



**Solar Backscatter Ultraviolet
Spectral Radiometer Mod 2**



SBUV/2

**Specification Compliance and
Calibration Data Book for SBUV/2
Engineering-Flight Unit (S/N 001)**



B6802-78

Specification Compliance and Calibration
Data Book
Volume I

for

Solar Backscatter Ultraviolet
Spectral Radiometer Mod 2
(SBUV/2 EMU-Flight)

Document No. B6802-78
January 11, 1984

Prepared for

NATIONAL AERONAUTICS AND SPACE ADMINISTRATION

Goddard Space Flight Center
Greenbelt, Maryland 20771

in accordance with
Contract NAS 5-26400, Item 40C

BASD Approvals:

Del Nelson
SBUV/2 Project Manager

Randall T. McConaughey
SBUV/2 System Engineer

Prepared By:

George E. Morris
SBUV/2 Test Engineer



TABLE OF CONTENTS

<u>Section</u>	<u>Title</u>	<u>Page</u>
1.	VIBRATION TEST.....	1-1
2.	THERMAL BALANCE TEST.....	2-1
3.	THERMAL VACCUM TEST.....	3-1
4.	EMI/EMC.....	4-1
5.	MASS PROPERTIES.....	5-1
6.	TIP COMPATIBILITY.....	6-1
7.	TELEMETRY CALIBRATION.....	7-1
8.	FIELD OF VIEW/UNIFORMITY.....	8-1
9.	POST ENVIRONMENTAL FOV VERIFICATION.....	9-1
10.	OPTICAL ALIGNMENT.....	10-1
11.	OUT OF FIELD RESPONSE.....	11-1
12.	GONIOMETRIC CALIBRATION.....	12-1
13.	SPECTRAL BANDPASS RESULTS.....	13-1
14.	OUT OF BAND RESPONSE.....	14-1
15.	POLARIZATION.....	15-1
16.	LIGHT LEAK RESPONSE.....	16-1
17.	SIGNAL TO NOISE RATIO.....	17-1
18.	SHORT TERM STABILITY.....	18-1
19.	WAVELENGTH CALIBRATION STABILITY.....	19-1
20.	ELECTRONIC CALIBRATION.....	20-1



LIST OF TABLES

<u>Table</u>	<u>Title</u>	<u>Page</u>
1-1	EMU-FLT Qualification Sinusoidal Vibration Levels.....	1-3
5-1	Instrument Weight.....	5-2
7-1	Digital A Analog Telemetry.....	7-2
7-2	Analog Telemetry.....	7-3
8-1	Horizontal Field-Of-View Scan.....	8-3
8-2	Horizontal Field-Of-View Scan Results.....	8-4
8-3	Vertical Field-Of-View Scan.....	8-5
8-4	Vertical Field-Of-View Scan Results.....	8-6
8-5	Horizontal Field-Of-View.....	8-7
8-6	Vertical Field-Of-View.....	8-8
8-7	Instantaneous Field-Of-View.....	8-9
9-1	FOV Size and Pointing Error Comparison.....	9-2
10-1	Optical Alignment.....	10-2
11-1	Pointing Position in Degrees.....	11-3
11-2	Out Of Field Response.....	11-6
12-1a	Goniometric Data at Wavelength (250 nm).....	12-3
12-1b	Goniometric Data at Wavelength (300 nm).....	12-3
12-1c	Goniometric Data at Wavelength (350 nm).....	12-4
12-1d	Goniometric Data at Wavelength (400 nm).....	12-4
13-1	Spectral Bandpass Results (Graphic Spline Interpolation From Three Measurement Points)	13-2
13-2	Discrete Mode Wavelength in the PROM are 1 to 3 Grating Steps out of Spec	13-4
14-1a	Out Of Band Response.....	14-2
14-1b	Out Of Band Response.....	14-2
16-1a	Light Leak Response for Side 1.....	16-2
16-1b	Light Leak Response for Side 2.....	16-3
16-1c	Light Leak Response for Side 3.....	16-4
16-1d	Light Leak Response for Side 4.....	16-5
16-1e	Light Leak Response for Side 5.....	16-6
16-2	Light Leak Response for Test (Discrete Wavelength 253.7 nm)	16-7



LIST OF TABLES (Cont'd)

<u>Table</u>	<u>Title</u>	<u>Page</u>
17-1	Signal-To-Noise Ratio Calculation.....	17-2
18-1	Short Term Stability	18-2
18-2	Short Term Stability	18-3
19-1	Wavelength Calibration Stability.....	19-2
20-1	Discrete Mode E-Cal.....	20-2
20-2	Sweep Mode E-Cal	20-3

LIST OF ILLUSTRATIONS

<u>Figure</u>	<u>Title</u>	<u>Page</u>
1-1	Modified Random Vibration Levels	1-4
3-1	Thermal Vacuum Test Profile.....	3-3
5-1	Sensor Module Center of Gravity	5-3
5-2	Electronics and Logic Module Center of Gravity	5-4
5-3	Sensor Module Envelope.....	5-5
5-4	Sensor Module Envelope.....	5-6
5-5	Sensor Module Interface Footprint.....	5-7
5-6	Electronics and Logic Module Y Dimensions.....	5-8
5-7	Electronics and Logic Module X-Z Dimensions...	5-9
7-1	Differential Reference Temperature	7-5
7-2	Temperature Sensor (PMT and CCR).....	7-6
7-3	Temperature Sensor (Sensor Module Shroud).....	7-7
7-4	Temperature Sensor (Diffuser Plate).....	7-8
7-5	Temperature Sensor (-15° to +45°C Range).....	7-9
7-6	Grating Motor Current	7-10
7-7	E-Cal Reference Voltage	7-11
7-8	5 Volt	7-12
7-9	+15 Volt Sensor and Servo.....	7-13
7-10	24 Volt Motor Power & 25 Volt Power.....	7-14
7-11	Chopper Error	7-15
7-12	Grating Course Error	7-16



LIST OF ILLUSTRATIONS (Cont'd)

<u>Figure</u>	<u>Title</u>	<u>Page</u>
7-13	Chopper Motor Current.....	7-17
7-14	Diffuser Motor Current.....	7-18
7-15	High Voltage.....	7-19
7-16	Thermistor Bias & 10 Volt Logic.....	7-20
7-17	-15 Volt Sensor and Servo.....	7-21
7-18	Lamp Motor Current.....	7-22
7-19	Grating Position Error.....	7-23
7-20	Baseplate and Diffuser Heater Current.....	7-24
7-21	Calibration Lamp Current.....	7-25
8-1 thru 26	Vertical and Horizontal Field of View Plot....	8-10 thru 35
9-1	Pre-Vibration Horizontal FOV.....	9-3
9-2	Pre-Vibration Vertical FOV.....	9-4
9-3	Pre-Vibration Horizontal CCR FOV.....	9-5
9-4	Pre-Vibration Vertical CCR FOV.....	9-6
9-5	Post Z-Axis Vibration Horizontal FOV.....	9-7
9-6	Post Z-Axis Vibration Vertical FOV.....	9-8
9-7	Post Z-Axis Vibration Horizontal CCR FOV.....	9-9
9-8	Post Z-Axis Vibration Vertical CCR FOV.....	9-10
9-9	Post Y-Axis Vibration Horizontal FOV.....	9-11
9-10	Post Y-Axis Vibration Vertical FOV.....	9-12
9-11	Post Y-Axis Vibration Horizontal CCR FOV.....	9-13
9-12	Post Y-Axis Vibration Vertical.....	9-14
9-13	Post X-Axis Vibration Horizontal FOV.....	9-15
9-14	Post X-Axis Vibration Vertical FOV.....	9-16
9-15	Post X-Axis Vibration Horizontal CCR FOV.....	9-17
9-16	Post X-Axis Vibration Vertical CCR FOV.....	9-18
9-17	Post T/V Horizontal FOV.....	9-19
9-18	Post T/V Vertical FOV.....	9-20
9-19	Post T/V Horizontal CCR FOV.....	9-21
9-20	Post T/V Vertical CCR FOV.....	9-22



LIST OF ILLUSTRATIONS (Cont'd)

<u>Figure</u>	<u>Title</u>	<u>Page</u>
10-1	Optical Alignment.....	10-3
11-1	Average Counts (CIF) in Field.....	11-4
11-2	Average Counts (COOF) out of Field.....	11-5
12-1	Goniometric Calibration Test Fixture.....	12-2
12-2 thru 10	Goniometric Response vs. Elevation Angle.....	12-5 thru 13
13-1	Graphic Spline Interpolation of Spectral..... Bandpass.....	13-3
14-1a thru g	Out of Band Sweep Plot.....	14-3 thru g
15-1	Residual Polarization Response.....	15-2
19-1 thru 10	Mercury Line Profiles.....	19-3 thru 12

FOREWORD

This document was prepared per item 40C of Contract NAS 5-26400 between the Goddard Space Flight Center (GSFC), Greenbelt, Maryland, and the Ball Aerospace Systems Division (BASD), Boulder, Colorado.

It is a compilation of all of the end-item test reports and calibration data applicable to the Engineering-Flight Unit Serial Number 001 of the Solar Backscatter Ultraviolet Spectral Radiometer Mod 2 (SBUV/2). Because of size, this document has been divided into two volumes. Volume I contains the specification compliance data whereas Volume II contains the calibration data. Reference to the Table of Contents of each volume will indicate the organization and contents of each document.

Prior to shipment of the instrument, a list of instrument non-conformances was created in the form of a waiver and submitted to GSFC for approval. A copy of this waiver (Number SBUV-W-002) is included for information.



REQUEST FOR DEVIATION/WAIVER
(SEE XIL-STD-480 OR 481 FOR INSTRUCTIONS)

DATE PREPARED
6 September 1983

PROCURING ACTIVITY NO.

1. ORIGINATOR NAME AND ADDRESS Ball Aerospace Systems Division, Boulder, Colorado 80306				2. <input type="checkbox"/> DEVIATION <input checked="" type="checkbox"/> WAIVER	
4. DESIGNATION FOR DEVIATION/WAIVER INO21A				3. <input checked="" type="checkbox"/> MINOR <input type="checkbox"/> MAJOR <input type="checkbox"/> CRITICAL	
6. MODEL/TYPE INO21A	8. MFR. CODE 13993	7. SYS. DESIG. TIROS-N	4. DEV/WAIVER NO. SBUV-W-002	5. BASE LINE AFFECTED <input checked="" type="checkbox"/> FUNCTIONAL <input type="checkbox"/> ALLOCATED	
7. SPECIFICATIONS AFFECTED-TEST PLAN				8. DRAWINGS AFFECTED	
9. SYSTEM 49671 IS-2280259 & IS-2295548				10. CONTRACT NO. & LINE ITEM NAS 5-26400, # 11A	
11. CONFIGURATION ITEM NOMENCLATURE Solar Backscatter Ultraviolet Spectral Radiometer Mod 2 (SBUV/2)				12. DEFECT CLASSIFICATION <input type="checkbox"/> MINOR <input type="checkbox"/> MAJOR <input type="checkbox"/> CRITICAL	
15. NAME OF PART OR LOWEST ASSEMBLY AFFECTED Instrument Assy		16. PART NO. OR TYPE DESIG. 67901-1		19. RECURRING DEVIATION/WAIVER <input type="checkbox"/> YES <input checked="" type="checkbox"/> NO	
20. EFFECT ON COST/PRICE None				21. EFFECT ON DELIVERY SCHEDULE	
22. EFFECT ON INTEGRATED LOGISTIC SUPPORT, INTERFACE, ETC. Refer to Section 5 of TCCR No. 3219.					
23. DESCRIPTION OF DEVIATION/WAIVER The instrument does not conform to some of the required design and performance requirements of the Interface Specifications IS-2280259 and IS-2295548 and the Instrument Design and Performance Specification S-480-12. These non-conformances are listed in Table 1.					

24. NEED FOR DEVIATION/WAIVER

The EMU/FLT Instrument S/N 001 is required to be shipped to RCA on 7 September, 1983. The out-of-spec conditions listed herein cannot possibly be corrected without major impacts on program cost and schedule.

25. PRODUCTION EFFECTIVITY BY SERIAL NUMBER S/N 001 Only.	
26. SUBMITTING ACTIVITY AUTHORIZING SIGNATURE <i>D. Nelson 6 Sept 83</i>	TITLE SBUV/2 Project Manager
27. APPROVAL/DISAPPROVAL	
6. <input type="checkbox"/> APPROVAL RECOMMENDED	8. <input type="checkbox"/> APPROVED <input type="checkbox"/> DISAPPROVED
7. GOVERNMENT ACTIVITY	SIGNATURE DATE

DD FORM 1694
1 DEC 56



Request for Waiver No. SBUV-W-002

TABLE I

LIST OF EMU/FLT UNIT NON-CONFORMANCES

No.	Parameter	Spec.No.	Spec.Ref.	Spec. Req'mt.	Measured Value	Remarks
1	Envelope (Sensor Module)	IS-2295548	Para. 3.2.1.1	See Fig's 1&2	See Fig's 1&2	
2	Power, Orbital Avg.	IS-2295548	Para. 3.1.3.1	12.0 Watts	12.1 Watts	
3	Peak Current	IS-2295548	Para. 3.1.3.1	0.93 Amp	1.265 Amps	
4	Conducted Emissions ● Fundamental Ripple Freq. ● +28V Telemetry Return Ripple ● +10V I/F Return Ripple	IS-2295548	Para. 3.1.3.2.6.1 Para. 3.1.3.3.2 Para. 3.1.3.5.5	30 KHz 0.14 mA 0.4 mA	≈ 100 KHz 14 mA P-P 10 mA P-P	
	Radiated Susceptibility	IS-2295548	Para. 3.4.2	29.1 V/M @ 135 - 139 MHz	≈ 10V/M	
6	Ground Isolation	IS-2280259	Para. 3.1.1.1 & Figure 12	>100 Kohms	14 Kohms	
7	Conducted Susceptibility +28V Main Bus	IS-2280259	Para. 3.6.1.2	Performance Shall Not Degrade		Susceptible to all Harmonics of 20 Hz.
8	Conducted Transient Susceptibility +28V Pulse Load Bus	IS-2280259	Para. 3.6.1.3	-13V	-12V	Loss of sync @ -12V
9	Field Non-Uniformity (Monochromator)	S-480-12	Para. 4.3.2.1	± 10% Max.	+7.3% -17.5%	



TABLE I (Cont'd)

No.	Parameter	Spec.No.	Spec. Ref.	Spec. Req't.	Measured Value	Remarks
10	Optical Alignment <ul style="list-style-type: none"> ● Monochromator To Instrument Reference ● Monochromator to CCR ● Changes During Test <ul style="list-style-type: none"> ● Monochromator ● CCR 	S-480-12	Para. 4.3.3	0.1° max. 0.1° max. 0.05° max. 0.05° max.	0.27° in +Y 0.18° in -Z 0.43° in +Y 0.21° in -Z 0.06° in +Y 0.06° in -Z 0.1° in -Y 0.1° in +Z	
11	Vibration Test	S-480-12	Para. 6.2.4	See Spec. S-480-12	-	Ran to modified levels. See Figure 3
12	Spectral Bandpass	S-480-12	Para. 4.3.4 Tab 4.1	See Figure 4	See Figure 4	
13	System Linearity	S-480-12	Para. 4.4.2.1	1% Max.	9% on Range 2	

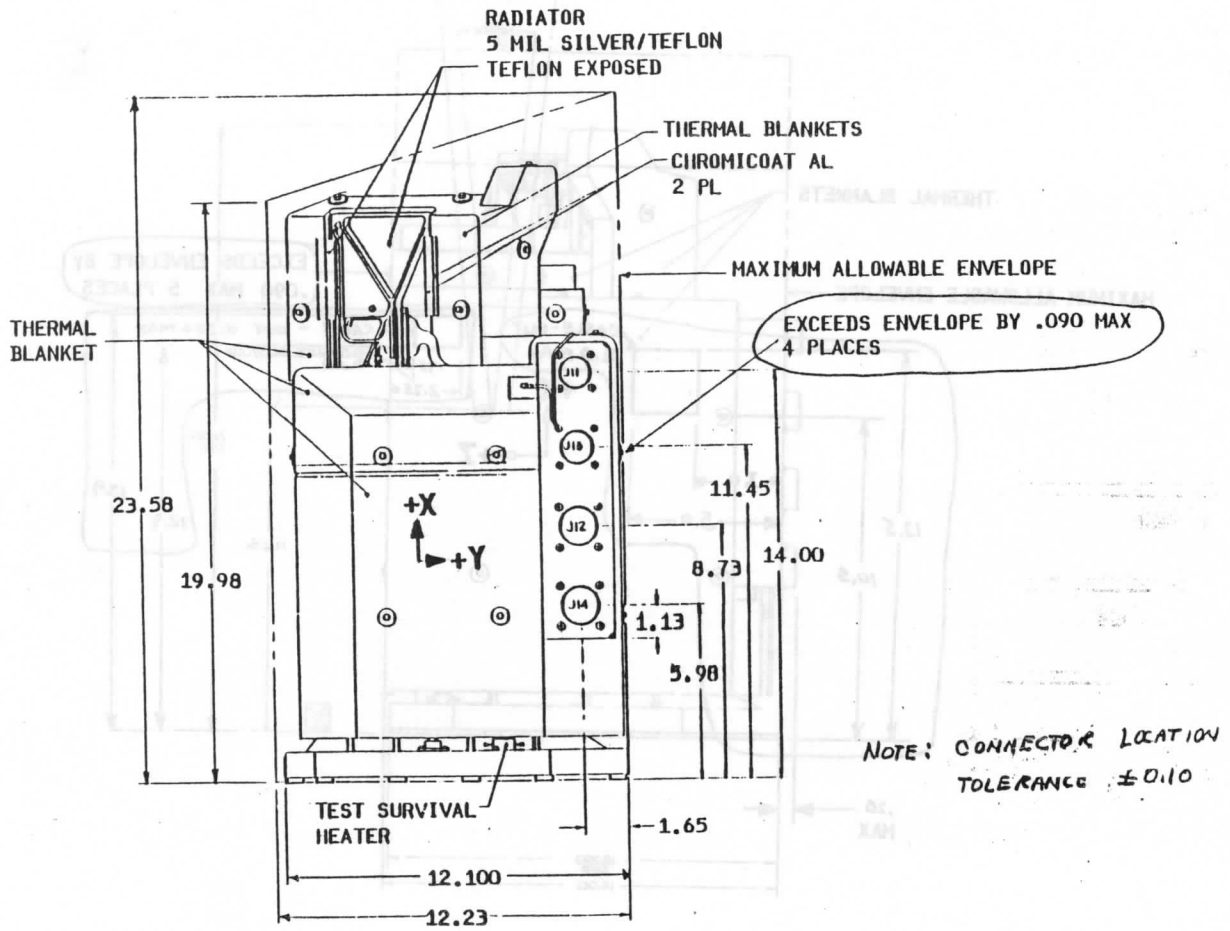


FIGURE 1

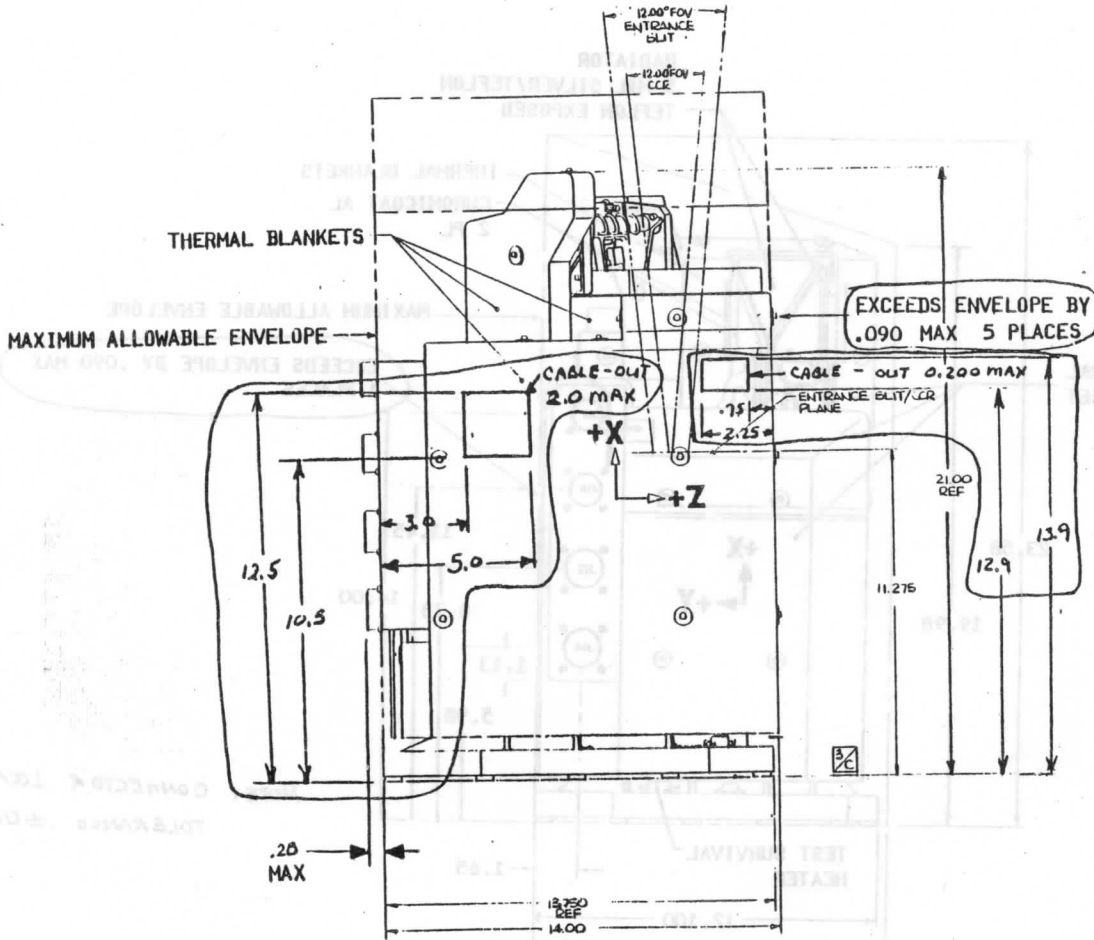
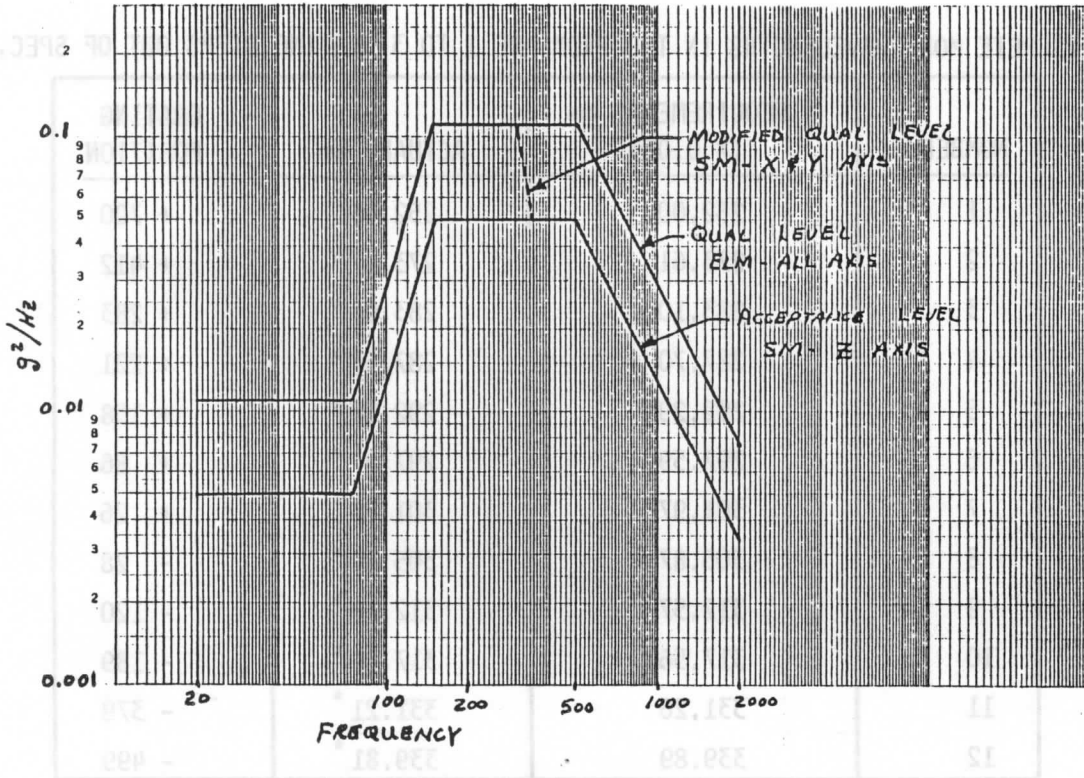


FIGURE 2



NOTE: Random vibration levels shown above for the Sensor Module do not meet Paragraph 6.2.4 of Specification S-480-12.

FIGURE 3



DISCRETE MODE WAVELENGTHS IN THE PROM ARE 1 TO 3 GRATING STEPS OUT OF SPEC.

NUMBER	REQUIREMENT, nm (± 0.05)	ACTUAL, nm	GRATING POSITION
1	252.00	252.03	+ 700
2	273.61	273.47 *	+ 412
3	283.10	283.00 *	+ 283
4	287.70	287.57 *	+ 221
5	292.29	292.20 *	+ 158
6	297.59	297.47 *	+ 86
7	301.97	301.86 *	+ 26
8	305.87	305.80 *	- 28
9	312.57	312.50 *	- 120
10	317.56	317.50 *	- 189
11	331.26	331.21 *	- 379
12	339.89	339.81 *	- 499

* Out-of-spec per Paragraph 4.3.4 of Specification S-480-12

FIGURE 4



Section 1
VIBRATION TEST

(Reference Test Procedure 68038)

The Sensor Module and Electronics and Logic Module were vibrated separately to minimize the size of the test fixture and allow for a maximum number of accelerometer data channels for the test. The instrument was tested at one of BASD's vibration/shock facilities - a Ling B335 Vibration System. The instrument was tested without thermal blankets and in a power off state.

A resonant survey of the test fixture was performed prior to vibration testing to assure no resonant frequencies which might present a problem. In each axis of vibration a low level sinusoidal survey was run before full level was applied. (See Figure 1-1 for levels). Because of greater than anticipated response from the grating shaft assembly the vibration levels for random were modified as was allowed by GSFC per the current TIROS vibration test data (see Table 1-1 for levels). Each test axis consisted of a qualification level sine, modified qualification level random and finally qualification level shock. The Electronics and Logic Module followed the same sequence except that it was subjected to full qualification level random.

The instrument was given a thorough visual inspection after each axis of vibration and shock. After each axis, it was returned to the clean room and an electrical/optical performance functional conducted. No problems were detected.

The primary resonances determined are listed below. (Requirement: None greater than 100HZ).

SENSOR MODULE

ELM

184HZ - Y AXIS LATERAL MODE
205HZ - Z AXIS LATERAL MODE
320HZ - CAL LAMP MODE
430HZ - GRATING BENDING MODE

210HZ - Y AXIS LATERAL MODE
250HZ - Z AXIS LATERAL MODE



B6802-78

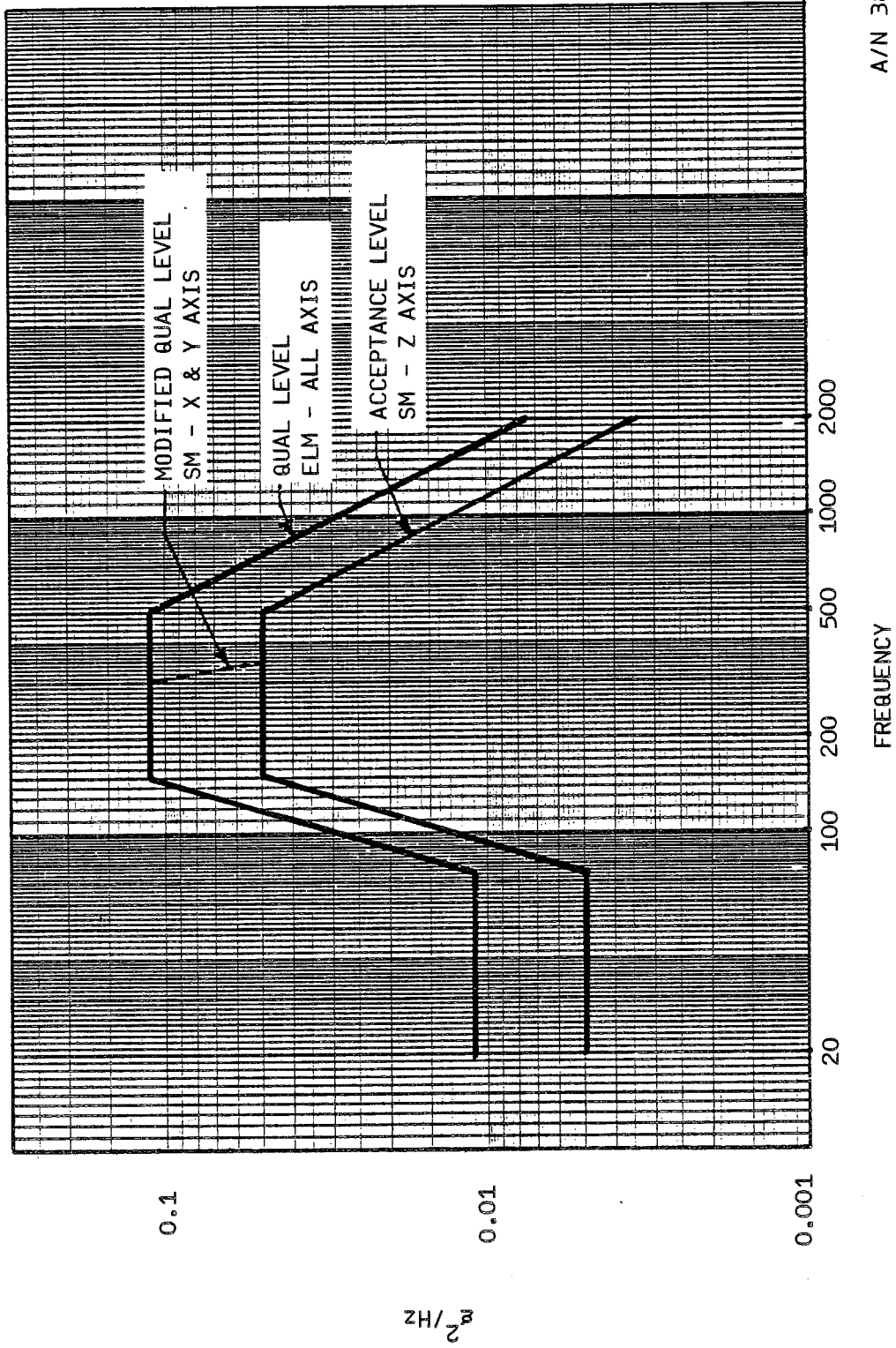
For detailed information, see EMU-FLT Vibration Test Report (BASD System Engineering Report (SER) No. SBUV-RP-83-391, Rev. A).



Table 1-1
EMU-FLT QUALIFICATION SINUSOIDAL VIBRATION LEVELS

AXIS	FREQUENCY RANGE	G LEVEL SPEC.	G LEVEL ACTUAL
X	5 - 70	4.5	4.5
	70 - 110	1.5	1.5
	110 - 2000	1.5	QUAL LEVEL SHOCK ALTERNATIVE
Y	5 - 70	5.0	5.0
	70 - 110	2.5	2.5
	110 - 2000	2.5	QUAL LEVEL SHOCK ALTERNATIVE
Z	5 - 70	4.0	4.0
	70 - 110	1.0	1.0
	110 - 2000	1.0	QUAL LEVEL SHOCK ALTERNATIVE

A/N 3875



A/N 3875

Figure 1-1 Modified Random Vibration Levels



Section 2

THERMAL BALANCE TEST

(Reference Test Procedure 68039)

A thermal balance test was conducted just prior to running the thermal vacuum test. This test was conducted in a BASD thermal vacuum facility modified for SBUV/2 requirements. A powered orbital "hot" and "cold" case, and an unpowered orbital "cold" case were simulated. The Sensor Module was mounted to a test fixture in a flight manner. The test fixture temperature was controlled to 0°C and +30°C to simulate a cold and hot spacecraft interface respectively. The instrument, fixture, and cables were wrapped in MLI. A vacuum chamber shroud provided the orbital cold and hot radiation conditions as it was controlled to -55°C and -29°C.

The tests were conducted by operating the instrument with power on or power off as the case required. Thermal equilibrium for each case was achieved when no temperature sensor changed more than 1°C per hour.

The purpose of the thermal balance test was to verify the thermal design of SBUV/2 and to verify and adjust the thermal math model so as to make accurate predictions of orbital thermal performance.

Both objectives were achieved with SBUV/2 operating within design limits despite some minor mechanical fit problems causing undesired heat leaks.

The thermal math model was changed to provide results in agreement with the test. The mechanical fit problems were corrected by some minor design changes thus eliminating the heat leak.

For detailed information see Thermal Balance Test and Updated Orbital Temperature Predictions, SER No. SBUV-TK-83-384.



Section 3

THERMAL VACUUM TEST

(Reference Test Procedure 68040)

Thermal vacuum testing was performed in a BASD vacuum chamber, COMBO. The Sensor Module was mounted onto the vacuum test fixture which had a cold plate attached to the mounting base for temperature control. Thermal blankets were removed from the instrument to expedite temperature change from plateau to plateau.

Thermal vacuum test began July 15 and was concluded on July 23. Figure 3-1 depicts the temperature profile used during the test. The testing consisted of radiometric data being taken at temperature plateaus of 0, 10, 20, and 30°C.

Electrical functionals were performed at the temperature extremes -10° and +40°C after a shutdown and restart. At the temperature extremes the instrument power was turned off and the instrument allowed to stabilize in temperature before restarting.

Radiometric data was taken at each of the mentioned temperature plateaus in sweep mode, discrete mode and position mode at the 12 discrete wavelengths, using these lamps - Argon Mini Arc, FEL and deuterium.

In conclusion, radiometric calibration data was successfully taken at 0°C, 10°C, 20°C, and 30°C with the FEL lamp, deuterium lamp and the Argon Mini Arc Lamp. No problems were found during cold start tests at -10°C or hot start tests at +40°C. Only two anomalies were noted during all of the calibration and electrical functionals:

- 1) Below about +16°C, the current through the on board mercury lamp began oscillating at approximately 7KHz. This was noticeable on some of the wavelength calibration and diffuser check data, but the data could still be used.

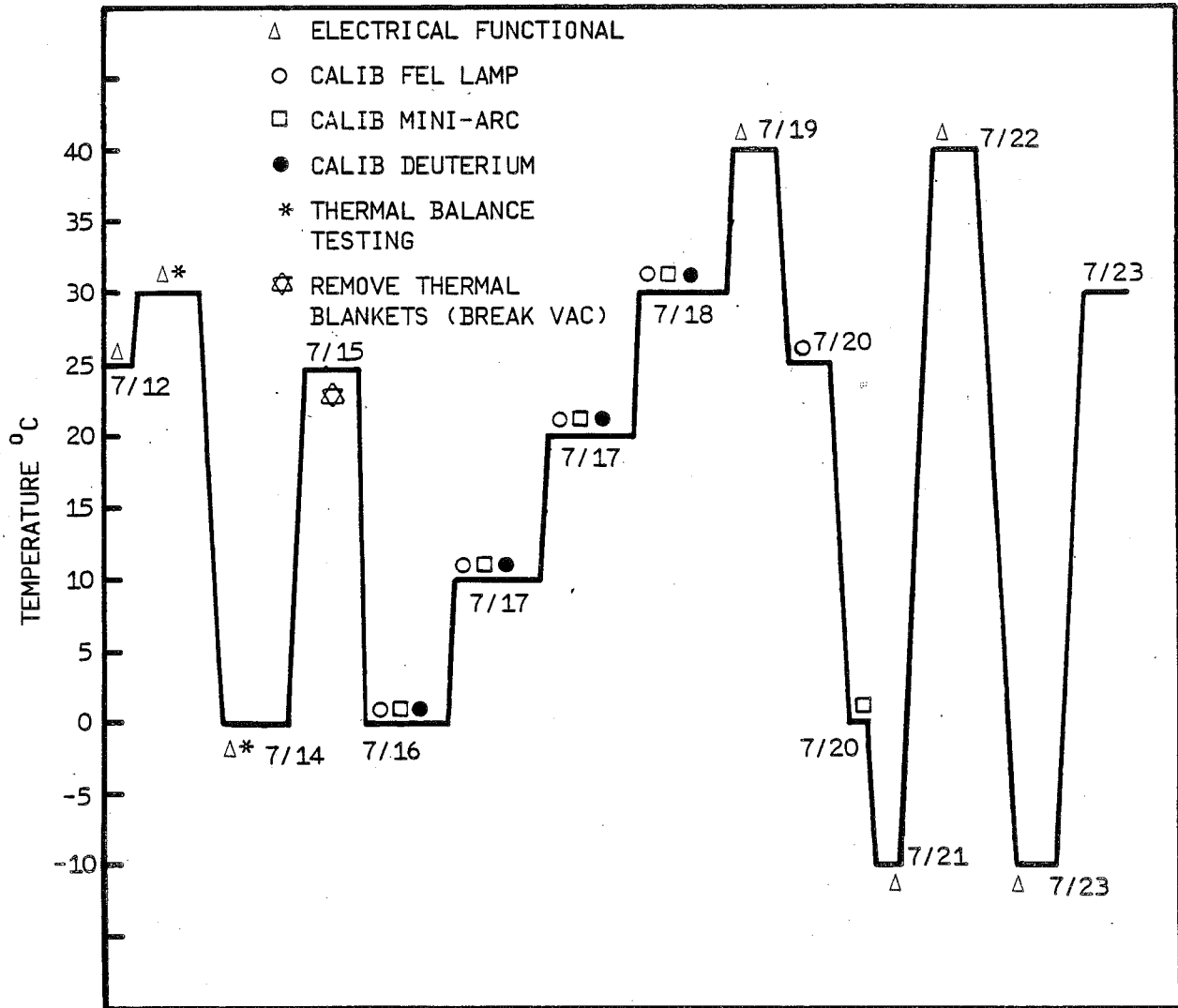


- 2) At the temperature extremes of -10°C and $+40^{\circ}\text{C}$, increased settling times were noted on the grating mechanism. Normal operation was observed at temperatures from 0°C to $+30^{\circ}\text{C}$.

Results of the thermal vacuum calibration data are given in Volume II of this document.



The figure below shows the temperature profile of the cold plate during the thermal balance and thermal vacuum tests.



A/N 3875

Figure 3-1 Thermal Vacuum Test Profile.



Section 4
EMI/EMC TESTING
(Reference Test Procedure 68035)

EMI/EMC testing was conducted in the BASD EMC Screen Room and Clean Room # 2, both are located in the John W. Fisher building at BASD. The testing consisted of the following:

Conducted Emission (CE01 and CE03)
Radiated Emissions (RE02)
Conducted Susceptibility (CS01 and CS06)
Radiated Susceptibility (RS03)
Special Radiated Emissions Test

The results of the Conducted Emission Tests (CE01 and CE03) reveal that most of the power and return lines tested met specification. Exceptions consisted of the following:

- 1) The Fundamental Ripple Frequencies were 100 kHz, a level exceeding the 30 kHz constraints described in DD68035.
- 2) The Ripple Current on the +28V Telemetry Return measured 14 mA p-p. The specification is 2 percent of average.
- 3) The Ripple Current on the +10V interface return measured 10 mA p-p. The specification is 5 percent of the average, or 0.4 mA.

The Radiated Emission testing (RE02) was performed per MIL-STD-462 from 14 kHz to 2 GHz with limits per MIL-STD-461. Exceptions occurred at eight frequency bands, where the limits were "Minimum Discernable Signal". Due to misinterpretation of MIL-STD-462, the initial testing was performed without the STE-to-ELM cables shielded. Retesting with the cables shielded showed reduced emission levels. It was then agreed that minimum discernable signal levels were met.

Conducted Susceptibility results demonstrated no susceptibility during CS01 testing. However, additional "Engineering Tests" did show susceptibility (increased noise in radiometric data) to all odd Harmonics of 20 Hz on the +28V main bus. Because the frequencies are precise multiples of 20 Hz, this was not



detected during earlier CS01 tests. Due to low probability of energy at precise multiples of 20 Hz on the spacecraft no changes were made. Also noted during the transient susceptibility testing (CS06) was a "Loss of Sync" detected with a -12V transient injected on the pulse load bus (specification is -13V). It was not determined whether the problem was in the STE or the instrument.

Radiated susceptibility tests showed no susceptibility at 1 Volt per meter from 14 kHz to 10 GHz. Initially, the instrument showed considerable susceptibility in the 135-139 MHz range, to field intensities above 1 Volt/Meter. (Specification is 29.1 Volts per Meter). Considerable improvement was made by adding a twisted, shielded pair cable from the anode Preamp output to the Electrometer. No susceptibility was noted with the added twisted shielded cable plus added filtering on the anode preamp power lines. If susceptibility is noted on the spacecraft, a jumper cable with required filters can be added. The jumper cable, will, however, violate the envelope. Susceptibility was noted after the EMU-FLT instrument was integrated onto the spacecraft. A jumper cable containing filtering was subsequently added to the EMU-FLT instrument at RCA. The design of the Sensor Module cable harness has been modified to incorporate this filtering on subsequent units.

Additional measurements were made during the initial radiated mission testing, in certain frequency bands using a low noise preamp and a spectrum analyzer. Review of the data after the test shows contamination from emissions of the unshielded STE-TO-ELM cables. Time limitations prevented repetition of measurements when the cables were shielded.

For detailed information see EMU-FLT EMI/EMC Test Report (BASD System Engineering Report (SER) # SBUV-DY-83-394.



Section 5

MASS PROPERTIES

(Reference Test Procedure 68037)

The weight, center of gravity, and envelope dimensions have been determined for the Electronics and Logic Module and the Sensor Module. The following table and figures give the weight, show the location of the center of gravity, and give the envelope dimensions for both the Sensor Module and Electronics and Logic Module.



Table 5-1
INSTRUMENT WEIGHT

ASSEMBLY	WEIGHT	
	SPECIFICATION	MEASUREMENT
SENSOR MODULE	55 POUNDS (TARGET)	55.75 POUNDS
ELECTRONICS AND LOGIC MODULE	29 POUNDS (TARGET)	24.25 POUNDS
TOTAL	84 POUNDS MAXIMUM	80.00 POUNDS

A/N 3875

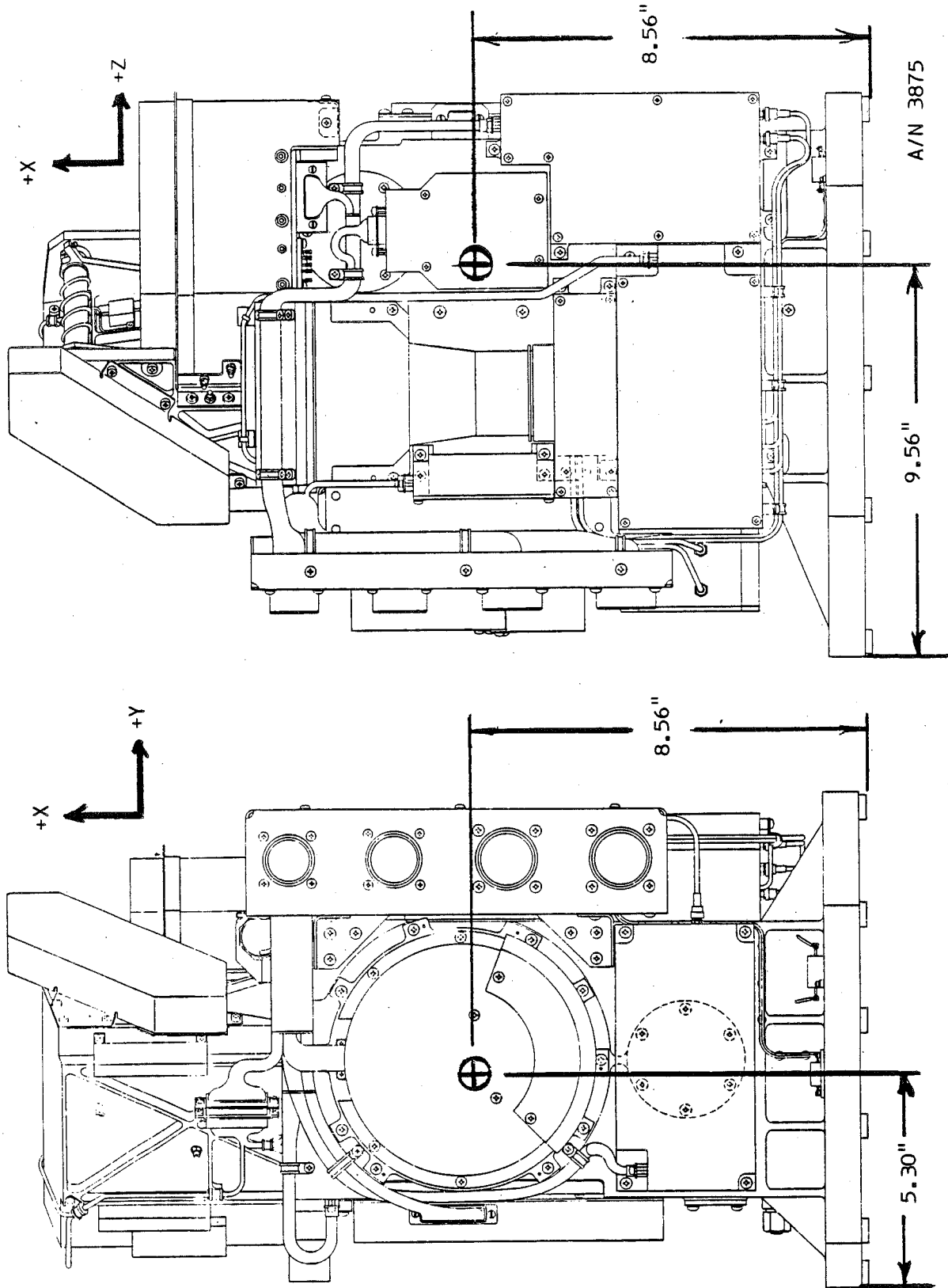


Figure 5-1 Sensor Module Center of Gravity



B6802-78

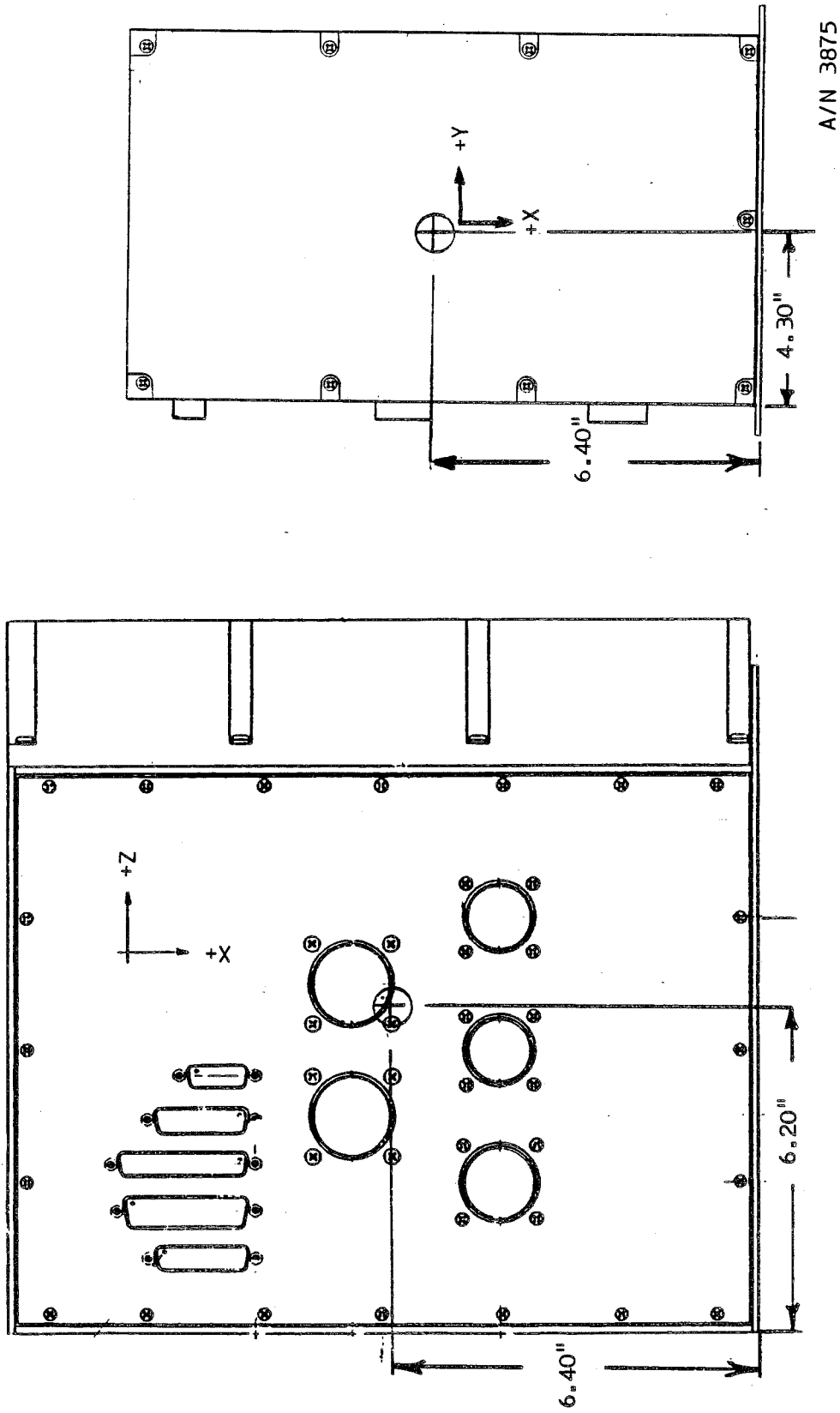
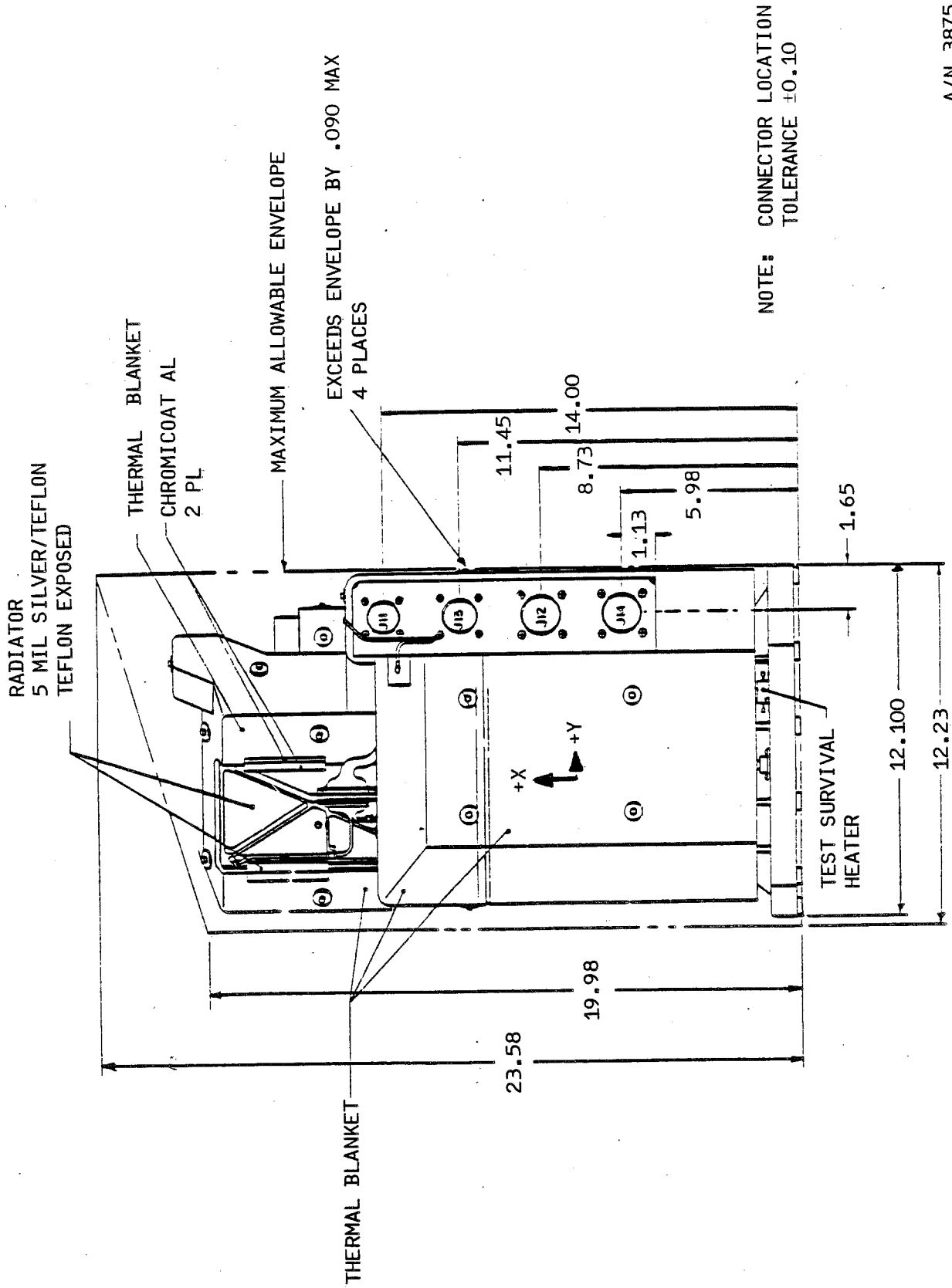
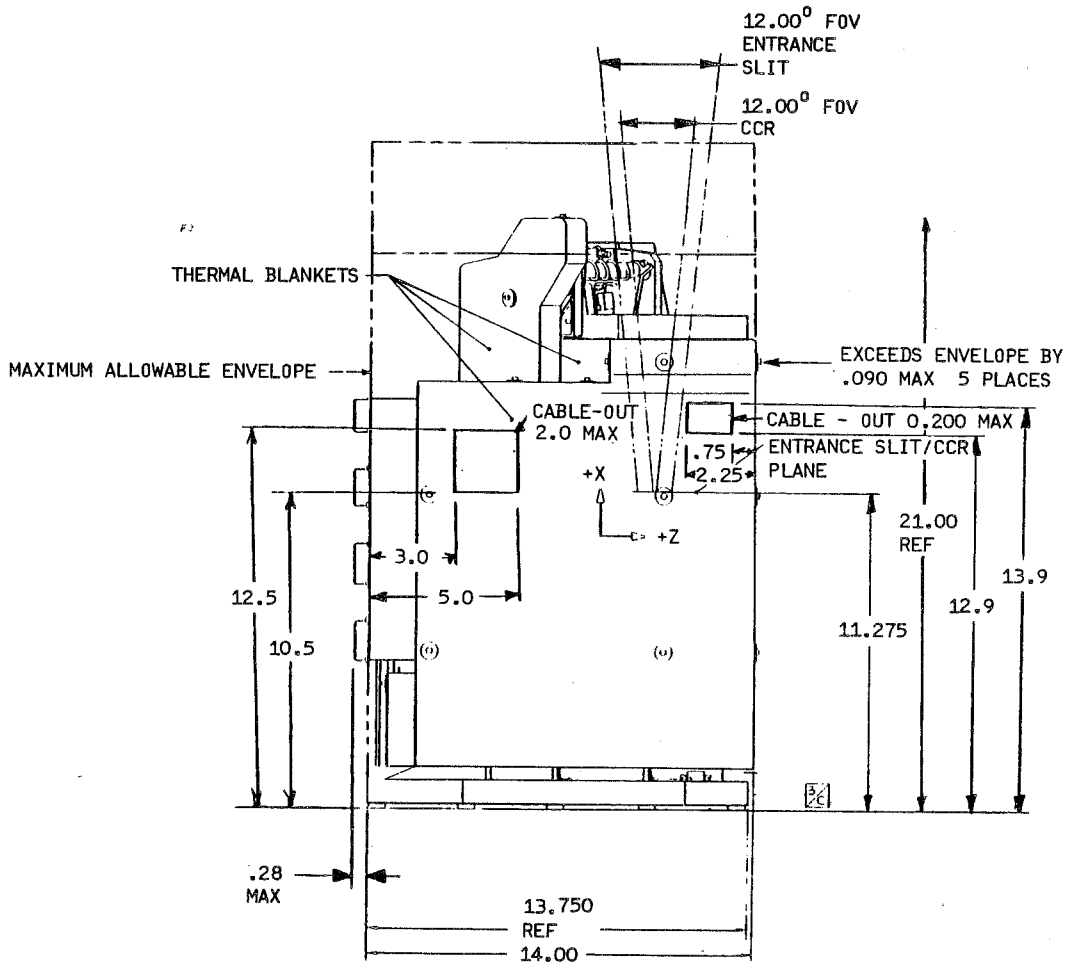


Figure 5-2 Electronics and Logic Module Center of Gravity



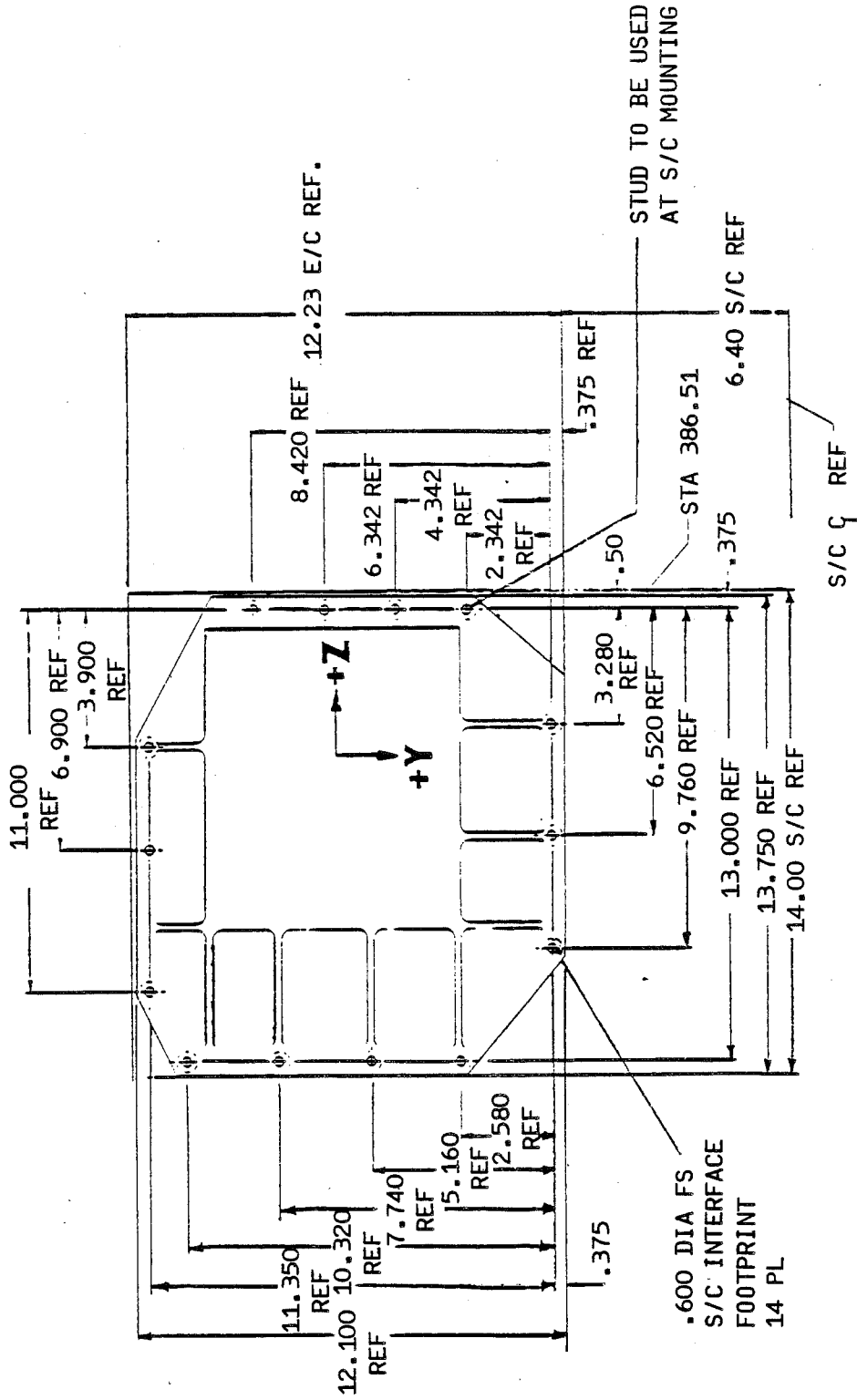
A/N 3875

Figure 5-3 Sensor Module Envelope



A/N 3875

Figure 5-4 Sensor Module Envelope



A/N 3875

Figure 5-5 Sensor Module Interface Footprint

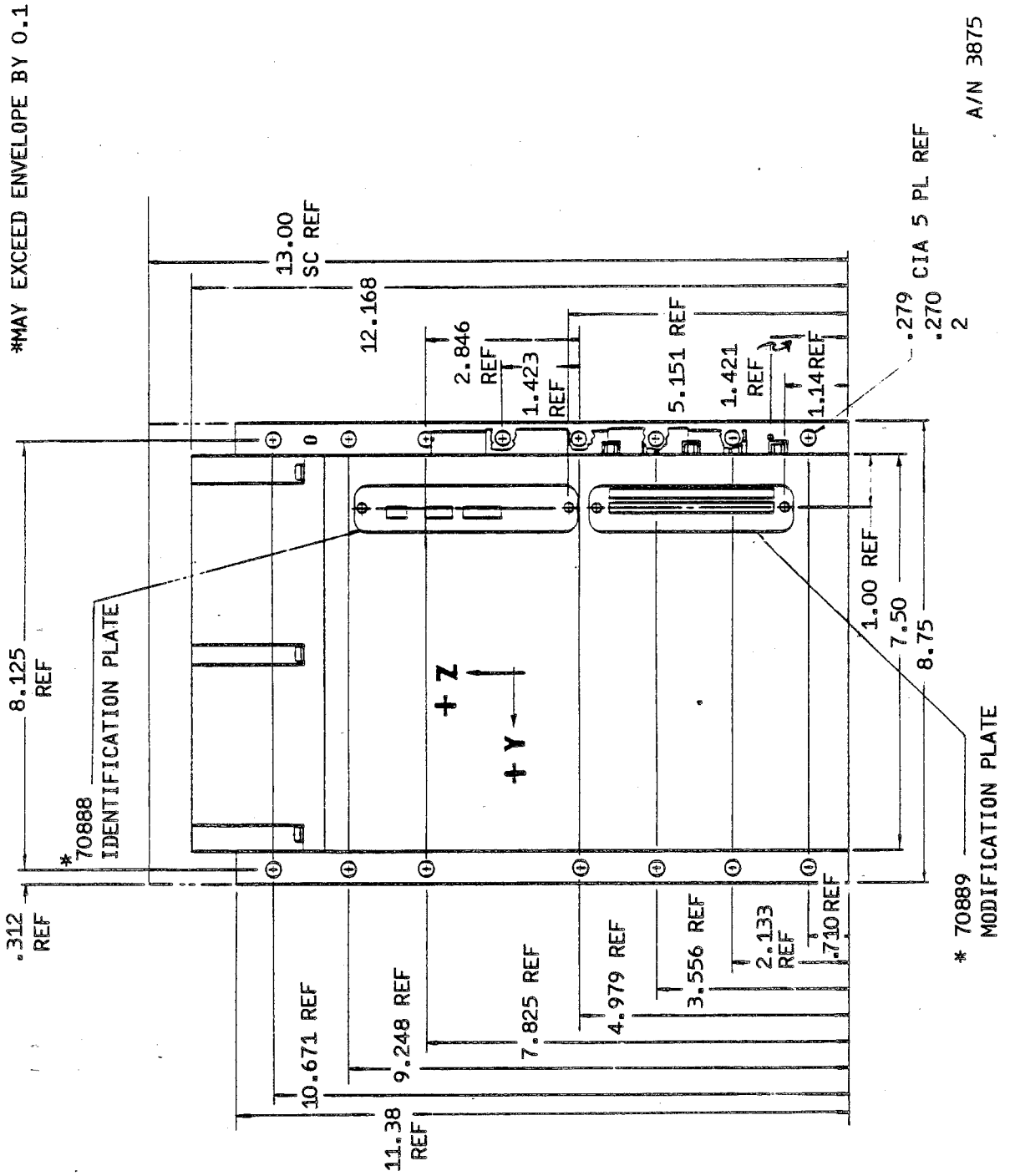


Figure 5-6 Electronics and Logic Module Y Dimensions



Section 6

TIP COMPATIBILITY

(Reference Test Procedure 68401)

The TIROS Interface Processor (TIP) compatibility test was performed at BASD. The test consisted of an electrical functional prior to connecting the TIROS Interface Processor Simulator. With instrument power off the TIP Simulator was connected. Three eight bit words were read out (Minor Frame 9, Word 36 Minor Frame 9, Word 37, and Minor Frame 4, Word 37). These words are read out under normal operation and again under degraded conditions (with noise, jitter, and reduced amplitude).

Under the nominal operating conditions the words were correctly read out. During the set up for the degraded portion of the test the TIP Simulator had a malfunction and it could not be repaired at BASD in time to complete the test. However, it was concluded that sufficient testing had been conducted to prove interface compatibility of SBUV/2 instrument to the spacecraft.



Section 7

TELEMETRY CALIBRATION

This section contains the calibration curves for the analog and Digital A analog data. Tables 7-1 and 7-2 list the Digital A and analog telemetry respectively. The calibration curves are shown in Figures 7-1 through 7-21.

Additional details can be found in the SBUV/2 Unique Instrument Interface Specification, RCA Document IS 2295548, Section 3.1.5



DIGITAL A ANALOG TELEMETRY

<u>Telemetry Point</u>	<u>Mnemonic</u>
Chopper Motor Current	CMCUR
Diffuser Motor Current	DCR
High Voltage Power Supply Volts	HVPS
Thermistor Bias Voltage (10V REF)	THB
Calibration Lamp Temperature Sensor	LMP
Electronic Calibration Reference Voltage	ECL
15 Volt Sensors Voltage	15SR
-15 Volt Sensors Voltage	-15SR
24 Volt Motor Voltage	24
5 Volt LED Voltage	5
10 Volt Logic Voltage	10
Calibration Lamp Current	LCR
Grating Coarse Error	CRSERR
Grating Motor Current	MOTRCUR
Calibration Lamp Motor Current	MCR
Diffuser Plate Temperature Sensor	DFP
Sensor Module Baseplate Temperature	SMB
25 Volt Power Voltage	25
15 Volt Servo Voltage	15SN
-15 Volt Servo Voltage	-15SN
CCR Diode Temperature	(CDT)
Sensor Module Differential Temperature Anti-Sun Side	(SDA)
Sensor Module Differential Temperature Sun Side	(SDS)
Differential Reference Temperature Sensor Anti-Sun Side	(DRA)
Differential Reference Temperature Sensor Sun Side	(DRS)
PMT Cathode Temperature Sensor	(PMT)
Chopper Motor Phase Error	CPERR
Digital A - Grating Position Error	POSERR

Table 7-1



ANALOG TELEMETRY

<u>Telemetry Point</u>	<u>Mnemonic</u>
Sensor Module Baseplate Temperature Sensor # 2	SM2
Sensor Module Shroud Temperature Sensor	SMS
Depolarizer Housing Temperature Sensor	DPH
High Voltage Power Supply Temperature Sensor	HVP
Diffuser Plate Temperature Sensor # 2	DF2
Choffer Motor Temperature Sensor	CHM
Grating Motor Temperature Sensor	GRM
Diffuser Motor Temperature Sensor	DFM
Calibration Lamp Motor Temperature Sensor	CLM
Electrometer Temperature Sensor	ELT
Calibration Lamp Power Supply Temperature Sensor	CLP
Diffuser Radiator Temperature Sensor	DFR
Electronics and Logic Module Temperature Sensor	ELM
Low Voltage Power Supply Temperature Sensor	LVP
Diffuser Heater Current	DFHTR
Baseplate Heater Current	BPHTR
28 Volt Main Power	28

Table 7-2



Conversion of Differential Temperature

- 1) Convert the differential reference temperature from counts to temperature using the conversion chart shown in Figure 7-1.

DRS or DRA = TD

- 2) Next, calculate the differential temperature counts from the following:

$$T_{(SDS)} = (.107499) (C_{SDS}) - (13.706) + C_{(DRS)}$$

where

$T_{(SDS)}$ = Differential Temperature in Counts

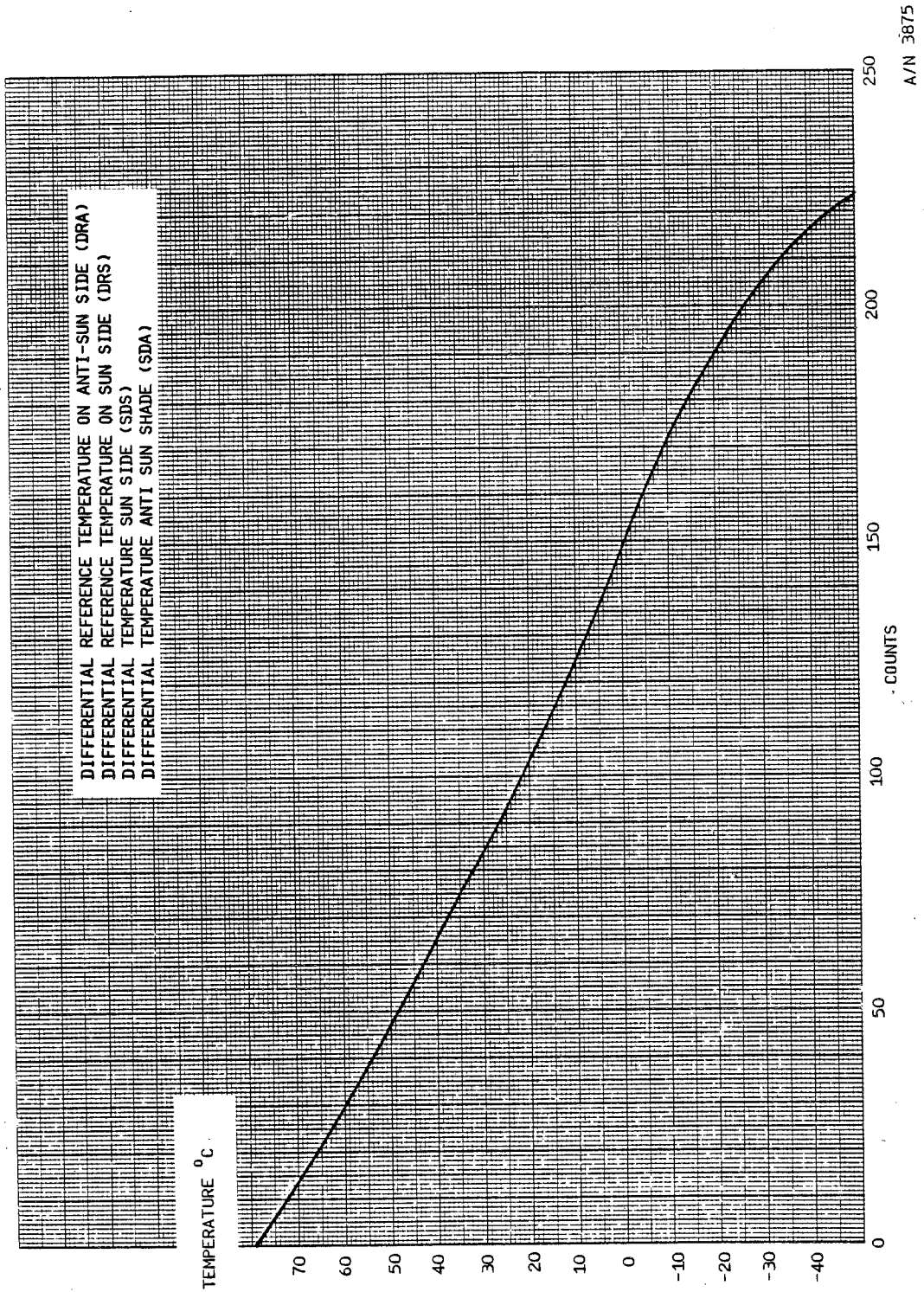
$C_{(SDS)}$ = Counts from Differential Temperature

$C_{(DRS)}$ = Counts from Differential Reference Temperature

- 3) Convert $T_{(SDS)}$ from counts calculated in the above equation to temperature (TS) using the conversion chart shown in Figure 7-1.

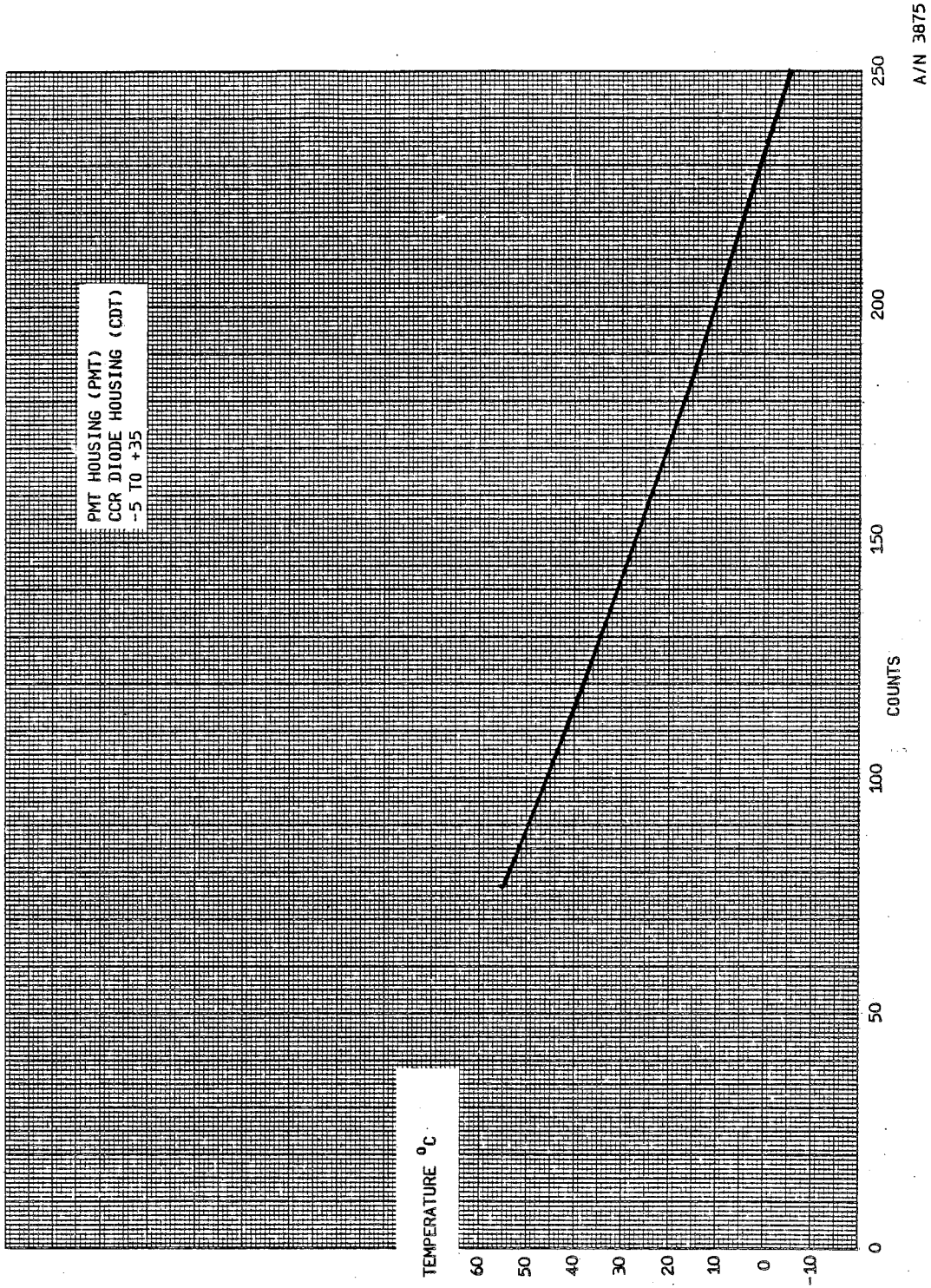
- 4) The differential temperature T, then is determined from the following:

$$T = TD - TS$$



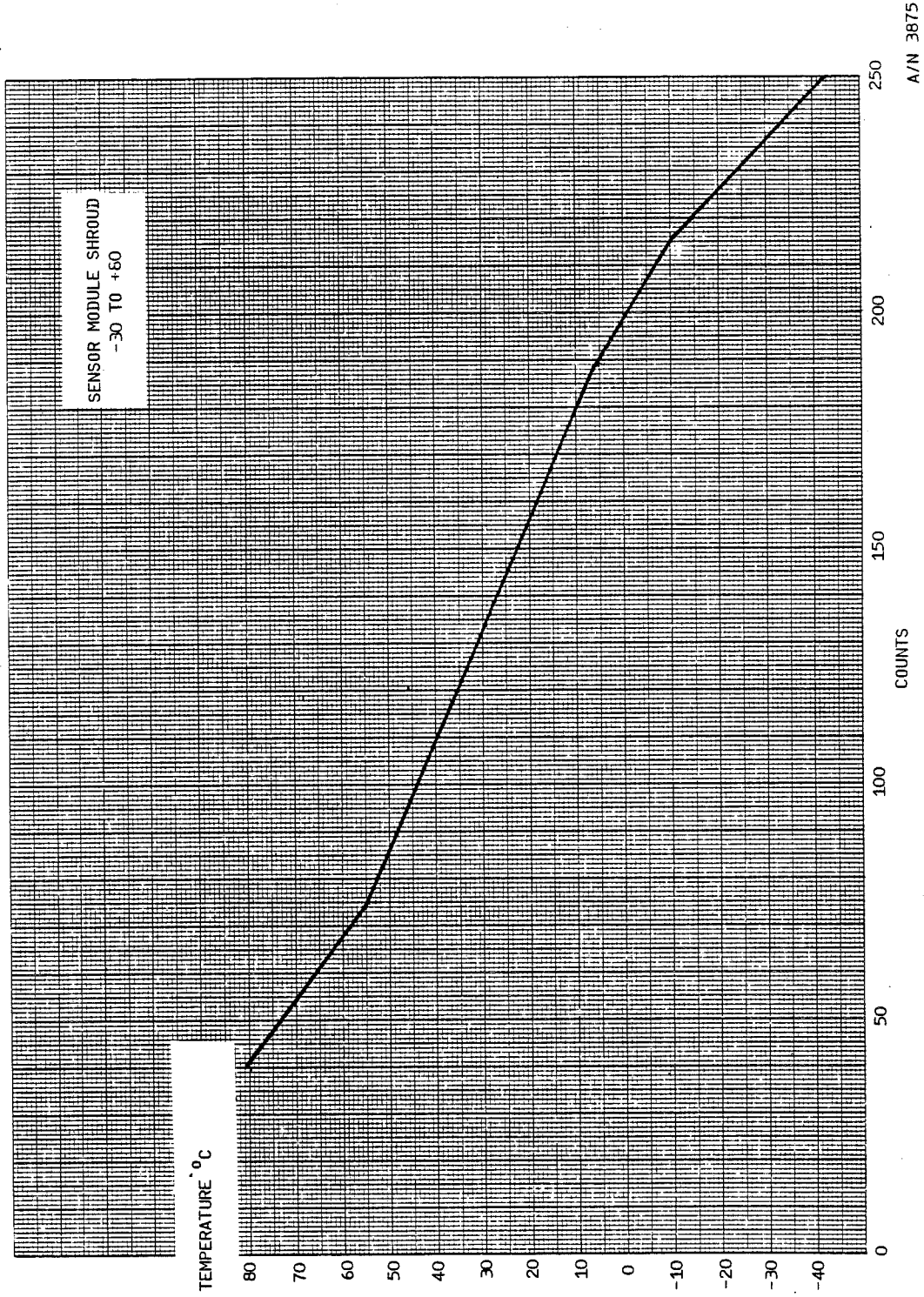
A/N 3875

Figure 7-1 Differential Reference Temperature



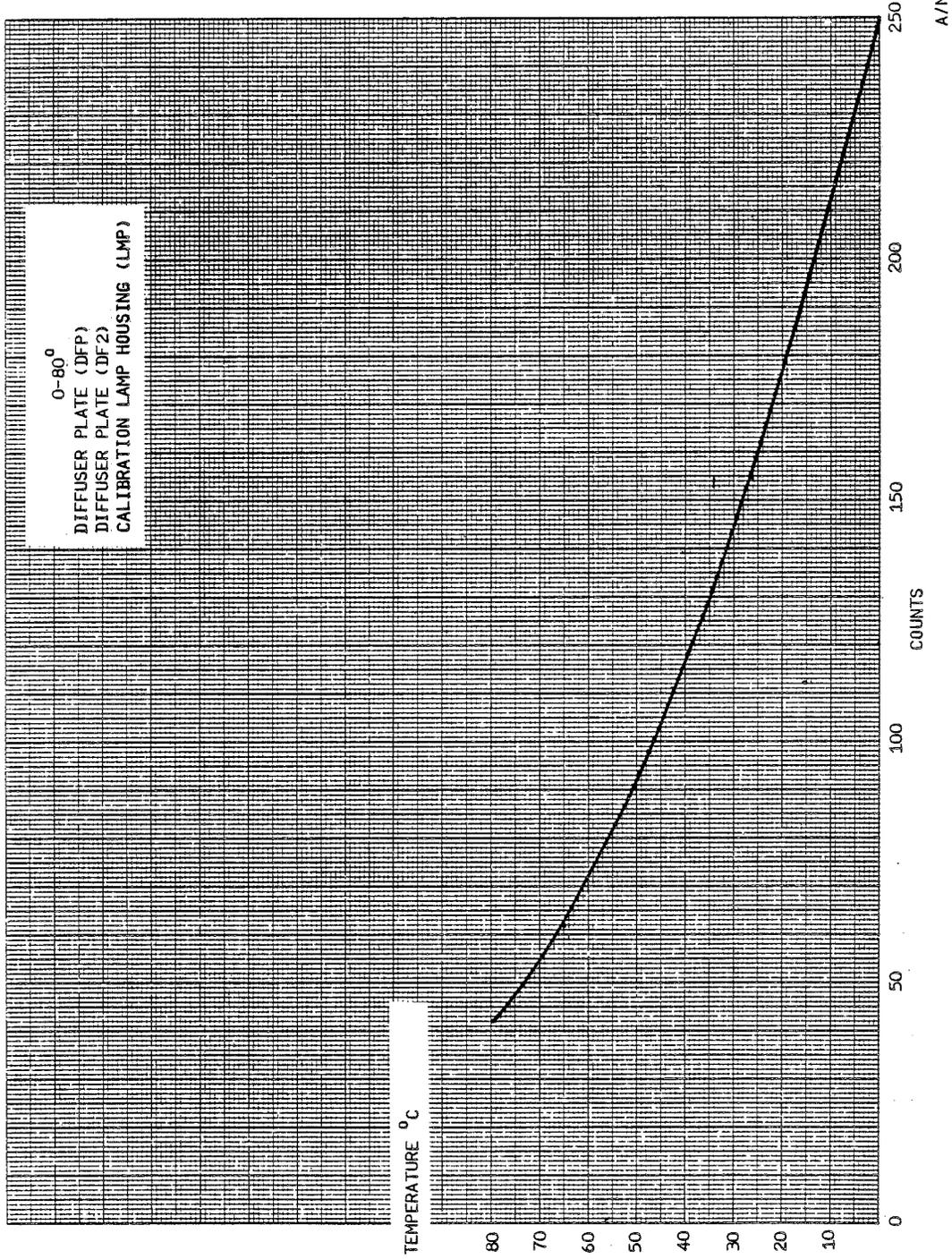
A/N 3875

Figure 7-2 Temperature Sensor (PMT and CCR)



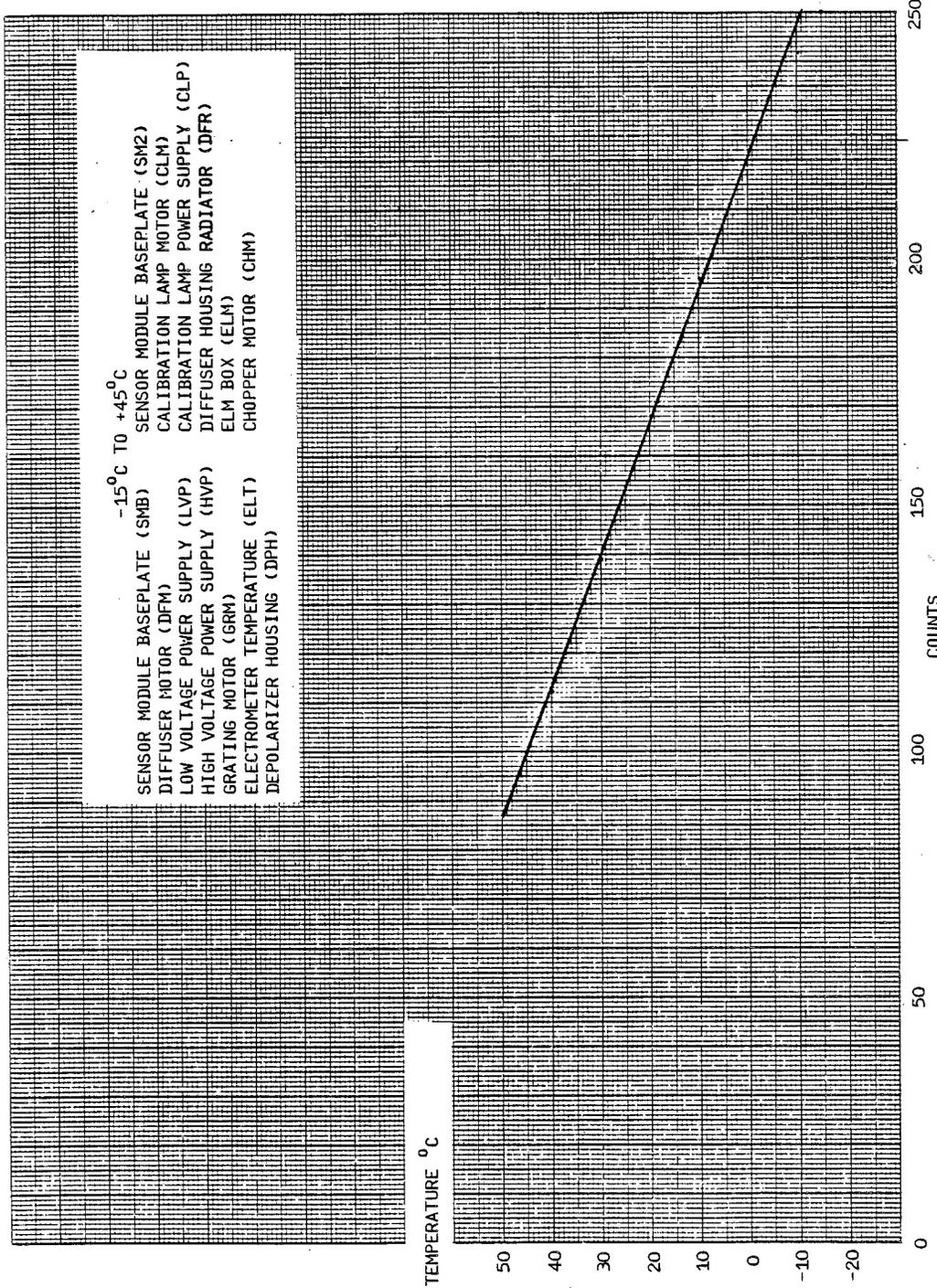
A/N 3875

Figure 7-3 Temperature Sensor (Sensor Module Shroud)



A/N 3875

Figure 7-4 Temperature Sensor (Diffuser Plate)



A/N 3675

Figure 7-5 Temperature Sensor (-15° to +45° C Range)



B6802-78

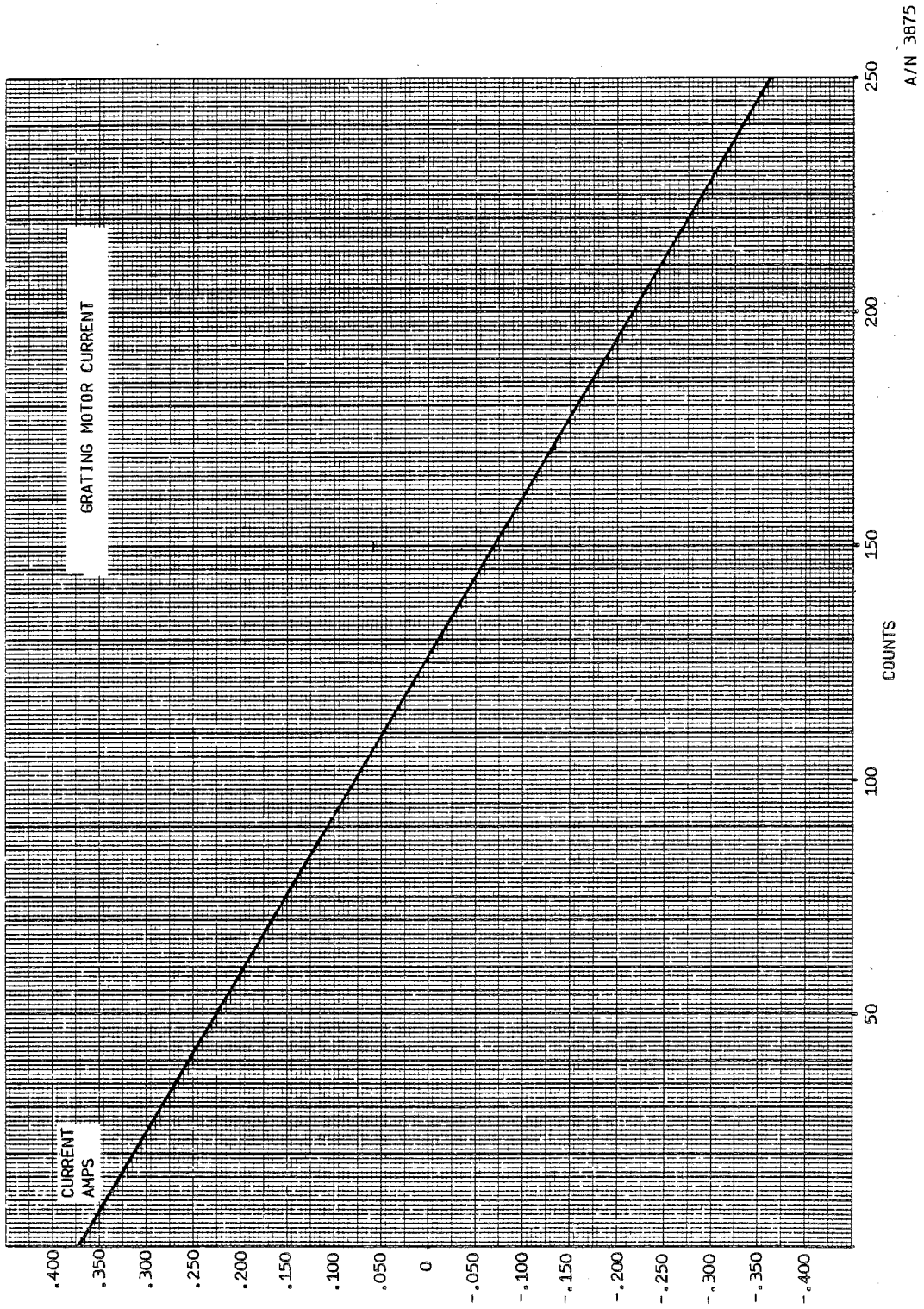


Figure 7-6 Grating Motor Current



B6802-78

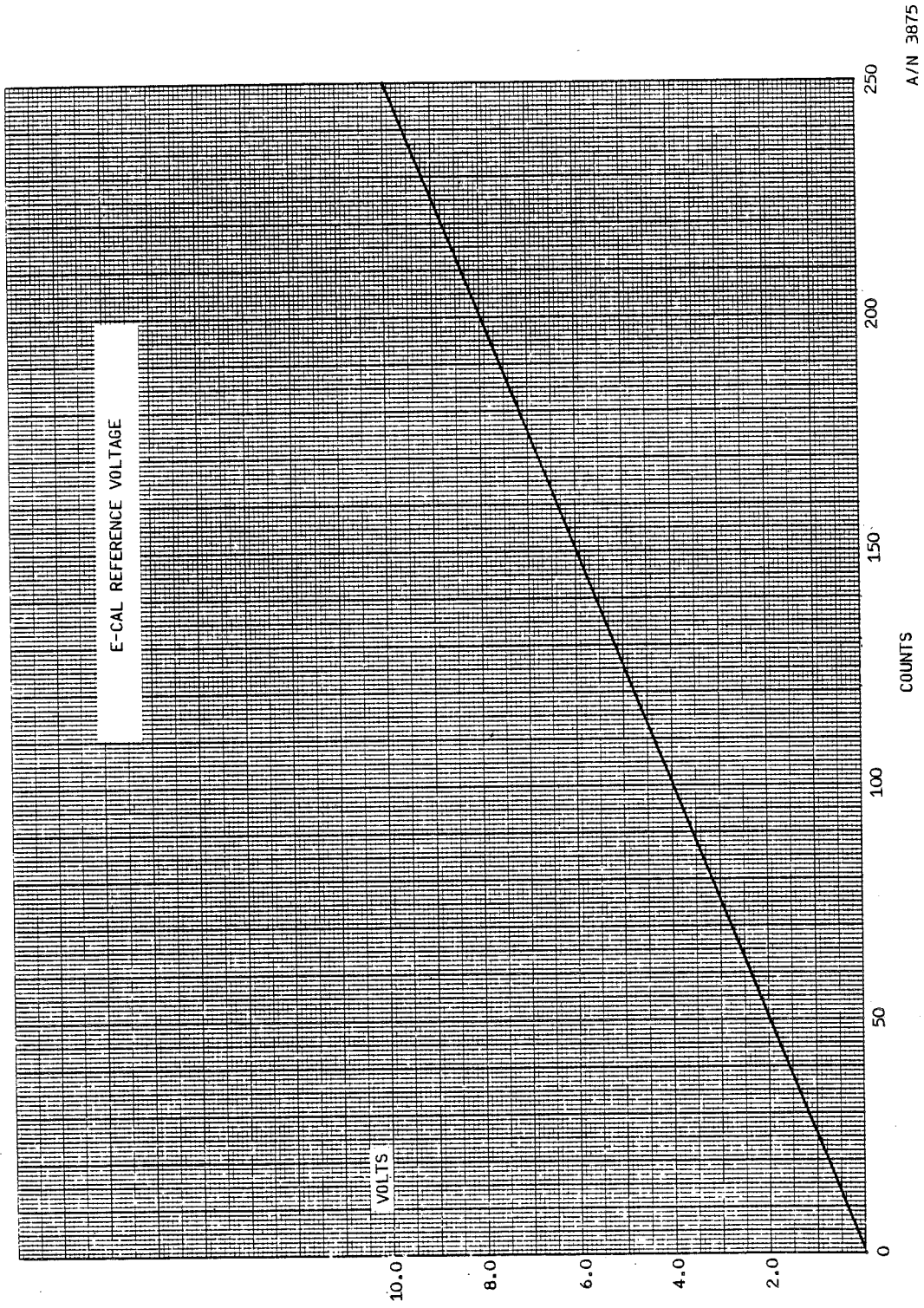


Figure 7-7 E-Cal Reference Voltage



B6802-78

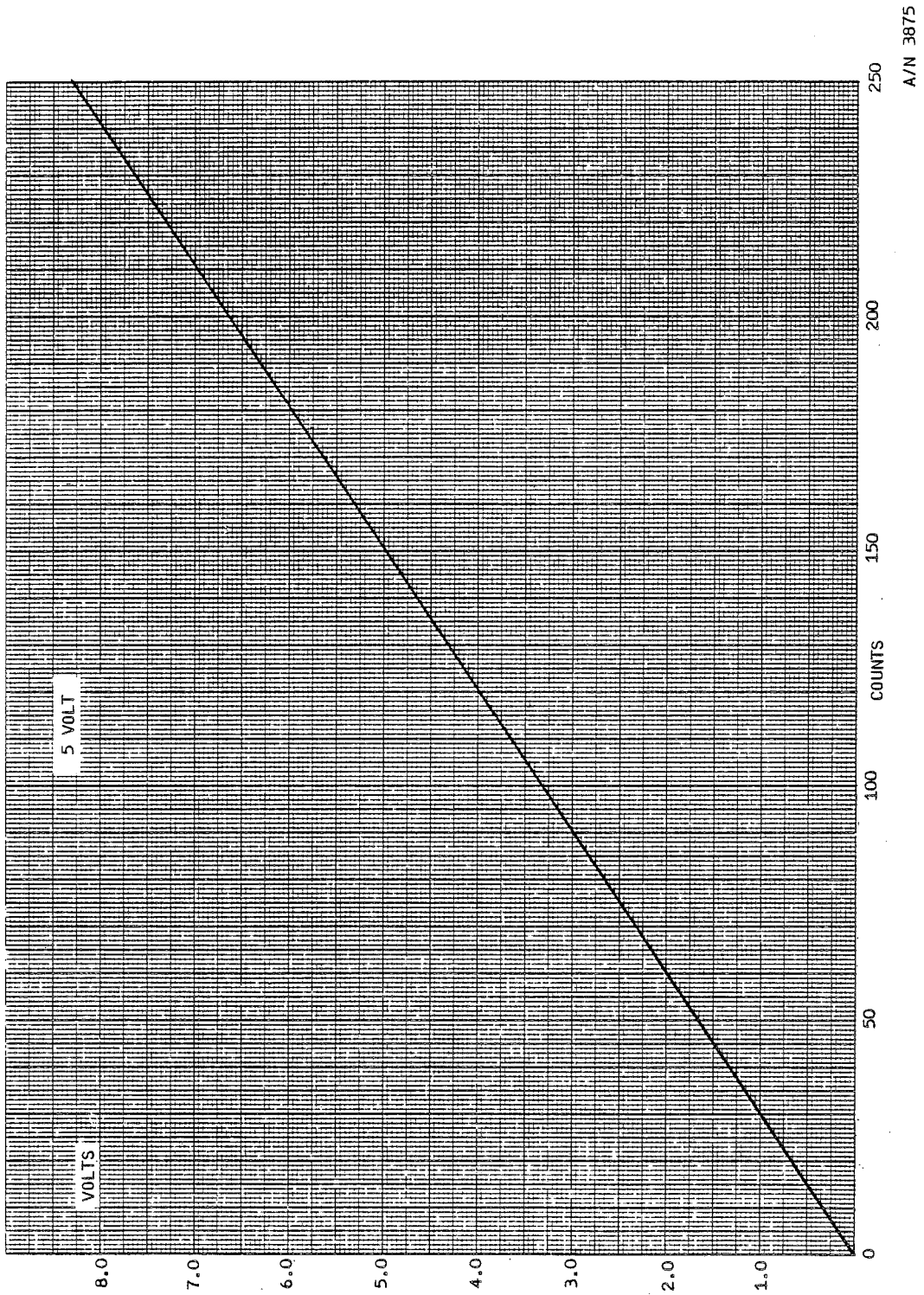
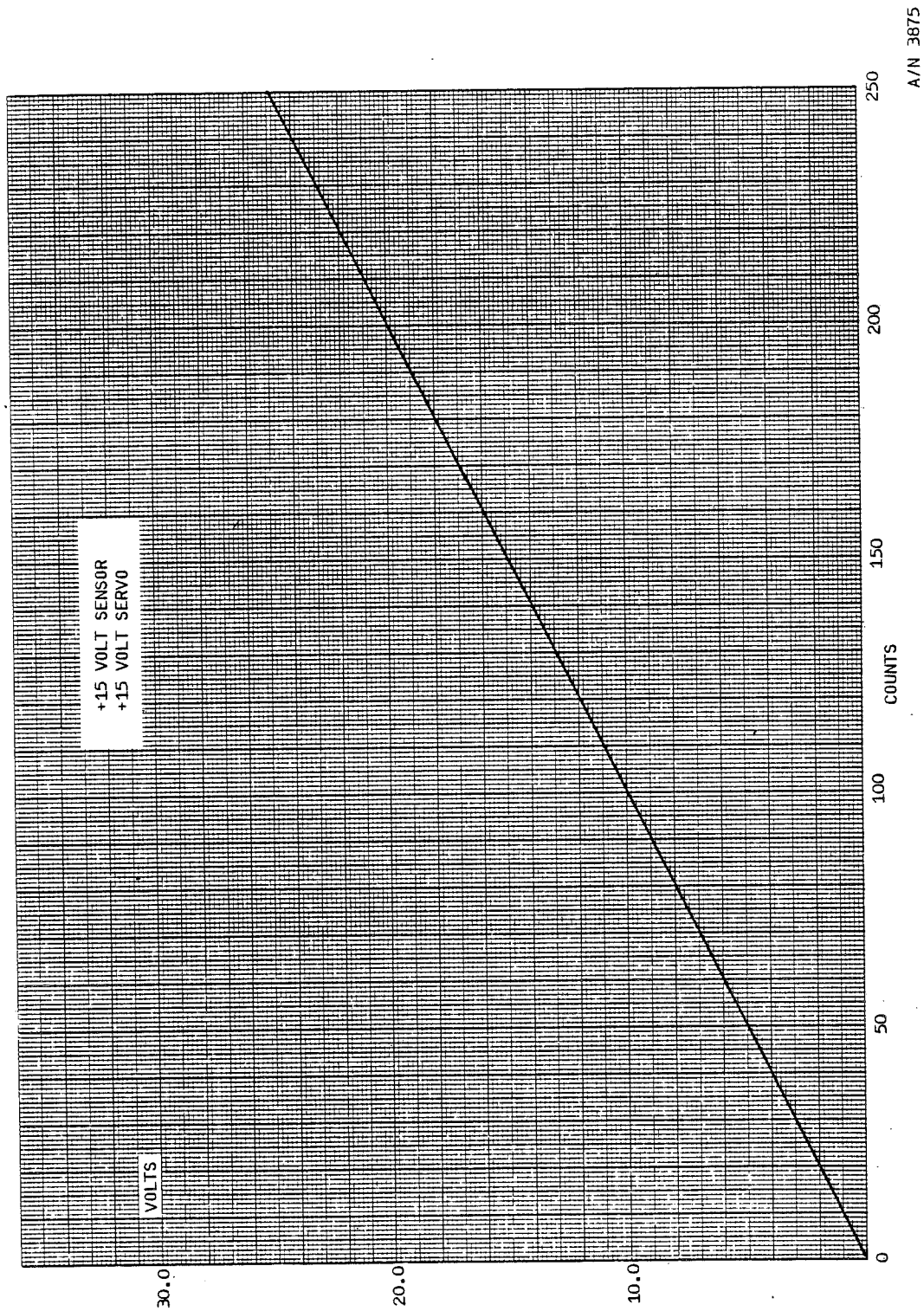


Figure 7-8 5 Volt

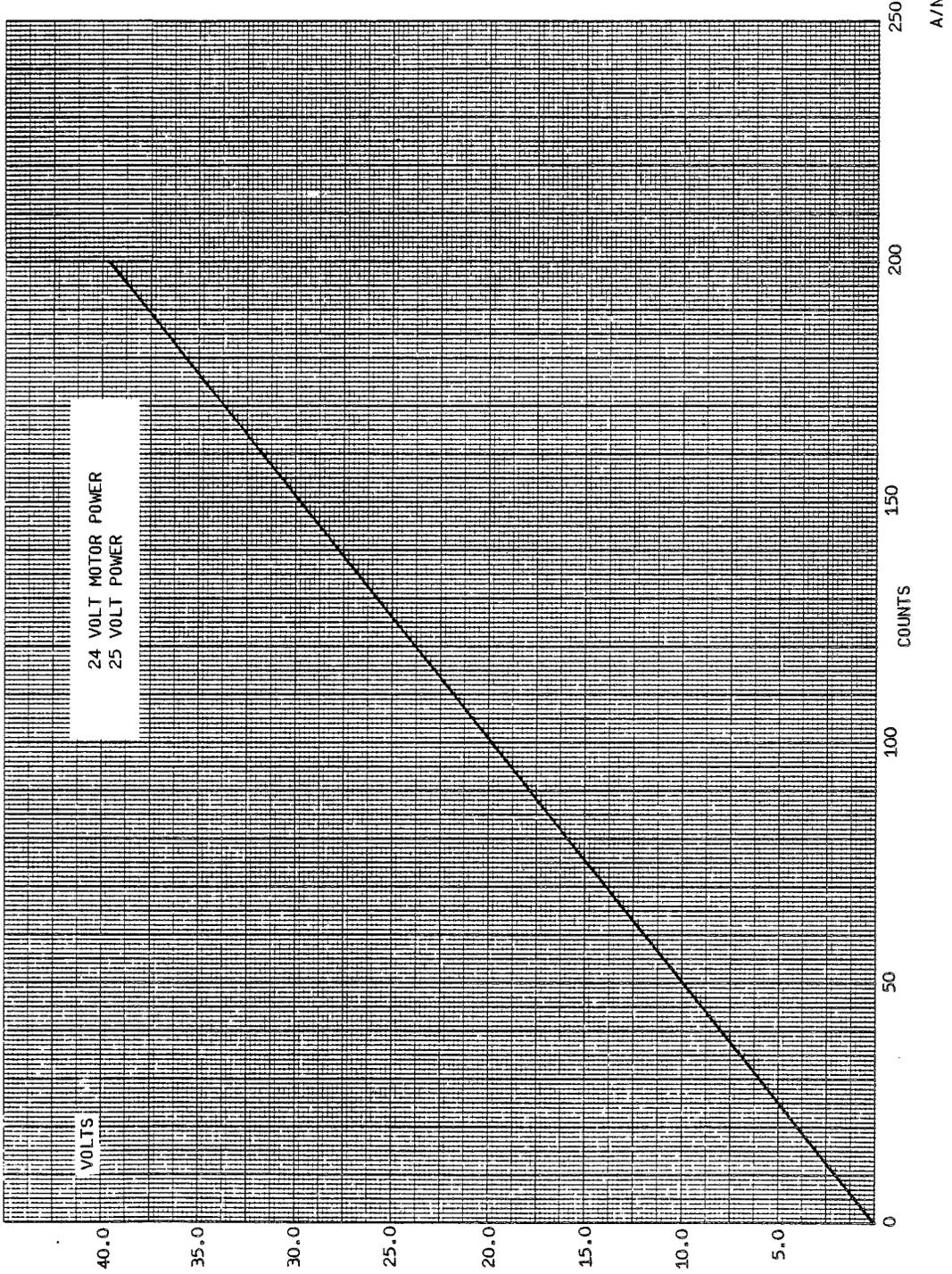


A/N 3875

Figure 7-9 +15 Volt Sensor and Servo

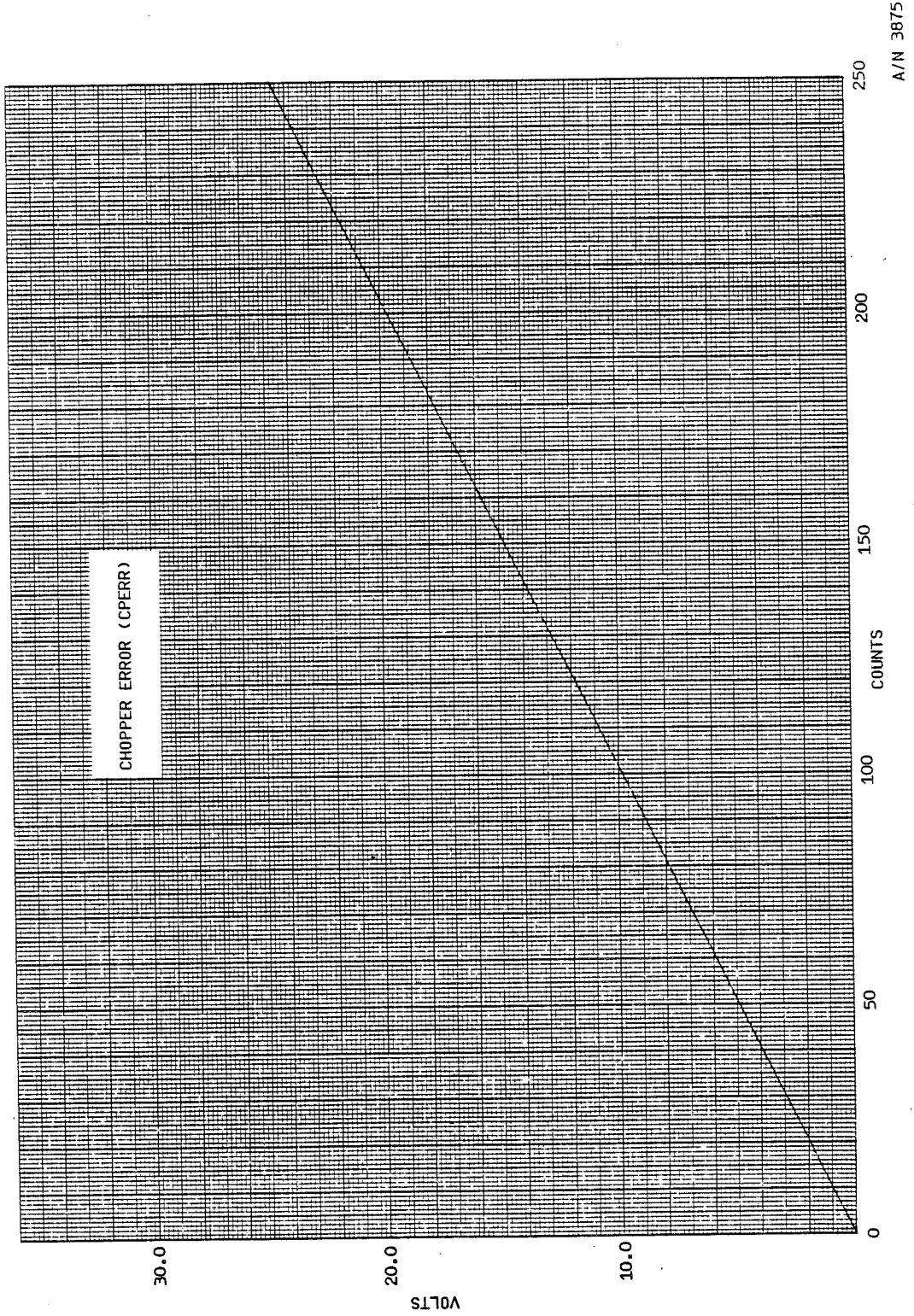


B6802-78



A/N 3875

Figure 7-10 24 Volt Motor Power and 25 Volt Power



A/N 3875

Figure 7-11 Chopper Error



B6802-78

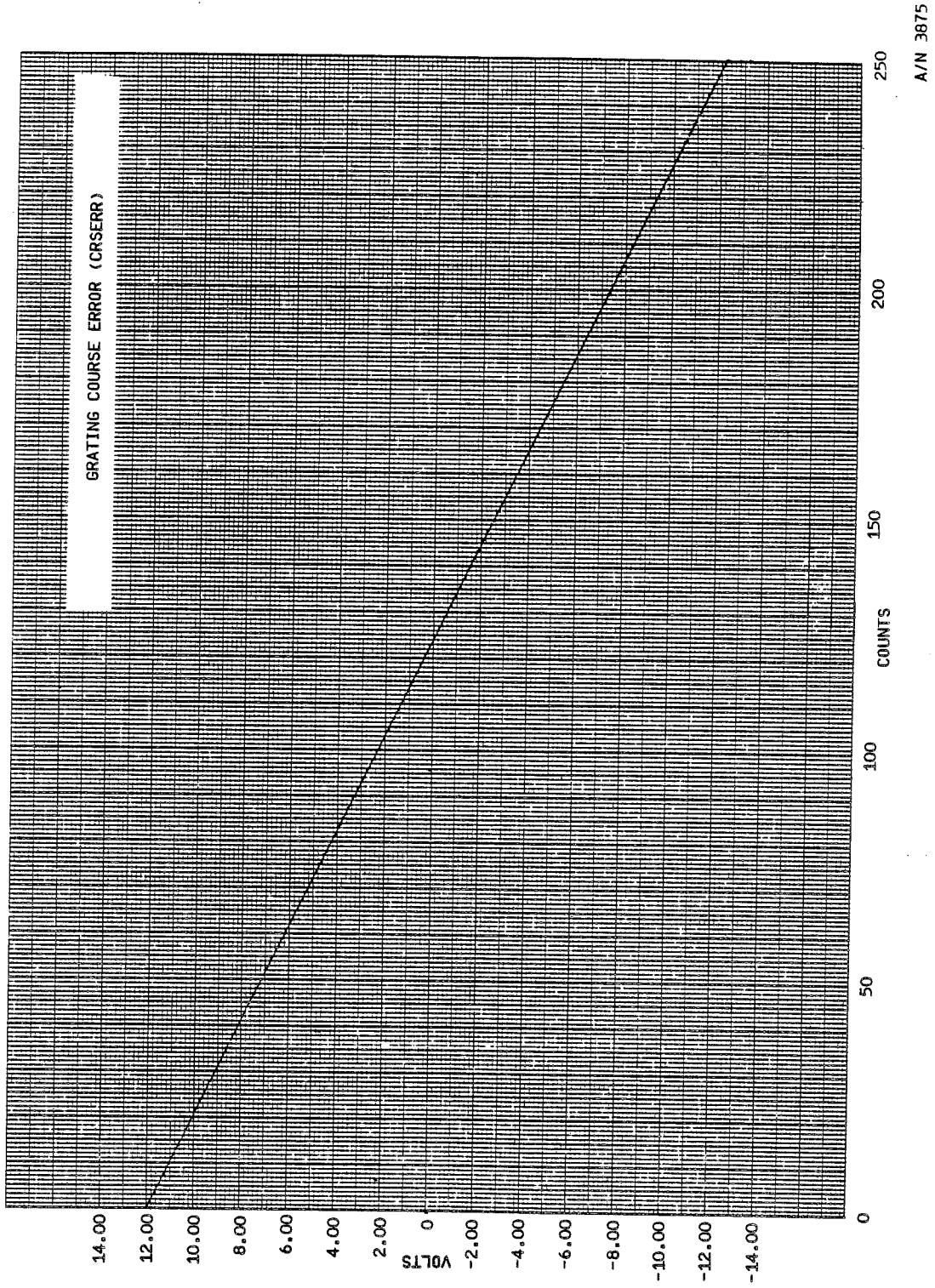


Figure 7-12 Grating Course Error

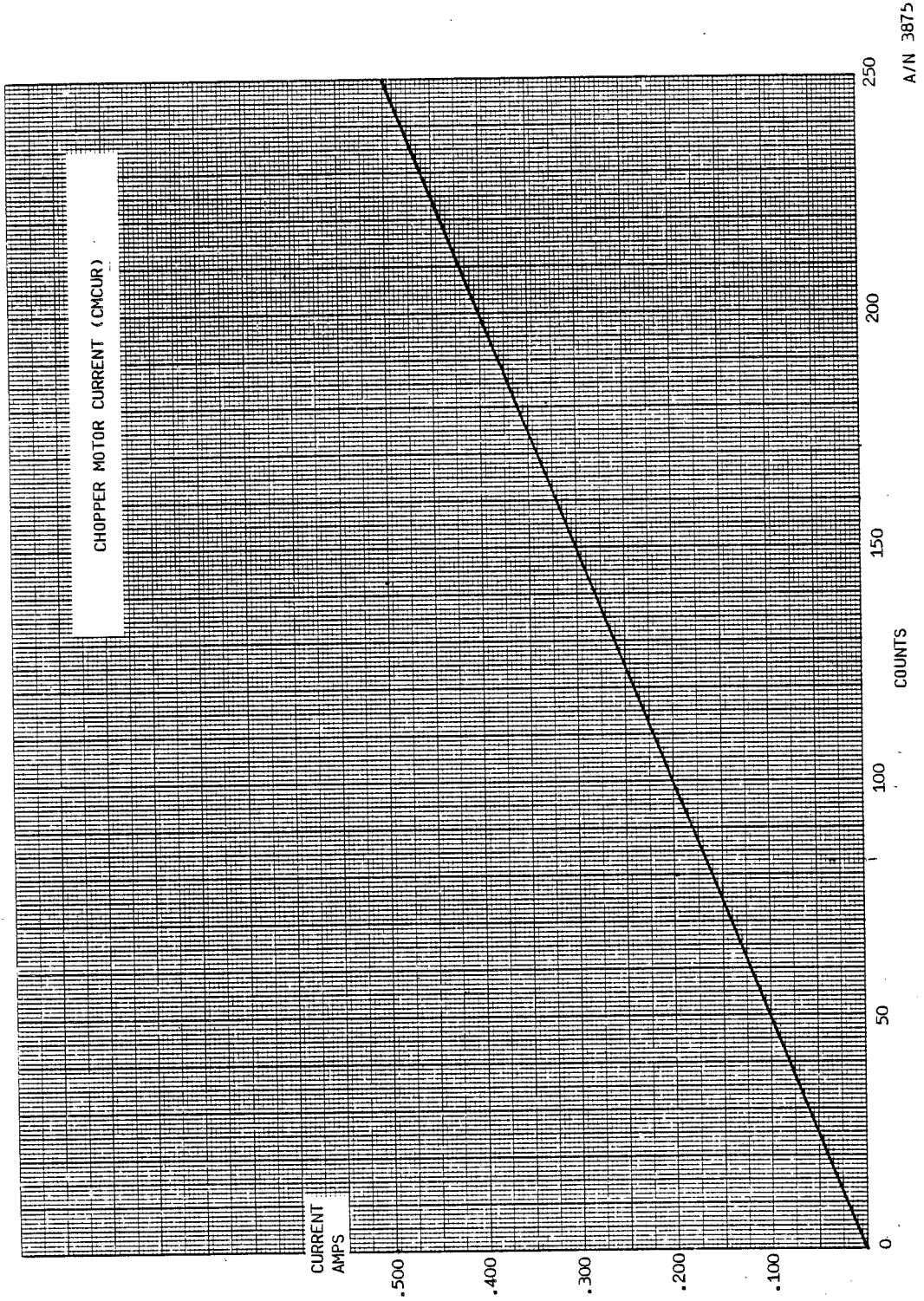


Figure 7-13 Chopper Motor Current

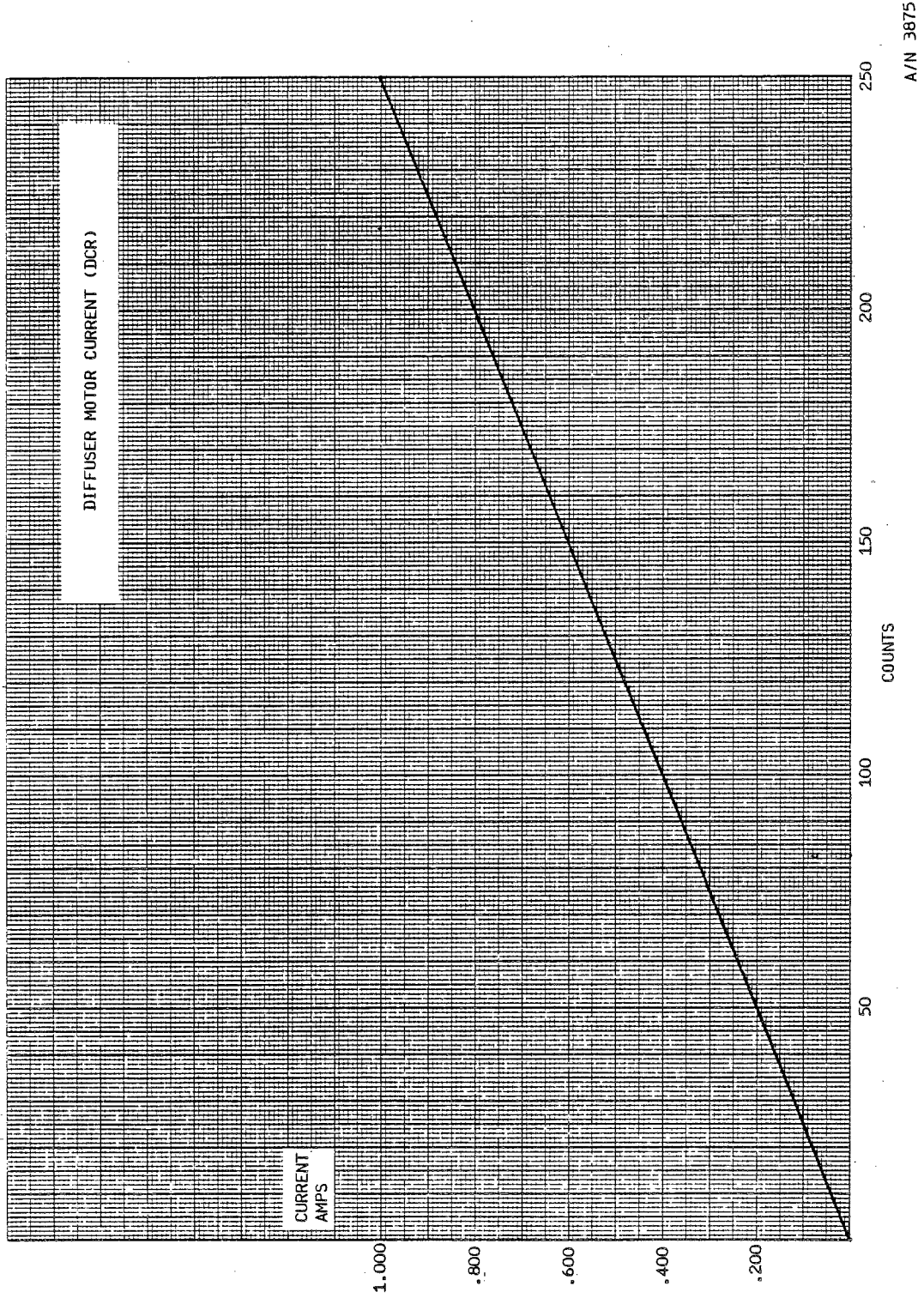


Figure 7-14 Diffuser Motor Current

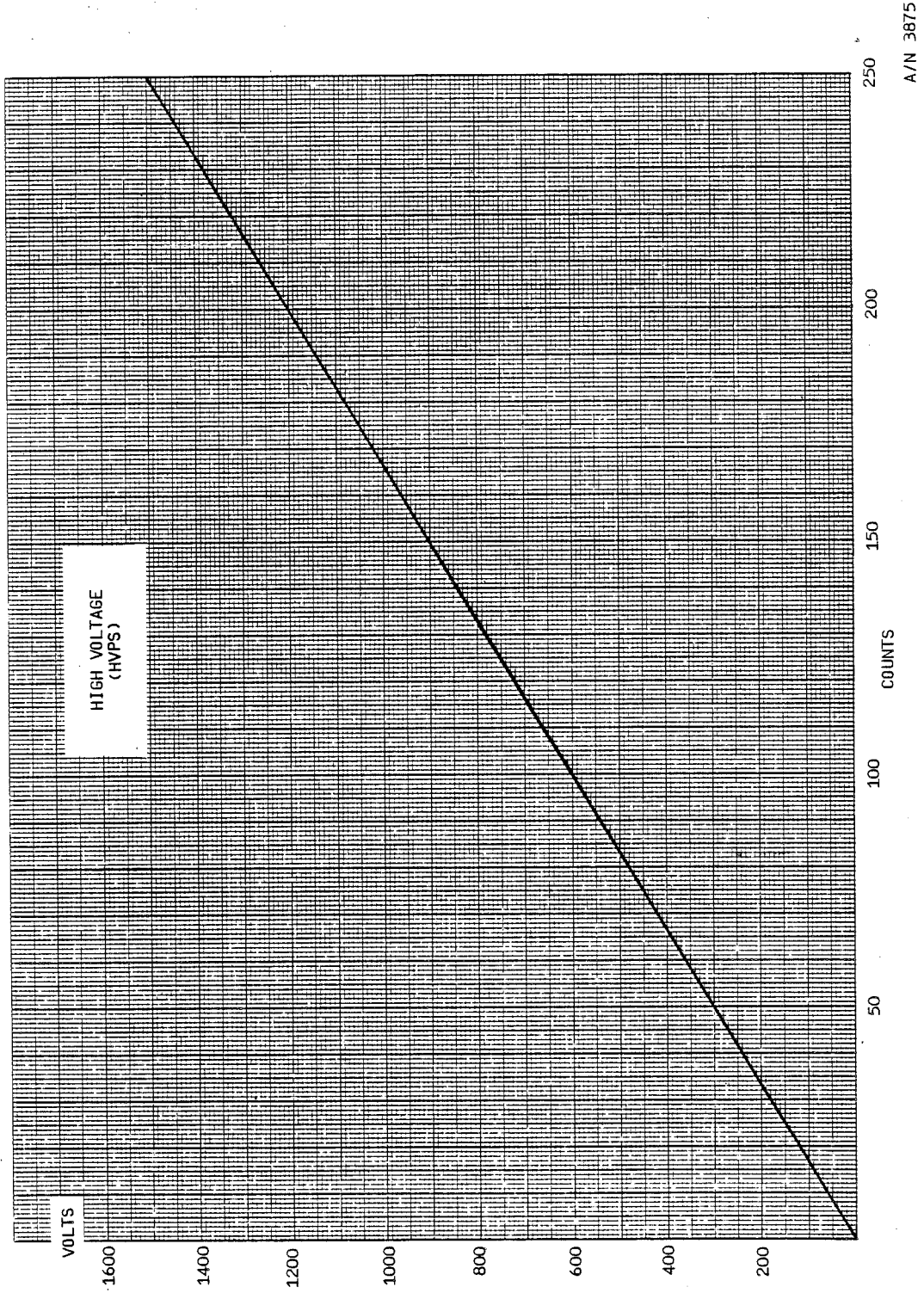
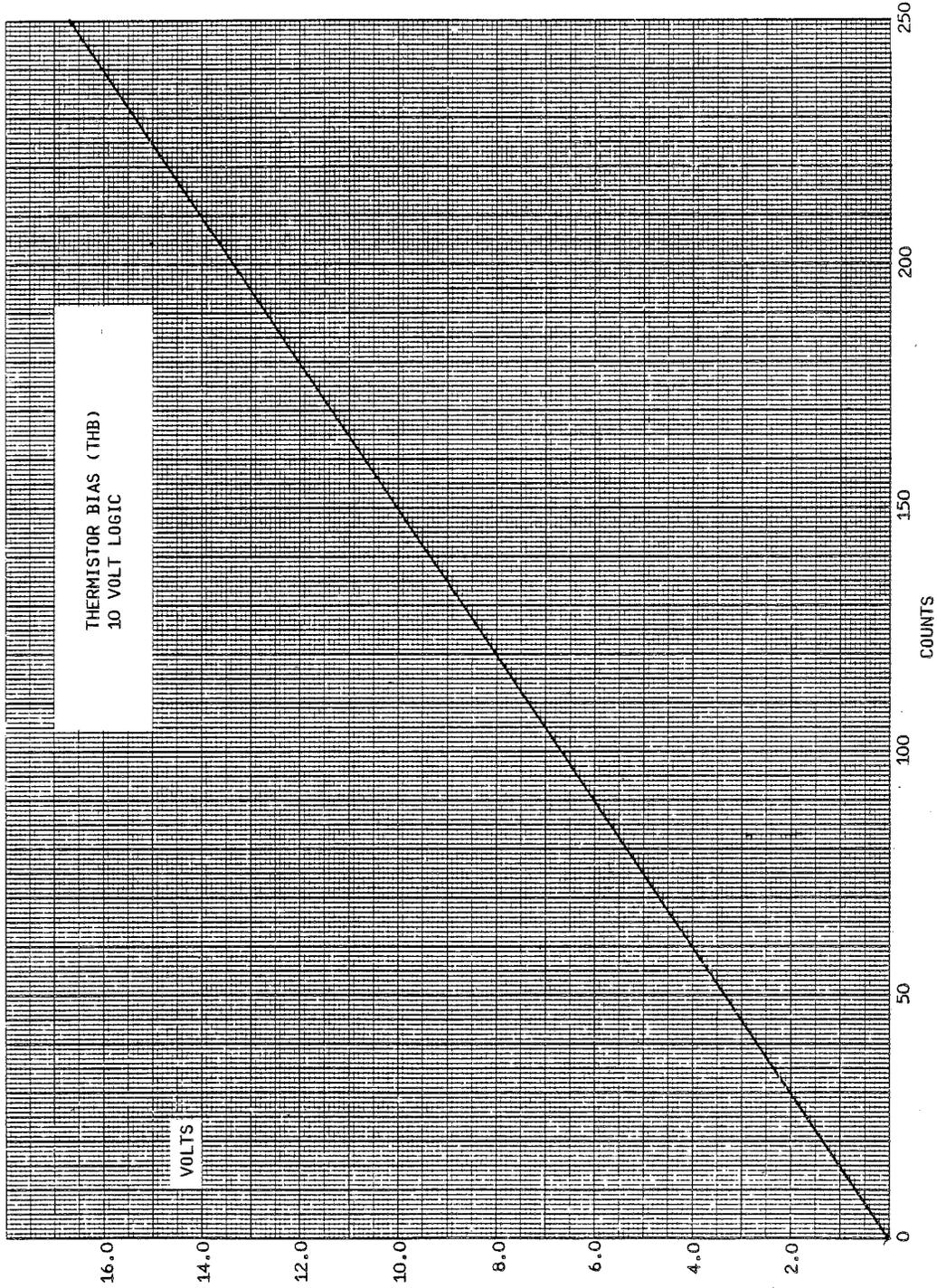
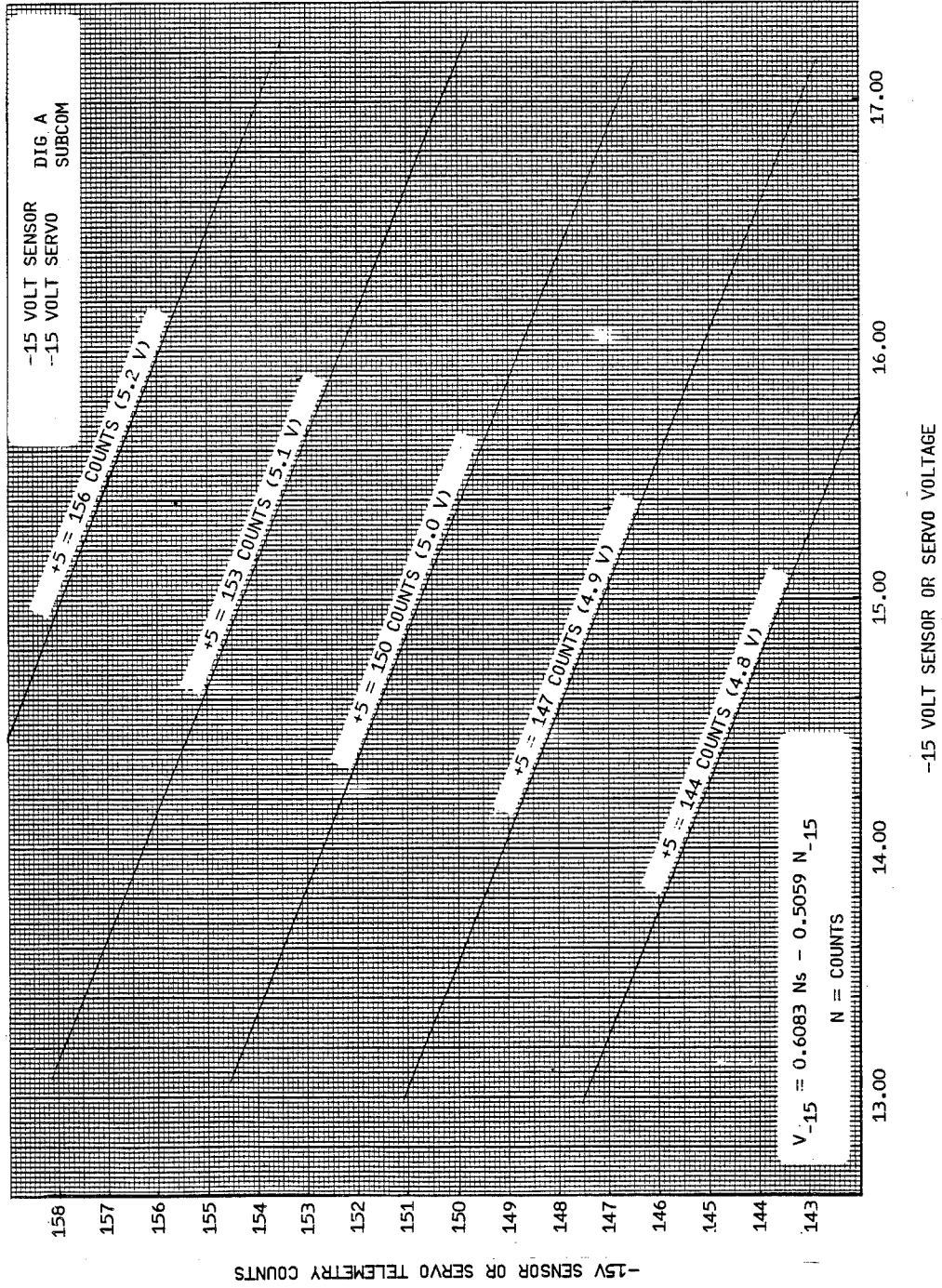


Figure 7-15 High Voltage



A/N 3875

7-16 Thermistor Bias and 10 Volt Logic



A/N 3875

Figure 7-17 -15 Volt Sensor and Servo

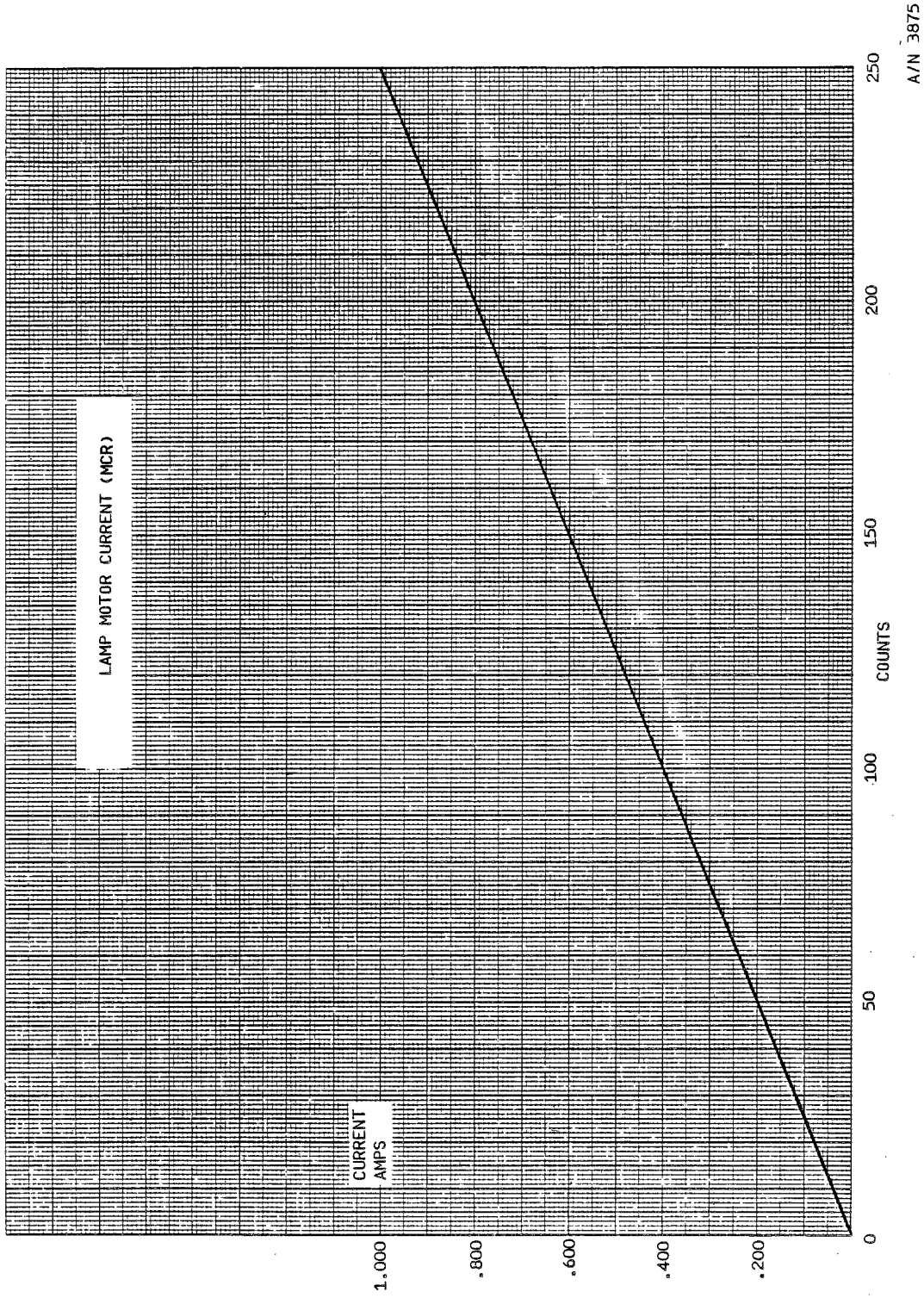


Figure 7-18 Lamp Motor Current

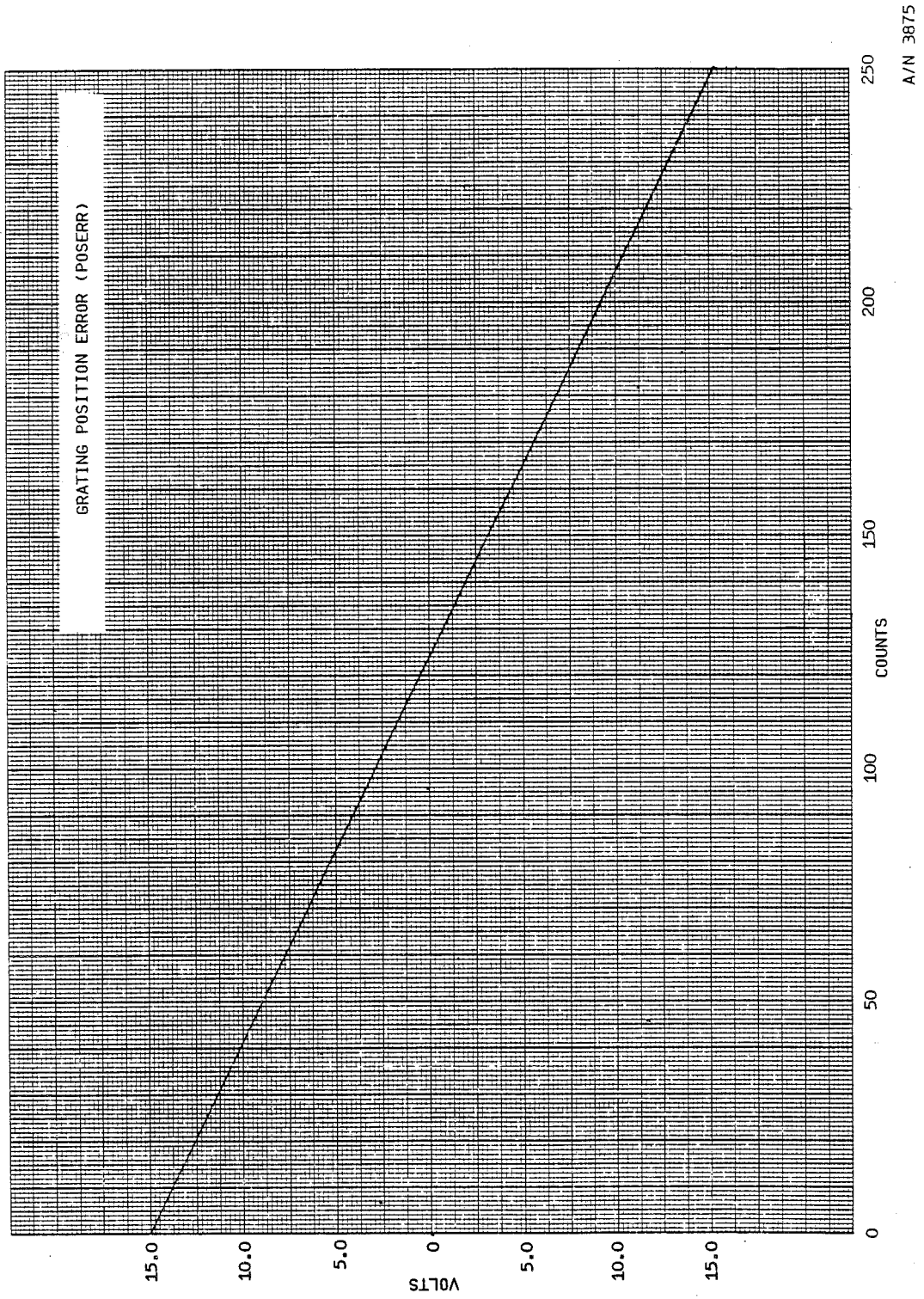
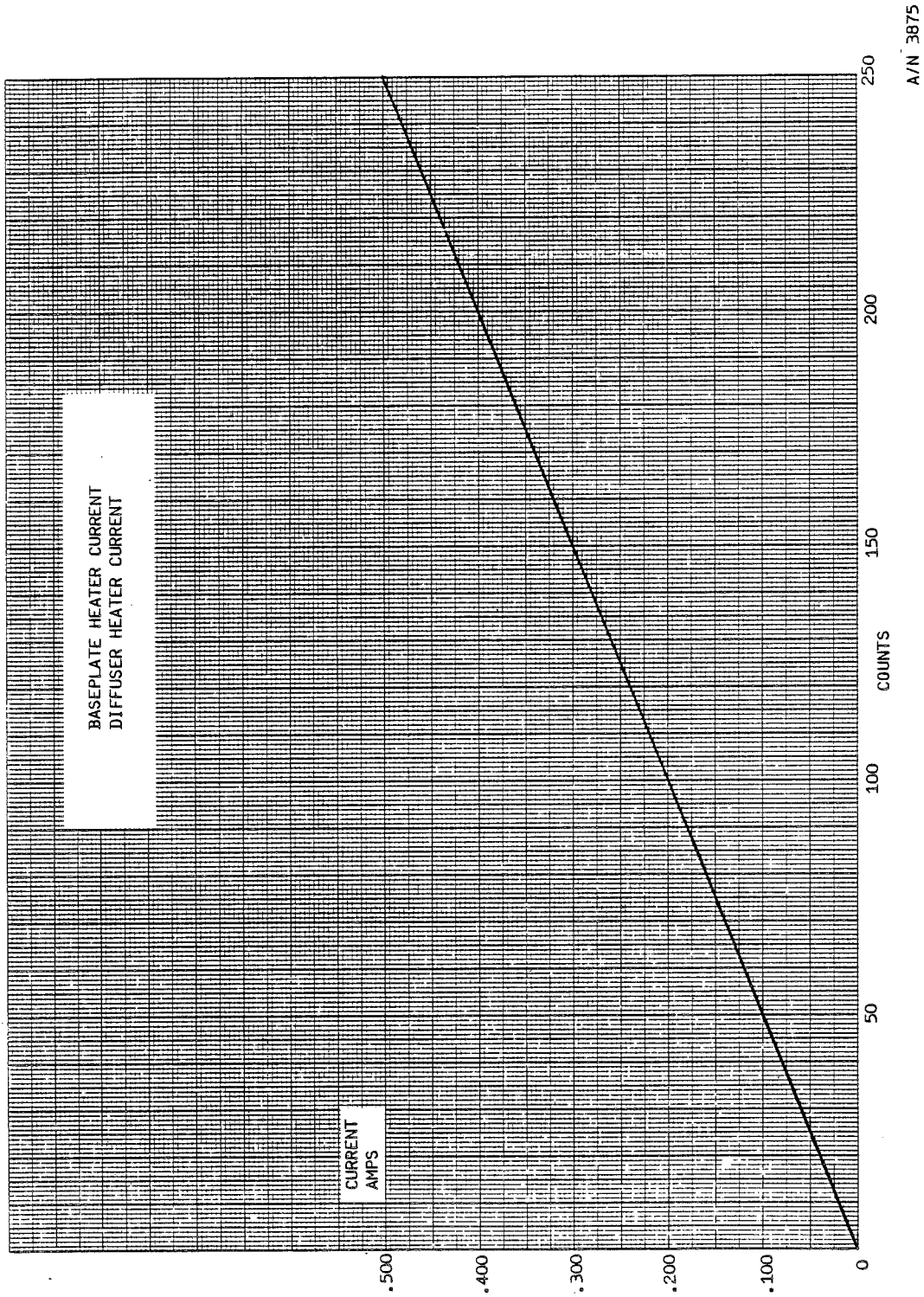


Figure 7-19 Grating Position Error



A/N 3875

Figure 7-20 Baseplate and Diffuser Heater Current

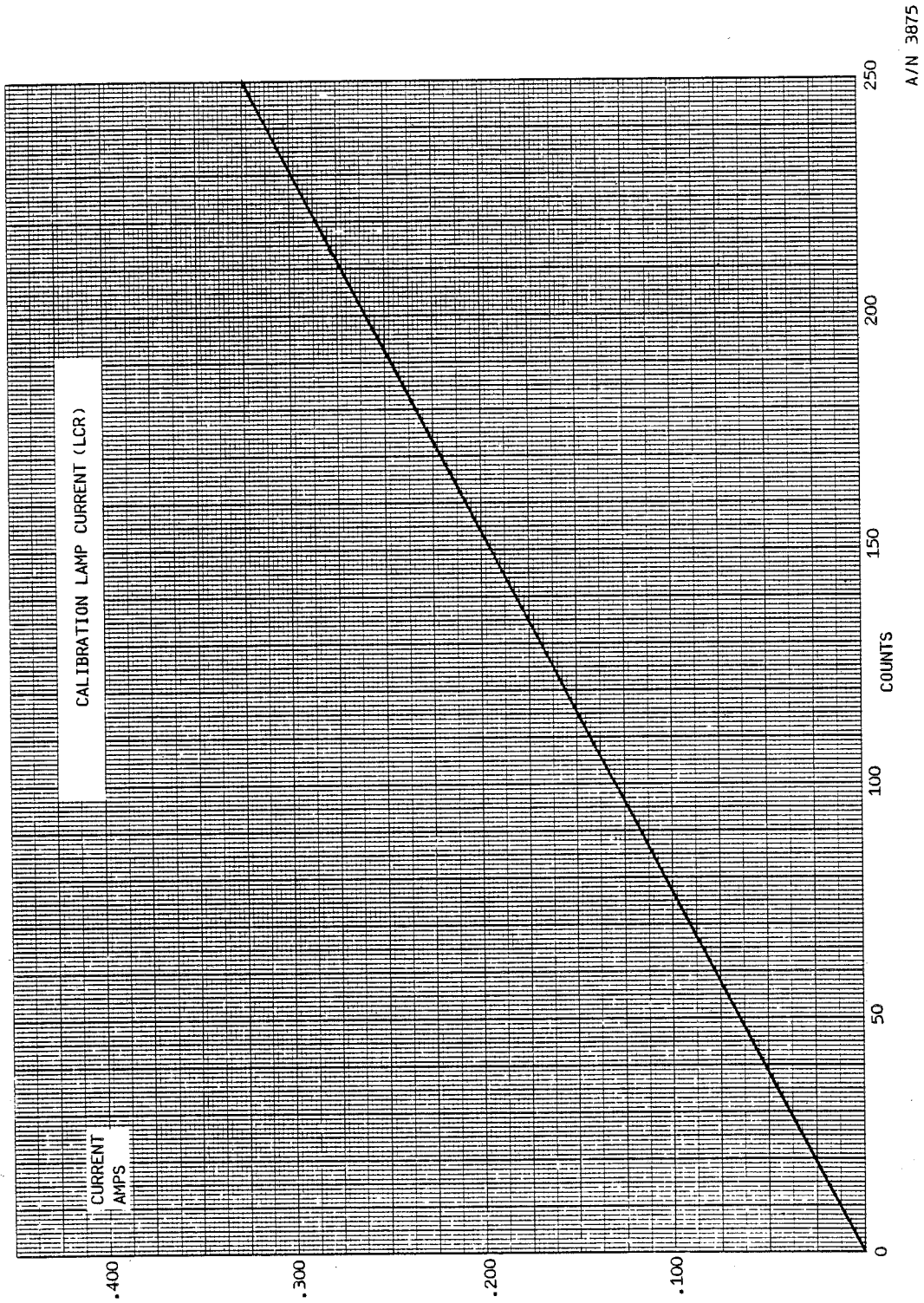


Figure 7-21 Calibration Lamp Current



Section 8

FIELD OF VIEW/UNIFORMITY
(Reference Test Procedure 68027)

Field of view measurements were made by scanning a target whose angular size is 11.33 X 1.13 degrees. Scans were made in both a horizontal (along Z axis) and vertical (along Y axis) with the target oriented perpendicular to the direction of scan.

Data was taken for each spectral band in the Discrete Mode and the Cloud Cover Radiometer.

The following pages contain

1. The method of calculation of the size of the Field of View (FWHM), the Pointing Error, and Uniformity.
2. Data sheets from the test along with the resulting calculations. (Table 8-1 through 8-7).
3. Plots of each discrete channel in both vertical and horizontal directions. (Figures 8-1 through 8-26).

Field of View Calculation

1. UNIFORMITY

$$\bar{Y} = \frac{\sum_{N=1}^{N=13} Y}{10}$$

where Y = PMT Counts
 N = Angular data position

2. FULL WIDTH HALF MAX (FWHM)

$$R = \frac{Y_{37} - Y_{40}}{0.5^{\circ}}$$

$$L = \frac{Y_{19} - Y_{16}}{0.5^{\circ}}$$

$$H_p = \frac{\bar{Y}}{2}$$

$$H_L = 5.4^{\circ} + \frac{(Y_{37} - H_p)}{L}$$

$$H_R = 5.4 + \frac{(Y_{19} - H_p)}{R}$$

$$FWHM = H_L + H_R$$

where R = Right Slope

L = Left Slope

H_p = Half Power Point

H_L = Half Max Left

H_R = Half Max Right

FWHM = Full Width Half Max

P = Pointing Error

Y_{xx} = Y Value for Point xx in Scan

3. POINTING ERROR

$$P = \frac{(H_L - H_R)}{2}$$



Table 8-2
HORIZONTAL FIELD OF VIEW SCAN RESULTS

CHANNEL	FWHM (DEGREES)	HORIZONTAL FIELD-OF-VIEW SCAN UNIFORMITY (%)	POINTING ERROR (DEGREES)
1	1103E+02	5007E-01	1408E+00
2	1101E+02	4592E-01	1184E+00
3	1101E+02	6158E-01	1370E+00
4	1101E+02	6914E-01	1417E+00
5	1101E+02	6740E-01	1507E+00
6	1101E+02	7104E-01	1610E+00
7	1102E+02	6873E-01	1665E+00
8	1102E+02	7155E-01	1726E+00
9	1102E+02	7235E-01	1773E+00
10	1103E+02	5827E-01	1833E+00
11	1103E+02	7261E-01	1512E+00
12	1103E+02	4032E-01	9225E-01
CCR	1110E+02	2289E-01	-3073E-01

A/N 3875



Table 8-3
VERTICAL FIELD OF VIEW SCAN

OPERATOR ID: GEM

TAPE NO: F027

TIME OF TEST: 1983:108/13/26/21

TEST: FIELD-OF-VIEW

VERTICAL FIELD-OF-VIEW SCAN

ANGLE	CHAN 1	CHAN 2	CHAN 3	CHAN 4	CHAN 5	CHAN 6	CHAN 7	CHAN 8	CHAN 9	CHAN 10	CHAN 11	CHAN 12	CCR
7300	439E-13	239E-13	549E-13	849E-13	1349E-13	1849E-13	2349E-13	2849E-13	3349E-13	3849E-13	4349E-13	4849E-13	000E+00
7400	1059E-13	305E-13	605E-13	905E-13	1405E-13	1905E-13	2405E-13	2905E-13	3405E-13	3905E-13	4405E-13	4905E-13	000E+00
7500	1819E-13	381E-13	681E-13	981E-13	1481E-13	1981E-13	2481E-13	2981E-13	3481E-13	3981E-13	4481E-13	4981E-13	000E+00
7600	2579E-13	457E-13	757E-13	1057E-13	1557E-13	2057E-13	2557E-13	3057E-13	3557E-13	4057E-13	4557E-13	5057E-13	000E+00
7700	3339E-13	533E-13	833E-13	1133E-13	1633E-13	2133E-13	2633E-13	3133E-13	3633E-13	4133E-13	4633E-13	5133E-13	000E+00
7800	4099E-13	609E-13	909E-13	1209E-13	1709E-13	2209E-13	2709E-13	3209E-13	3709E-13	4209E-13	4709E-13	5209E-13	000E+00
7900	4859E-13	685E-13	985E-13	1285E-13	1785E-13	2285E-13	2785E-13	3285E-13	3785E-13	4285E-13	4785E-13	5285E-13	000E+00
8000	5619E-13	761E-13	1061E-13	1361E-13	1861E-13	2361E-13	2861E-13	3361E-13	3861E-13	4361E-13	4861E-13	5361E-13	000E+00
8100	6379E-13	837E-13	1137E-13	1437E-13	1937E-13	2437E-13	2937E-13	3437E-13	3937E-13	4437E-13	4937E-13	5437E-13	000E+00
8200	7139E-13	913E-13	1213E-13	1513E-13	2013E-13	2513E-13	3013E-13	3513E-13	4013E-13	4513E-13	5013E-13	5513E-13	000E+00
8300	7899E-13	989E-13	1289E-13	1589E-13	2089E-13	2589E-13	3089E-13	3589E-13	4089E-13	4589E-13	5089E-13	5589E-13	000E+00
83225	8659E-13	1065E-13	1365E-13	1665E-13	2165E-13	2665E-13	3165E-13	3665E-13	4165E-13	4665E-13	5165E-13	5665E-13	000E+00
83390	9419E-13	1141E-13	1441E-13	1741E-13	2241E-13	2741E-13	3241E-13	3741E-13	4241E-13	4741E-13	5241E-13	5741E-13	000E+00
84110	10179E-13	1217E-13	1517E-13	1817E-13	2317E-13	2817E-13	3317E-13	3817E-13	4317E-13	4817E-13	5317E-13	5817E-13	000E+00
84440	10939E-13	1293E-13	1593E-13	1893E-13	2393E-13	2893E-13	3393E-13	3893E-13	4393E-13	4893E-13	5393E-13	5893E-13	000E+00
84770	11699E-13	1369E-13	1669E-13	1969E-13	2469E-13	2969E-13	3469E-13	3969E-13	4469E-13	4969E-13	5469E-13	5969E-13	000E+00
85500	12459E-13	1445E-13	1745E-13	2045E-13	2545E-13	3045E-13	3545E-13	4045E-13	4545E-13	5045E-13	5545E-13	6045E-13	000E+00
86250	13219E-13	1521E-13	1821E-13	2121E-13	2621E-13	3121E-13	3621E-13	4121E-13	4621E-13	5121E-13	5621E-13	6121E-13	000E+00
87000	13979E-13	1607E-13	1907E-13	2207E-13	2707E-13	3207E-13	3707E-13	4207E-13	4707E-13	5207E-13	5707E-13	6207E-13	000E+00
88000	14739E-13	1683E-13	1983E-13	2283E-13	2783E-13	3283E-13	3783E-13	4283E-13	4783E-13	5283E-13	5783E-13	6283E-13	000E+00
89000	15499E-13	1759E-13	2059E-13	2359E-13	2859E-13	3359E-13	3859E-13	4359E-13	4859E-13	5359E-13	5859E-13	6359E-13	000E+00
90000	16259E-13	1835E-13	2135E-13	2435E-13	2935E-13	3435E-13	3935E-13	4435E-13	4935E-13	5435E-13	5935E-13	6435E-13	000E+00
91000	17019E-13	1911E-13	2211E-13	2511E-13	3011E-13	3511E-13	4011E-13	4511E-13	5011E-13	5511E-13	6011E-13	6511E-13	000E+00
92000	17779E-13	1987E-13	2287E-13	2587E-13	3087E-13	3587E-13	4087E-13	4587E-13	5087E-13	5587E-13	6087E-13	6587E-13	000E+00
93000	18539E-13	2063E-13	2363E-13	2663E-13	3163E-13	3663E-13	4163E-13	4663E-13	5163E-13	5663E-13	6163E-13	6663E-13	000E+00
94500	19299E-13	2139E-13	2439E-13	2739E-13	3239E-13	3739E-13	4239E-13	4739E-13	5239E-13	5739E-13	6239E-13	6739E-13	000E+00
95500	20059E-13	2215E-13	2515E-13	2815E-13	3315E-13	3815E-13	4315E-13	4815E-13	5315E-13	5815E-13	6315E-13	6815E-13	000E+00
96500	20819E-13	2291E-13	2591E-13	2891E-13	3391E-13	3891E-13	4391E-13	4891E-13	5391E-13	5891E-13	6391E-13	6891E-13	000E+00
97000	21579E-13	2367E-13	2667E-13	2967E-13	3467E-13	3967E-13	4467E-13	4967E-13	5467E-13	5967E-13	6467E-13	6967E-13	000E+00
97500	22339E-13	2443E-13	2743E-13	3043E-13	3543E-13	4043E-13	4543E-13	5043E-13	5543E-13	6043E-13	6543E-13	7043E-13	000E+00
98000	23099E-13	2519E-13	2819E-13	3119E-13	3619E-13	4119E-13	4619E-13	5119E-13	5619E-13	6119E-13	6619E-13	7119E-13	000E+00
99000	23859E-13	2595E-13	2895E-13	3195E-13	3695E-13	4195E-13	4695E-13	5195E-13	5695E-13	6195E-13	6695E-13	7195E-13	000E+00
100000	24619E-13	2671E-13	2971E-13	3271E-13	3771E-13	4271E-13	4771E-13	5271E-13	5771E-13	6271E-13	6771E-13	7271E-13	000E+00
101000	25379E-13	2747E-13	3047E-13	3347E-13	3847E-13	4347E-13	4847E-13	5347E-13	5847E-13	6347E-13	6847E-13	7347E-13	000E+00
102000	26139E-13	2823E-13	3123E-13	3423E-13	3923E-13	4423E-13	4923E-13	5423E-13	5923E-13	6423E-13	6923E-13	7423E-13	000E+00
103000	26899E-13	2899E-13	3199E-13	3499E-13	3999E-13	4499E-13	4999E-13	5499E-13	5999E-13	6499E-13	6999E-13	7499E-13	000E+00
104000	27659E-13	2975E-13	3275E-13	3575E-13	4075E-13	4575E-13	5075E-13	5575E-13	6075E-13	6575E-13	7075E-13	7575E-13	000E+00
105000	28419E-13	3051E-13	3351E-13	3651E-13	4151E-13	4651E-13	5151E-13	5651E-13	6151E-13	6651E-13	7151E-13	7651E-13	000E+00
106000	29179E-13	3127E-13	3427E-13	3727E-13	4227E-13	4727E-13	5227E-13	5727E-13	6227E-13	6727E-13	7227E-13	7727E-13	000E+00
107000	29939E-13	3203E-13	3503E-13	3803E-13	4303E-13	4803E-13	5303E-13	5803E-13	6303E-13	6803E-13	7303E-13	7803E-13	000E+00
108000	30699E-13	3279E-13	3579E-13	3879E-13	4379E-13	4879E-13	5379E-13	5879E-13	6379E-13	6879E-13	7379E-13	7879E-13	000E+00
109000	31459E-13	3355E-13	3655E-13	3955E-13	4455E-13	4955E-13	5455E-13	5955E-13	6455E-13	6955E-13	7455E-13	7955E-13	000E+00
110000	32219E-13	3431E-13	3731E-13	4031E-13	4531E-13	5031E-13	5531E-13	6031E-13	6531E-13	7031E-13	7531E-13	8031E-13	000E+00
111000	32979E-13	3507E-13	3807E-13	4107E-13	4607E-13	5107E-13	5607E-13	6107E-13	6607E-13	7107E-13	7607E-13	8107E-13	000E+00
112000	33739E-13	3583E-13	3883E-13	4183E-13	4683E-13	5183E-13	5683E-13	6183E-13	6683E-13	7183E-13	7683E-13	8183E-13	000E+00
113000	34499E-13	3659E-13	3959E-13	4259E-13	4759E-13	5259E-13	5759E-13	6259E-13	6759E-13	7259E-13	7759E-13	8259E-13	000E+00
114000	35259E-13	3735E-13	4035E-13	4335E-13	4835E-13	5335E-13	5835E-13	6335E-13	6835E-13	7335E-13	7835E-13	8335E-13	000E+00
115000	36019E-13	3811E-13	4111E-13	4411E-13	4911E-13	5411E-13	5911E-13	6411E-13	6911E-13	7411E-13	7911E-13	8411E-13	000E+00
116000	36779E-13	3887E-13	4187E-13	4487E-13	4987E-13	5487E-13	5987E-13	6487E-13	6987E-13	7487E-13	7987E-13	8487E-13	000E+00
117000	37539E-13	3963E-13	4263E-13	4563E-13	5063E-13	5563E-13	6063E-13	6563E-13	7063E-13	7563E-13	8063E-13	8563E-13	000E+00
118000	38299E-13	4039E-13	4339E-13	4639E-13	5139E-13	5639E-13	6139E-13	6639E-13	7139E-13	7639E-13	8139E-13	8639E-13	000E+00
119000	39059E-13	4115E-13	4415E-13	4715E-13	5215E-13	5715E-13	6215E-13	6715E-13	7215E-13	7715E-13	8215E-13	8715E-13	000E+00
120000	39819E-13	4191E-13	4491E-13	4791E-13	5291E-13	5791E-13	6291E-13	6791E-13	7291E-13	7791E-13	8291E-13	8791E-13	000E+00

A/N 3875



Table 8-4
VERTICAL FIELD OF VIEW SCAN RESULTS

CHANNEL	FWHM (DEGREES)	VERTICAL FIELD-OF-VIEW SCAN		POINTING ERROR (DEGREES)
		UNIFORMITY (%)		
1	1107E+02	6832E-01	1600E+00	2187E+00
2	1107E+02	6499E-01	1631E+00	2087E+00
3	1106E+02	5935E-01	1538E+00	2393E+00
4	1106E+02	6148E-01	1700E+00	2379E+00
5	1106E+02	6131E-01	1725E+00	2433E+00
6	1105E+02	6718E-01	1472E+00	2332E+00
7	1105E+02	6703E-01	1468E+00	2390E+00
8	1105E+02	6501E-01	1449E+00	2518E+00
9	1104E+02	6629E-01	1495E+00	2538E+00
10	1103E+02	5845E-01	1602E+00	2700E+00
11	1103E+02	5652E-01	1746E+00	2374E+00
12	1113E+02	2608E-01	9955E-01	2355E+00
CLR				1618E+00

A/N 3875



Table 8-5
HORIZONTAL FIELD OF VIEW

Wavelength in Nanometers	FWHM Degrees Limit: 11.33 +.57	Uniformity Limits $\pm 10\%$ *		Pointing Error Degrees Limit: 0.10
		% POSITIVE	% NEGATIVE	
252.00	11.03	5.007	11.35	.1408
273.61	11.01	4.592	10.42	.1184
283.10	11.01	6.158	12.93	.1370
287.70	11.01	6.514	13.65	.1417
292.29	11.01	6.740	14.51	.1507
297.59	11.01	7.104	15.06	.1610
301.97	11.02	6.873	15.57	.1665
305.87	11.02	7.155	15.69	.1726
312.57	11.02	7.235	16.22	.1773
317.56	11.03	7.261	16.45	.1833
331.26	11.03	5.827	12.70	.1512
339.89	11.03	4.032	7.368	0.09226
CCR	11.10	2.289	4.801	-0.0307

A/N 3875

*CCR LIMITS $\pm 5\%$



Table 8-6
VERTICAL FIELD OF VIEW

Wavelength in Nanometers	FWHM Degrees Limit: 11.33 ± .57	Uniformity Limits ±10% *		Pointing Error Degrees LIMIT: 0.10
		% POSITIVE	% NEGATIVE	
252.00	11.07	6.832	16.00	-.2187
273.61	11.07	6.499	16.31	-.2087
283.10	11.07	5.935	15.38	-.2303
287.70	11.06	6.146	15.00	-.2379
292.29	11.06	6.168	14.72	-.2453
297.59	11.06	6.131	14.79	-.2552
301.97	11.05	6.458	14.72	-.2590
305.87	11.05	6.403	14.66	-.2618
312.57	11.05	6.601	14.49	-.2658
317.56	11.04	6.629	14.55	-.2700
331.26	11.05	5.845	16.02	-.2574
339.89	11.03	5.652	17.46	-.2255
CCR	11.03	2.608	5.955	+.1618

A/N 3875

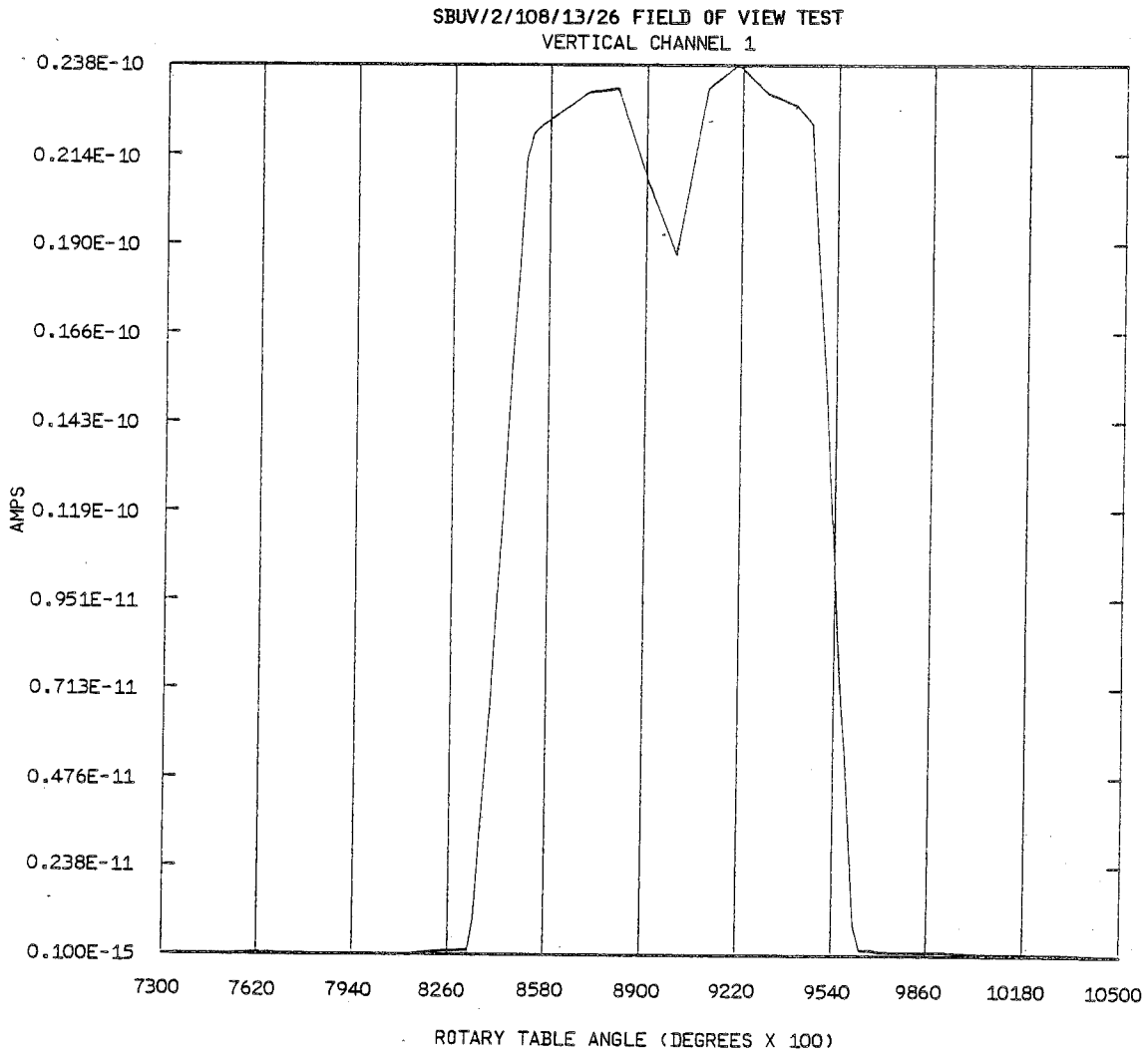
* CCR LIMITS ±5%



Table 8-7
INSTANTANEOUS FIELD OF VIEW

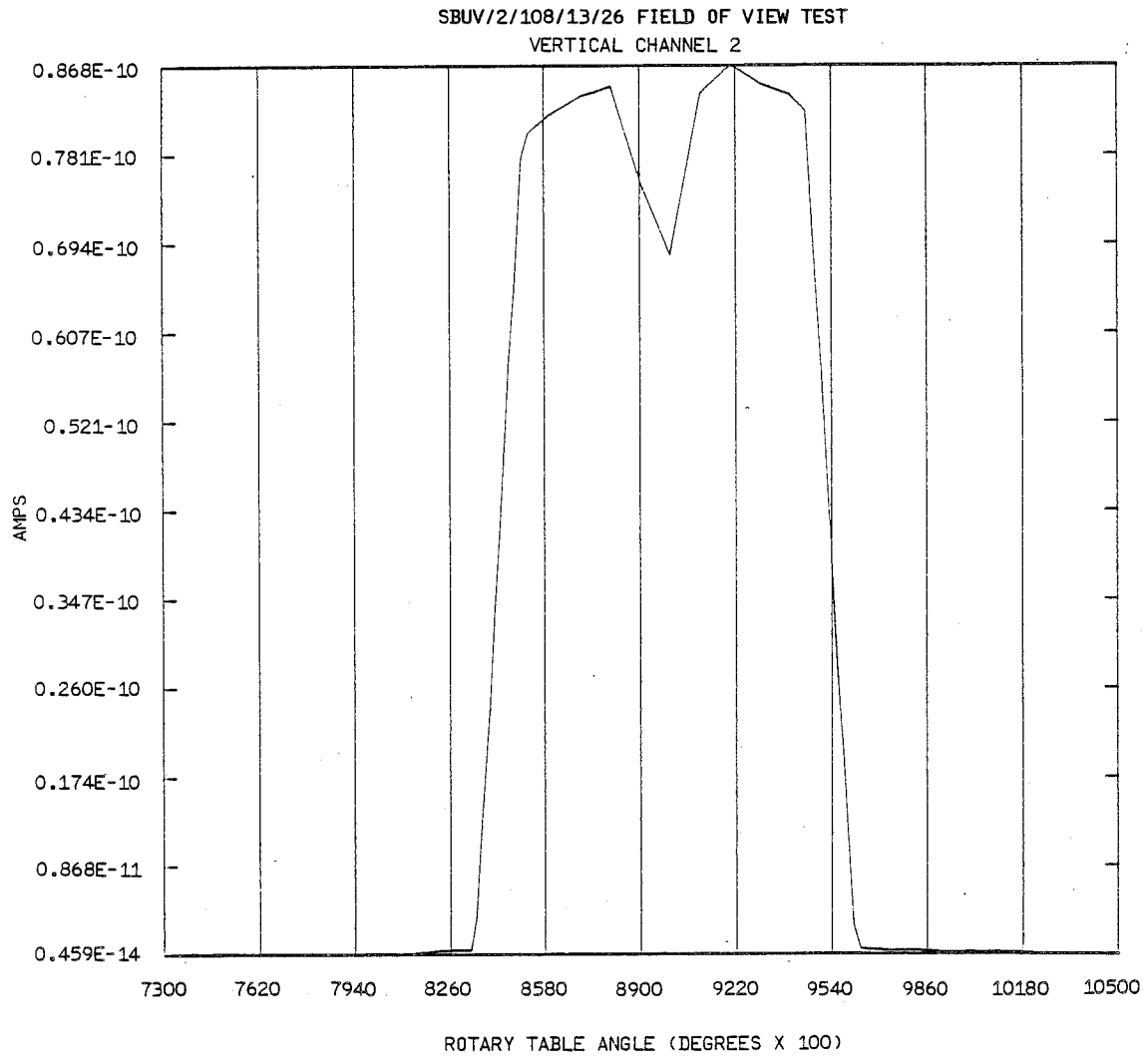
Wavelength in Nanometers	LIMITS: $11.33 \pm .570$		Limit: 0.1° Squareness Y-Z	Limit: 0.1° Y-YCCR	Limit: 0.1° Z-ZCCR
	Y-SIZE Vertical	Z-SIZE Horizontal			
252.00	11.07	11.03	.04	.06	.07
273.61	11.07	11.01	.06	.06	.09
283.10	11.07	11.01	.06	.06	.09
287.70	11.06	11.01	.05	.07	.09
292.29	11.06	11.01	.05	.07	.09
297.59	11.06	11.01	.05	.07	.09
301.97	11.05	11.02	.03	.08	.08
305.87	11.05	11.02	.03	.08	.08
312.57	11.05	11.02	.03	.08	.08
317.56	11.04	11.03	.01	.09	.07
331.26	11.05	11.03	.02	.08	.07
339.89	11.03	11.03	.00	.10	.07
CCR	11.13	11.10	.03		

A/N 3875



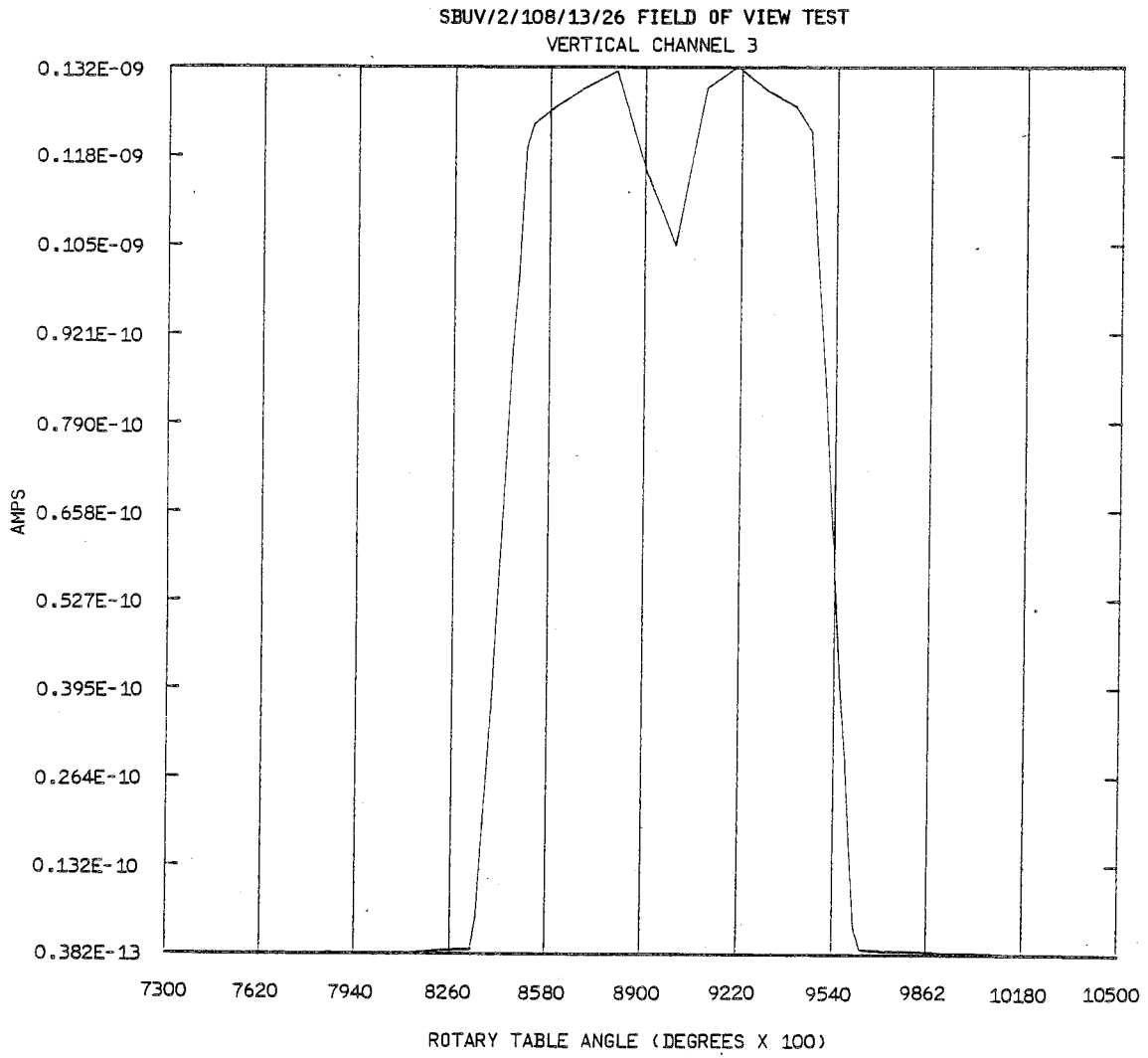
A/N 3875

Figure 8-1 Vertical and Horizontal Field of View Plot



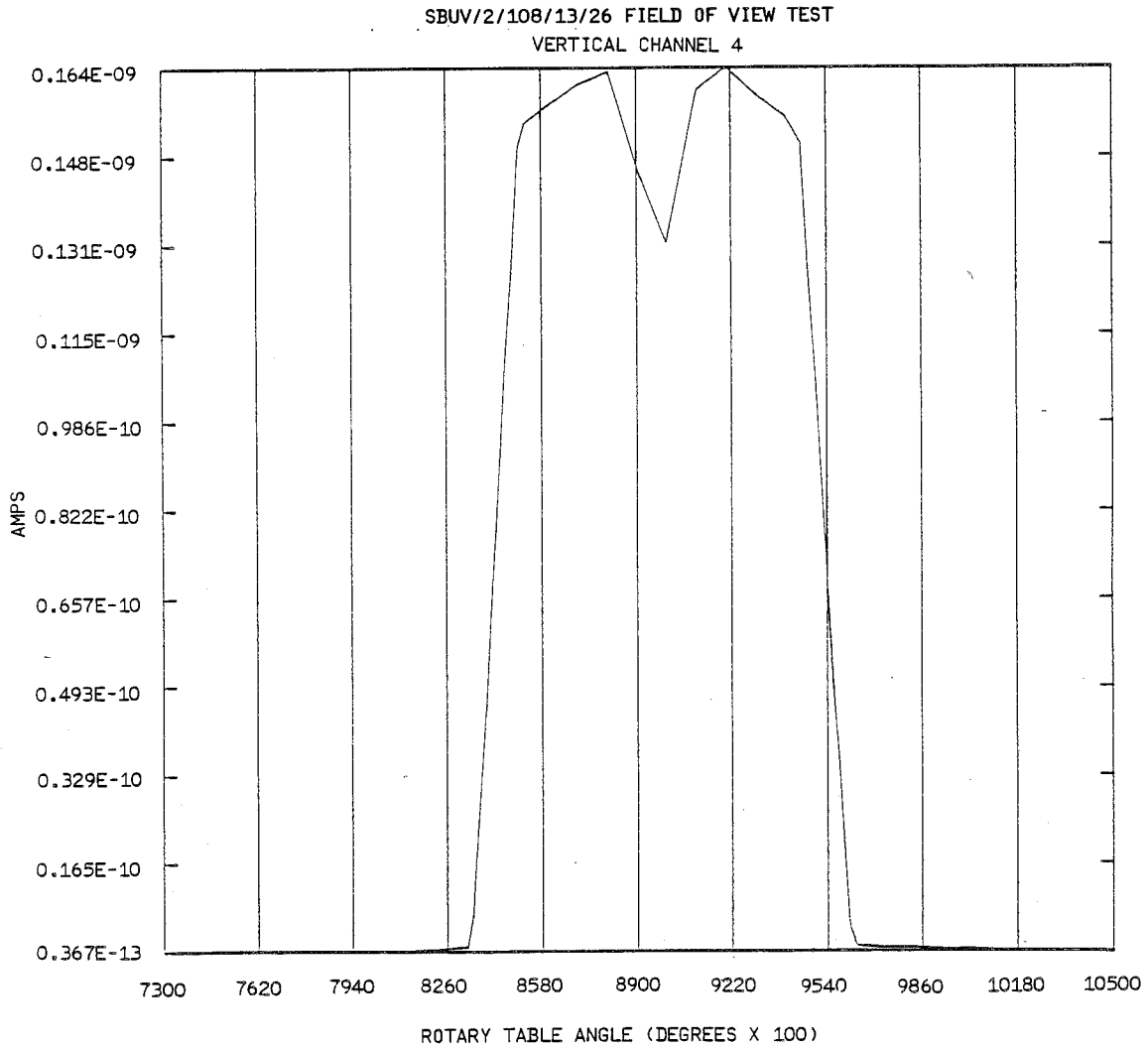
A/N 3875

Figure 8-2 Vertical and Horizontal Field of View Plot



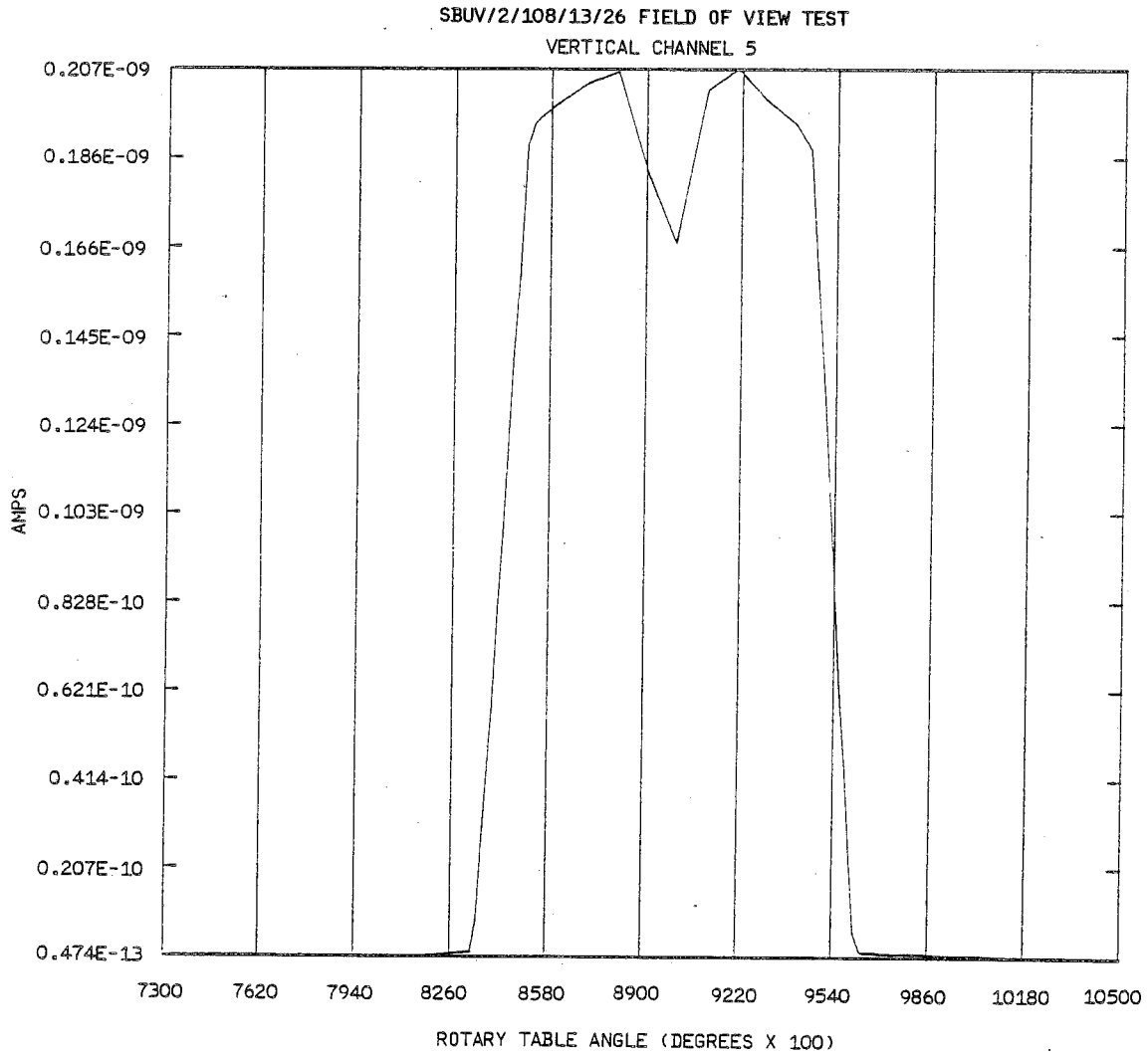
A/N 3875

Figure 8-3 Vertical and Horizontal Field of View Plot



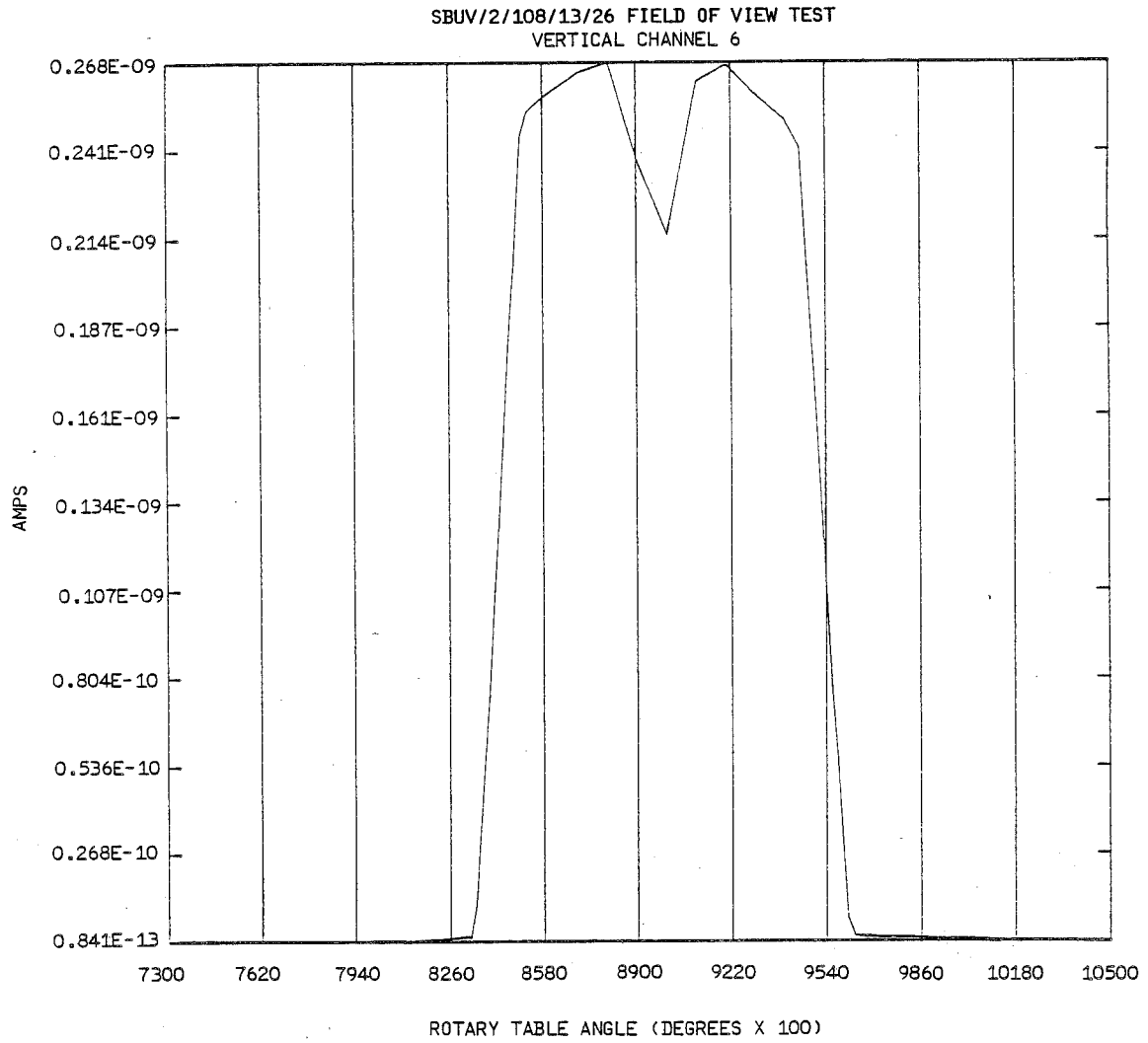
A/N 3875

Figure 8-4 Vertical and Horizontal Field of View Plot



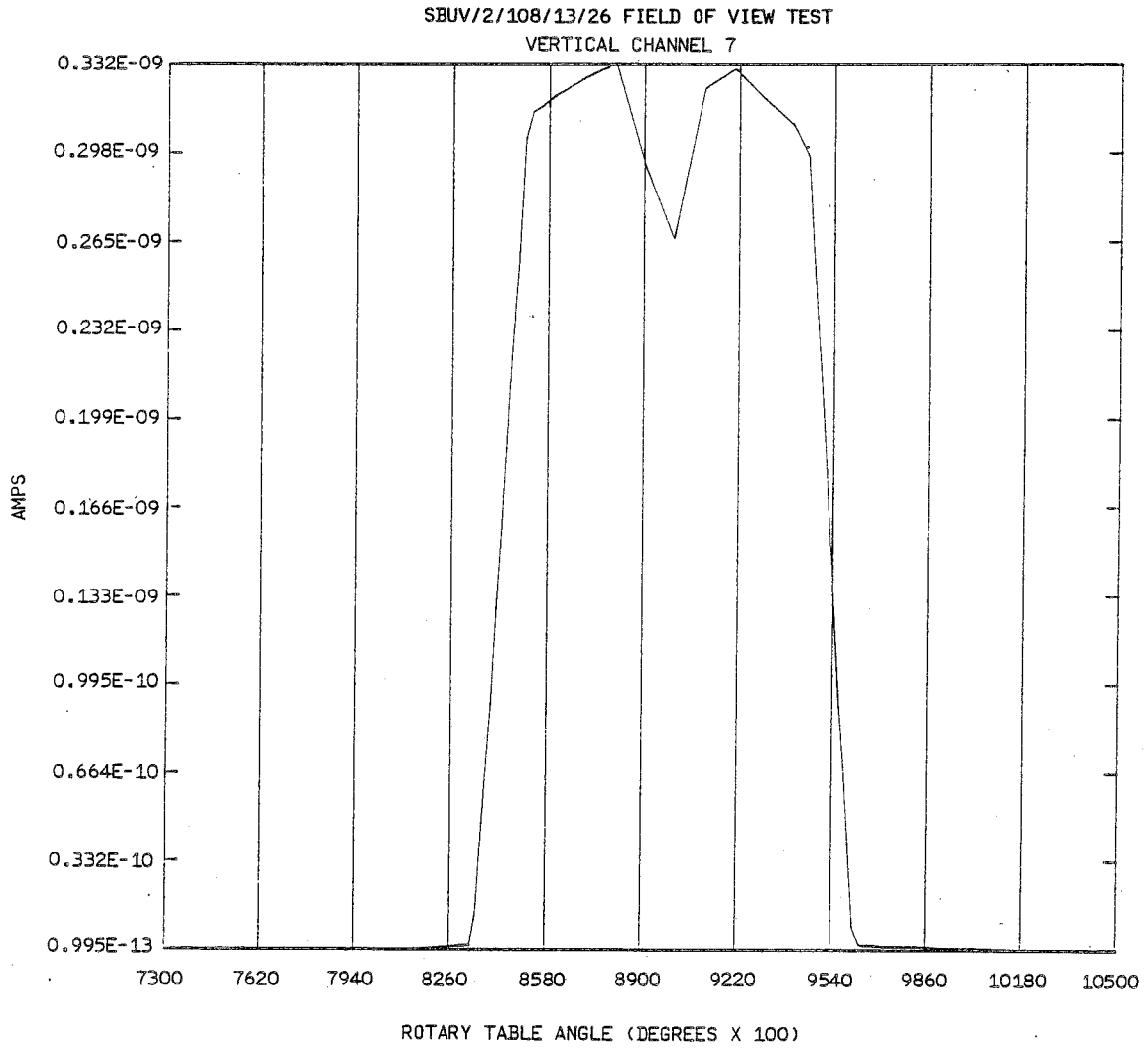
A/N 3875

Figure 8-5 Vertical and Horizontal Field of View Plot



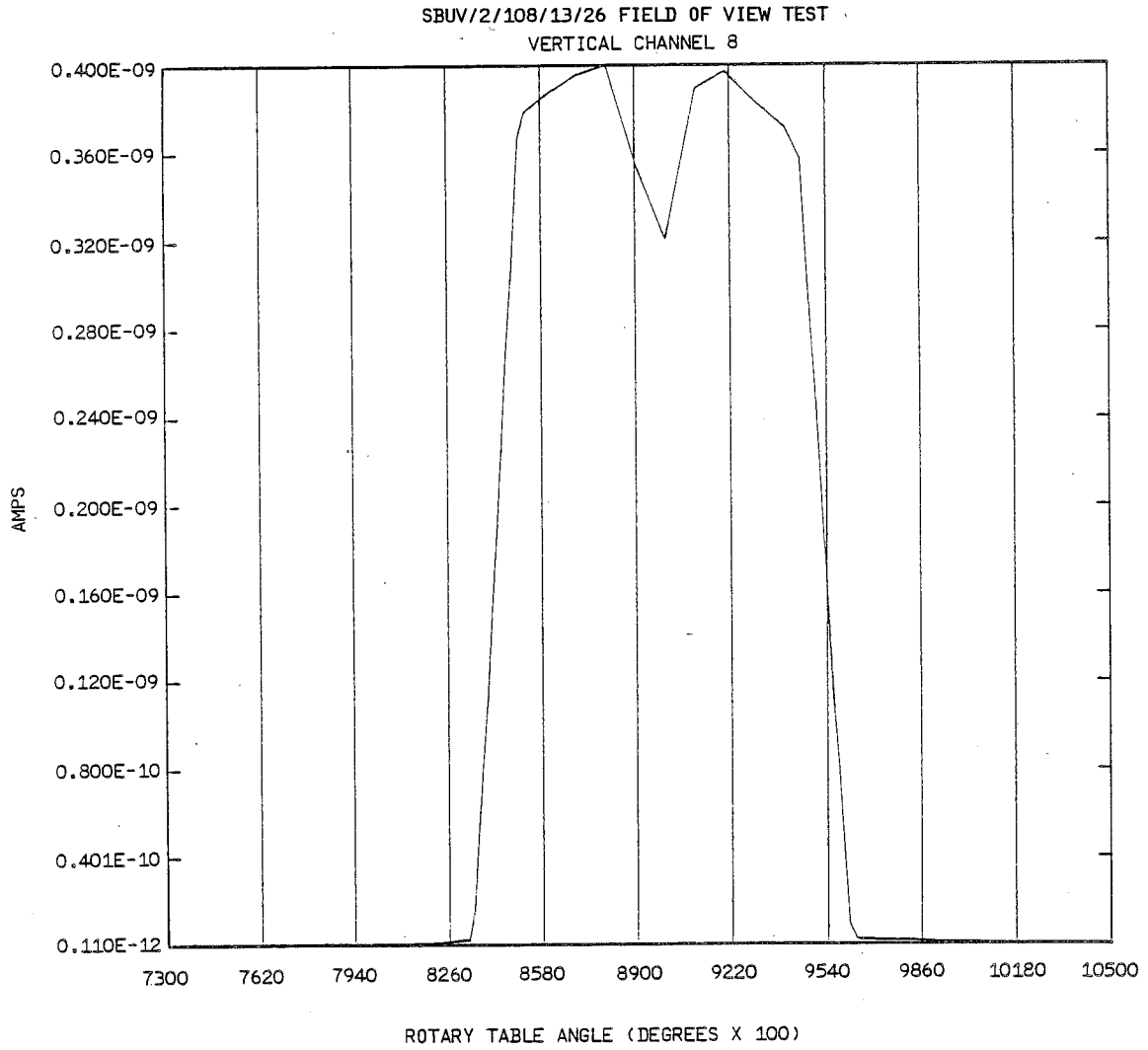
A/N 3875

Figure 8-6 Vertical and Horizontal Field of View Plot



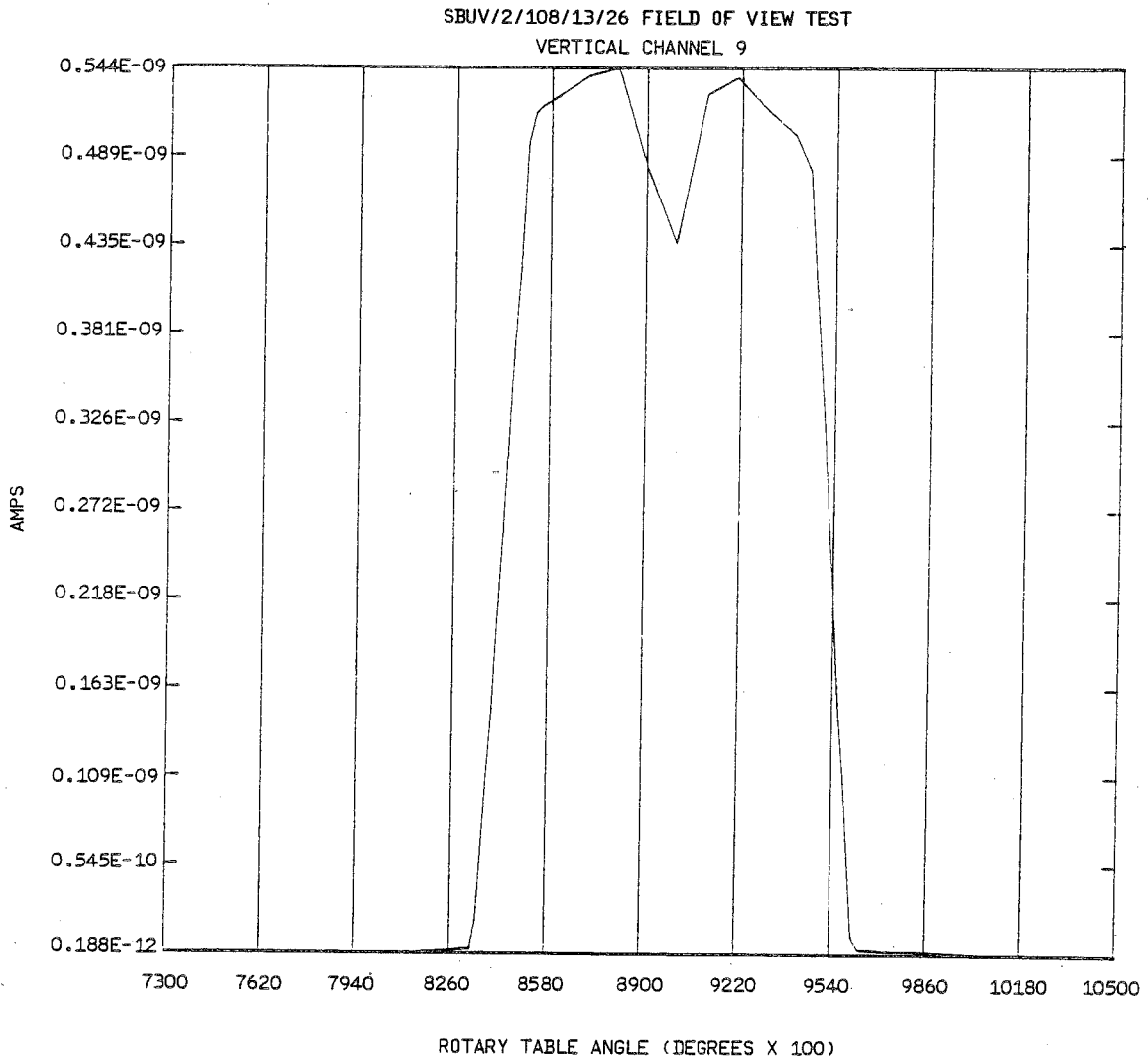
A/N 3875

Figure 8-7 Vertical and Horizontal Field of View Plot



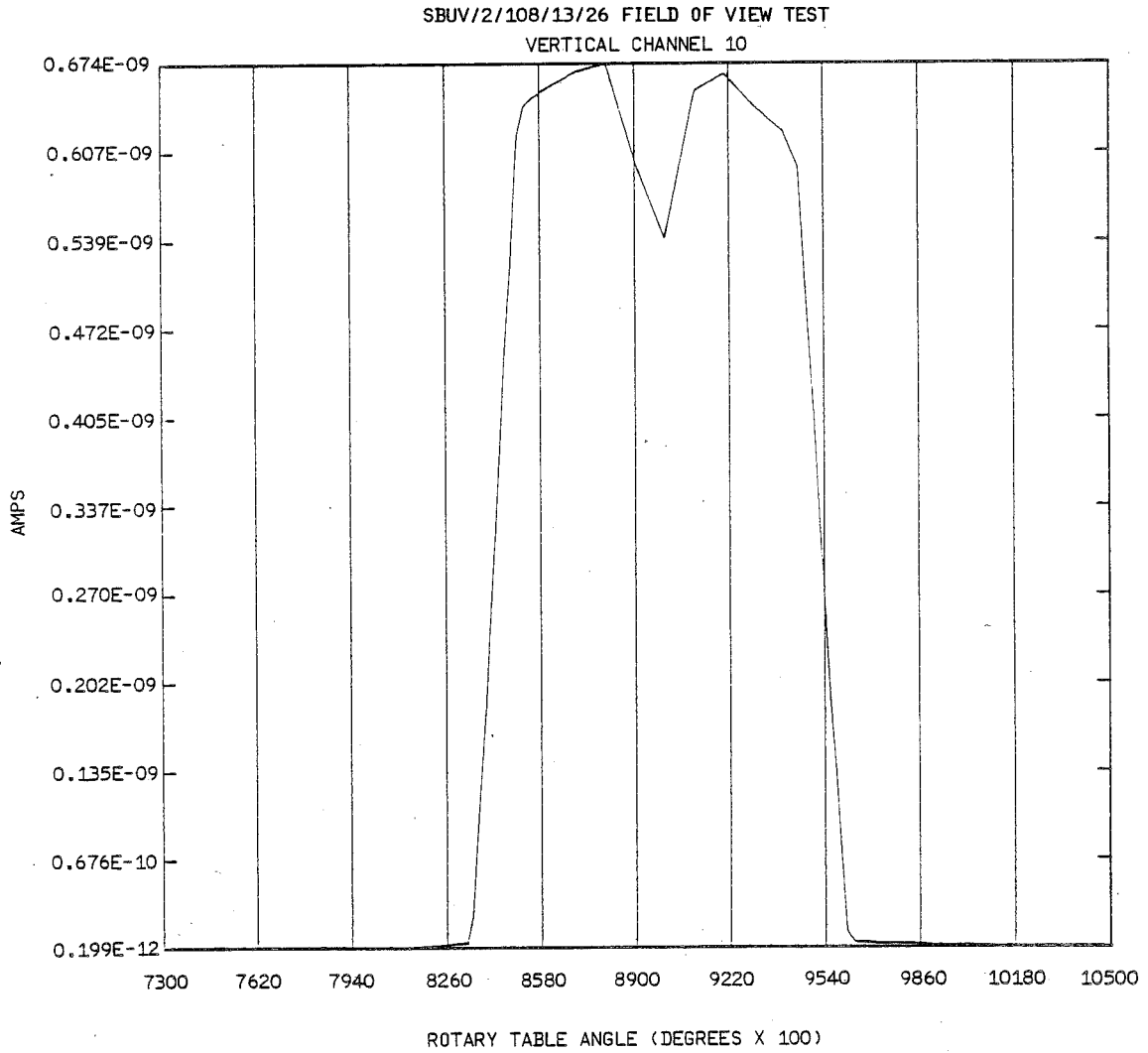
A/N 3875

Figure 8-8 Vertical and Horizontal Field of View Plot



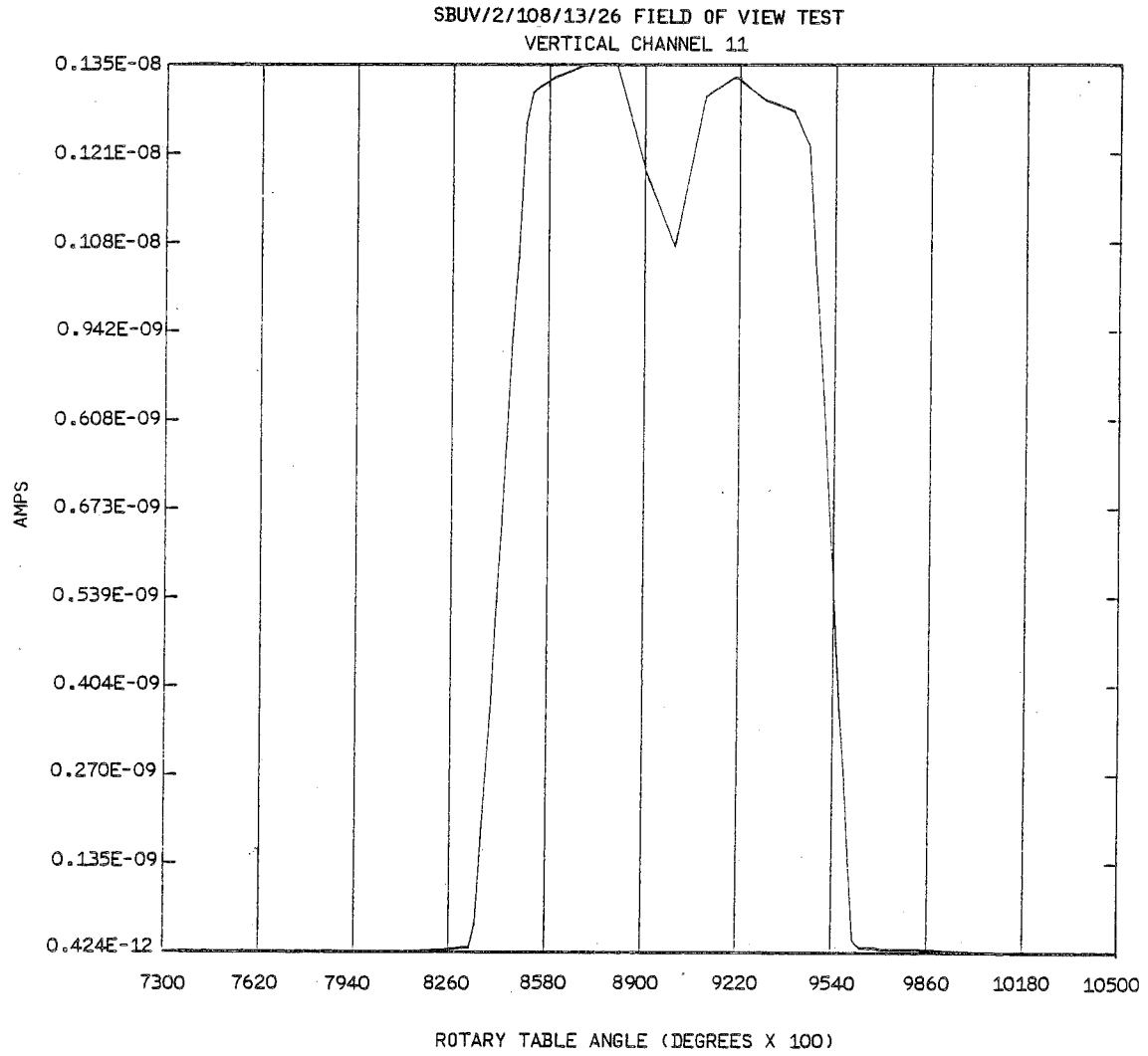
A/N 3875

Figure 8-9 Vertical and Horizontal Field of View Plot



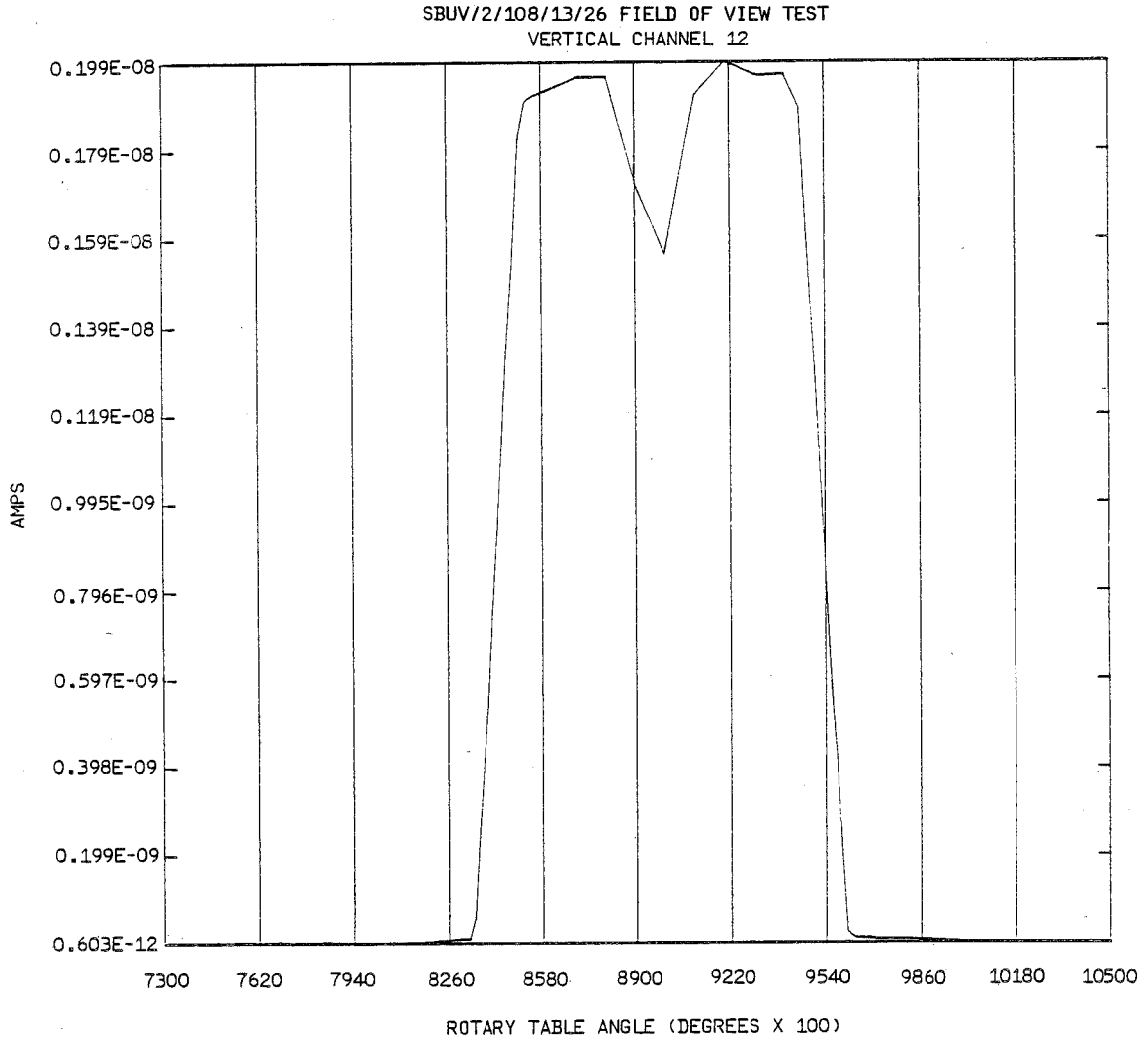
A/N 3875

Figure 8-10 Vertical and Horizontal Field of View Plot



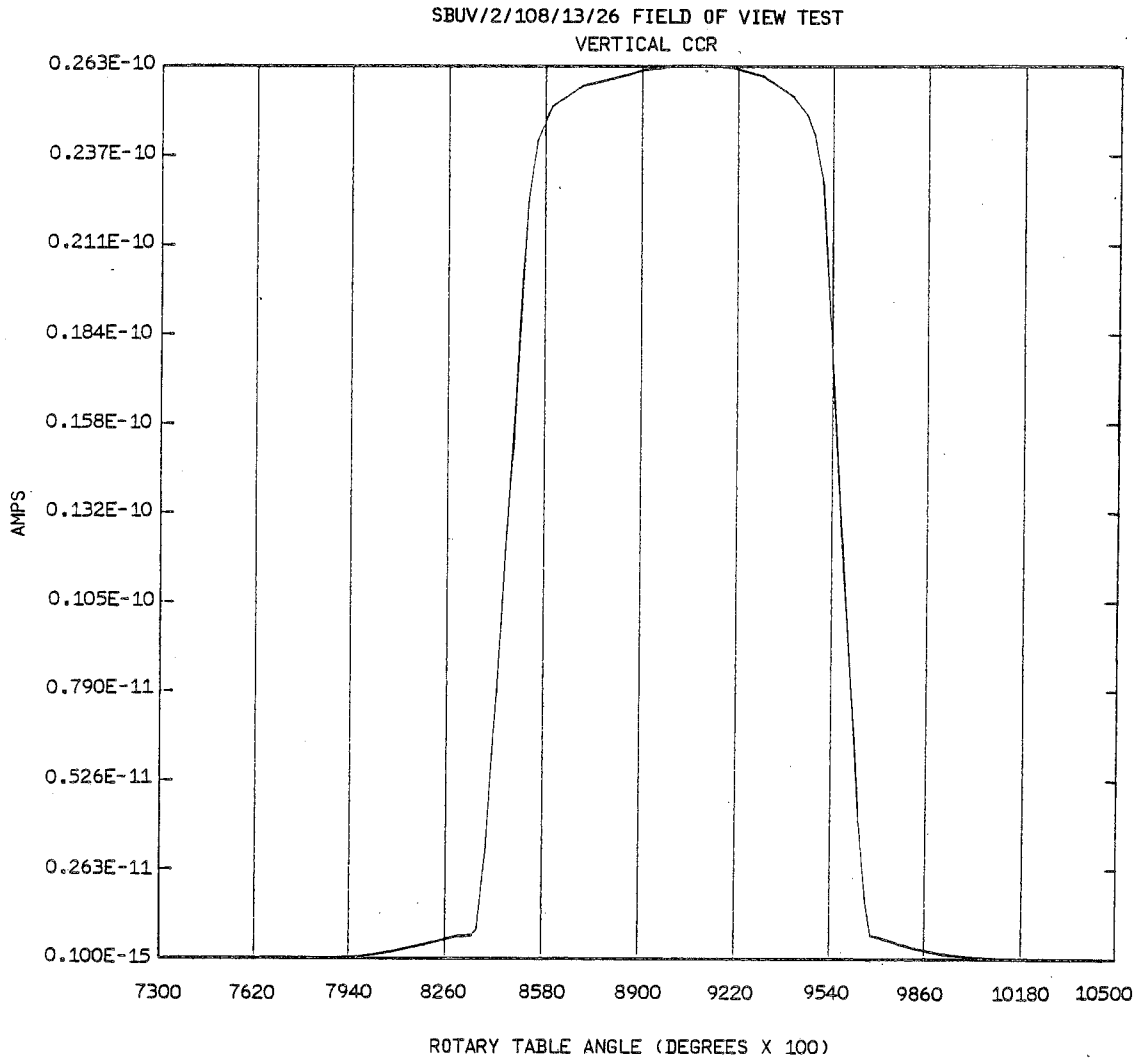
A/N 3875

Figure 8-11 Vertical and Horizontal Field of View Plot



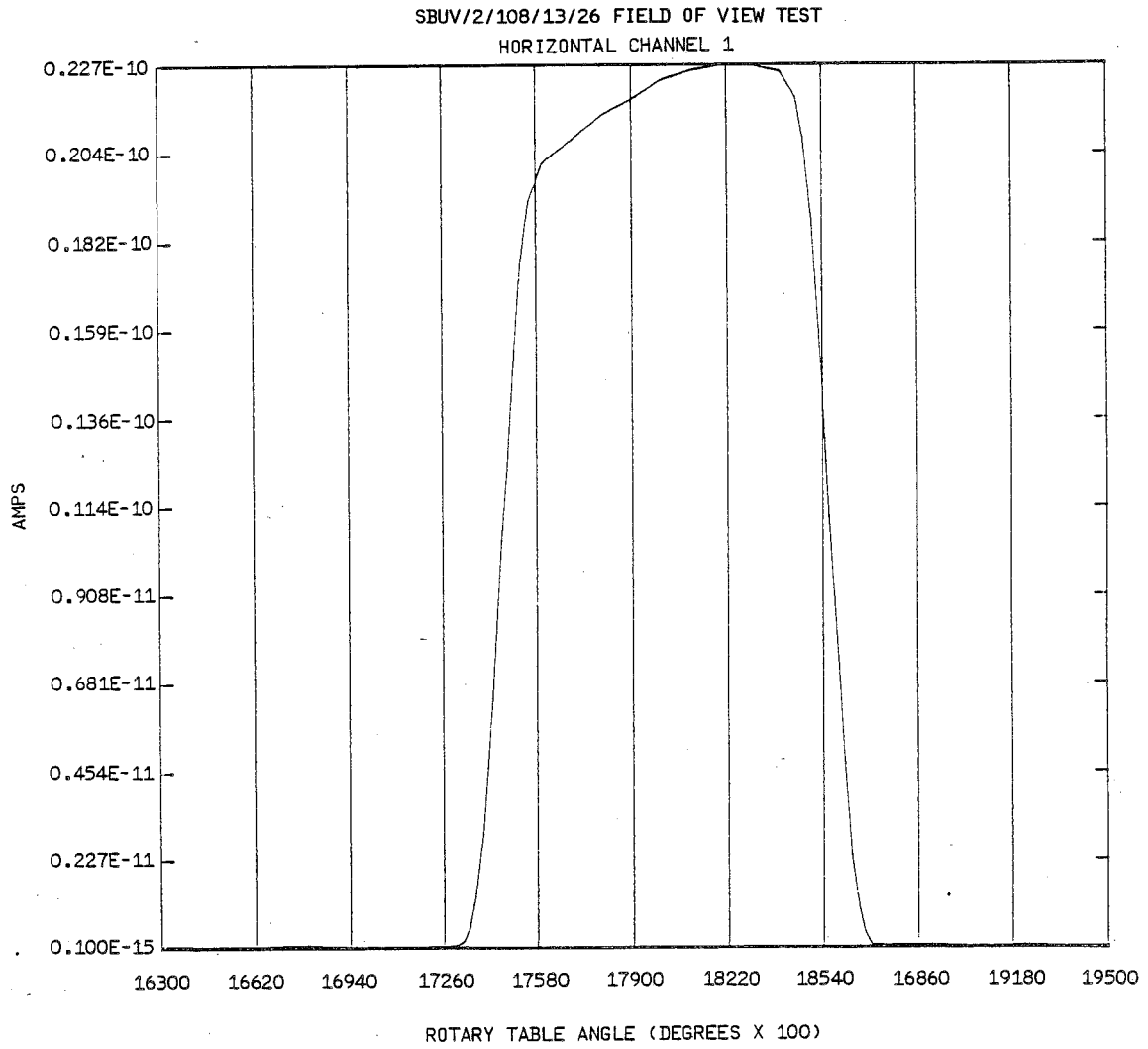
A/N 3875

Figure 8-12 Vertical and Horizontal Field of View Plot



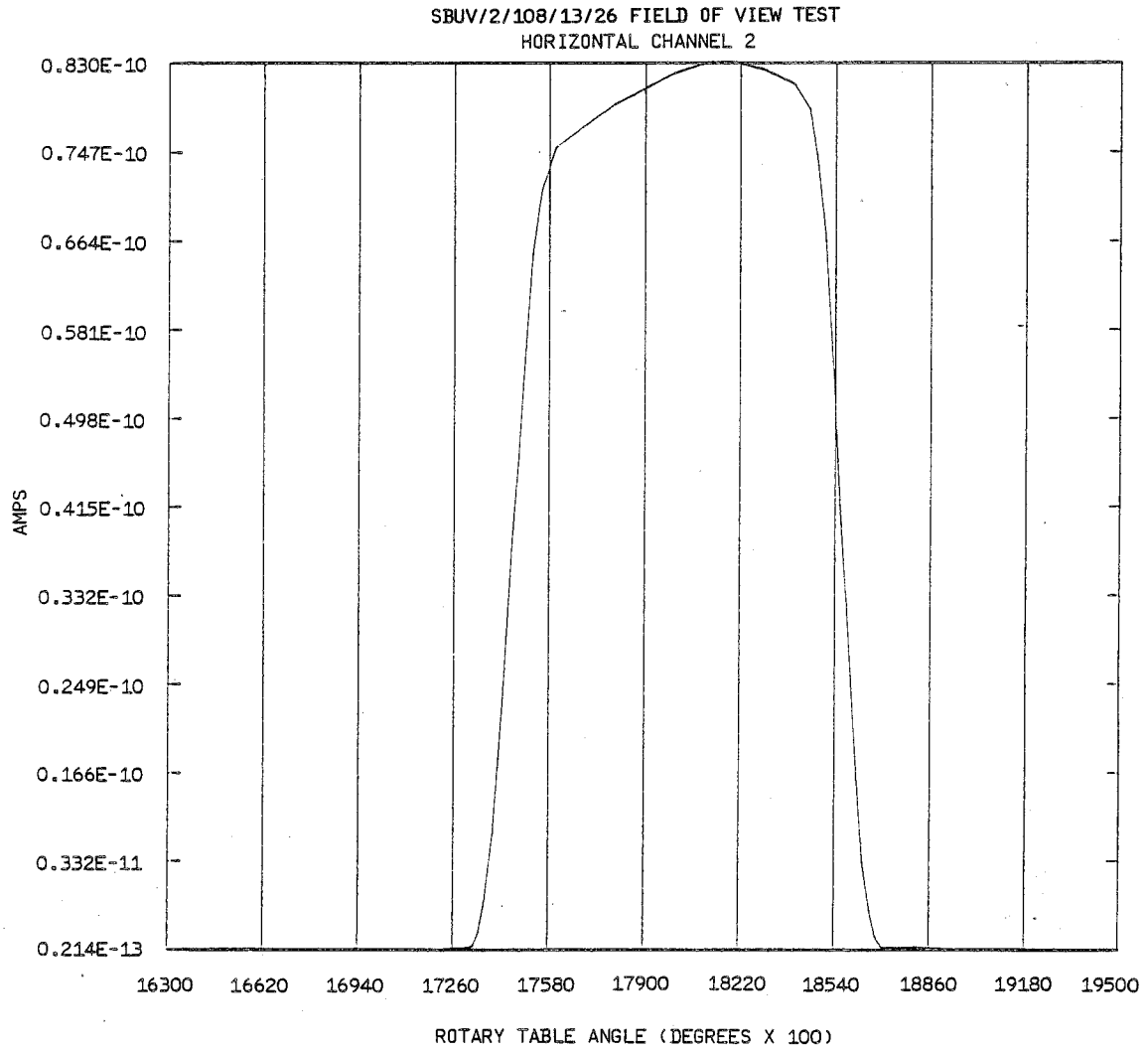
A/N 3875

Figure 8-13 Vertical and Horizontal Field of View Plot



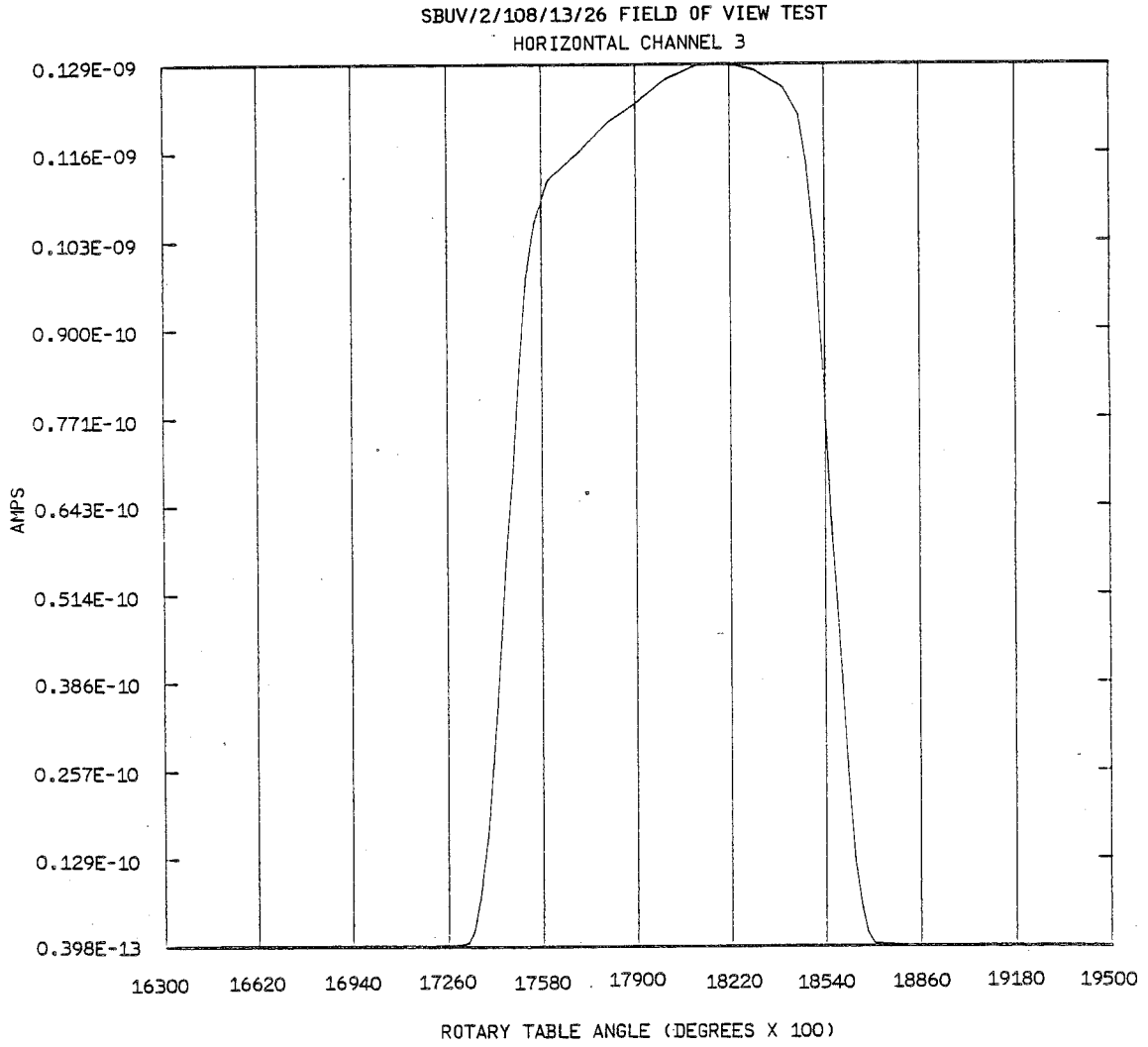
A/N 3875

Figure 8-14 Vertical and Horizontal Field of View Plot



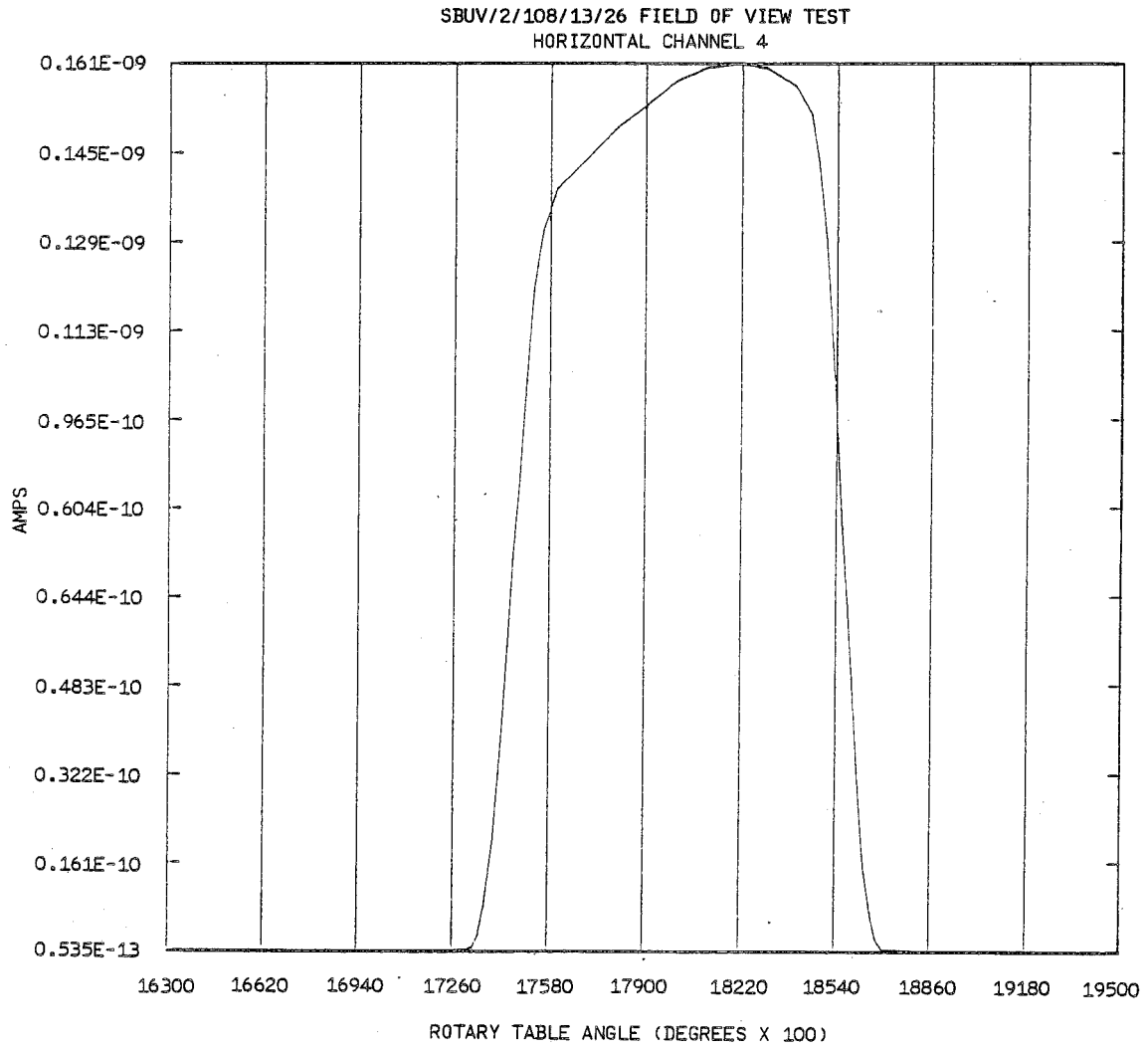
A/N 3875

Figure 8-15 Vertical and Horizontal Field of View Plot



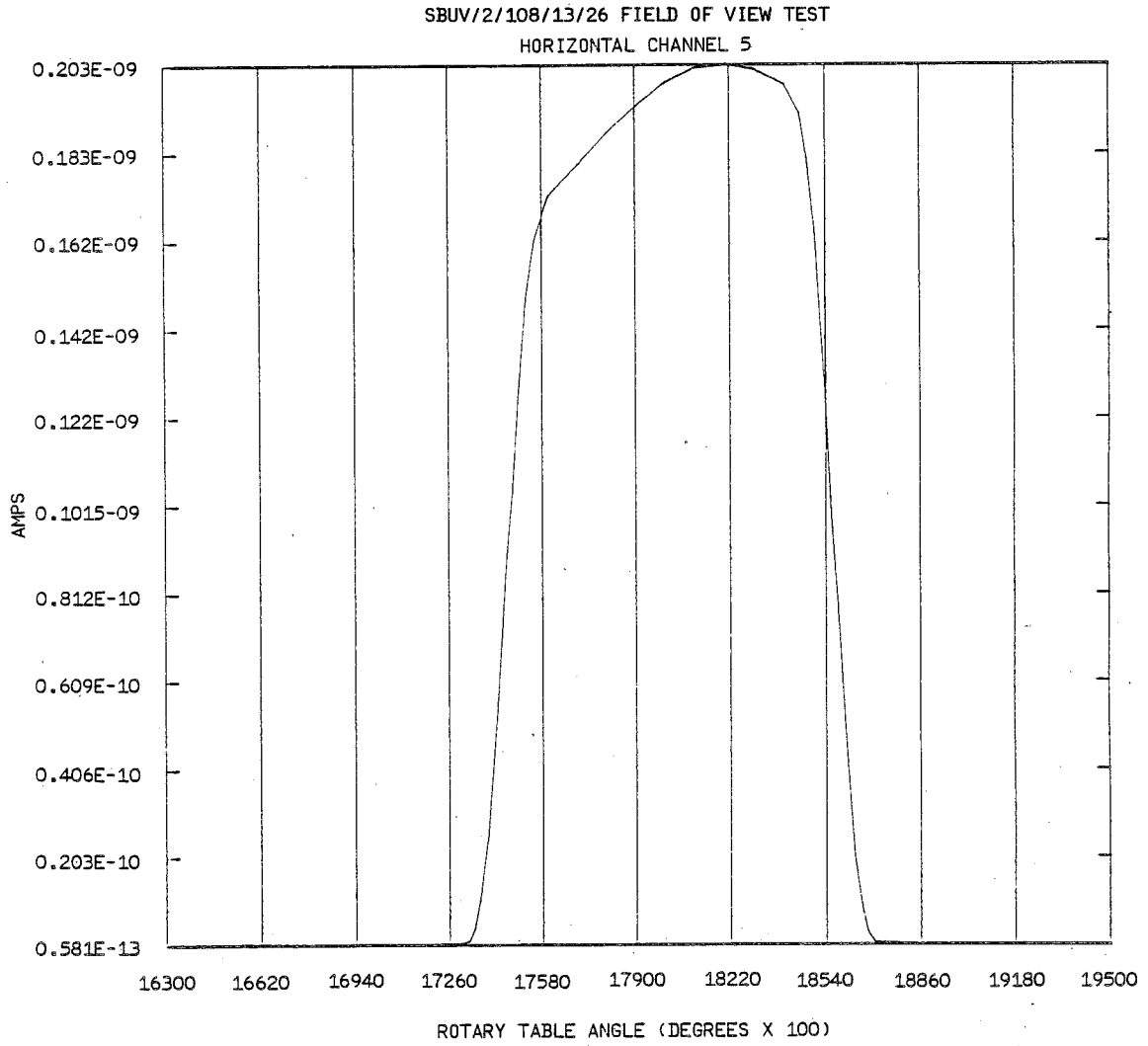
A/N 3875

Figure 8-16 Vertical and Horizontal Field of View Plot



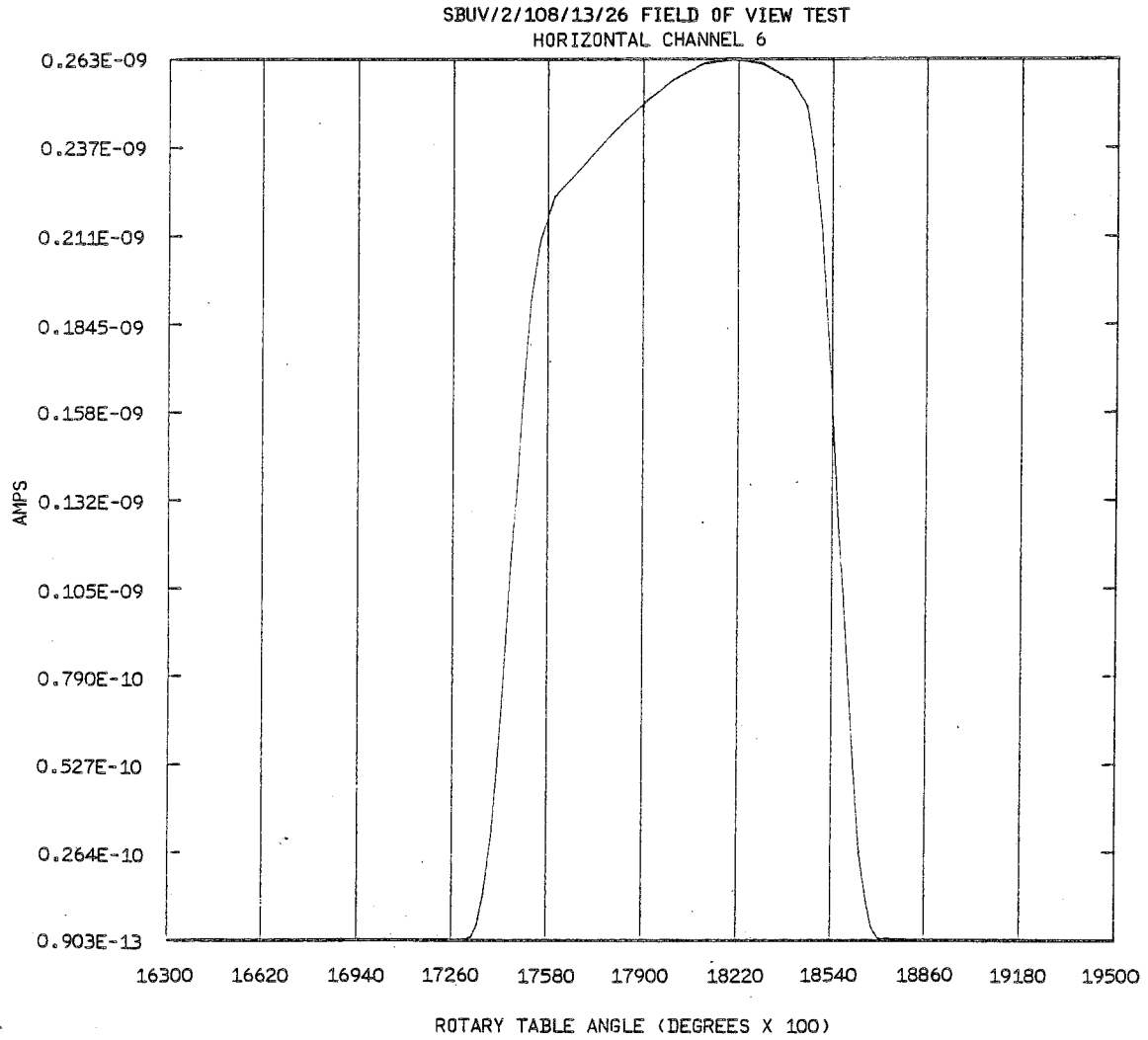
A/N 3875

Figure 8-17 Vertical and Horizontal Field of View Plot



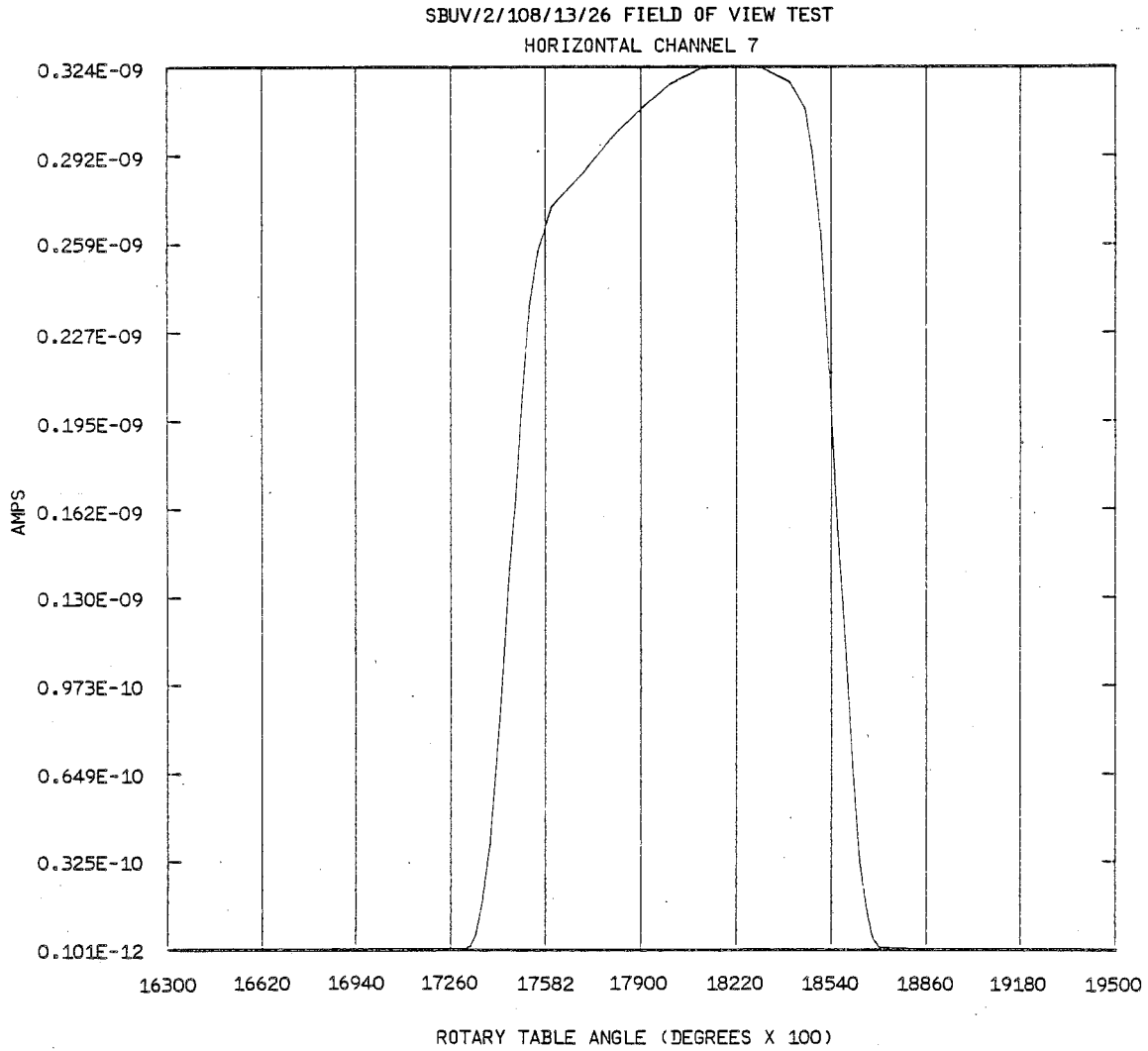
A/N 3875

Figure 8-18 Vertical and Horizontal Field of View Plot



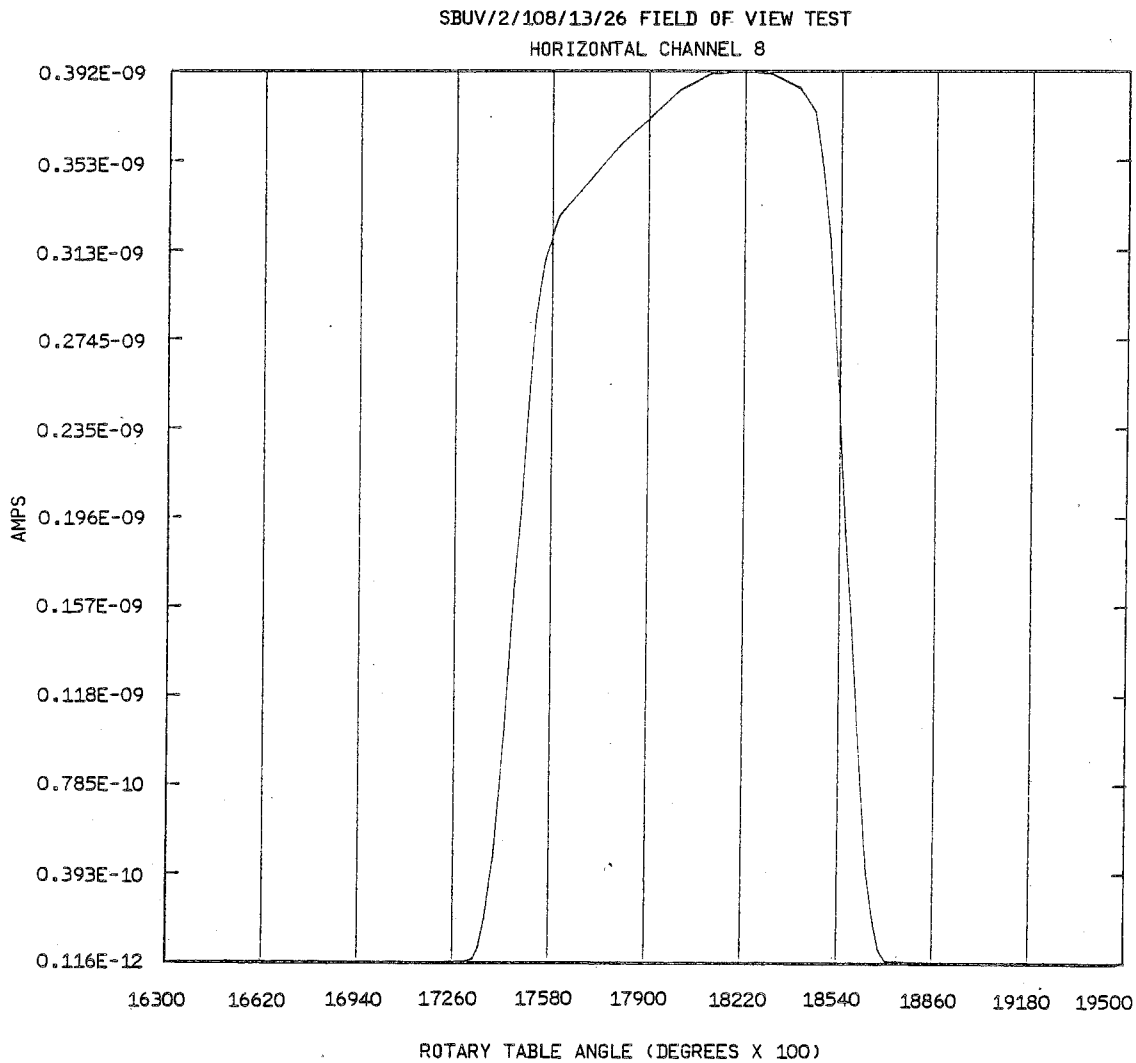
A/N 3875

Figure 8-19 Vertical and Horizontal Field of View Plot



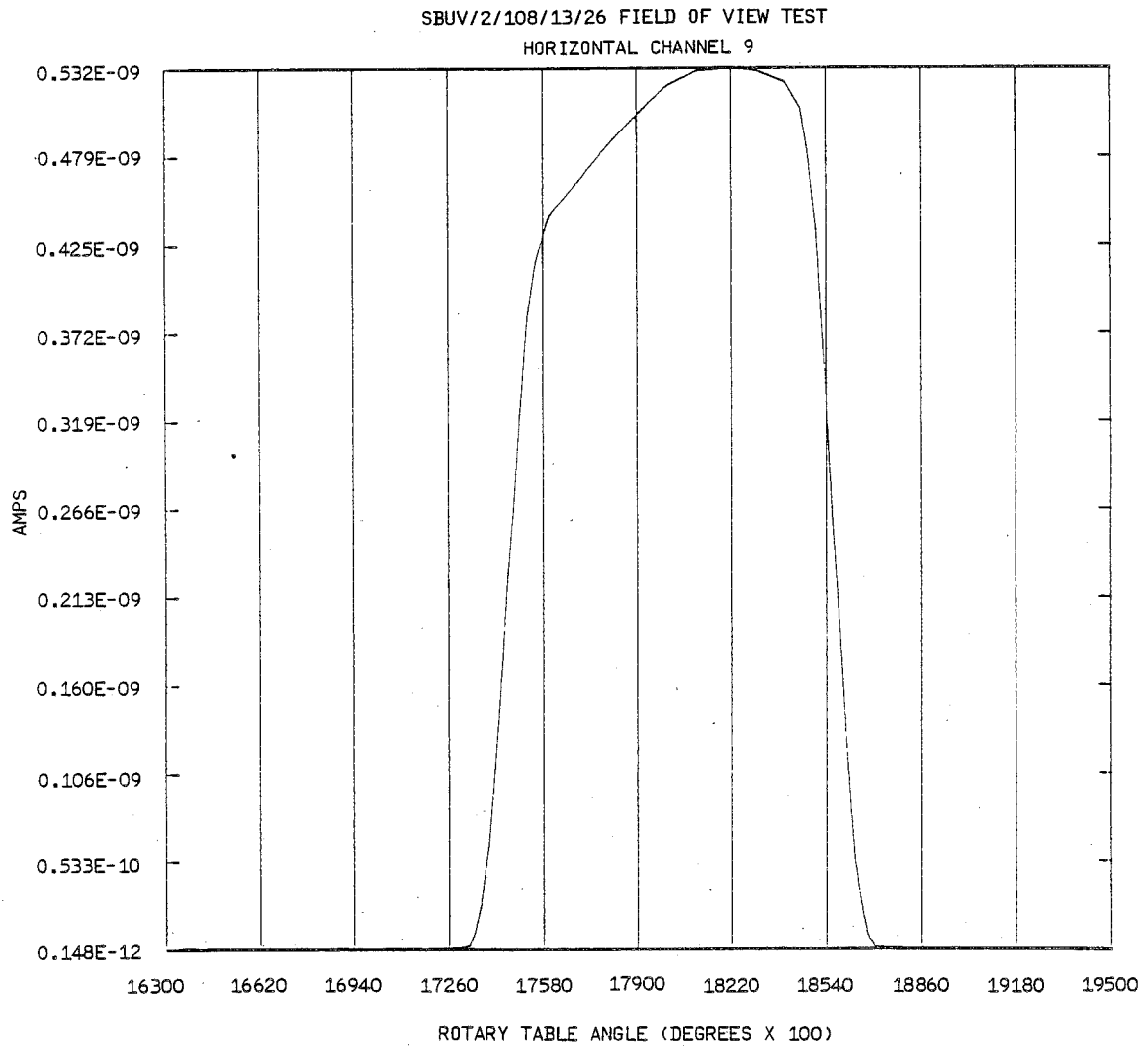
A/N 3875

Figure 8-20 Vertical and Horizontal Field of View Plot



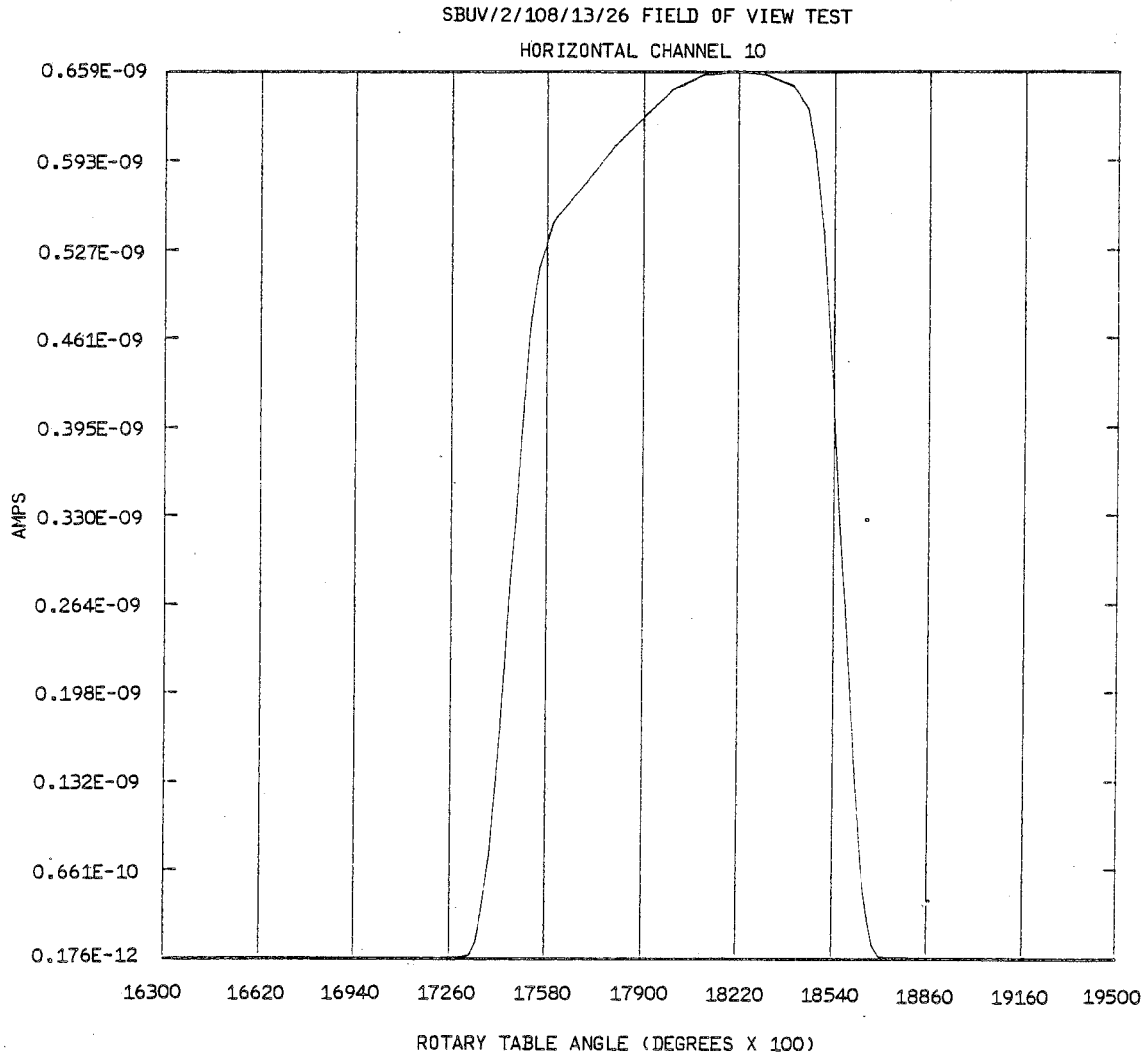
A/N 3875

Figure 8-21 Vertical and Horizontal Field of View Plot



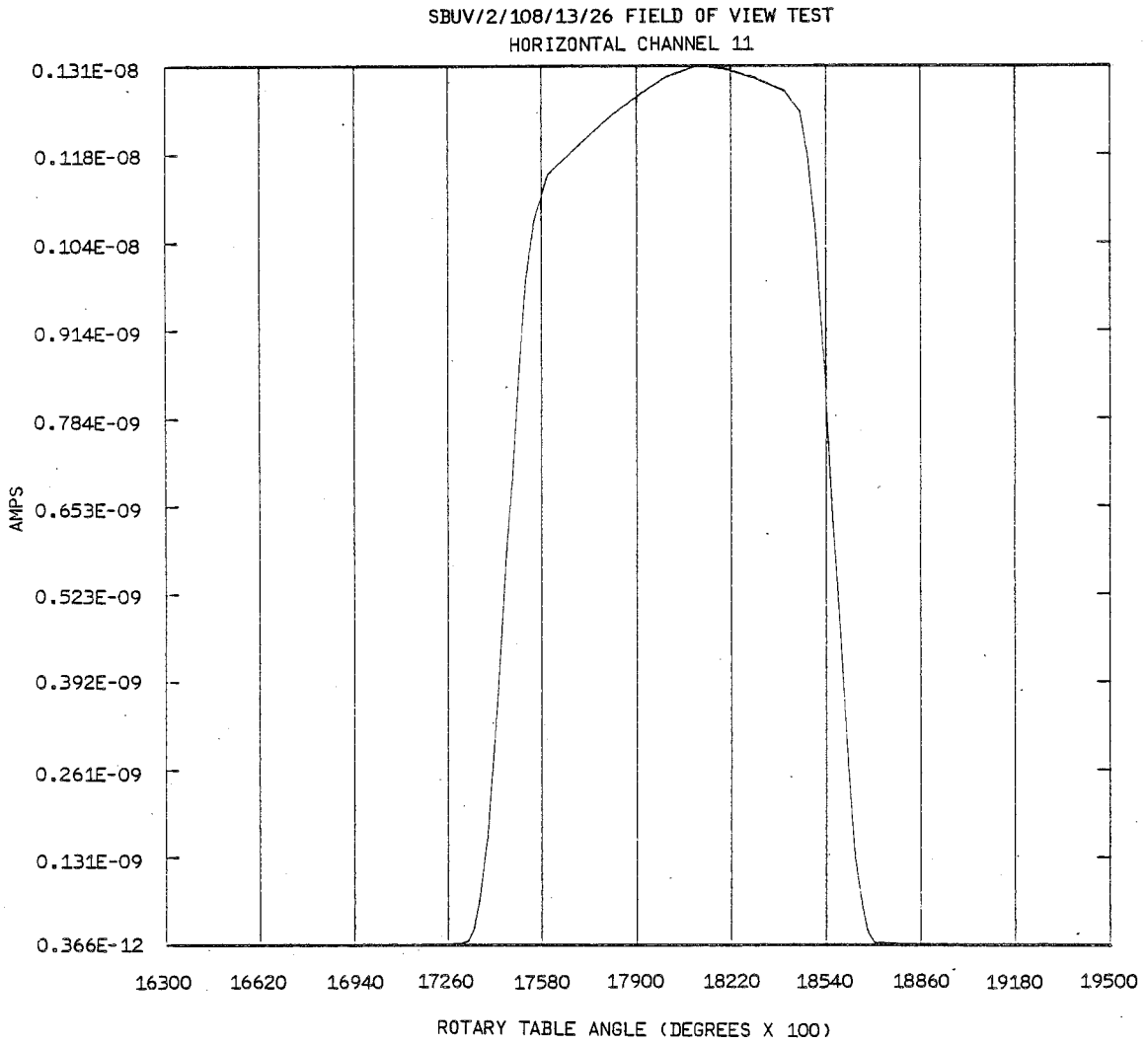
A/N 3875

Figure 8-22 Vertical and Horizontal Field of View Plot



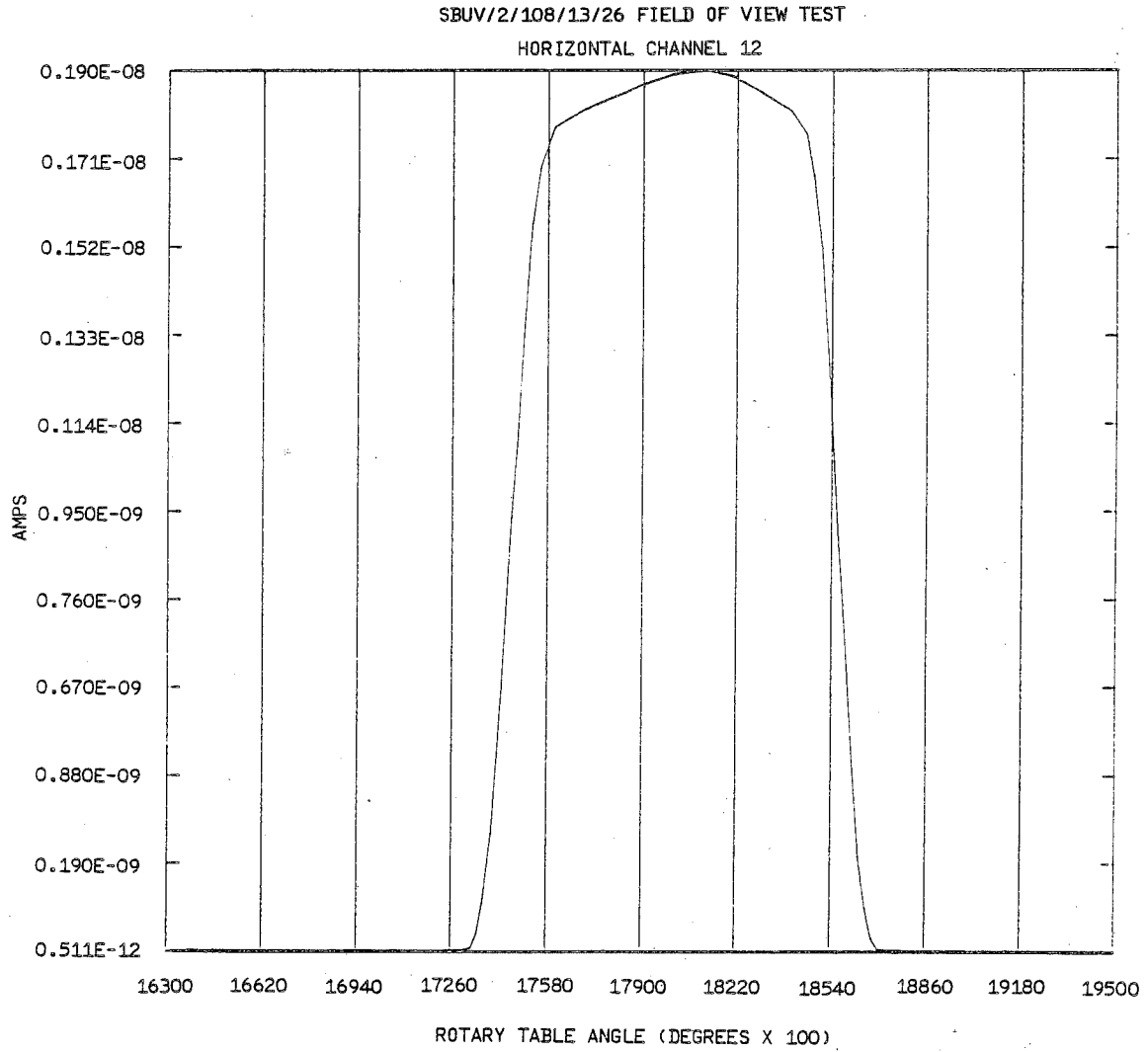
A/N 3875

Figure 8-23 Vertical and Horizontal Field of View Plot



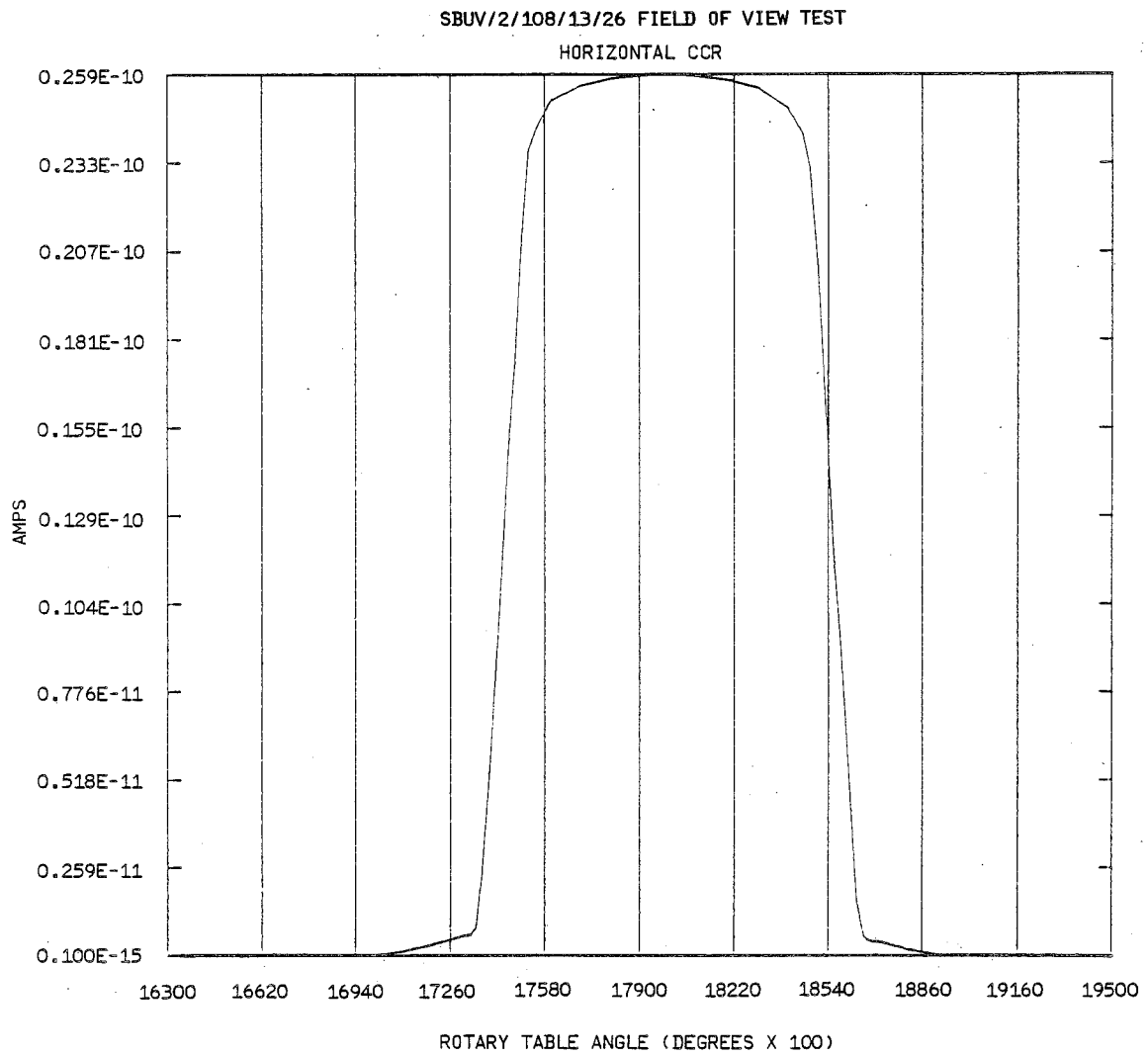
A/N 3875

Figure 8-24 Vertical and Horizontal Field of View Plot



A/N 3875

Figure 8-25 Vertical and Horizontal Field of View Plot



A/N 3875

Figure 8-26 Vertical and Horizontal Field of View Plot



Section 9

POST ENVIRONMENT FOV VERIFICATION

(Reference Test Procedure 68042)

Field of view measurements were made at five different points during the test program. The results are summarized in Table 9-1. Plots of the individual measurements follow also in Figures 9-1 through 9-20.

The FOV size was determined by first normalizing the PMT data to 1.0. Graphs were plotted. Selected data points along both the right and left slopes were fitted to a straight line using a linear regression method. The 50% points are determined from the equation of each side. The full width half maximum (size) is found from the sum of the absolute value of the 50% points. The pointing error is found from the sum of 50% points divided by 2.



Table 9-1
FOV SIZE AND POINTING ERROR COMPARISON

	MONOCHROMATOR (283 μm)				CLOUD COVER RADIOMETER			
	SIZE		POINTING ERROR		SIZE		POINTING ERROR	
	HORIZ.	VERTICAL	HORIZ.	VERTICAL	HORIZ.	VERTICAL	HORIZ.	VERTICAL
PRE-VIBRATION	10.88	10.98	+0.006	-0.08	11.17	11.08	-0.71	+0.5
POST-Z AXIS VIB.	10.89	10.98	+0.03	-0.09	11.09	11.06	-0.64	+0.50
POST-Y AXIS VIB.	10.89	11.09	+0.04	-0.14	11.06	11.18	-0.65	+0.45
POST-X AXIS VIB.	10.89	10.99	+0.03	-0.08	11.09	11.07	-0.63	+0.51
POST THERMAL VAC	10.87	10.98	+0.06	+0.01	11.10	11.08	-0.62	+0.61

A/N 3875



B6802-78

A/N 3875

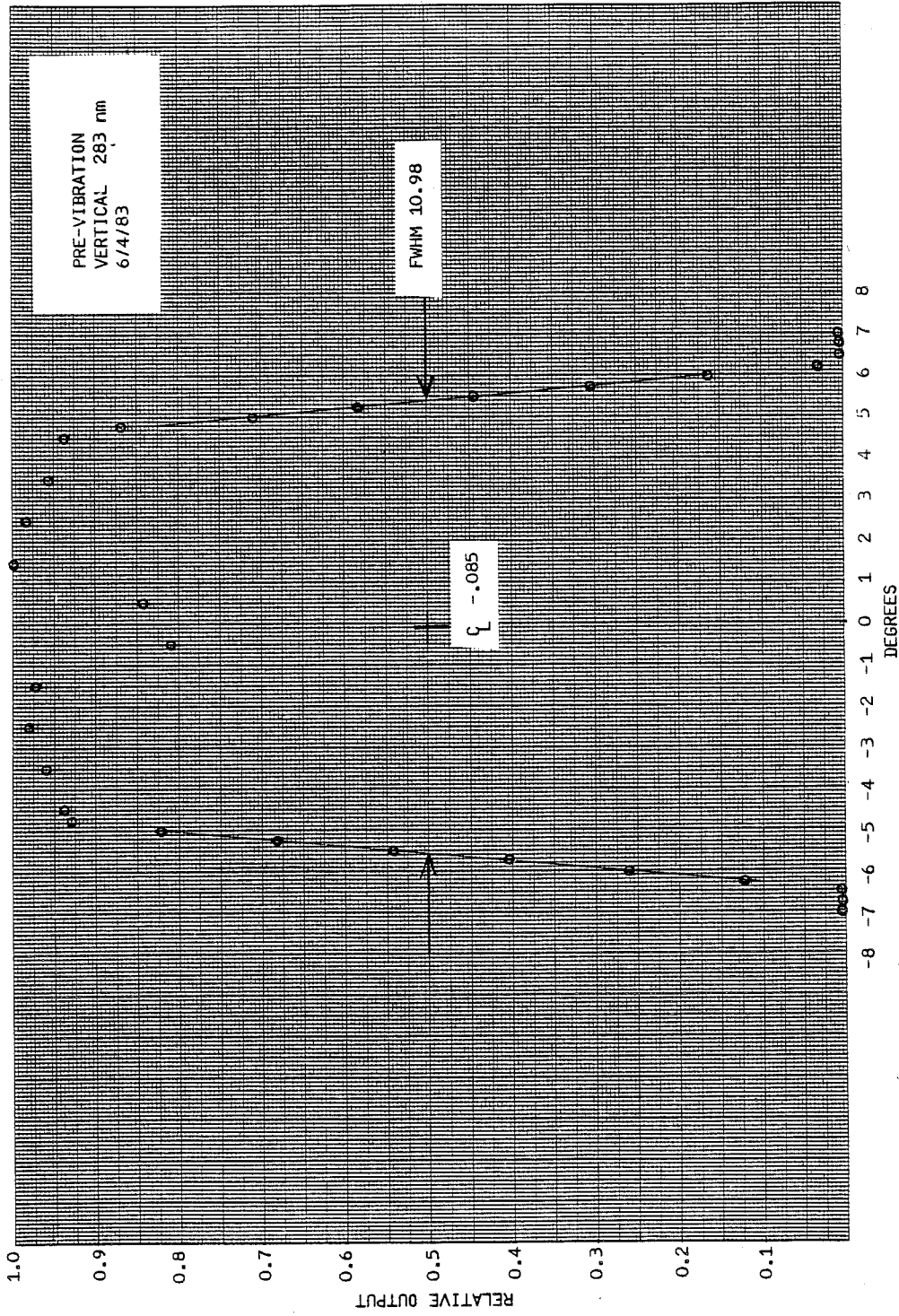


Figure 9-1 Pre-Vibration Horizontal FOV

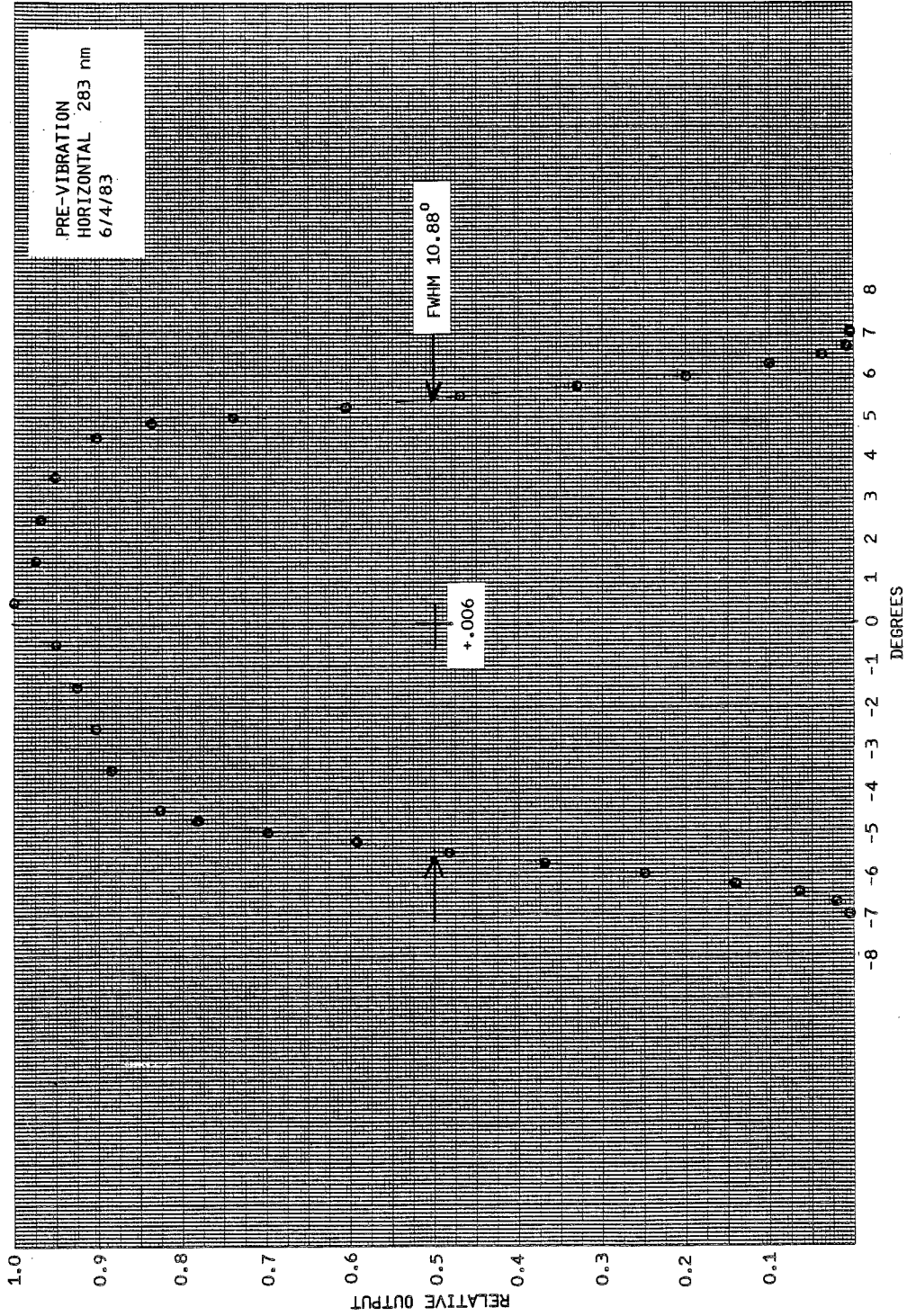


Figure 9-2 Pre-Vibration Vertical FOV

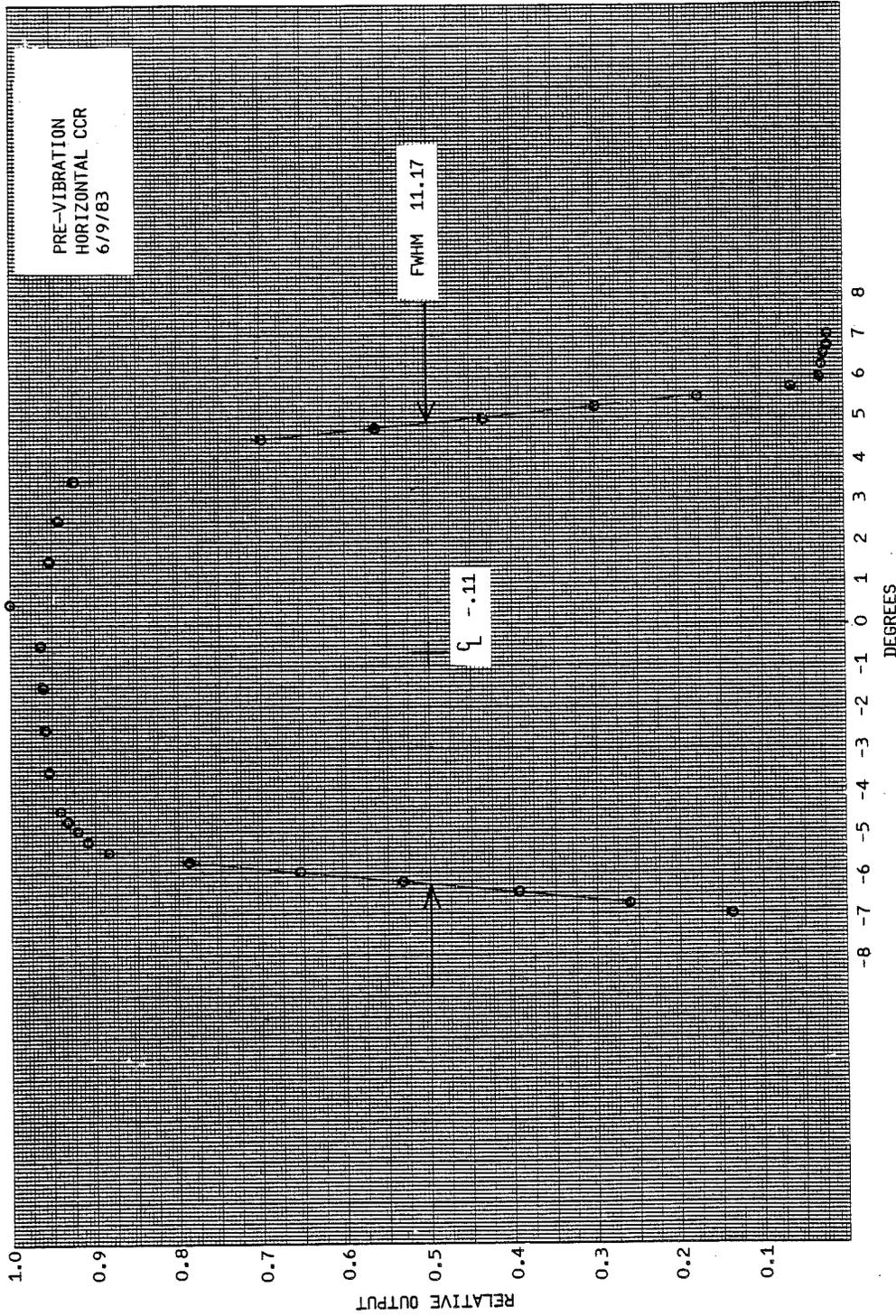


Figure 9-3 Pre-Vibration Horizontal CCR FOV

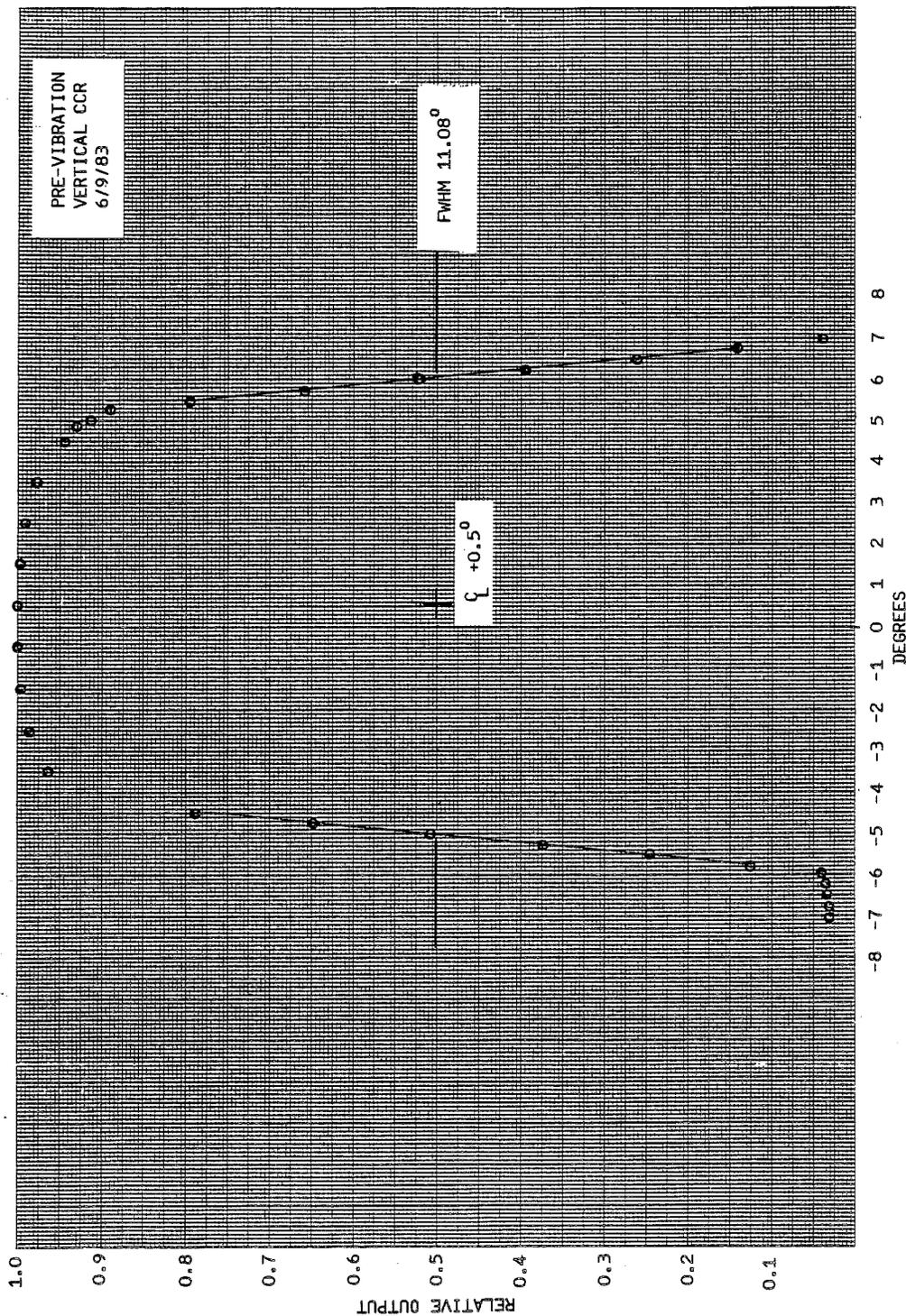


Figure 9-4 Pre-Vibration Vertical CCR FOV

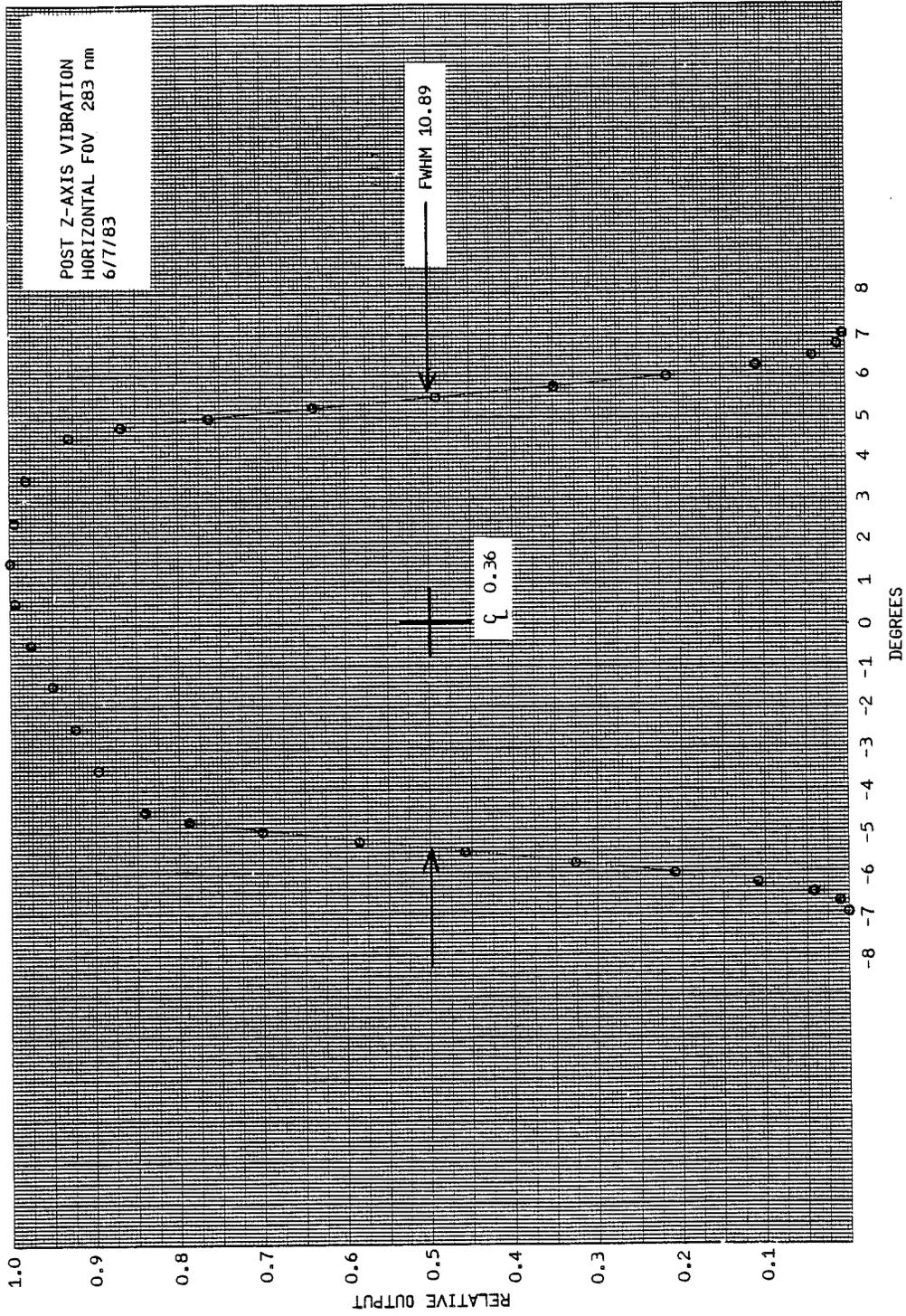


Figure 9-5 Post Z-Axis Vibration Horizontal FOV

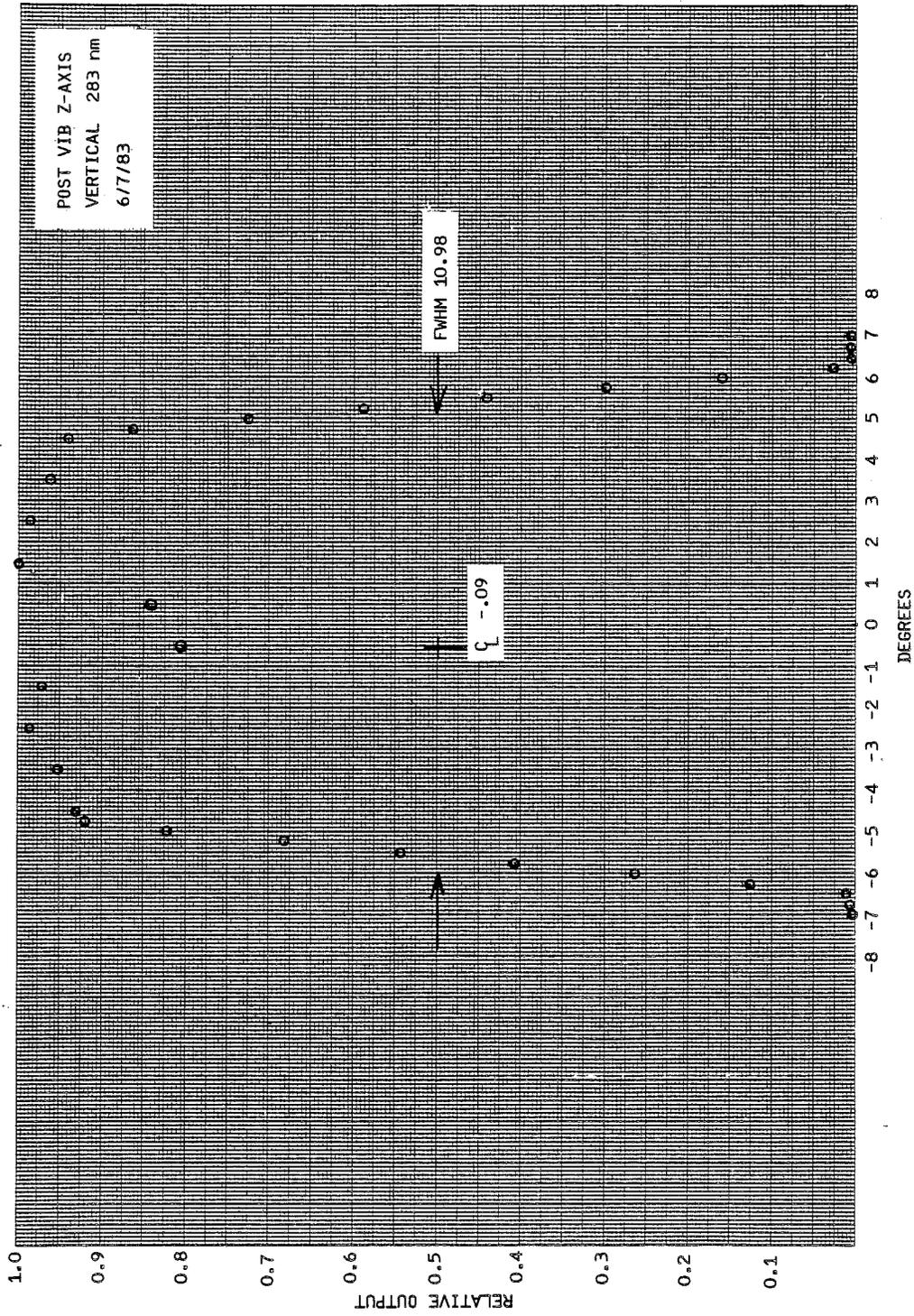


Figure 9-6 Post Z-Axis Vibration Vertical FOV

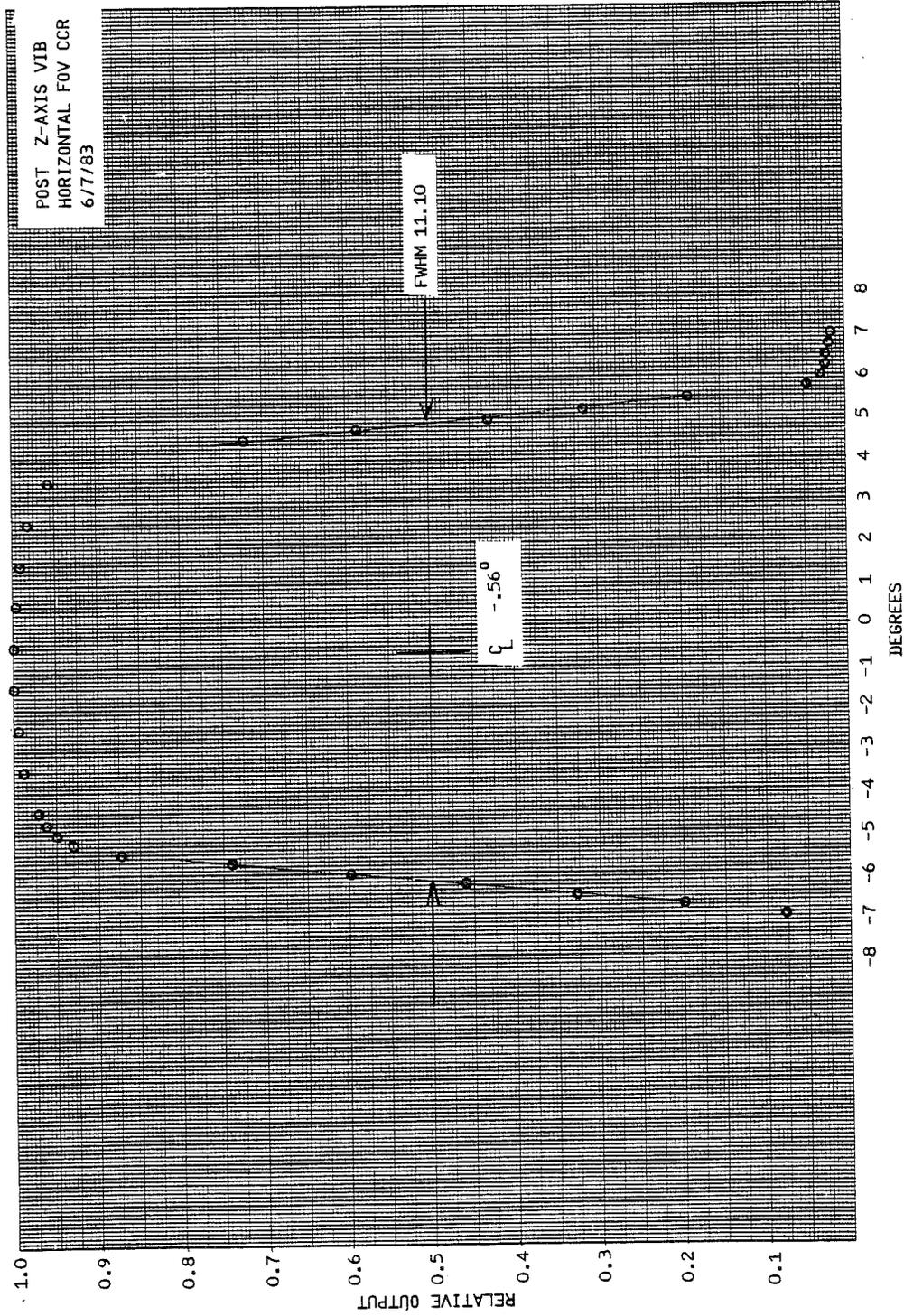


Figure 9-7 Post Z-Axis Vibration Horizontal CCR Fov

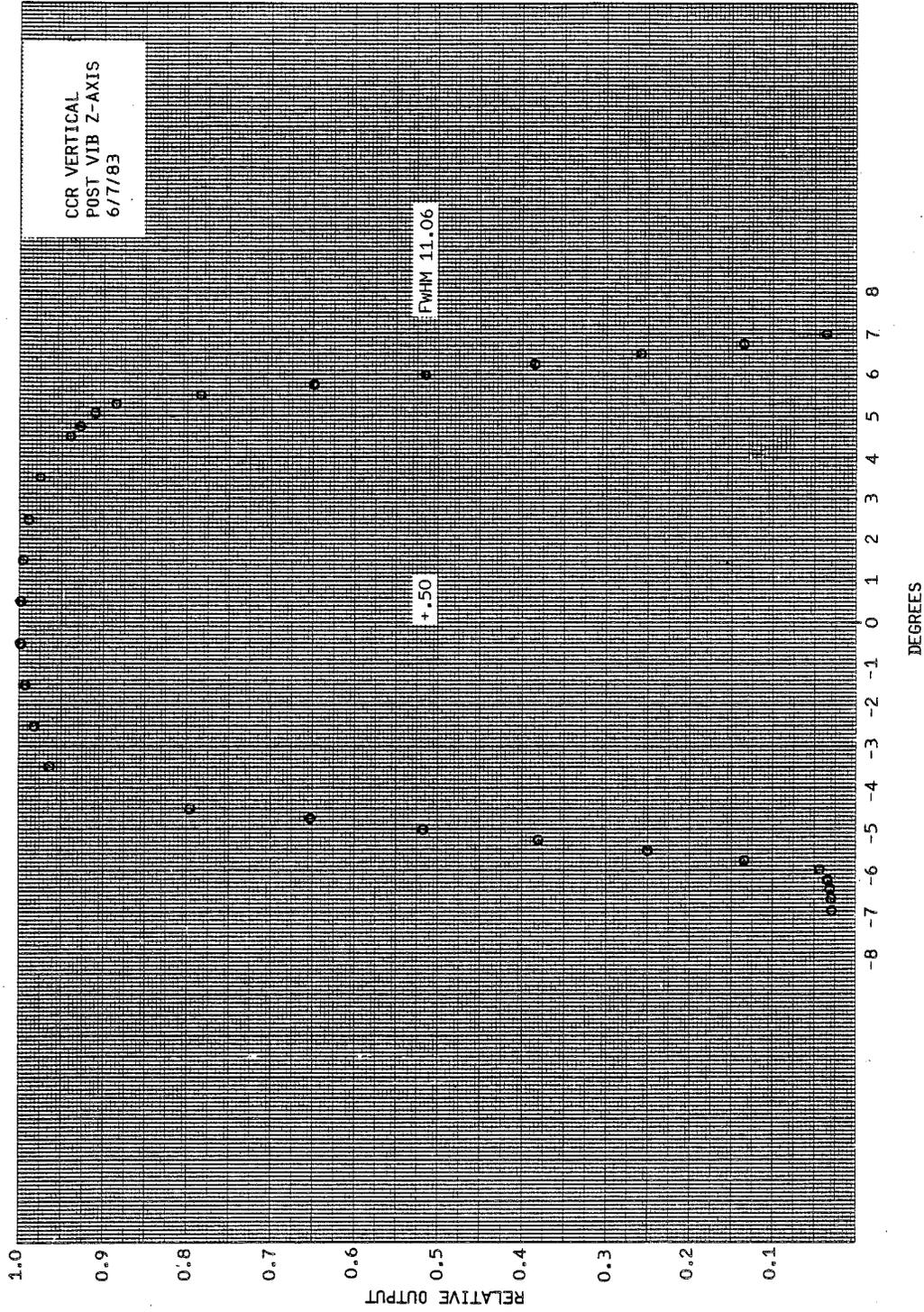


Figure 9-8 Post Z-Axis Vibration Vertical CCR FOV

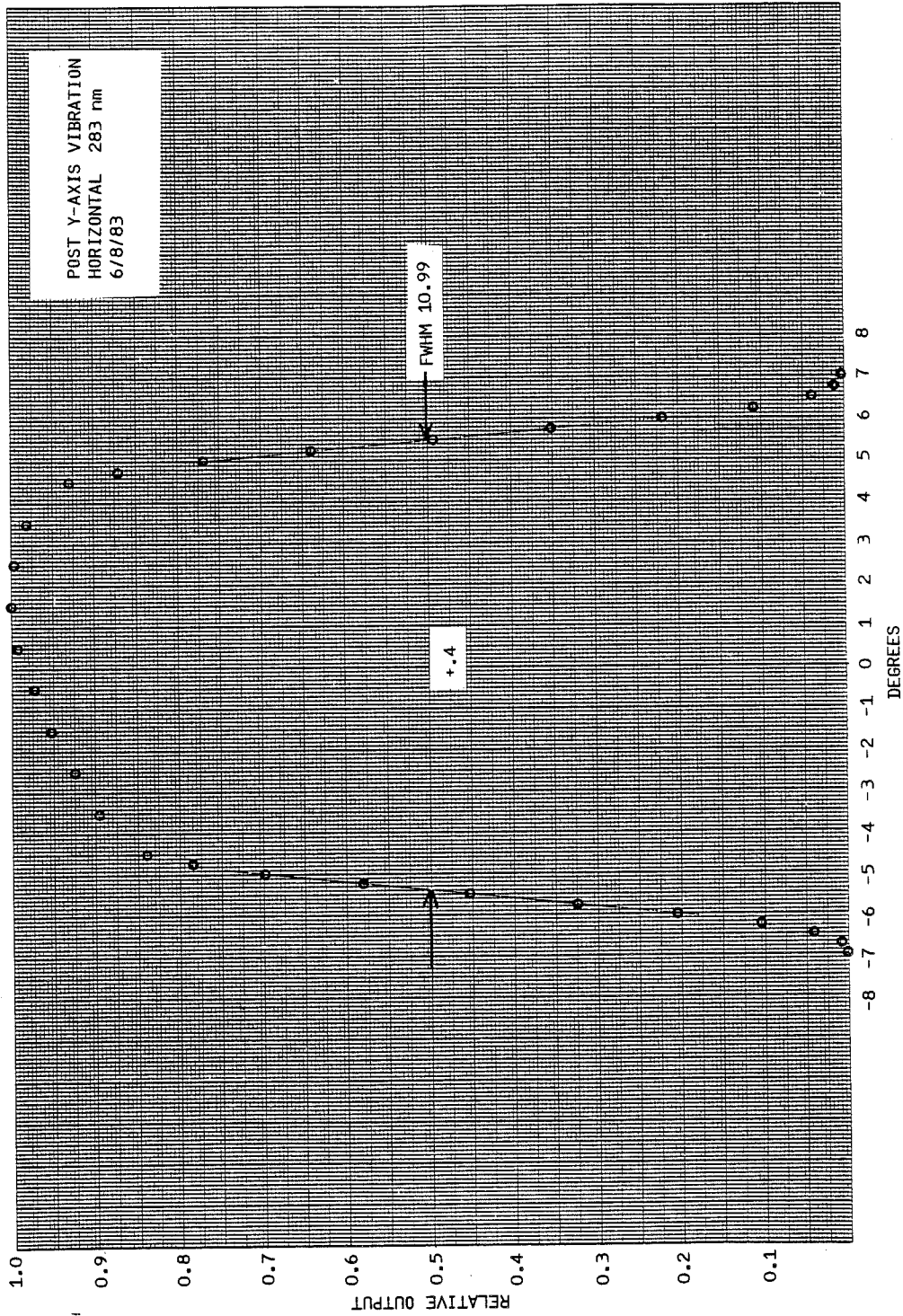
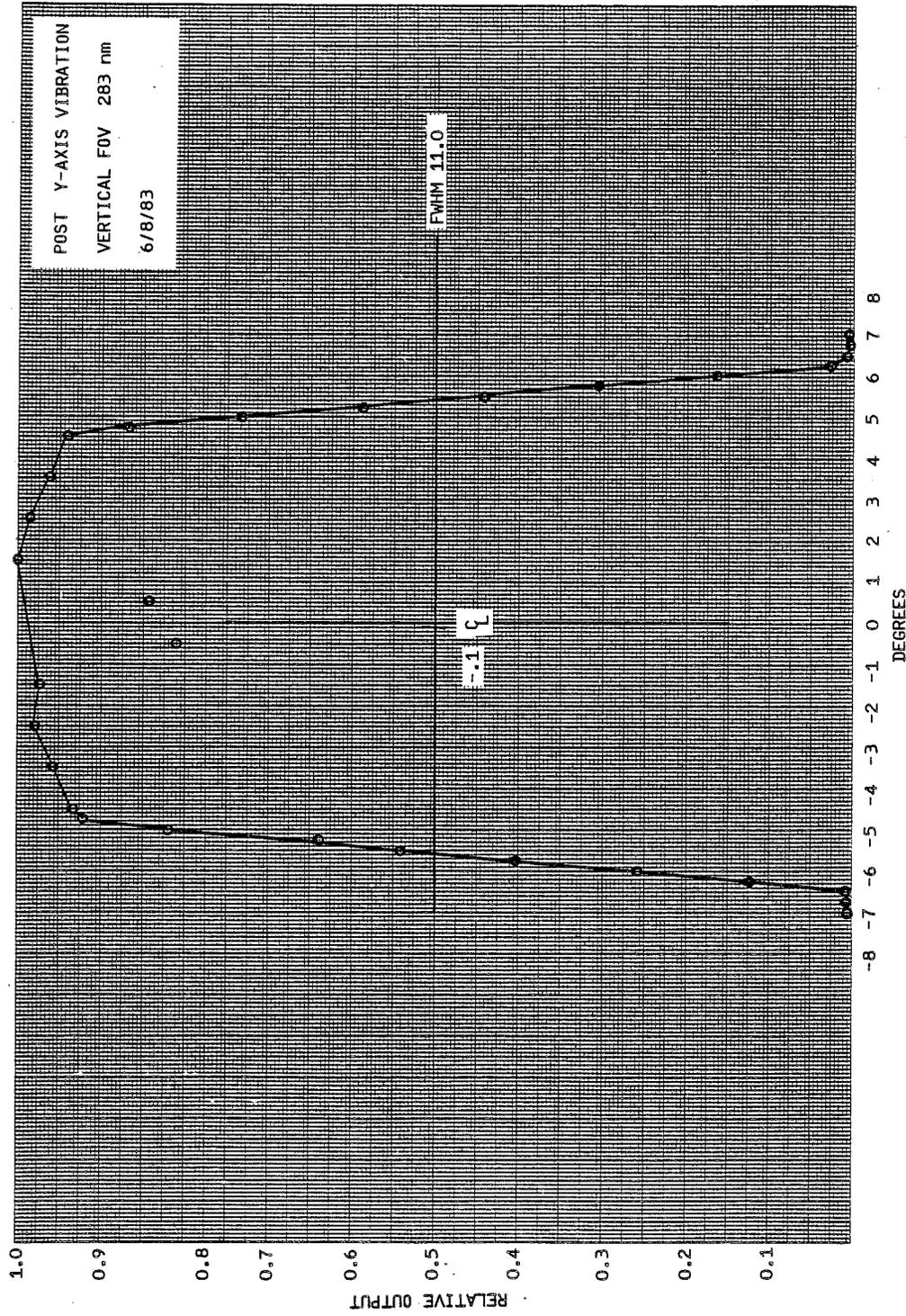


Figure 9-9 Post Y-Axis Vibration Horizontal FOV



A/N 3875

Figure 9-10 Post Y-Axis Vibration Vertical FOV

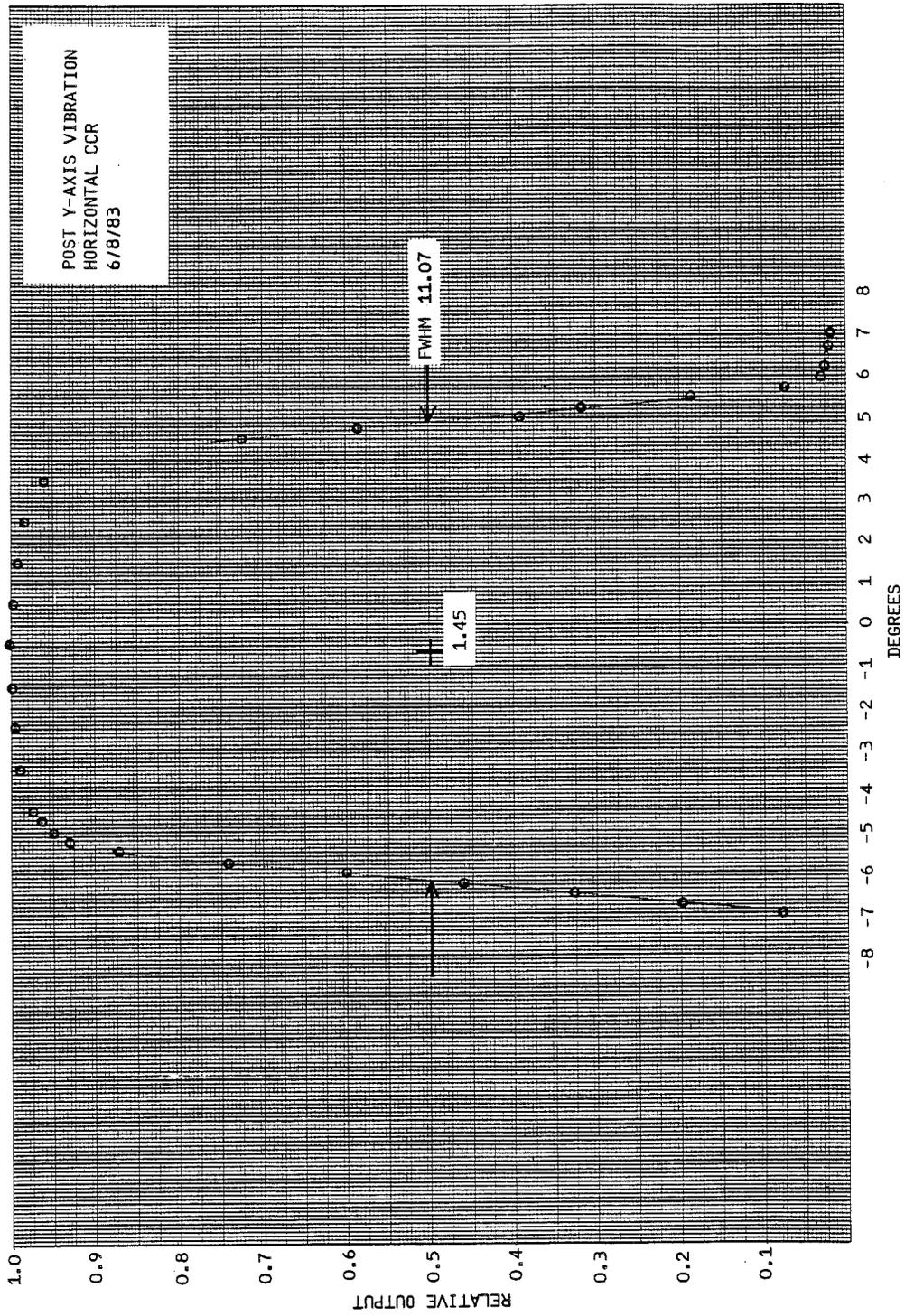


Figure 9-11 Post Y-Axis Vibration Horizontal CCR FOV

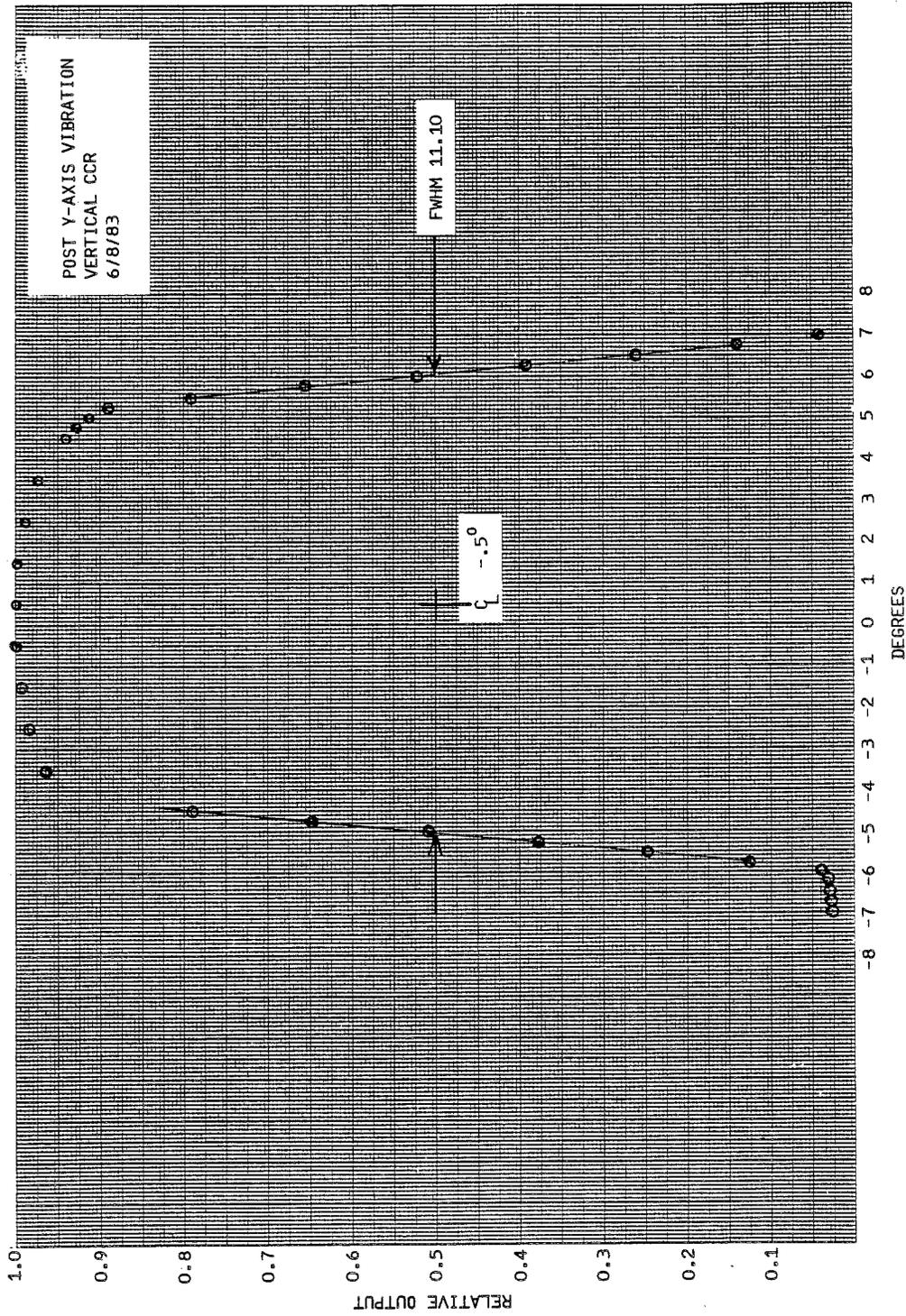


Figure 9-12 Post Y-Axis Vibration Vertical CCR FOV



B6802-78

A/N 3875

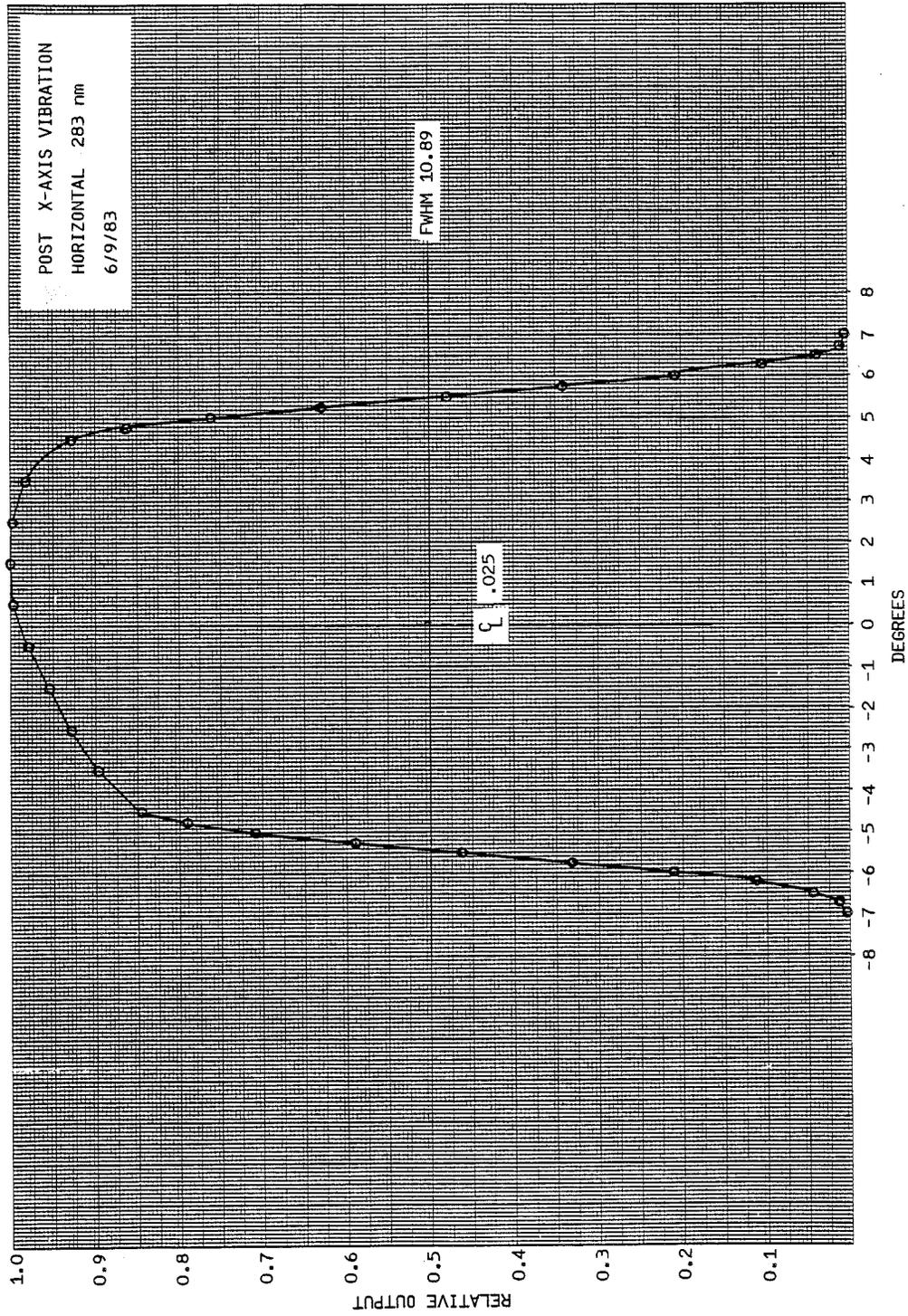


Figure 9-13 Post X-Axis Vibration Horizontal FOV

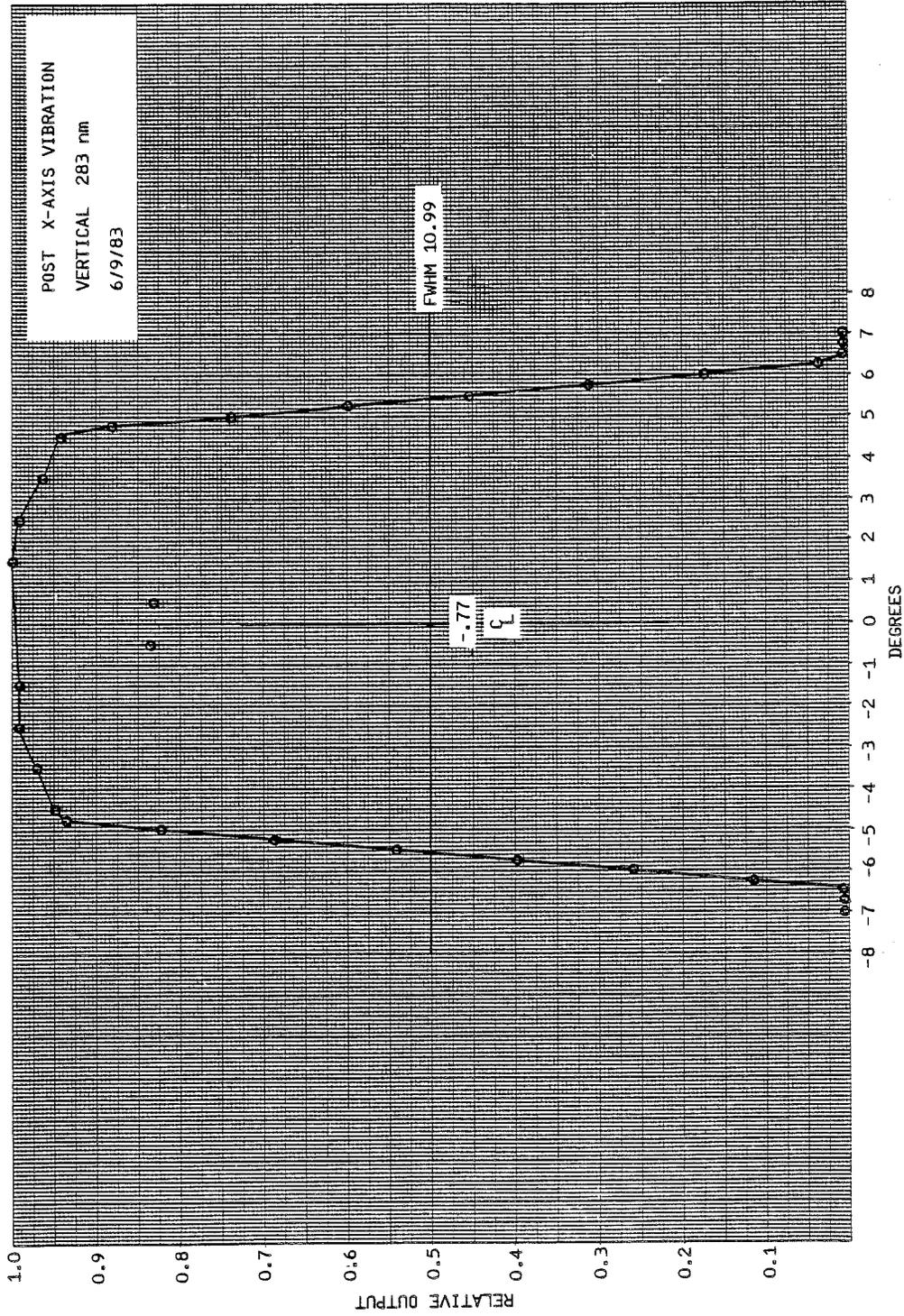


Figure 9-14 Post X-Axis Vibration Vertical FOV

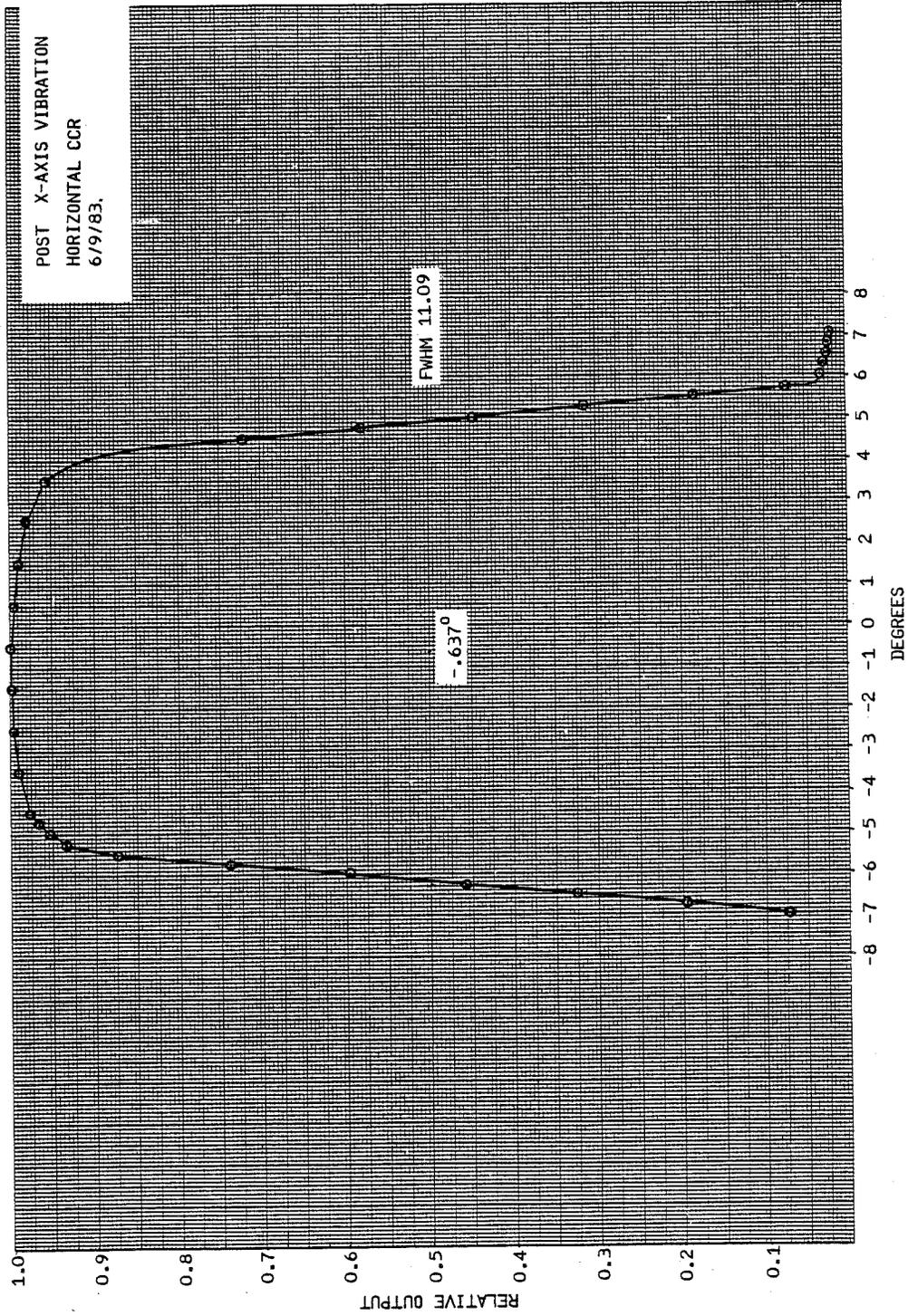


Figure 9-15 Post X-Axis Vibration Horizontal CCR FOV

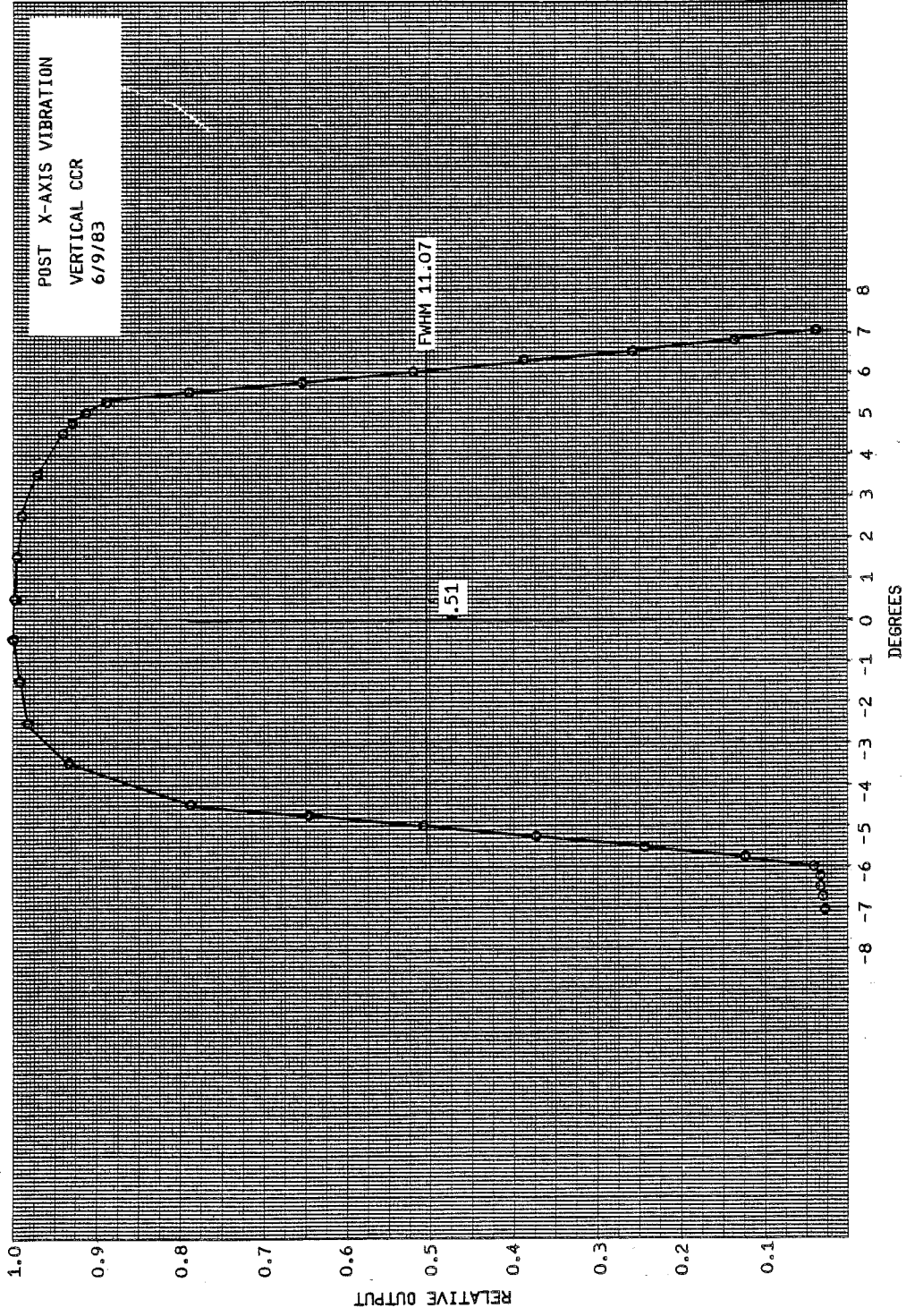


Figure 9-16 Post X-Axis Vibration Vertical CCR FOV

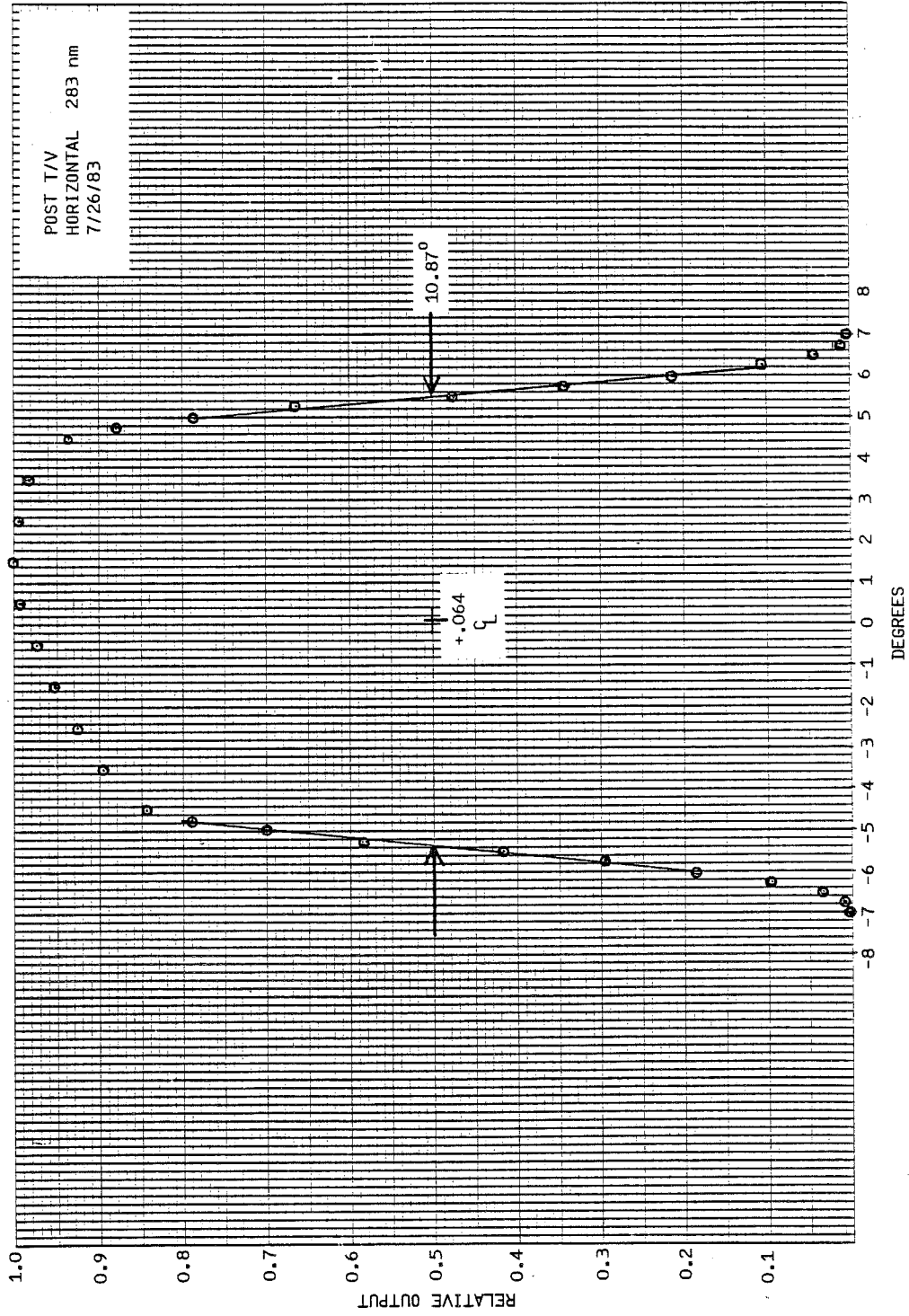


Figure 9-17 Post T/V Horizontal FOV



B6802-78

A/N 3875

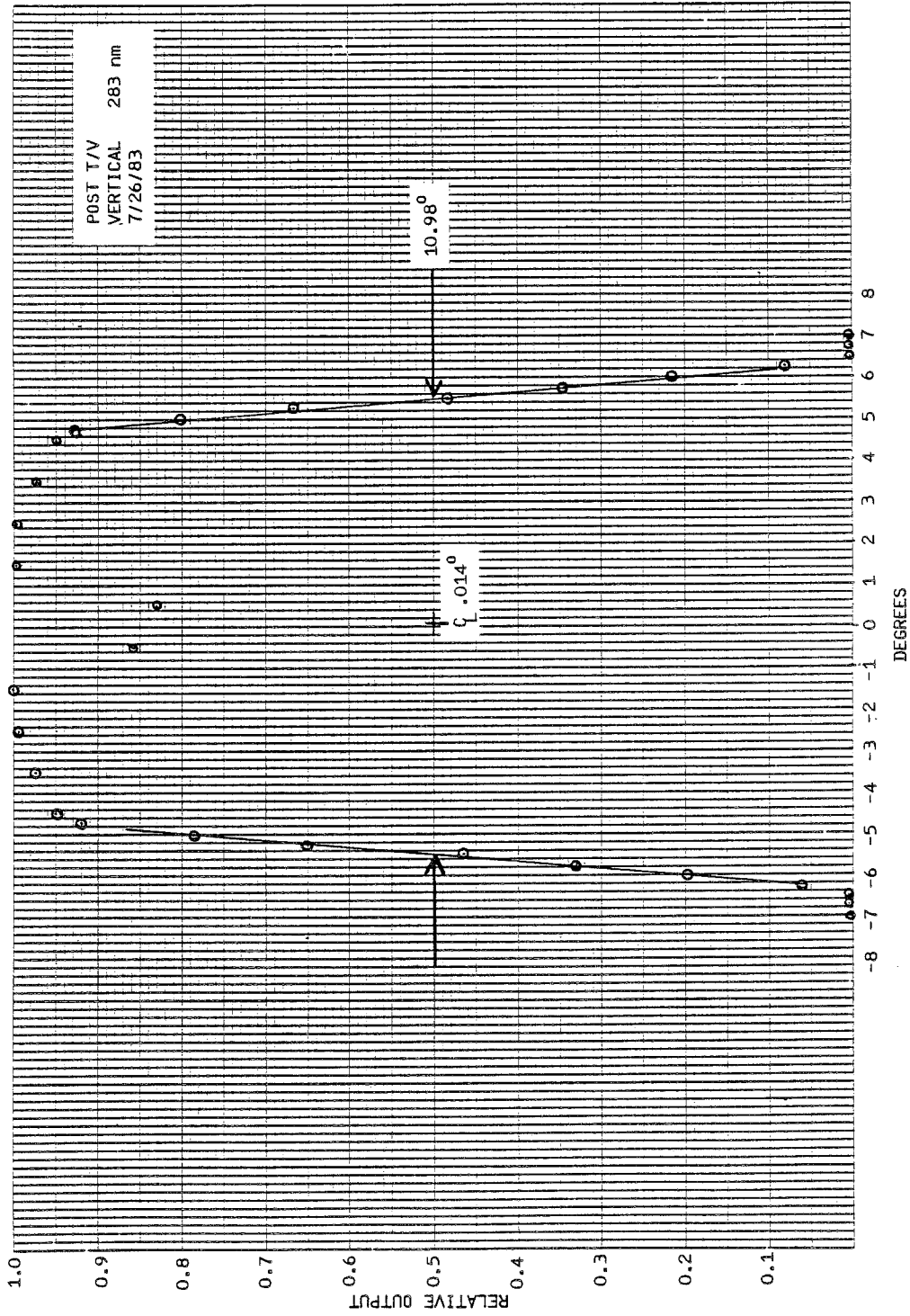


Figure 9-18 Post T/V Vertical FOV

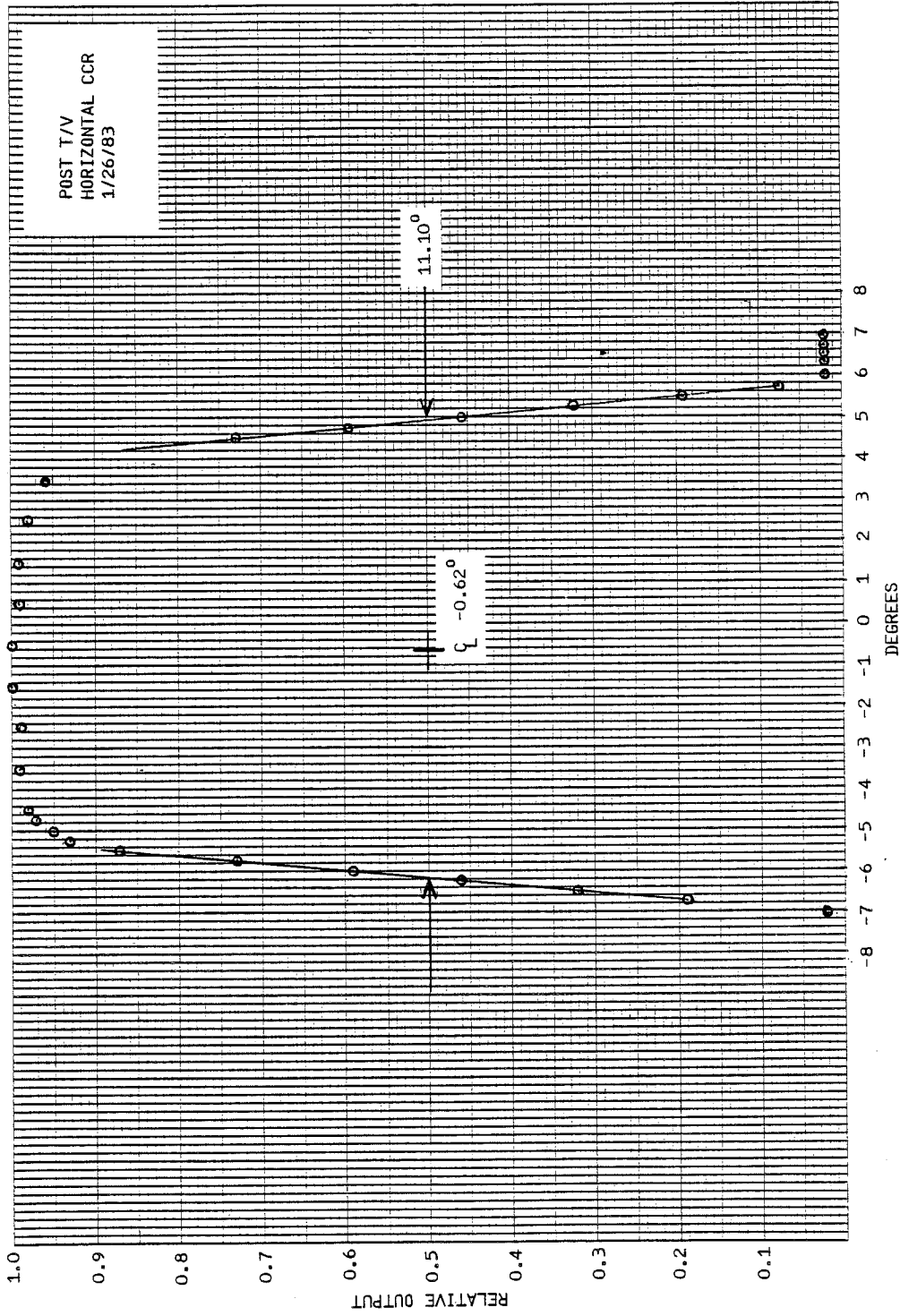


Figure 9-19 Post T/V Horizontal CCR FOV



A/N 3875

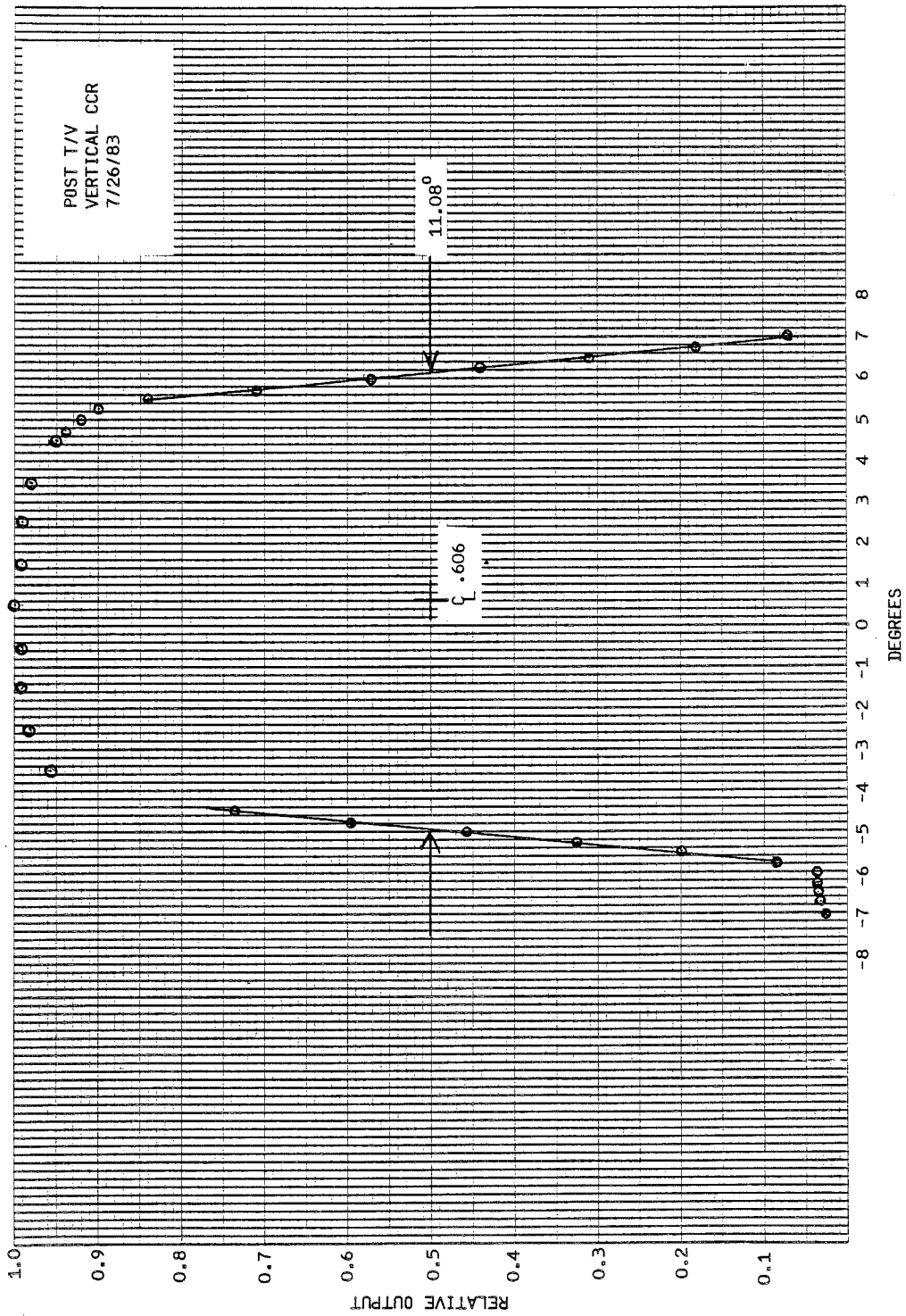


Figure 9-20 Post T/V Vertical CCR FOV



Section 10

OPTICAL ALIGNMENT

(Reference Test Procedure 68021)

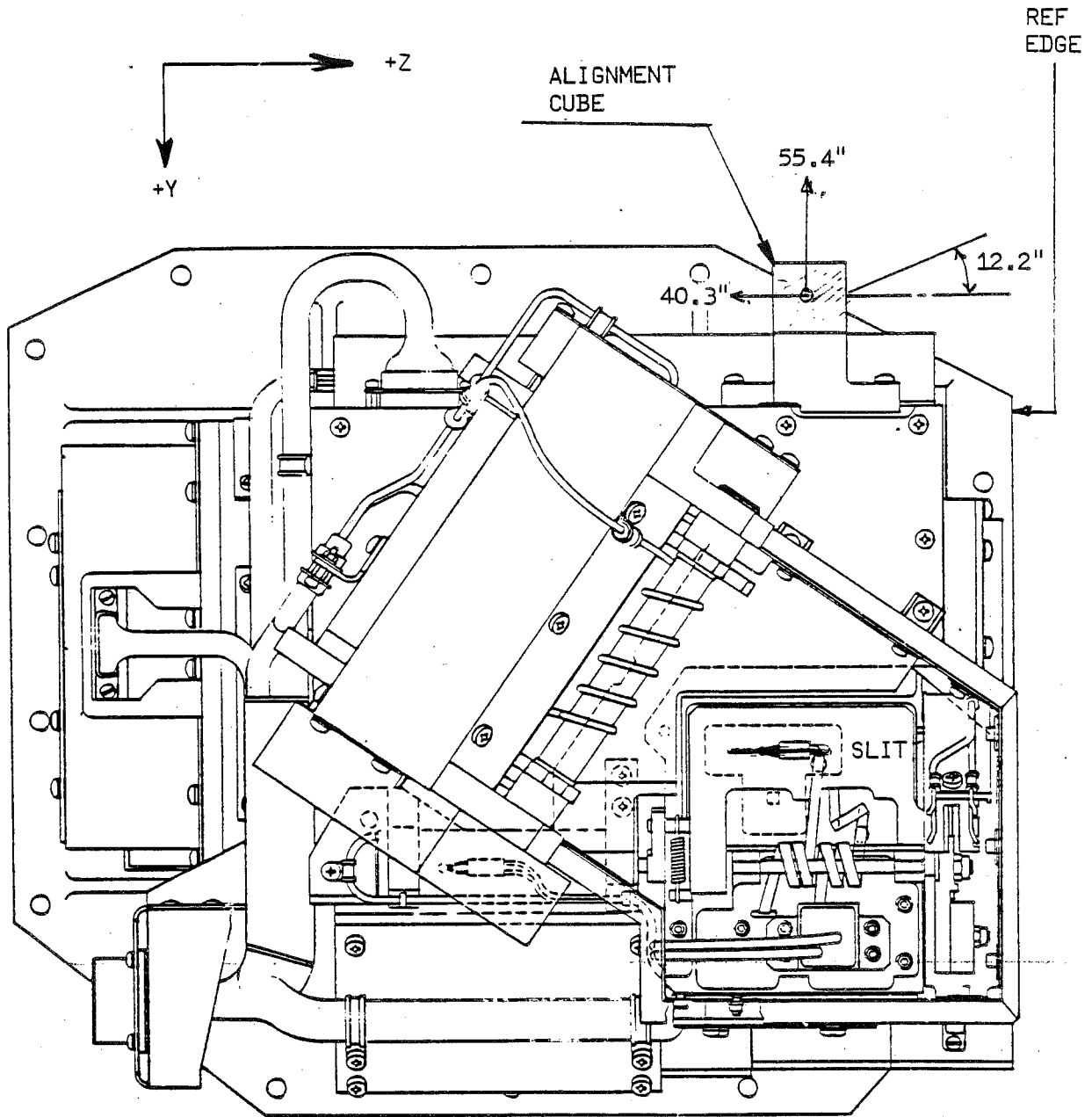
Alignment of the optical reference cube was performed and checked at baseline testing of the instrument. The normals to the reference cube are misaligned with respect to the Sensor Module Base as shown in Figure 10-16 and Table 10-1.

The monochromator to instrument reference (cube) and monochromator to Cloud Cover Radiometer alignment is determined from the field of view data.

Alignment changes during test are data taken from field of view measurements made at 283.0 nm during functional checks after environmental tests. These values represent the maximum changes observed when comparing all these test data. Details are given in the section on post environmental field of view measurements.

Table 10-1
OPTICAL ALIGNMENT

PARAMETER	SPECIFICATION	MEASURED
<u>OPTICAL ALIGNMENT</u>		
● INSTRUMENT REFERENCE (CUBE) TO X AXIS	0.1° MAX	Y-Z SURFACE NORMAL 0.015° IN -Y 0.011° IN -Z XY SURFACE NORMAL 0.003° IN -Y
● MONOCHROMATOR TO INSTRUMENT REFERENCE	0.1° MAX	0.27° IN -Y 0.18° IN -Z
● MONOCHROMATOR TO CCR	0.1° MAX	0.43° IN +Y 0.21° IN +Z
● ALIGNMENT CHANGES DURING TEST		
- MONOCHROMATOR	0.05° MAX	0.06° IN +Y 0.06° IN -Z
- CCR	0.05° MAX	0.1° IN +Y 0.1° IN -Z



A/N 3875

Figure 10-1 Optical Alignment



Section 11

OUT OF FIELD RESPONSE

(Reference Test Procedure 68027)

A mini-arc lamp was used as an intense UV source to illuminate the instrument while it is viewing a black background. The Sensor Module was pointed in four directions plus and minus 15 degrees along the horizontal and vertical axis.

Due to test fixture setup it was not possible to eliminate all the background radiation while viewing the black panels. As can be seen from the data (Table 11-1), the horizontal plus, horizontal minus, and vertical plus 15 degree positions are approximately the same values, whereas the minus 15 degree vertical location is at a much lower level.

The out of field response is determined from measurements of instrument response made during field of view testing. Scans of both the vertical and horizontal directions were made out to 17 degrees on each side of the center of the field of view.

Out of field response is determined from the ratio of the energy in field to out of field.

$$\text{Out of Field Response} = \frac{C_{\text{out of field}}}{C_{\text{in field}}} = \frac{C_{\text{OOF}}}{C_{\text{IF}}}$$

To determine C_{OOF} and C_{IF} a curve of the instrument response in counts at each angle measured was plotted. An average value of counts is determined from each radially symmetric angular position.

$$\bar{C}_{\theta} = \frac{C_{\text{H}+} + C_{\text{H}-} + C_{\text{V}+} + C_{\text{V}-}}{4}$$

A curve of $(\bar{C}_{\theta})(\theta)$ vs. θ is plotted over the range of values for $\theta = 0$ to $\theta = 17$. The following curves are examples at 283.0 nm.



From the curve a close approximation of the areas underneath $\theta = 0$ to θ_1 and $\theta = \theta_2 = \theta_3$ for

$$C_{IF} = \int_0^{\theta_1} \frac{\partial C}{\partial A} 2\pi\theta d\theta = \frac{2\pi}{\partial A} \int_0^{\theta_1} \bar{C}_\theta d\theta$$

and

$$C_{OOF} = \frac{2\pi}{\partial A} \int_{\theta_2}^{\theta_3} \bar{C}_\theta \theta d\theta$$

where

C = counts per unit area

A = angular area of the source of illumination in radians

θ_1 = upper limit of in field response in radians

(determined from the $\frac{(\text{FWHM} + \text{width of source})}{2}$ to 1

θ_2 = lower limit of out of field response in radians

θ_3 = upper limit of out of field response band in radians

using the Trapezoidal rule to evaluate the integral:

$$C_{IF} = \frac{2\pi}{\partial A} \int_0^{\theta_1} \bar{C}_\theta d\theta = \left[\frac{2\pi}{\partial A} \right] \frac{1}{2} \Delta C (\bar{C}_0 + 2\bar{C}_1 + 2\bar{C}_2 + \dots + 2\bar{C}_{N-1} + \bar{C}_N)$$

$$A = 3.87 \times 10^{-3} \text{ radians}$$

$$\theta_1 = .1178 \text{ radians}$$

$$\theta_2 = .1274 \text{ radians}$$

$$\theta_3 = .2967 \text{ radians}$$

Values for $(\bar{C} \times \theta)$ are determined for the curve at increments of ΔC .

Finally, the out of field response is determined from,

$$\text{OOF Response} = \frac{C_{OOF}}{C_{IF}}$$

The following Table (11-2) gives the results for all discrete wavelengths.



Table 11-1
POINTING POSITION IN DEGREES

WAVELENGTH	Horiz Vert 0 0	Horiz Vert 15 0	Horiz Vert -15 0	Horiz Vert 0 15	Horiz Vert 0 -15
252.0	4.24X10 ⁻⁹	4.96X10 ⁻¹³	4.75X10 ⁻¹³	4.93X10 ⁻¹³	7.34X10 ⁻¹⁴
273.5	4.54	5.19	4.87	4.58	7.34
283.0	4.62	5.19	4.94	4.64	7.34
287.5	4.72	5.52	5.14	4.77	7.80
292.2	4.86	5.52	5.37	4.90	7.80
297.5	5.04	5.74	5.58	5.08	8.11
301.9	5.19	5.94	5.80	5.28	8.4
305.8	5.38	6.14	5.97	5.42	9.18
312.5	5.65	6.47	6.23	5.62	8.57
317.5	5.90	6.72	6.52	6.04	9.03
331.2	7.40	8.49	8.28	7.28	1.18X10 ⁻¹³
339.8	8.69	9.98	9.87	8.51	1.29X10 ⁻¹³
CCR	3.57x10 ⁻¹¹	0	0	0	0

A/N 3875



A/N 3675

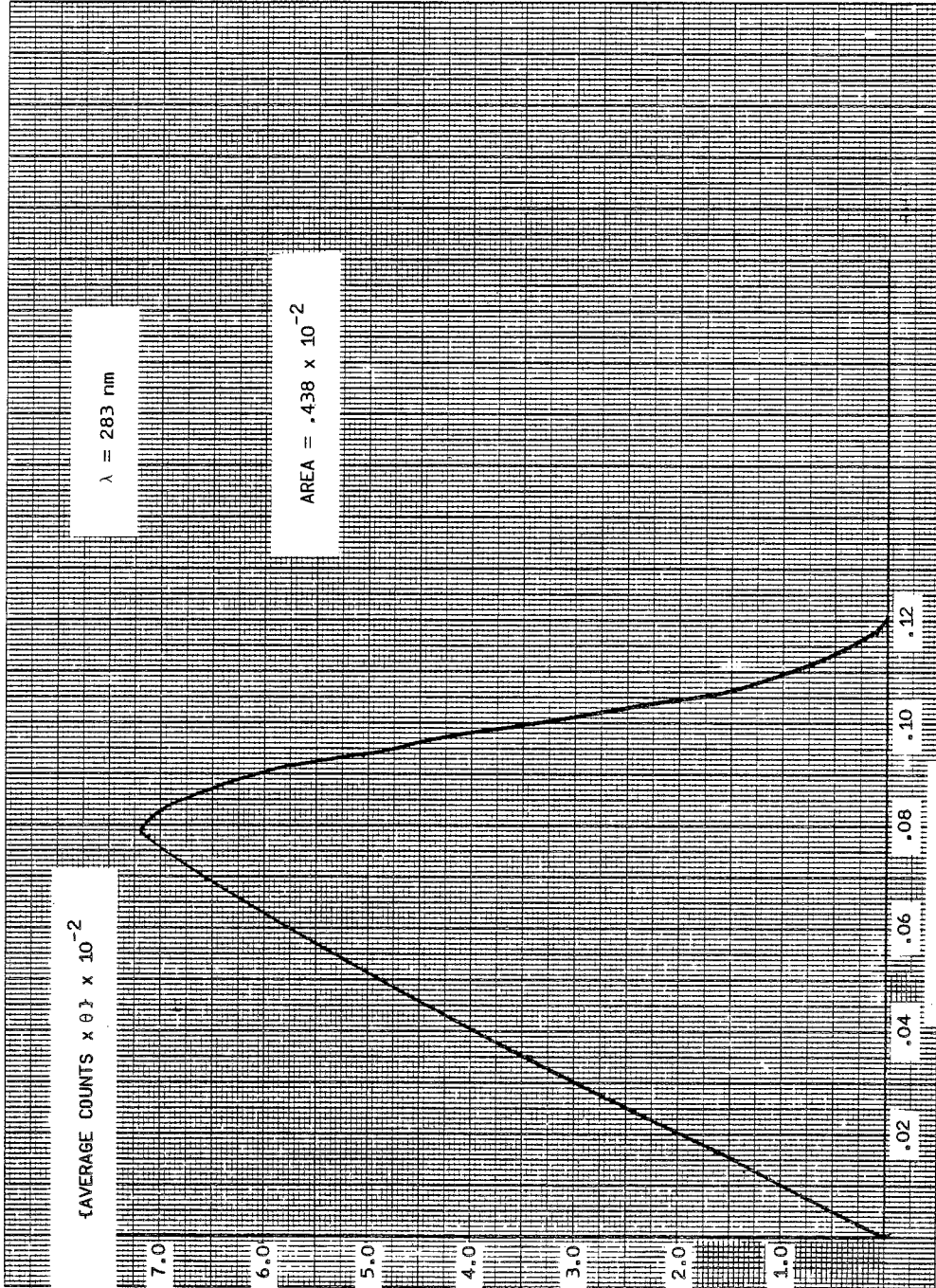


Figure 11-1 Average Counts (\bar{C}_{IF}) in Field

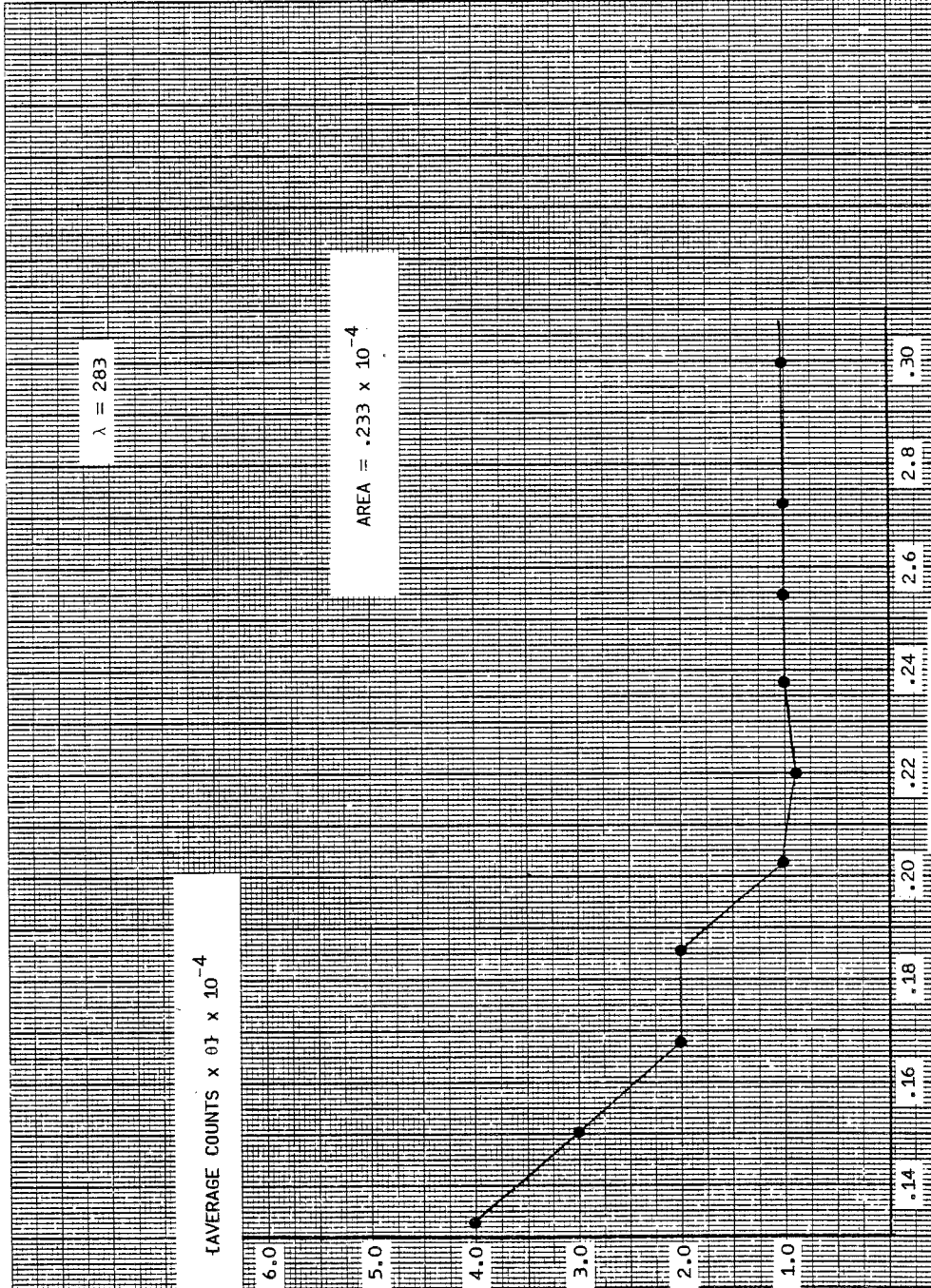


Figure 11-2 Average Counts (\bar{C}_{OOF}) Out of Field



Table 11-2
OUT OF FIELD RESPONSE

WAVELENGTH	OUT-OF-FIELD RESPONSE
252.0	0.93 %
273.5	0.89 %
283.0	0.50 %
287.5	0.64 %
292.2	1.07 %
297.6	0.68 %
301.9	0.70 %
305.8	0.59 %
312.5	0.84 %
317.5	0.64 %
331.2	0.50 %
339.8	0.69 %
AVERAGE	0.72 %
CCR	0.17 %

A/N 3875



Section 12

GONIOMETRIC CALIBRATION

(Reference Test Procedure 68034)

Goniometric calibration was performed using the fixture illustrated in Figure 12-1. This fixture locates the center of the instrument diffuser at the intersection of the horizontal and vertical axes of rotation. A target (FEL Lamp) placed 3 meters from the Sensor Module provides it with nearly parallel, uniform illumination.

Data was taken over an angular field which covers the expected angles of illumination during orbit. Scans were made in increments of 2 degrees in elevation and 5 degrees in azimuth. Two SERs (SBUV-GC-83-386 and SBUV-GC-83-390) cover the use of the data with respect to the spacecraft position.

Included here are the raw data in instrument counts (Table 12-1a,b,c,d) plots of the center wavelength at each Azimuth angle (Figures 12-2 through 12-10).

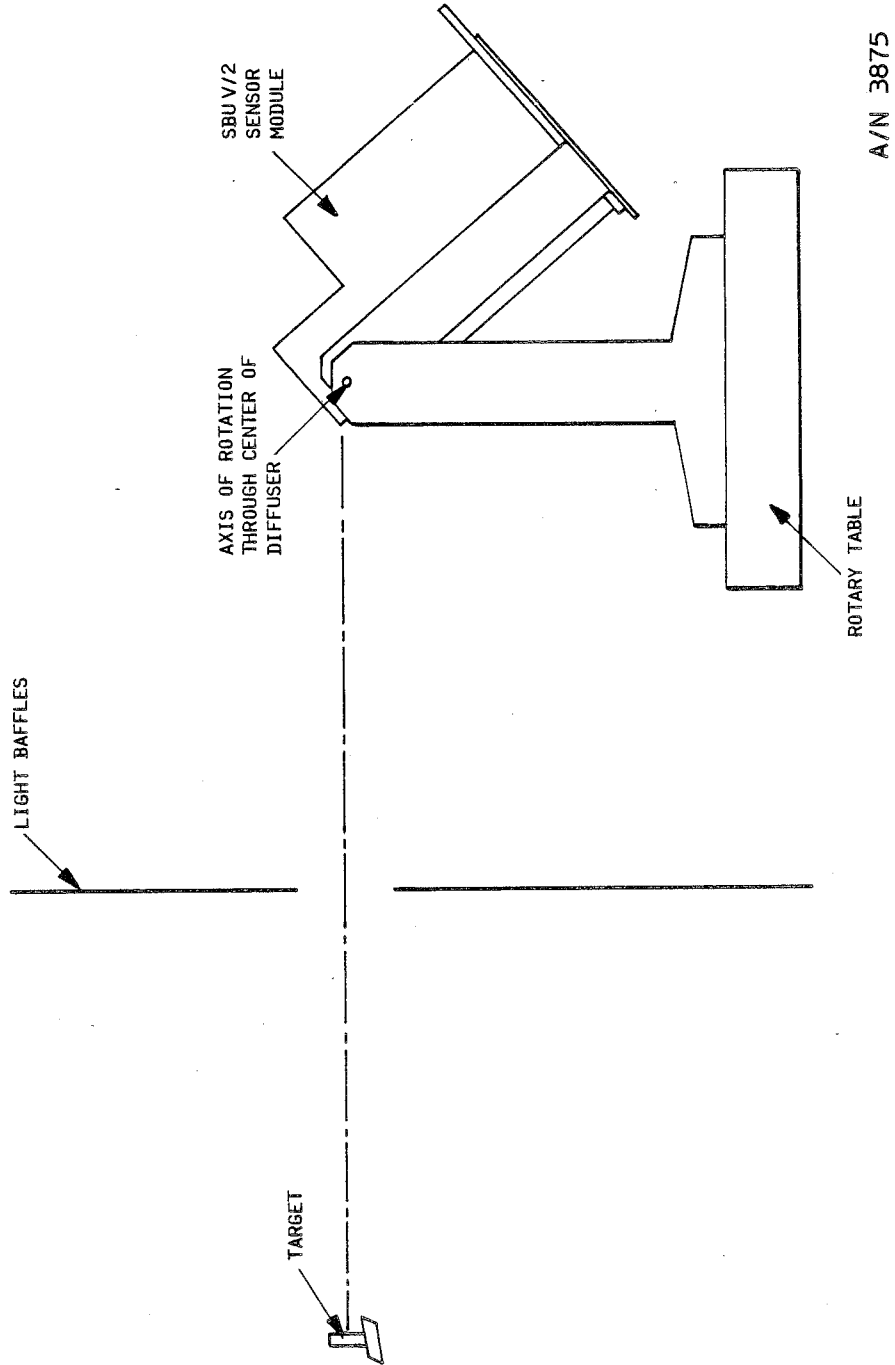


Figure 12-1 Goniometric Calibration Test Fixture



Table 12-1a
GONIOMETRIC DATA AT WAVELENGTH (250 nm)

ELEVATION	AZIMUTH								
	30	34	35	40	46	50	55	60	65
0	423	433	427	418	408	380	350	339	303
2	399	397	398	394	363	350	337	305	296.59
4	366	377	371	370	351	341	328	292.39	277.19
6	347	351	356	342	325	320	305	287.39	266
8	317	316	317	322	302	282.59	283	270.79	246.79
10	294.19	302	304	294.39	287.79	277.79	244.59	243.79	213.99
12	268.79	269.19	264.79	264.19	263.59	242.79	234.19	225.59	212.99
14	254.19	252.39	244.59	252.79	232.99	228.99	212.79	195.79	184.19
16	216.19	230.79	225.19	220.59	207.79	205.59	195.19	180.79	171.00
18	208.79	194.79	206.59	205.59	197.79	178.79	171.19	172.79	165.79
20	167.79	169.79	177.99	169.99	173.79	164.59	154.39	142.59	139.59

A/N 3875

Table 12-1b
GONIOMETRIC DATA AT WAVELENGTH (300 nm)

ELEVATION	AZIMUTH								
	30	34	35	40	46	50	55	60	65
0	3373	3404	3375	3319	3181	3008	2797	2577	2333
2	3118	3137	3134	3096	2954	2809	2610	2382	2187
4	2882	2903	2889	2851	2749	2598	2430	2238	2029
6	2654	2670	2669	2634	2519	2378	2248	2061	1877
8	2424	2432	2438	2405	2310	2188	2049	1898	1714
10	2198	2219	2208	2181	2113	1986	1845	1720	1546
12	1978	1995	1989	1965	1877	1806	1666	1543	1400
14	1748	1756	1752	1752	1671	1584	1481	1357	1249
16	1542	1550	1564	1526	1461	1389	1294	1189	1073
18	1339	1332	1329	1308	1260	1187	1109	1011	933
20	1083	1098	1090	1072	1024	971	916	828	760

A/N 3875



Table 12-1c
GONIOMETRIC DATA AT WAVELENGTH (350 nm)

ELEVATION	AZIMUTH								
	30	34	35	40	46	50	55	60	65
0	19610	19774	19708	19386	18600	17567	16297	14967	13530
2	18152	18240	18224	17931	17235	16325	15117	13893	12604
4	16698	16841	16856	16545	15937	15050	14014	12868	11666
6	15373	15481	15472	15196	14667	13849	12904	11847	10736
8	14022	14127	14096	13874	13360	12670	11800	10797	9790
10	12740	12787	12732	12527	12116	11471	10656	9801	8866
12	11390	11435	11449	11253	10867	10282	9562	8791	7930
14	10094	10139	10137	9969	9611	9059	8445	7759	6982
16	8756	8821	8868	8708	8381	7916	7352	6725	6070
18	7534	7572	7537	7395	7103	6705	6212	5698	5124
20	6100	6153	6134	6019	5804	5445	5070	4614	4158

A/N 3875

Table 12-1d
GONIOMETRIC DATA AT WAVELENGTH (400 nm)

ELEVATION	AZIMUTH								
	30	34	35	40	46	50	55	60	65
0	35002	35275	35214	34600	33286	31353	29131	26785	24265
2	32368	32531	32535	31932	30812	29157	27066	24885	22585
4	29833	30012	30024	29494	28448	26937	25054	23046	20948
6	27394	27560	27551	27097	26140	24784	23095	21212	19277
8	24964	25102	25116	24656	23810	22601	21037	19328	17544
10	22585	22734	22682	22350	21592	20437	19066	17497	15864
12	20313	20365	20413	20066	19347	18345	17066	15712	14250
14	17904	18065	18008	17727	17055	16163	15085	13852	12562
16	15602	15676	15702	15457	14895	14092	13114	12043	10873
18	13298	13396	13351	13155	12643	11931	11075	10156	9179
20	10819	10870	10852	10695	10298	9689	9045	8277	7482

A/N 3875

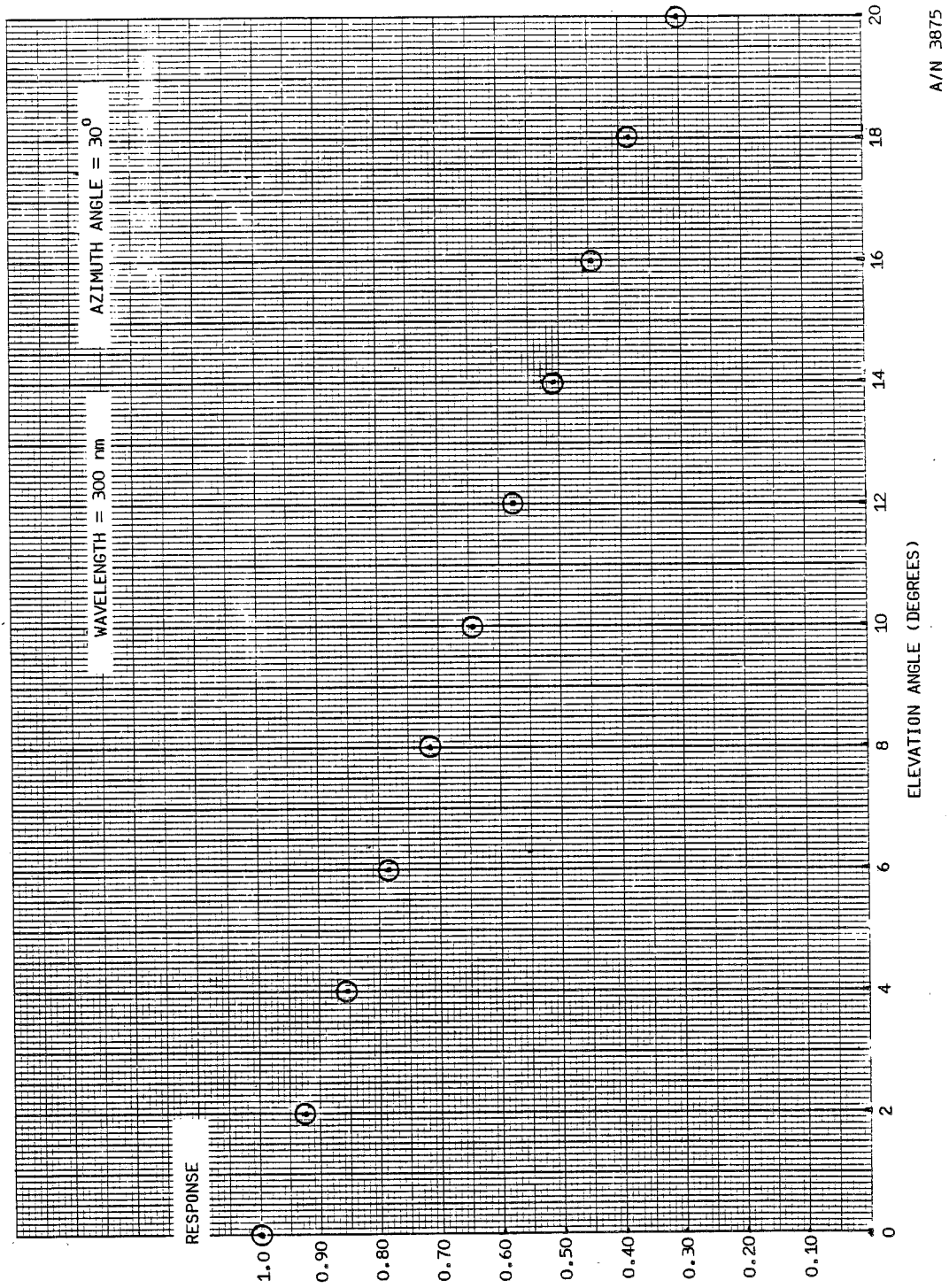


Figure 12-2 Goniometric Response vs. Elevation Angle



B6802-78

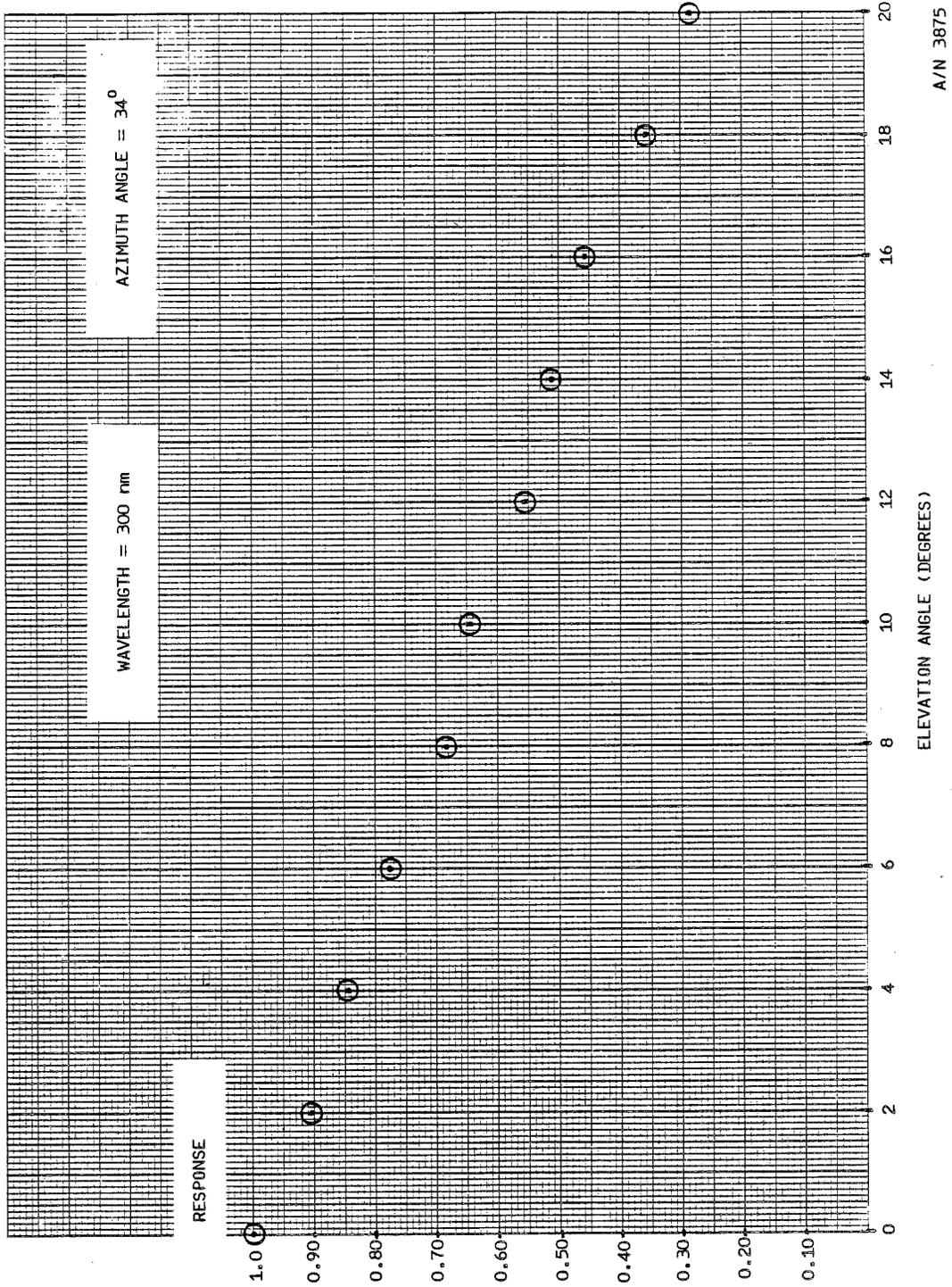
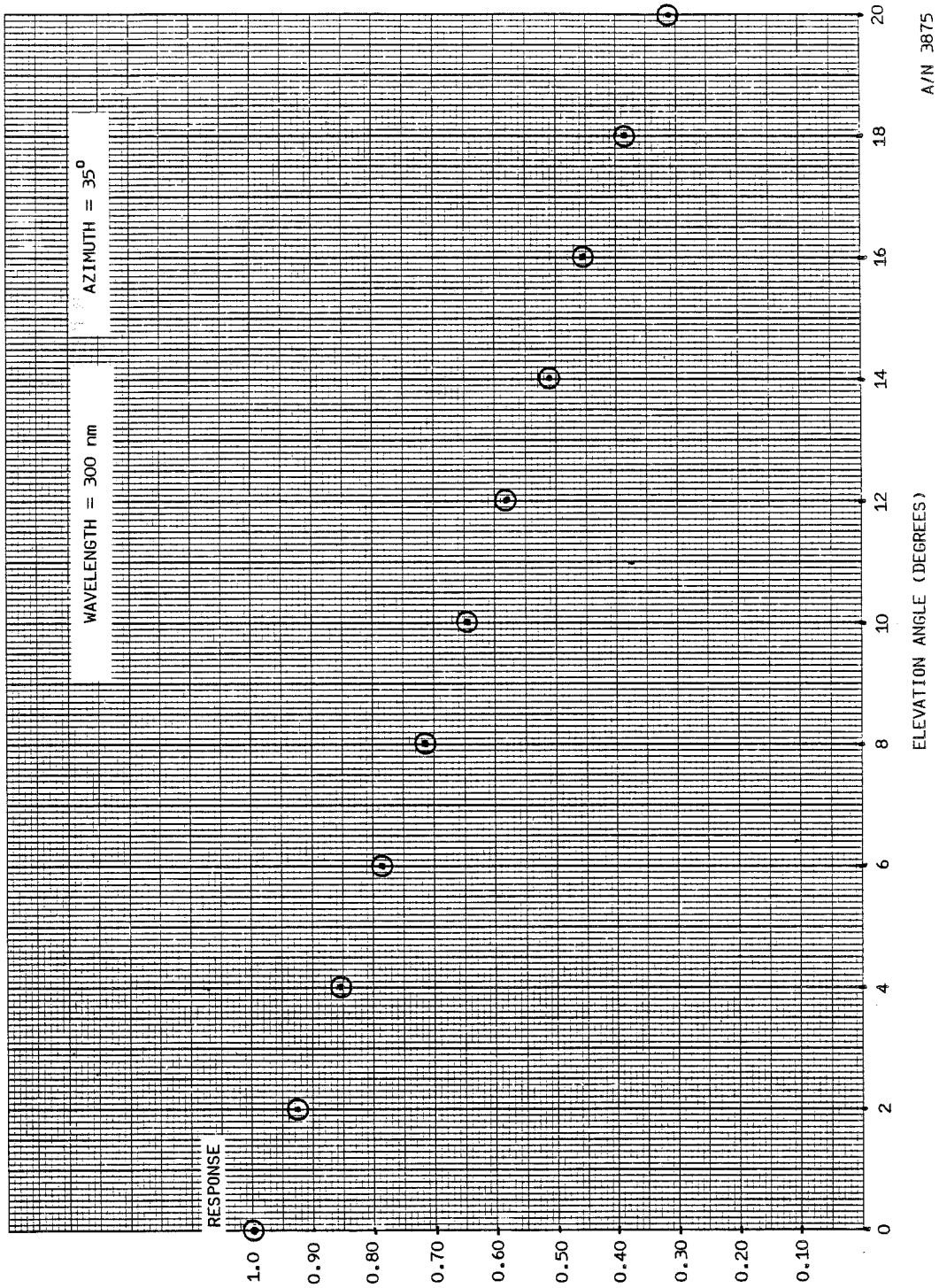


Figure 12-3 Goniometric Response vs. Elevation Angle



A/N 3875

Figure 12-4 Goniometric Response vs. Elevation Angle

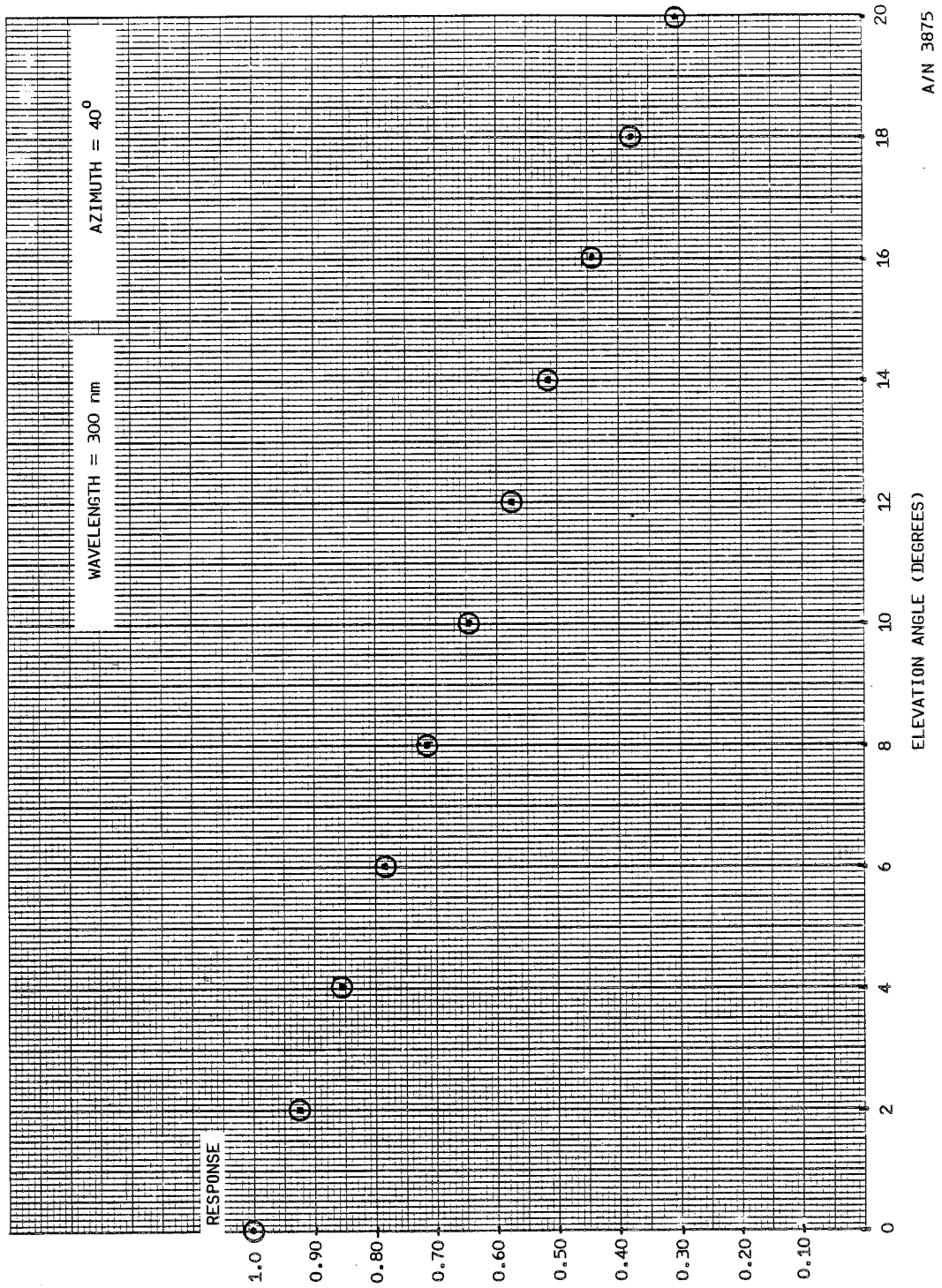


Figure 12-5 Coniometric Response vs. Elevation Angle

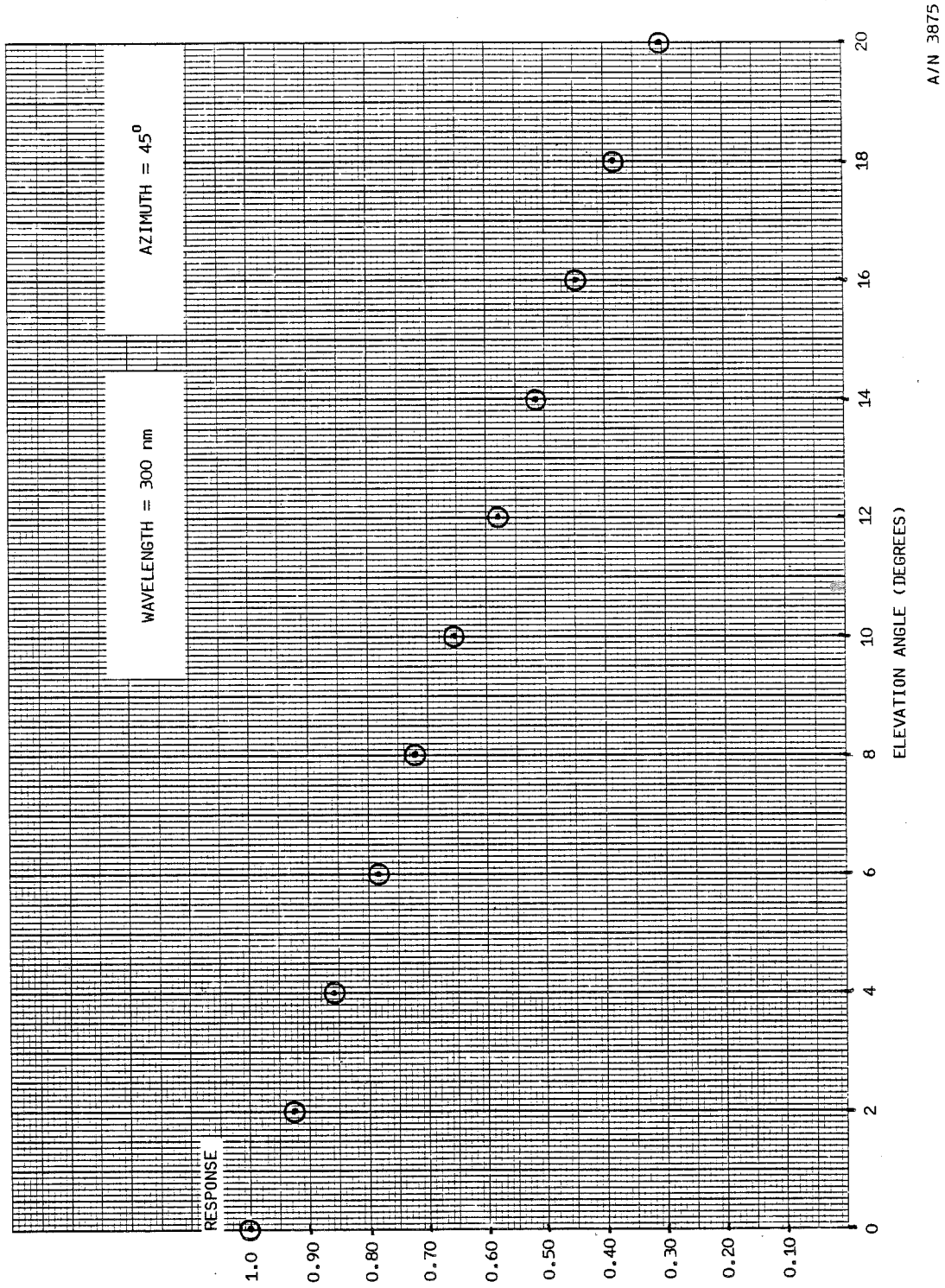


Figure 12-6 Goniometric Response vs. Elevation Angle

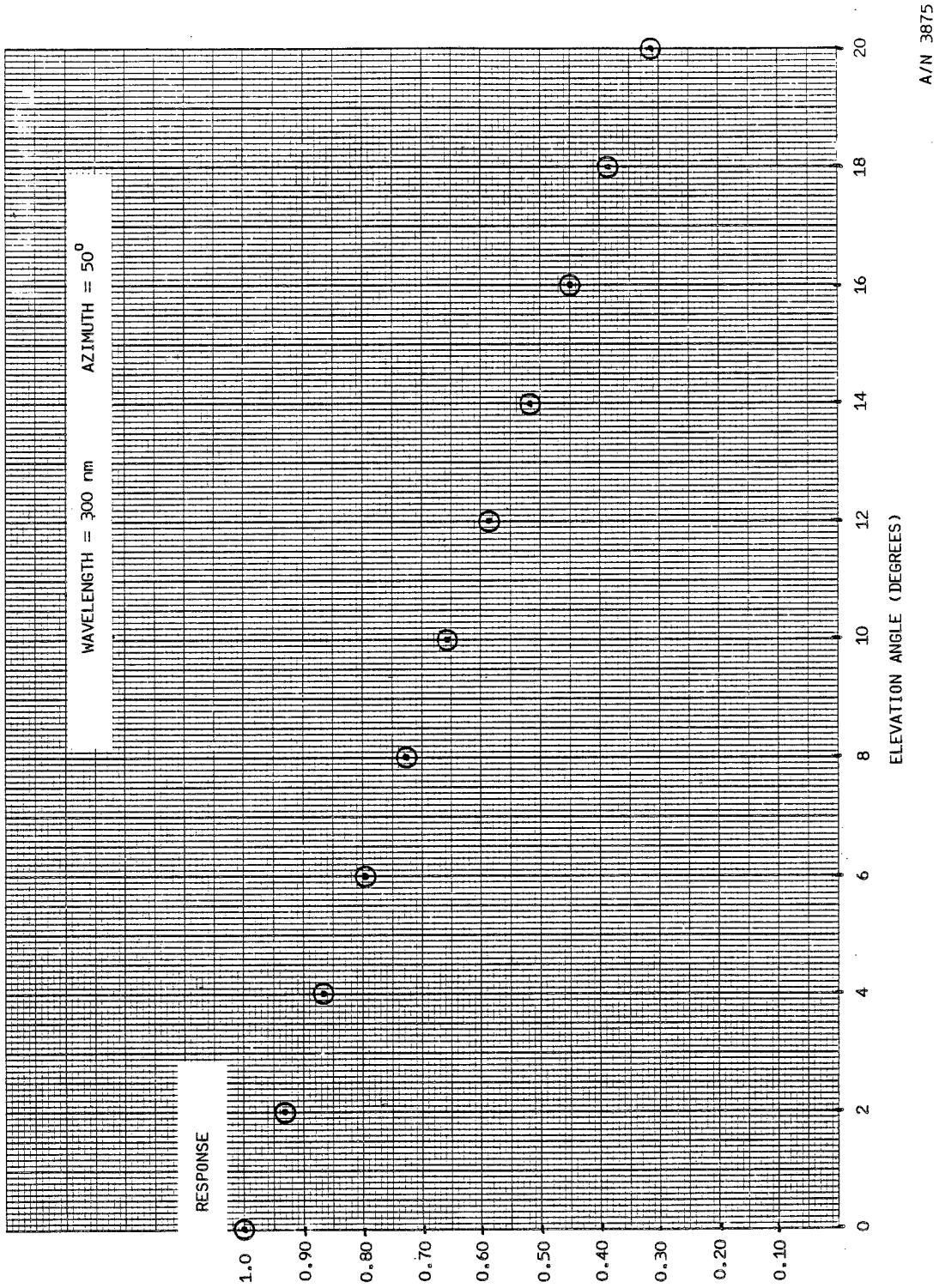
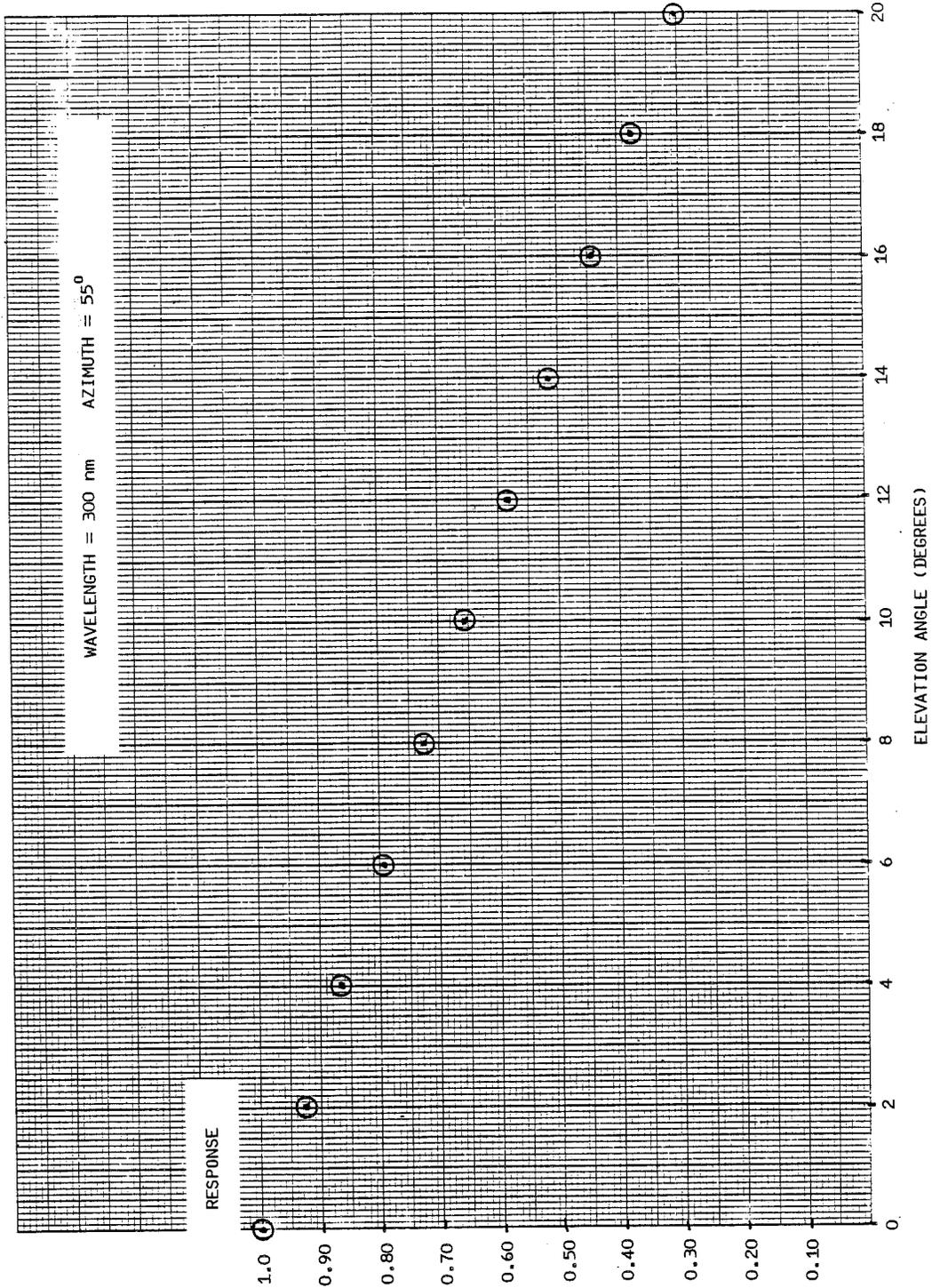


Figure 12-7 Goniometric Response vs. Elevation Angle



A/N 3875

Figure 12-8 Coniometric Response vs. Elevation Angle



B6802-78

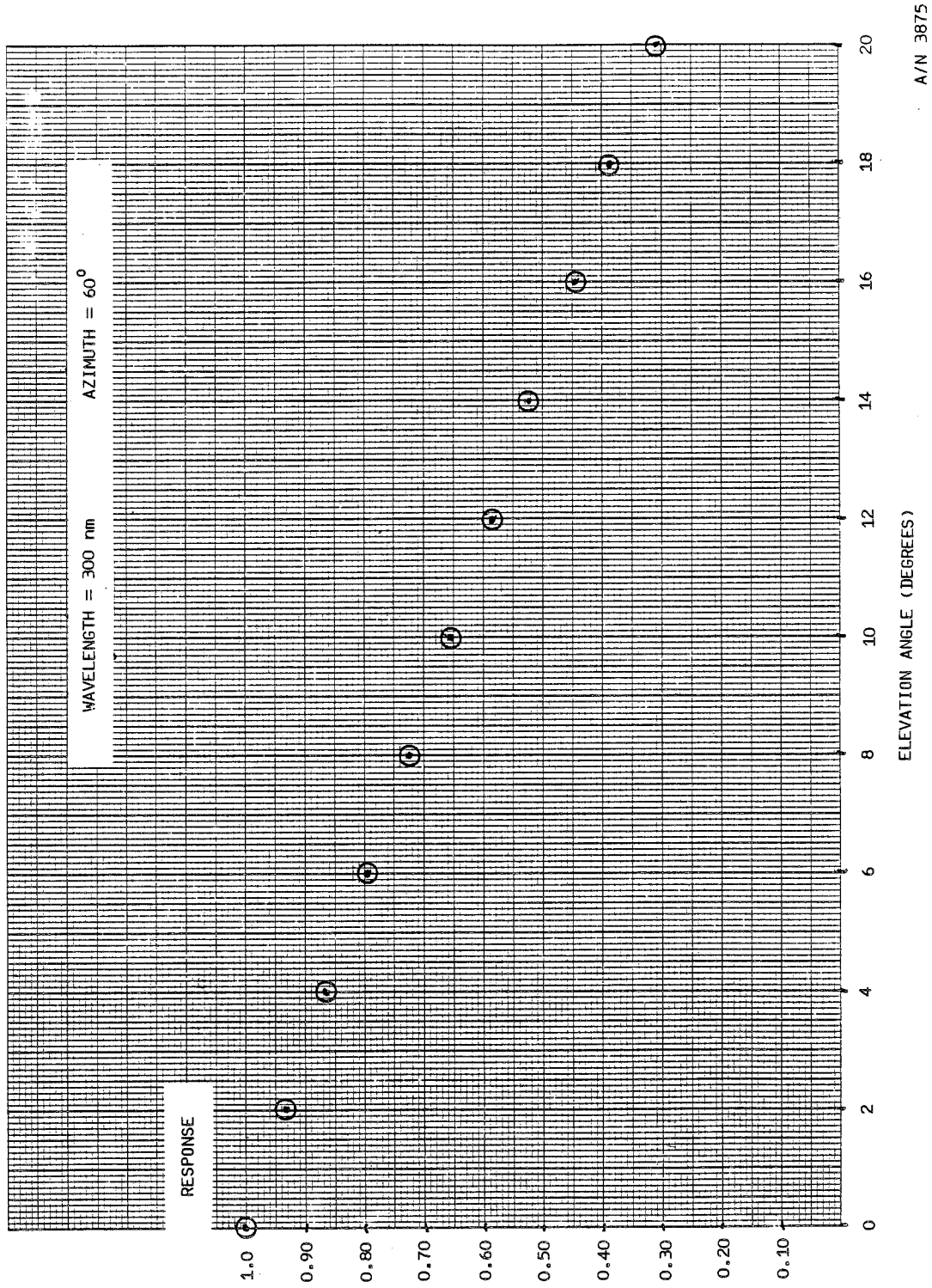
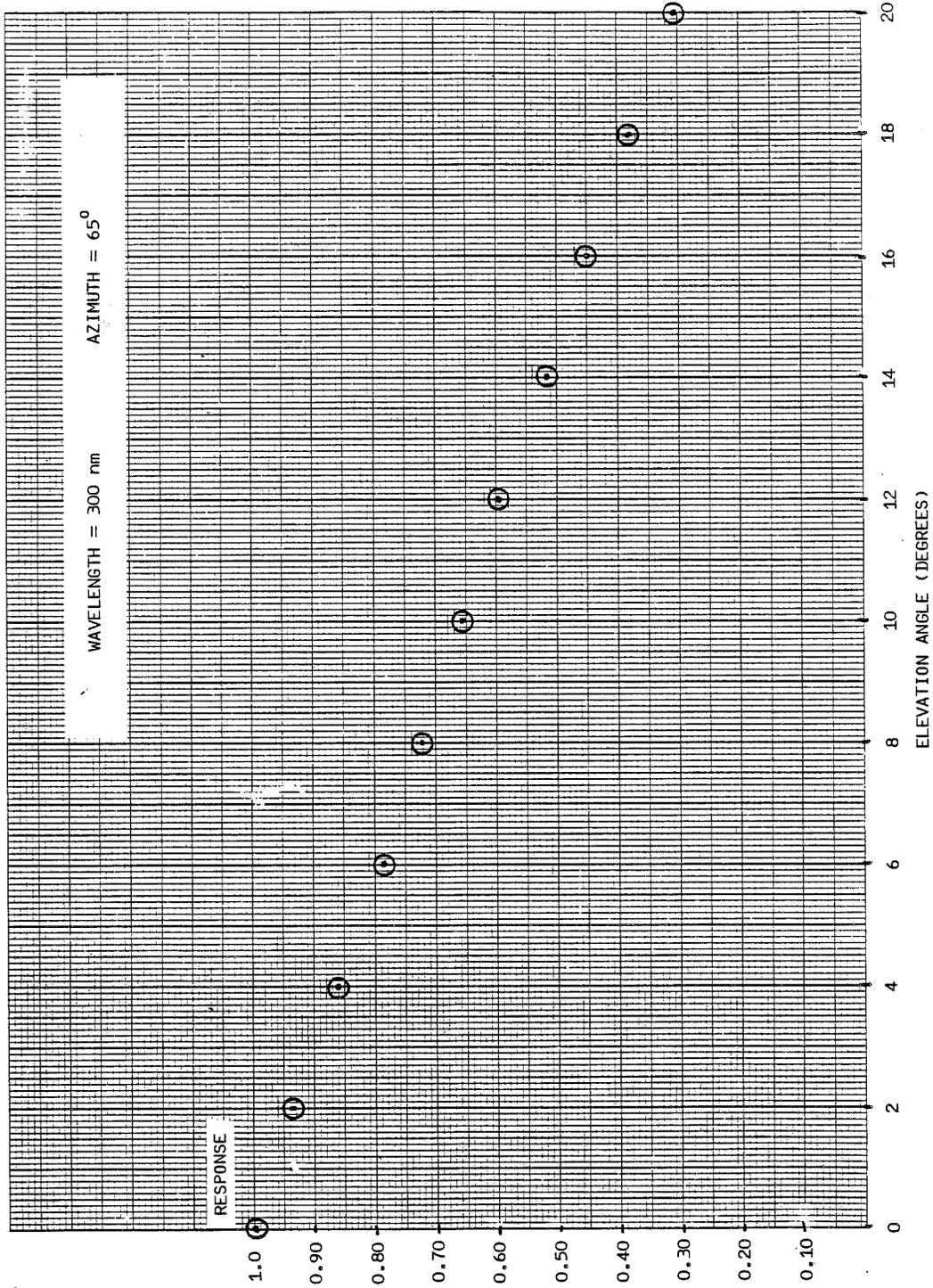


Figure 12-9 Goniometric Response vs. Elevation Angle



B6802-78



A/N 3875

Figure 12-10 Coniometric Response vs. Elevation Angle



System Engineering Report

REPORT NO. SBUV-GC-83-386 DATE 3-19-83

PROJECT SBUV/2

TITLE Use of The Goniometric Test Fixture: Determination of the True Angles of Azimuth and Elevation

PREPARED BY F. Gary Cunningham T.O. SBUV/2 DATE 8-19-83 APPROVED BY DATE

SCOPE/TEXT:(ATTACH ADDITIONAL SHEETS AS REQUIRED) The goniometric properties of the on-board diffuser are measured by use of the goniometric test fixture, which is designed to simulate the motion of the sun (source) by rotating the instrument about the center of the diffuser while keeping the source fixed. Because of the geometry of the situation, the azimuth and elevation angles of measurement, alpha_s and epsilon_s respectively, are not the true angles alpha and epsilon, and are referred to herein as pseudo-angles.

When deployed in the solar viewing position, the plane of the on-board diffuser makes an angle of 28 degrees with the instrument/spacecraft Y-Z plane, and the projection of the diffuser normal onto the Y-Z plane is offset 34 degrees from the +Z axis, in the +Y direction, to accommodate the wide variation in orbital gamma angle..

In this exercise the Y-Z plane is represented by a parellel plane passing through the center of the diffuser. The azimuth angle is measured in this plane relative to the +Z axis and the elevation angle is the angle between the source and the Y-Z plane.

Figure 1 depicts the problem which can be outlined as follows:

- 1) The projection OL of diffuser normal n onto the Y-Z plane is offset from the Z-axis by +34 degrees.
2) Goniometric calibration is made by azimuthal rotation phi about the line OX' (OX when the elevation epsilon is zero).

Table with 3 columns: Name, GSEC (2), and a blank column. Rows include D. Nelson, R. McConaughy, W. Nelson, G. Morris, K. Kelly, W. Fowler, and A. Olsen.



SBUV-GC-83-386

Page 2

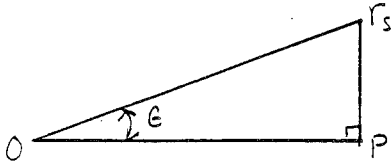
- 3) The line $\overline{AA'}$ is the intersection of the diffuser with the Y-Z plane and is the axis of rotation for setting the elevation angle ζ .
- 4) The plane $XO\bar{n}$ is one of the symmetry planes of the diffuser.
- 5) The psuedo-elevation angle ζ_s is set by a rotation about $\overline{AA'}$ as measured from \overline{OL} .
- 6) Unit vector \overline{Or} represents the instantaneous position of the source (sun) when the elevation angle is zero: The true azimuth angle is $\alpha = \psi - 56^\circ$. The arc $A'LA$ is the locus of \bar{r} as the azimuth angle (rotary table) is varied from -56° to $+124^\circ$.
- 7) The unit vector \overline{Or}_s is equivalent and equal to \overline{Or} for an elevation angle $\zeta_s = 0$ and $\alpha_s = \psi - 56^\circ$; likewise, unit vector \overline{OL}_s is equivalent and equal to \overline{OL} and lies in the plane $XO\bar{n}$, and the arc $A'L_sA$ is equivalent and equal to $A'LA$.
- 8) The psuedo-azimuth angle α_s is the angle of measurement referenced to the line \overline{OZ} on the rotary table, determined when the elevation angle is zero. The true azimuth angle α is defined by the lines \overline{OZ} and \overline{OP} where P is the projection of \bar{r}_s onto the Y-Z plane.
- 9) If α_s is held constant while the elevation angle is changed, the locus of \bar{r} will scribe the arc \overline{rr}_s which defines a plane normal to both the Y-Z plane and the line $\overline{AA'}$.

Gary Cunningham



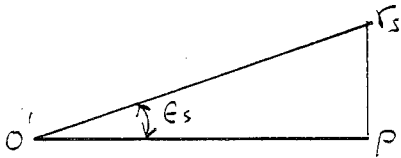
SBUV-6C-83-386
PAGE 4

From $\Delta r_s O P$:



$$\overline{r_s P} = \overline{O r_s} \sin \epsilon \equiv \sin \epsilon \quad (1)$$

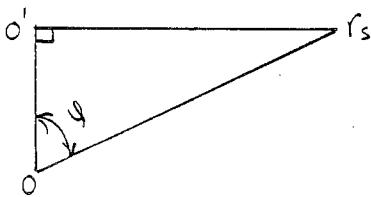
From $\Delta r_s O' P$:



$$\overline{r_s P} = \sin \epsilon_s \overline{O' r_s} \quad (2)$$

$$\overline{O' P} = \cos \epsilon_s \overline{O' r_s} \quad (3)$$

From $\Delta O O' r_s$:



$$\overline{O' r_s} = \overline{O r_s} \sin \phi \equiv \sin \phi \quad (4)$$

$$\overline{O O'} = \overline{O r_s} \cos \phi \equiv \cos \phi \quad (5)$$

Now, from Eqs. (1), (2) & (4)

$$\sin \epsilon = \sin \epsilon_s \sin \phi \quad (6)$$

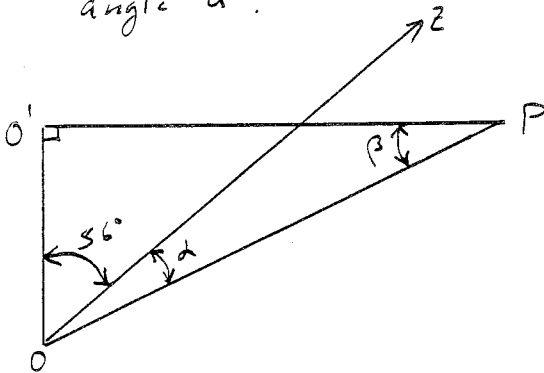
and from Eqs. (3) & (4)

$$\overline{O' P} = \cos \epsilon_s \sin \phi \quad (7)$$



SBUV-6C-83-326
PAGE 5

Now, From $\Delta O'O P$ we can determine the azimuthal angle α .



$$\text{From } \beta + (56^\circ + \alpha) = 90^\circ$$

We have

$$\alpha = 34^\circ - \beta \quad \text{and,} \quad (8)$$

$$\overline{O'P} \sin \beta = \overline{OO'} \quad (9)$$

$$\overline{OP}^2 = \overline{OO'}^2 + \overline{O'P}^2 \quad (10)$$

Using Eq's (6), (7) & (10) :

$$\overline{OP}^2 = \cos^2 \varphi + \cos^2 \epsilon_s \sin^2 \varphi = \cos^2 \varphi$$

From which

$$\overline{OP}^2 = 1 - \sin^2 \epsilon_s \sin^2 \varphi \quad (11)$$



STUV-GC-83-386
PAGE 6

Then, from Eqs. (5), (9) & (10)

$$\sin \beta = \frac{\cos \varphi}{[1 - \sin^2 \epsilon_s \sin^2 \varphi]^{1/2}} \quad (12)$$

Hence, the equations for determining the true angles of azimuth and elevation when the angles of measurement are known are:

$$\sin \epsilon = \sin \epsilon_s \cdot \sin(56^\circ + \alpha_s) \quad (13)$$

and

$$\alpha = 34^\circ - \arcsin \left\{ \frac{\cos(56^\circ + \alpha_s)}{[1 - \sin^2 \epsilon_s \cdot \sin^2(56^\circ + \alpha_s)]^{1/2}} \right\} \quad (14)$$

Figure 2 provides a plot of the true angles (α, ϵ) parameterized by the angles of measurement (α_s, ϵ_s) over the range of interest for an afternoon, ascending node orbit: $35^\circ \leq \gamma \leq 65^\circ$.



System Engineering Report

REPORT NO. SBUV-GC-83-390 DATE 30 Aug. 83

PROJECT SBUV/2

TITLE Determination of the Solar Angles of Azimuth and Elevation from the Instantaneous Position of the Sun in Orbit; and Use of the SBUV/2 Goniometric Calibration : Determination of the Solar Angle of Incidence with the On-Board Diffuser

PREPARED BY F. Gary Cunningham SBUV/2 Technical Officer

DATE 29 Aug. '83

APPROVED BY

DATE

SCOPE/TEXT:(ATTACH ADDITIONAL SHEETS AS REQUIRED)

For the Tiros Spacecraft (S/C), on which the SBUV/2 will fly, the S/C Z-Axis is maintained parallel to the orbit normal at all times. Therefore, the solar angle, which is the angle between the solar vector and the orbit normal, is the angular position of the sun off the Z-Axis. For all orbits in which the sun will appear, from a position on the S/C, to precess about the Z-Axis making one revolution per orbit of the S/C about Earth. In order to determine the solar irradiance the position of the sun in terms of angle and orbital position, taken during the measurement, must be transformed to angles of azimuth, and elevation, which are measured relative to the Z-Axis and Y-Z Plane, respectively.

SBUV/2 will fly on S/C in afternoon, ascending node orbits. The orientation of the S/C with respect to Earth in such an orbit is shown in Figure 1. We can see that from sunrise over the South Pole to sunset over the North Pole the sun will lie on the -X side of the Y-Z Plane, or in other words, above the earth facing panel of the S/C for all angles. As the S/C passes over the poles (orbital position nearest the poles but 90 orbital degrees from S/C noon) the sun lies in the S/C Y-Z Plane. As the S/C moves beyond its local sunset (moving now toward the South Pole) the sun becomes visible from the +X side of the Y-Z Plane and the +Y side of the X-Z Plane. At this time, and only this time, SBUV/2 solar irradiance measurements are possible.

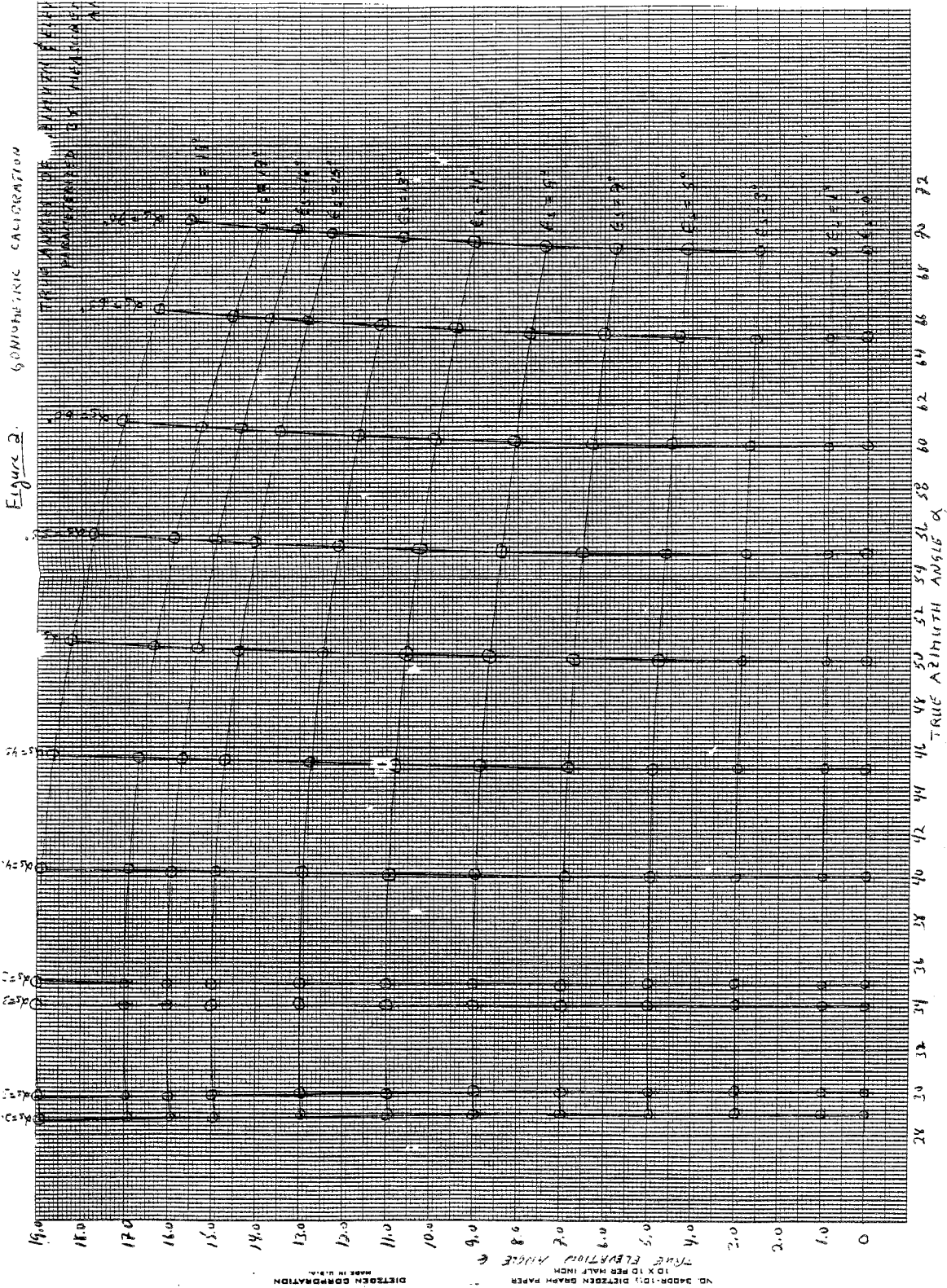
Figure 2 shows the apparent precessional motion of the sun, as seen from the S/C, and depicts the geometry of the situation. The problem is to define and compute the angles of azimuth, and elevation.

DISTRIBUTION

Table with 3 columns: Name, Signature line, and Date line. Rows include D. Nelson, W. Nelson, A. Olsen, W. Fowler, G. Morris, R. McConaughy, K. Kelly, and GSAC (2).



Figure 2. GEOMETRIC CALIBRATION





SBUV-GC-83-390
Page 4

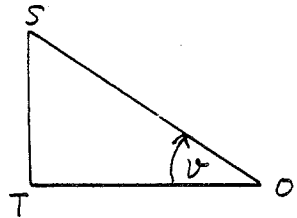
In Figure 2, the locus of the sun \overline{OS} describes a circle of unit radius about the origin O' ; i.e., $\overline{O'S} = \overline{O'S_1} = \overline{O'S_2} = 1$, and a cone of half angle γ whose apex is located at origin O . Therefore, $\overline{OS} = \overline{OS_1} = \overline{OS_2}$. S_1 , the position of the sun at S/C sunset, lies in the Y-Z Plane of the S/C, and $O'T$ is the projection of $\overline{O'S}$ onto the Y-Z Plane; while, the angle ν gives the angular position of $\overline{O'S}$, measured from the Y-Z Plane, as the sun revolves about the Z-Axis.

The angle ZOT is, by definition, the azimuth angle α , and the angle SOT is, by definition, the elevation angle ϵ .

The SBUV/2 will have an unobstructed view of the sun for the following range of elevation angles ϵ : $0^\circ \leq \epsilon \leq 15^\circ$. When ϵ is less than zero the sun view is obstructed by the S/C, and when ϵ is greater than 15+ degrees, the solar array obstructs the view.

Now, from Figure 2:

Using triangle $O'ST$, we have:

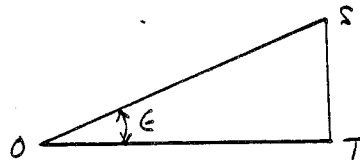


$$\overline{O'T} = \overline{O'S} \cdot \cos \nu = \cos \nu \quad (1)$$

and

$$ST = \overline{O'S} \cdot \sin \nu = \sin \nu \quad (2)$$

From triangle $O'ST$, we have:



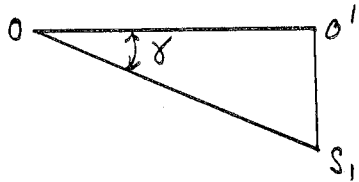
$$\overline{OS} \cdot \sin \epsilon = \overline{ST} \quad \text{Therefore, from Eq. (1)}$$

$$\sin \epsilon = \frac{\sin \nu}{\overline{OS}} \quad (3)$$



SBUV -GC-83- 396
Page 5

To determine \overline{OS} we need triangle $OO'S_1$:



$$\overline{O'S_1} = \overline{OS_1} \cdot \sin \gamma = 1$$

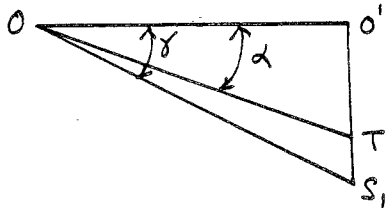
Since $\overline{OS_1} = \overline{OS}$, we have

$$\overline{OS} = \frac{1}{\sin \gamma} \quad (4)$$

Then, using Eqs. (3) & (4):

$$\sin \epsilon = \sin \gamma \cdot \sin \nu \quad (5)$$

From triangles $O'OT$ and $O'OS_1$, we have:



$$\overline{OT} \cdot \cos \alpha = \overline{OO'} \quad (6)$$

and

$$\overline{OS_1} \cdot \cos \gamma = \overline{OO'} \quad (7)$$

Then,

$$\overline{OT} \cdot \cos \alpha = \overline{OS_1} \cdot \cos \gamma, \text{ and from Eq. (4)}$$

$$\cos \alpha = \frac{\cos \gamma}{\overline{OT} \cdot \sin \gamma} \quad (8)$$



SBUV-GC-83-390
 Page 6

Again, from triangle OST, we have:

$$(\overline{OT})^2 + (\overline{ST})^2 = (\overline{OS})^2 \quad (9)$$

Then, using Eqs. (2) & (4):

$$(\overline{OT})^2 = \frac{1}{\sin^2 \gamma} - \sin^2 \nu \quad (10)$$

Now, Equation (8) becomes:

$$\cos \alpha = \frac{\cos \gamma}{(1 - \sin^2 \gamma \cdot \sin^2 \nu)^{1/2}} \quad (11)$$

Equation (5) gives the elevation angle ϵ in terms of the γ angle and the angular position of the sun ν , while equation (11) provides the equivalent relationship for the azimuth angle α .

Note: The apparent angular position of the sun, ν , measured from the Y-Z Plane bears a one-to-one correspondence to the angular position of the S/C in orbit, measured from the position of S/C sunset.

Equations (5) and (11) can be rewritten in terms of the angle γ and the other angle by eliminating the angle ν :

$$\sin \epsilon = \left(1 - \frac{\cos^2 \gamma}{\cos^2 \alpha} \right)^{1/2} \quad (12)$$

and

$$\cos \alpha = \frac{\cos \gamma}{\cos \epsilon} \quad (13)$$



SBUV-GC-83- 390
Page 7

Use of the SBUV/2 Goniometric Calibration Data: A simplistic approach.

1. Fit the goniometric test data to an equation(s) which will provide instrument relative response as a function of test angles α_s and ϵ_s .
2. For any instantaneous solar irradiance measurement, determine the true angles of azimuth and elevation, α and ϵ , respectively, by using the equations provided herein, or by some other technique.
3. From data provided by RCA correct the angles determined in (2) so that all angular measurements are made relative to the SBUV/2 alignment cube.
4. Using equations provided in System Engineering REport No. 386, BASD Document SBUV-GC-83-386, correct the angles from (3) to determine their test angles α_s and ϵ_s .
5. The equation(s) from (1) are then used to correct the measured instrument solar irradiance response data from which the solar irradiance can be deduced.

Determination of the Instantaneous Angle of incidence of the Sun on the On-Board Diffuser:

To follow this calculation it is necessary to add the on-board diffuser to Figure 2; The essential elements are shown in Figure 3.

In Figure 3, $\overline{AA'}$ is the intersection of the on-board diffuser with a plane parallel to the S/C Y-Z Plane, and which passes through the center of the diffuser. $\overline{AA'}$ makes an angle of 34 degrees with the S/C Y-Axis. The line \overline{OC} is normal to $\overline{AA'}$ and, likewise, makes an angle of 34 degrees with the Z-Axis. The projection of the diffuser normal \overline{ON} , which makes an angle of 62 degrees with the Y-Z Plane, onto the Y-Z Plane lies along \overline{OC} . The intersection of the diffuser plane with the plane containing the locus of the sun, as it precesses about the Z-Axis, is line \overline{BM} . \overline{MC} is normal to the Y-Z Plane and to the line \overline{BC} , and line \overline{MD} is normal to \overline{ON} ; the angle MOC is, therefore, 28 degrees.



SBUU - GC-83-390
Page 8

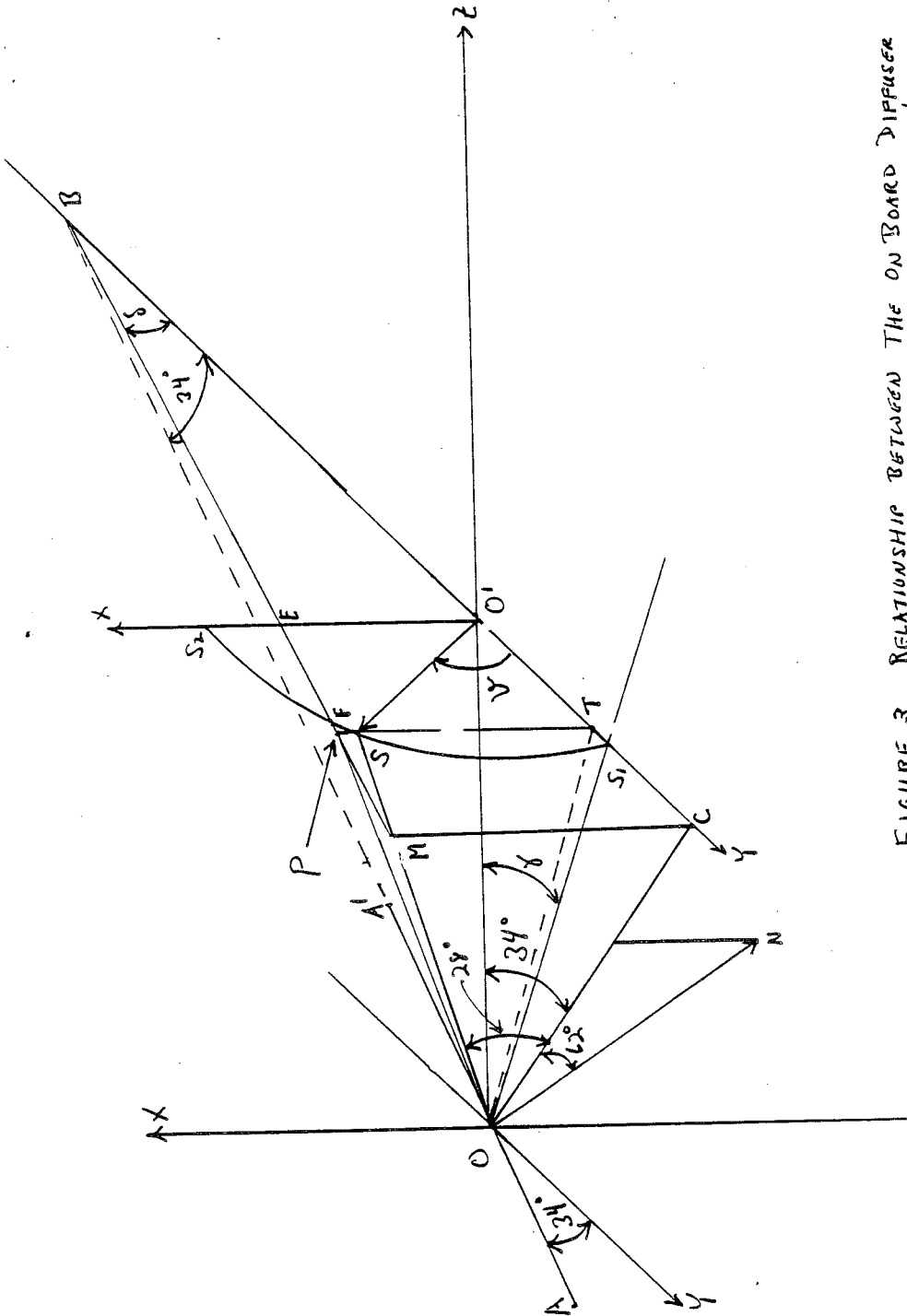


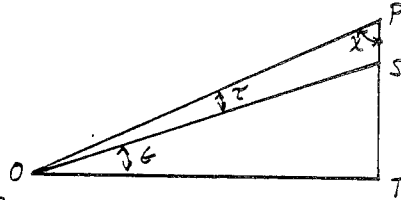
FIGURE 3. RELATIONSHIP BETWEEN THE ON BOARD DIFFUSER AND THE SOLAR VECTOR - SHOWN IN S/C COORDINATES



SBUV-GC-83-390
 Page 9

Now, from Figure 3:

The angle between the sun and the diffuser plane, τ , is defined by using triangles OTP and OST: ρ is the intersection of \overline{TS} with \overline{BM} .



Then, from triangle OSP:

$$\frac{\overline{SP}}{\sin \tau} = \frac{\overline{OS}}{\sin \chi}, \text{ and using Eq. (4) we have,}$$

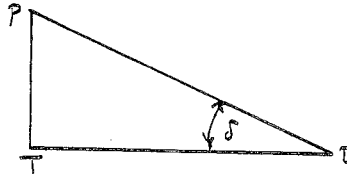
$$\sin \tau = \overline{SP} \cdot \sin \chi \cdot \sin \gamma \tag{14}$$

We need to compute the line \overline{SP} and $\sin \chi$: To do so a series of new triangles must be introduced.

Firstly, from triangle OTP"

$$\overline{SP} = \overline{TP} - \overline{ST} \tag{15}$$

Then, using new triangle TPB:



$$\frac{\overline{TP}}{\sin \delta} = \frac{\overline{BT}}{\sin(90 - \delta)} = \frac{\overline{BT}}{\cos \delta}, \text{ and therefore}$$

$$\overline{TP} = \overline{BT} \cdot \tan \delta \tag{16}$$

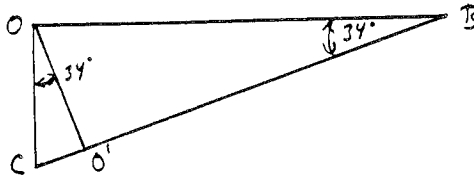
And, from Figure 3:

$$\overline{BT} = \overline{O'B} + \overline{O'T} \tag{17}$$



SBUV-GC-83- 390
 Page 10

To determine $\overline{O'B}$ we need new triangle $OO'B$



$$\overline{OB} \cdot \cos 34^\circ = \overline{O'B} \tag{18}$$

and

$$\overline{OB} \cdot \sin 34^\circ = \overline{OO'}$$

but, from Eqs. (4) and (7) we have,

$$\overline{OB} \cdot \sin 34^\circ = \cot \gamma$$

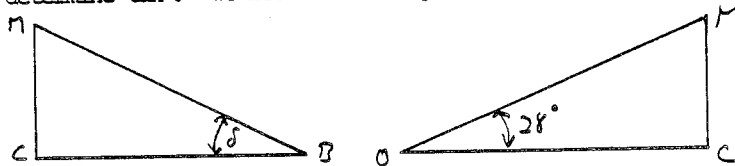
, therefore Eq. (18) becomes:

$$\overline{O'B} = \cot 34^\circ \cdot \cot \gamma \tag{19}$$

Then, from Eqs. (1), (17) and (19), Eq. (16) becomes:

$$\overline{TP} = (\cot 34^\circ \cdot \cot \gamma + \cos 24^\circ) \cdot \tan \delta \tag{20}$$

To determine $\tan \delta$ we need new triangles BMC and MOC :



From which we have,

$$\begin{aligned} \overline{BM} \cdot \cos \delta &= \overline{BC} \\ \overline{BM} \cdot \sin \delta &= \overline{MC} \end{aligned} \quad \Rightarrow \quad \frac{\overline{BM} \cdot \sin \delta}{\overline{BM} \cdot \cos \delta} = \tan \delta = \frac{\overline{MC}}{\overline{BC}} \tag{21}$$

$$\begin{aligned} \overline{OM} \cdot \sin 28^\circ &= \overline{MC} \\ \overline{OM} \cdot \cos 28^\circ &= \overline{OC} \end{aligned} \quad \Rightarrow \quad \frac{\overline{OC} \cdot \sin 28^\circ}{\cos 28^\circ} = \overline{MC} = \overline{OC} \cdot \tan 28^\circ \tag{22}$$



SBUV-GC-83-390
 Page 11

Now from triangles OO'C and BOC we have,

$$\overline{OC} \cdot \cos 34^\circ = \overline{OO'}$$

$$\overline{OC} \cdot \sin 34^\circ = \overline{O'C}$$

and

$$\overline{BC} = \overline{O'B} + \overline{O'C} \quad (23)$$

Using Eqs. (4) and (7), OC becomes

$$\overline{OC} = \frac{\cot \gamma}{\cos 34^\circ} \quad (24)$$

and then,

$$\overline{O'C} = \cot \gamma \cdot \tan 34^\circ \quad (25)$$

Then, from Eqs. (19), (22), (23) and (25), Eq. (21) becomes,

$$\tan \delta = \sin 34^\circ \cdot \tan 28^\circ \quad (26)$$

Then, from Eqs. (2) and (20), Eq. (15) becomes,

$$\overline{SP} = (\cot 34^\circ \cdot \cot \gamma + \cos \psi) \cdot \tan \delta - \sin \psi \quad (27)$$

To determine $\sin \chi$, refer back to triangle OPT:

$$\overline{OP} \cdot \sin \chi = \overline{OT}$$

and

$$(\overline{OP})^2 = (\overline{TP})^2 + (\overline{OT})^2 \quad \text{and, from Eqs. (10) and}$$



SBUV-GC-83-390
Page 12

(20) we have:

$$\overline{OP} = \frac{1}{\sin \gamma} \left[(1 - \sin^2 \gamma \cdot \sin^2 \psi) + (\cot 34^\circ \cdot \cot \gamma + \cos \psi)^2 \cdot \tan^2 \delta \cdot \sin^2 \gamma \right]^{1/2} \quad (28)$$

Using Eqs. (10) and (28)

$$\sin \chi = \frac{(1 - \sin^2 \psi \cdot \sin^2 \gamma)^{1/2}}{\left[(1 - \sin^2 \gamma \cdot \sin^2 \psi) + (\cot 34^\circ \cdot \cot \gamma + \cos \psi)^2 \tan^2 \delta \cdot \sin^2 \gamma \right]^{1/2}}$$

or

$$\sin \chi = \frac{1}{\left[1 + \frac{(\cot 34^\circ \cdot \cot \gamma + \cos \psi)^2 \tan^2 \delta \cdot \sin^2 \gamma}{(1 - \sin^2 \gamma \cdot \sin^2 \psi)} \right]^{1/2}} \quad (29)$$

Then, from Eqs. (27) and (29), Eq. (14) becomes:

$$\sin \tau = \frac{[(\cot 34^\circ \cdot \cot \gamma + \cos \psi) \tan \delta - \sin \psi] \sin \gamma}{\left[1 + \frac{(\cot 34^\circ \cdot \cot \gamma + \cos \psi)^2 \tan^2 \delta \cdot \sin^2 \gamma}{(1 - \sin^2 \gamma \cdot \sin^2 \psi)} \right]^{1/2}} \quad (30)$$

Where $\tan \delta$ is given by Eq. (26).



Section 13
SPECTRAL BANDPASS RESULTS
(Reference Test Procedure 68030)

To measure the spectral bandpass of the monochromator, three line sources (one at each end of the spectral range and one in the center) were spectrally scanned. The full width at half maximum was measured on each profile. The results are:

<u>Wavelength (nm)</u>	<u>FWHM (nm)</u>
180	1.14
285	1.13
405	1.18

These profile widths represent the bandpass of the instrument at these wavelengths, which are specified to be $1.0^{+0.2}_{-0.0}$ nm.

The spectral bandpass of the Cloud Cover Radiometer was determined by a separate measurement on the CCR filter.

The following Table 13-1 and Figure 13-1 give the bandpass values for the discrete, sweep and cloud cover radiometer.

Table 13-2 shows the actual discrete wavelength positions and the amount they are out of specification.

To measure the resolution capability (resolution limit with arbitrarily narrow slits) of the instrument, the profile of the Mg 2830 Å line was differentiated twice. (Refer to SER# A0-82-330. "Manipulating Spectral Data", by Art Olson, for an explanation of this process.) The widths of the second derivative spikes are about 2 to 3 data points wide. If the profile is Fourier interpolated, increasing the number of points by a factor of eight, the spikes appear to be 20 Fourier interpolated points wide. This translates to a spectral width 1.85Å, and represents the instruments' resolution capability. The specification calls for no greater than 2 Å resolution capability.



Table 13-1
SPECTRAL BANDPASS RESULTS (GRAPHIC SPLINE INTERPOLATION FROM
THREE MEASUREMENT POINTS)

Central Wavelength Nanometers	Bandwidth in Nanometers Limits: 1.0 + 0.2, -0
Discrete Mode:	
339.89 ± 0.05	1.14
331.26 ± 0.05	1.14
317.56 ± 0.05	1.14
312.57 ± 0.05	1.13
305.87 ± 0.05	1.13
301.97 ± 0.05	1.13
297.59 ± 0.05	1.13
292.29 ± 0.05	1.13
287.70 ± 0.05	1.13
283.10 ± 0.05	1.13
273.61 ± 0.05	1.13
252.00 ± 0.05	1.13
SWEEP MODE 160-400 ± 0.25	LIMITS: 1.0 + 0.2 - 0 1.13 + 0.05 - 0
Cloud Cover Radiometer 379 ± 1.0	LIMITS: 3.0 ± 0.3 2.95
Actual Peak Wavelength 378.62	

A/N 3875

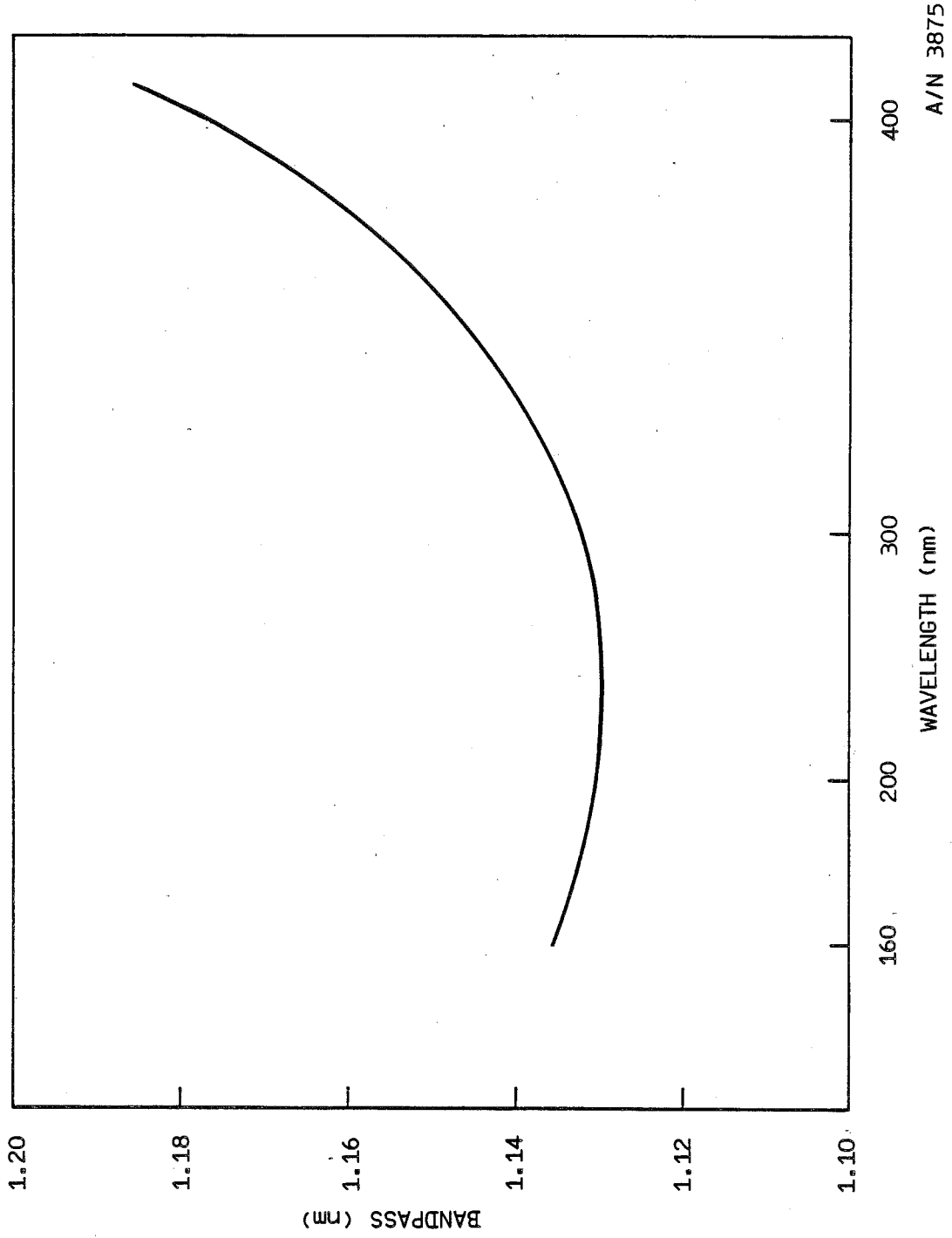


Figure 13-1 Graphic Spline Interpolation of Spectral Bandpass



Table 13-2
DISCRETE MODE WAVELENGTHS IN THE PROM ARE 1 TO 3 GRATING STEPS OUT OF SPEC

CHANNEL NUMBER	REQUIREMENT, (nm) (+0.05)	ACTUAL IN NANOMETERS	GRATING POSITION	BANDWIDTH IN NANOMETERS
1	252.00	252.03	+700	1.13
2	273.61	273.47	+412	1.13
3	283.10	283.00	+283	1.13
4	287.70	287.57	+221	1.13
5	292.29	292.20	+158	1.13
6	297.59	297.47	+ 86	1.13
7	301.97	301.86	+ 26	1.13
8	305.87	305.80	- 28	1.13
9	312.57	312.50	-120	1.13
10	317.56	317.50	-189	1.14
11	331.26	331.21	-379	1.14
12	339.89	339.81	-499	1.14

A/N 3875



Section 14
OUT OF BAND RESPONSE
(Reference Test Procedure 68032)

Out of band response is defined as the instrument response to energy integrated over all wavelengths outside a spectral region three times the measured bandwidth. Viewing the sky with the SBUV/2 instrument and scanning wavelengths from 400 nm down to 160 nm shows the out of band response of the instrument at short wavelengths and those far from the central wavelength. Two versions of this test were performed. One test enabled the SBUV/2 instrument to view the sky. The second test allowed the instrument to view a large, ground aluminum diffuser which was illuminated by direct sunlight. Sweep Mode scans and plots were made from the data. The ratio of maximum signal to minimum signal was determined from the data and used as the criteria for passing the out of band response.

A ratio of at least 1×10^6 was used as the pass/fail criteria.

The following plot is an average of 4 sweeps viewing a ground aluminum diffuser (Figures 14-1a through 14-1g).

Data taken from these sweeps, shown in Table 14-1a&b was used for the ratio calculation.



Table 14-1-a
OUT OF BAND RESPONSE

WAVELENGTH OF RESPONSE											
SWEEP	400.08	399.94	399.81	399.67	399.53	399.39	399.26	399.12	398.98	398.85	
1	747	758	751	748	749	746	745	742	731	728	
2	763	748	742	742	744	739	734	730	725	724	
3	768	753	753	752	753	750	743	739	734	730	
4	771	751	749	748	750	745	738	736	728	728	
AVERAGE	762	753	749	748	749	745	740	737	730	728	

MEAN OF ALL POINTS
ANODE CURRENT

1.301×10^{-7}

Table 14-1-b

WAVELENGTH OF RESPONSE											
SWEEP	200.77	200.62	200.46	200.31	200.16	200.01	199.85	199.70	199.55	199.40	
1	71	68	72	66	73	68	70	65	72	63	
2	75	62	70	67	70	65	70	66	72	65	
3	71	64	71	65	68	66	70	67	72	66	
4	72	69	70	64	71	64	69	68	71	67	
AVERAGE	72	66	71	66	71	66	70	67	72	65	

MEAN OF

ANODE CURRENT 8.798×10^{-14}

$$\frac{1.301 \times 10^{-7}}{8.798 \times 10^{-14}} = 1.479 \times 10^6$$

A/N 3875

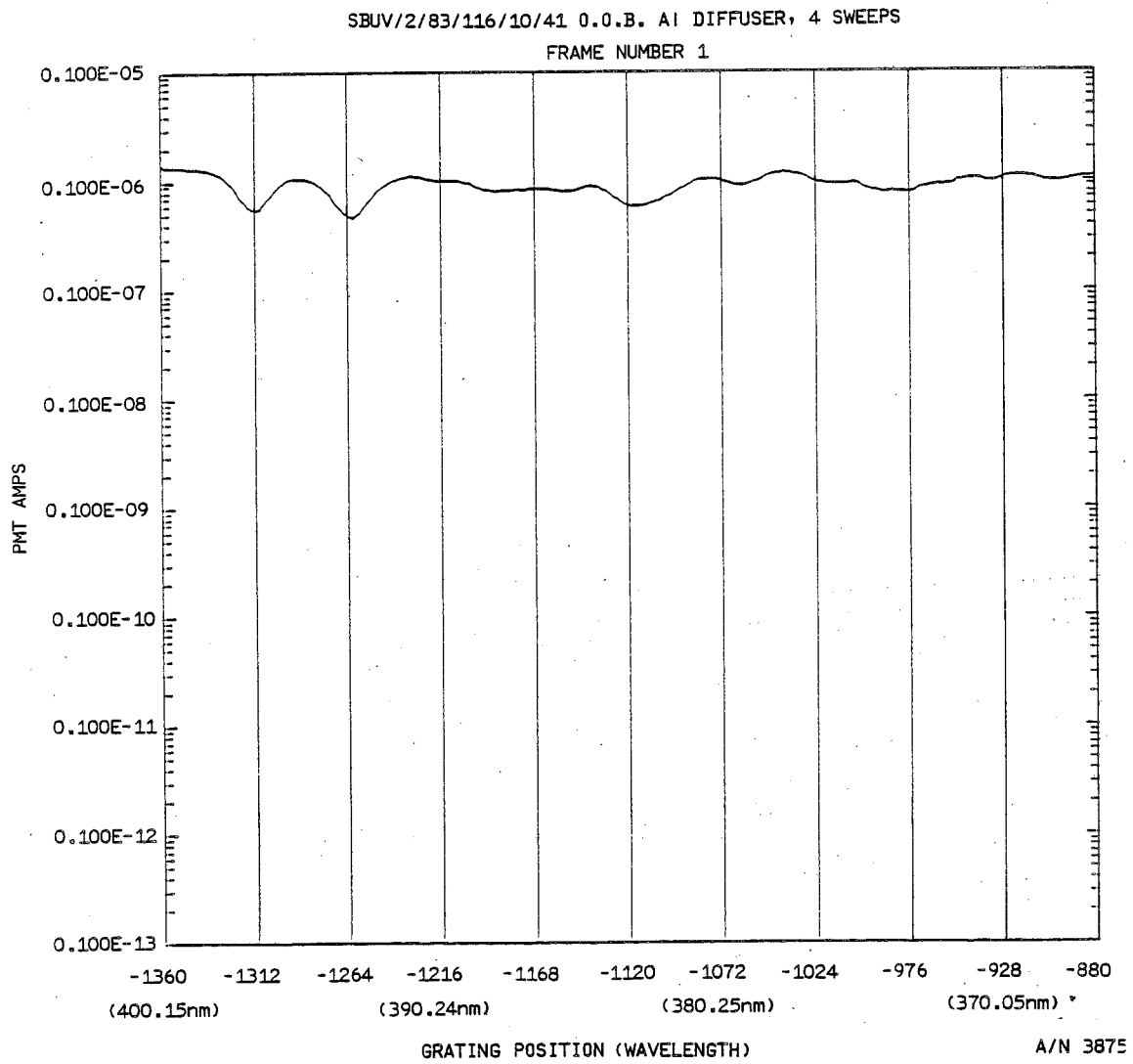


Figure 14-1a Out of Band Sweep Plot

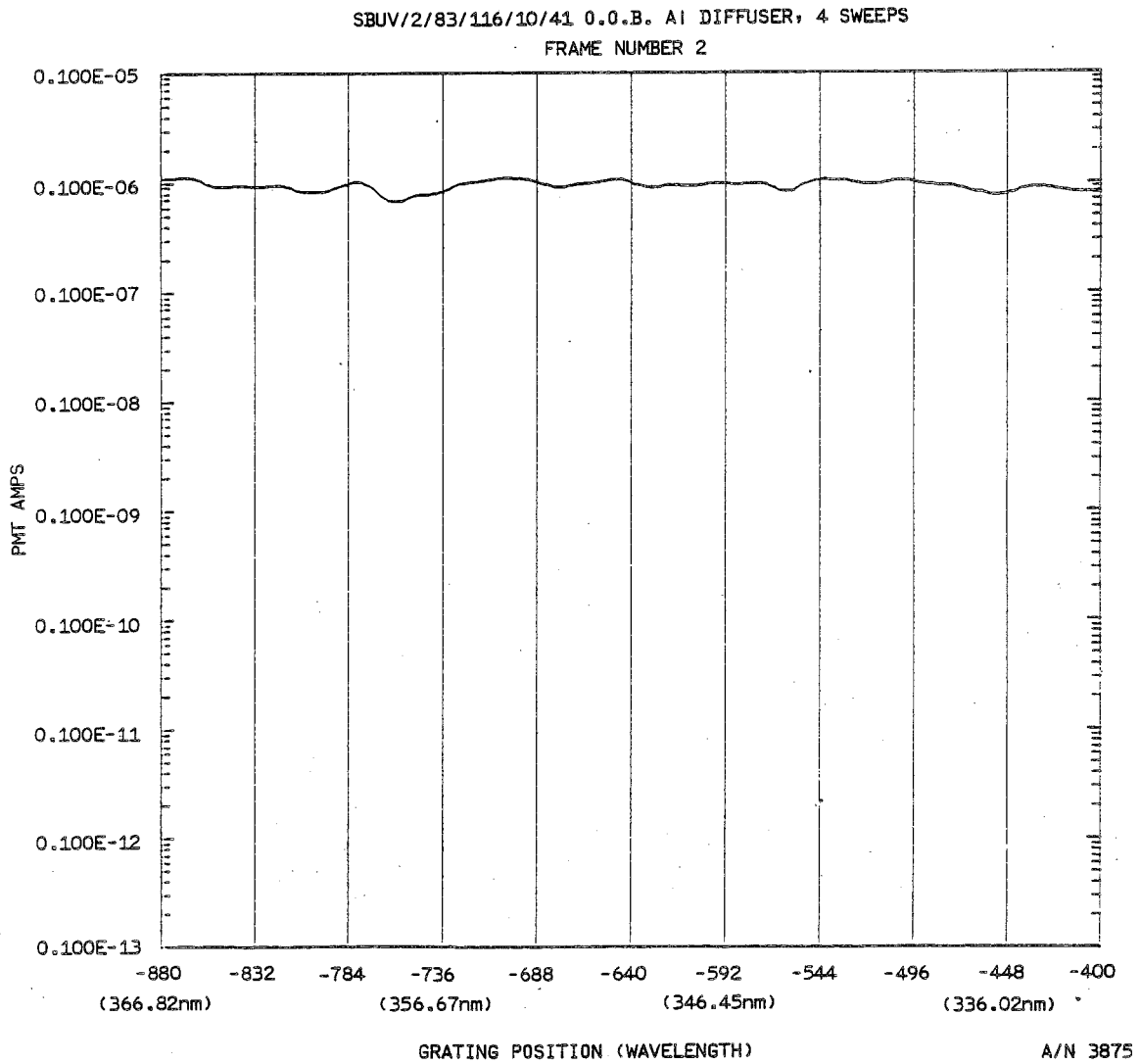


Figure 14-1b Out of Band Sweep Plot

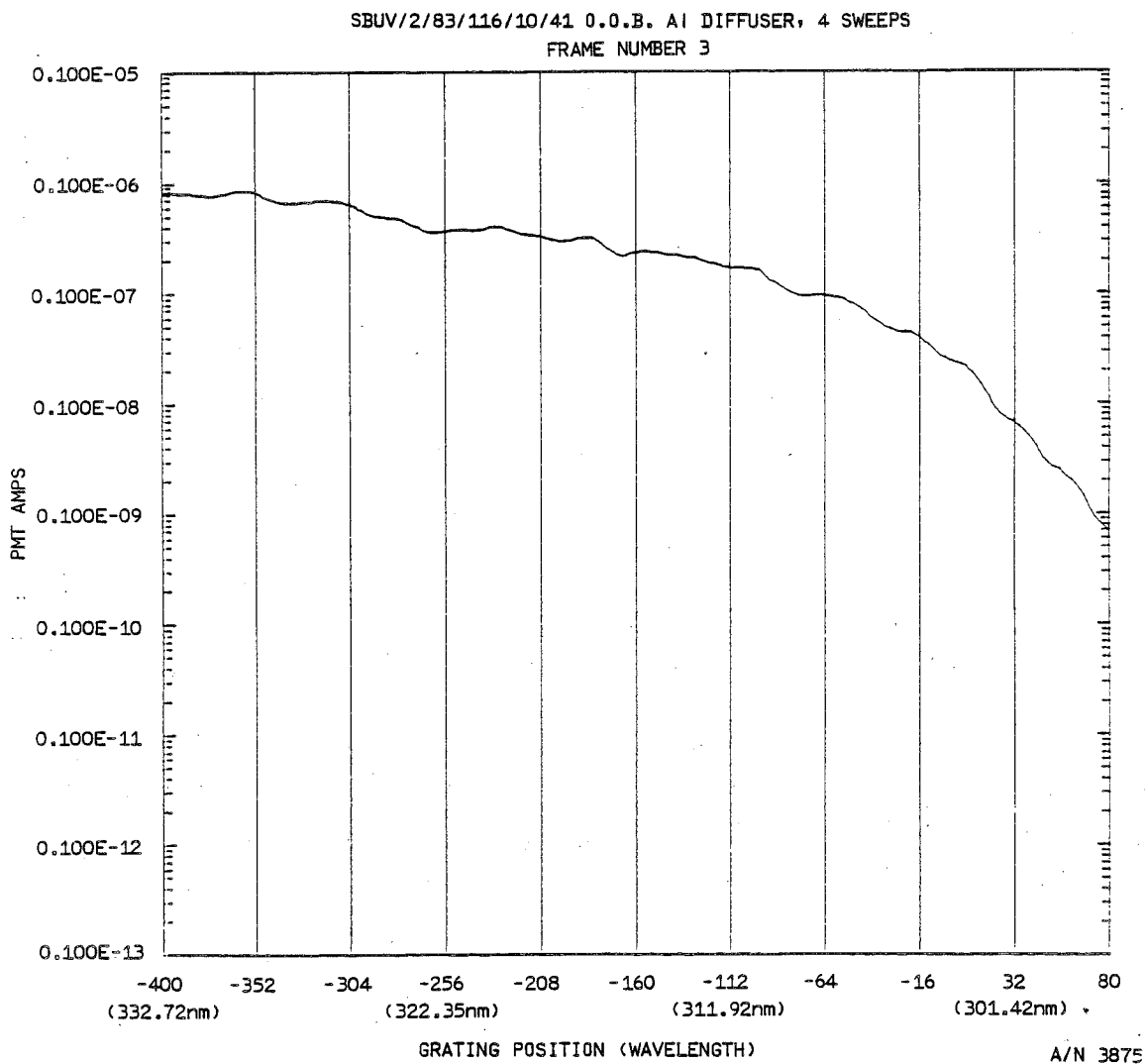
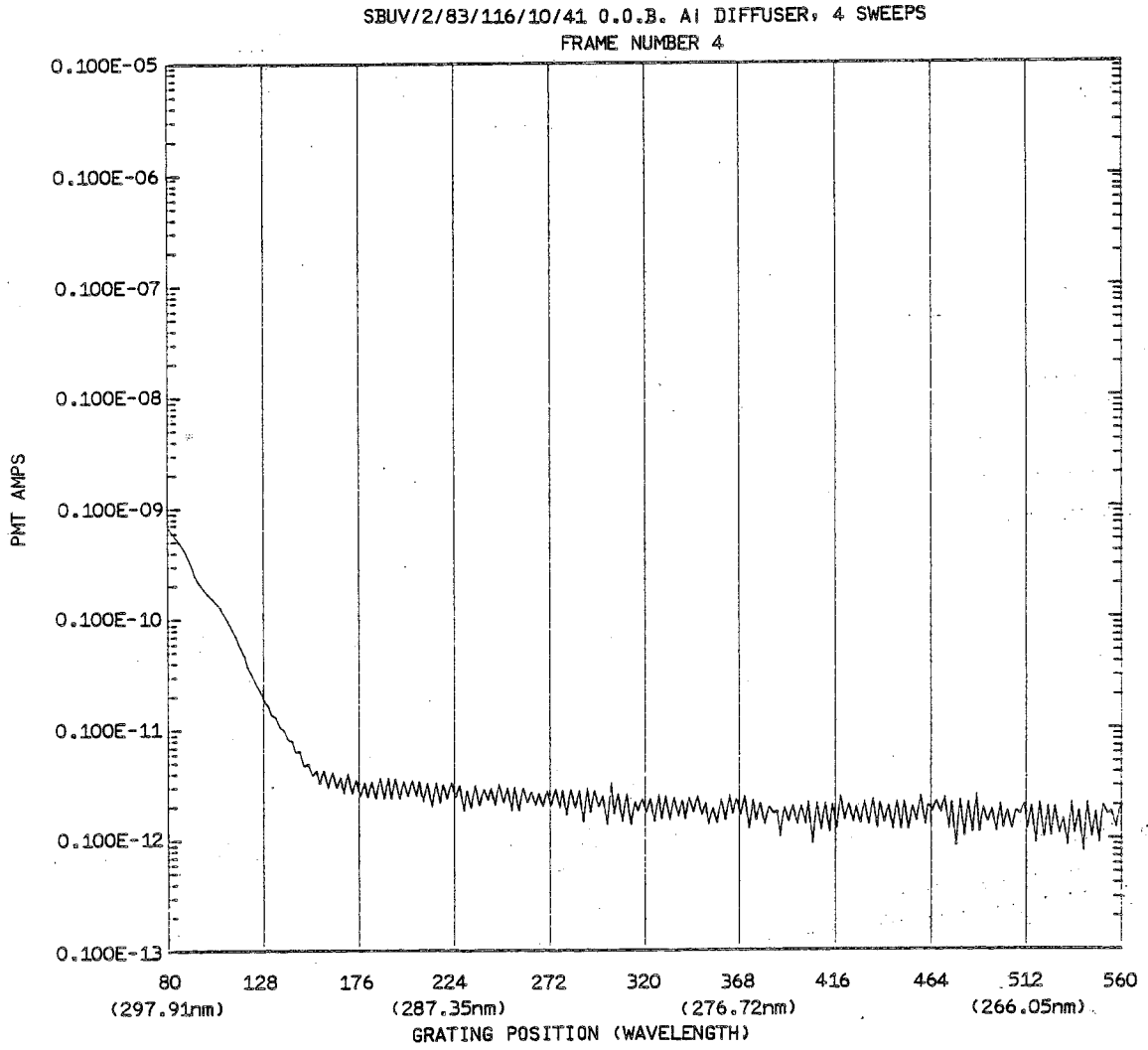


Figure 14-1c Out of Band Sweep Plot



A/N 3875

Figure 14-1d Out of Band Sweep Plot

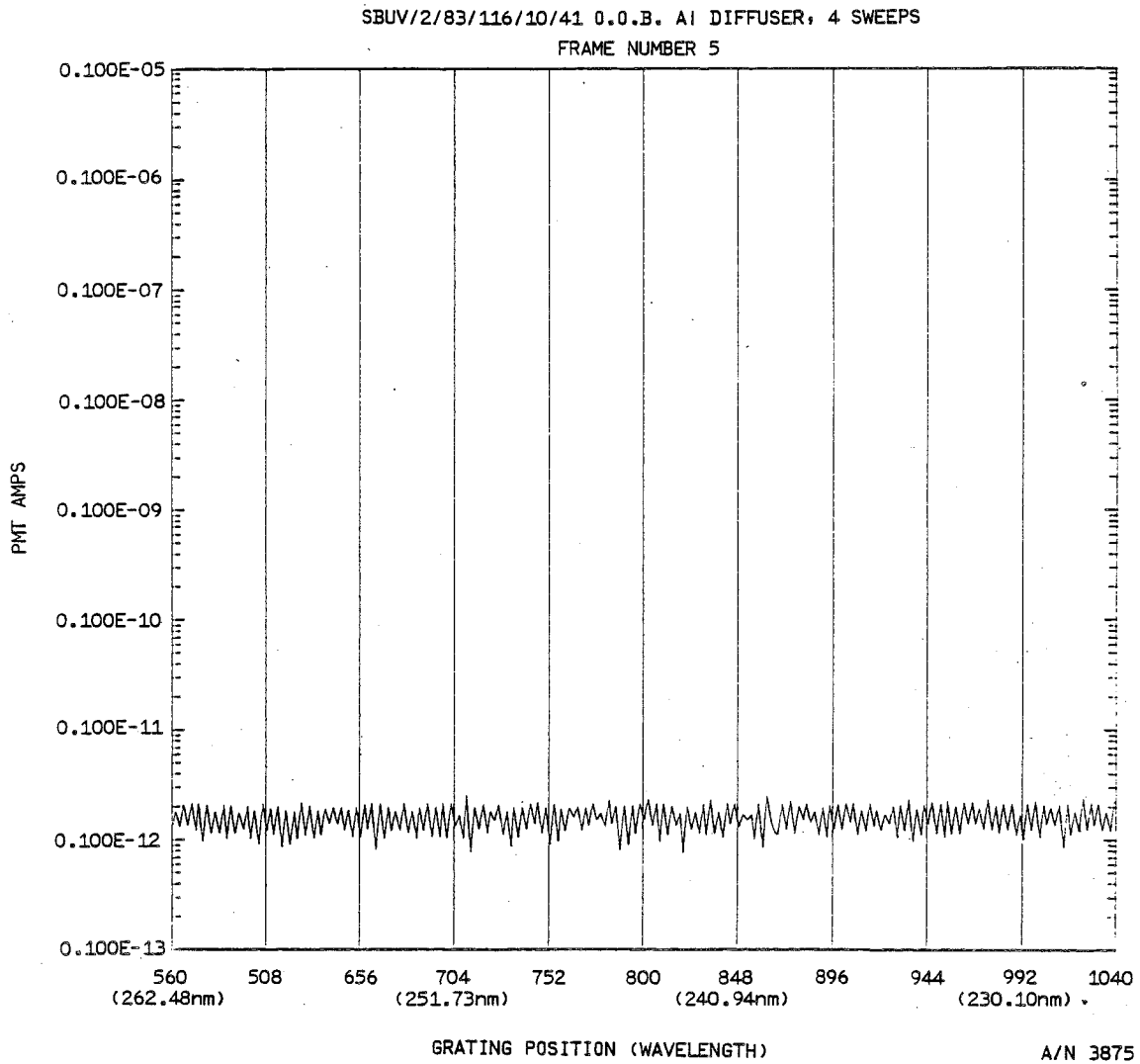


Figure 14-1e Out of Band Sweep Plot

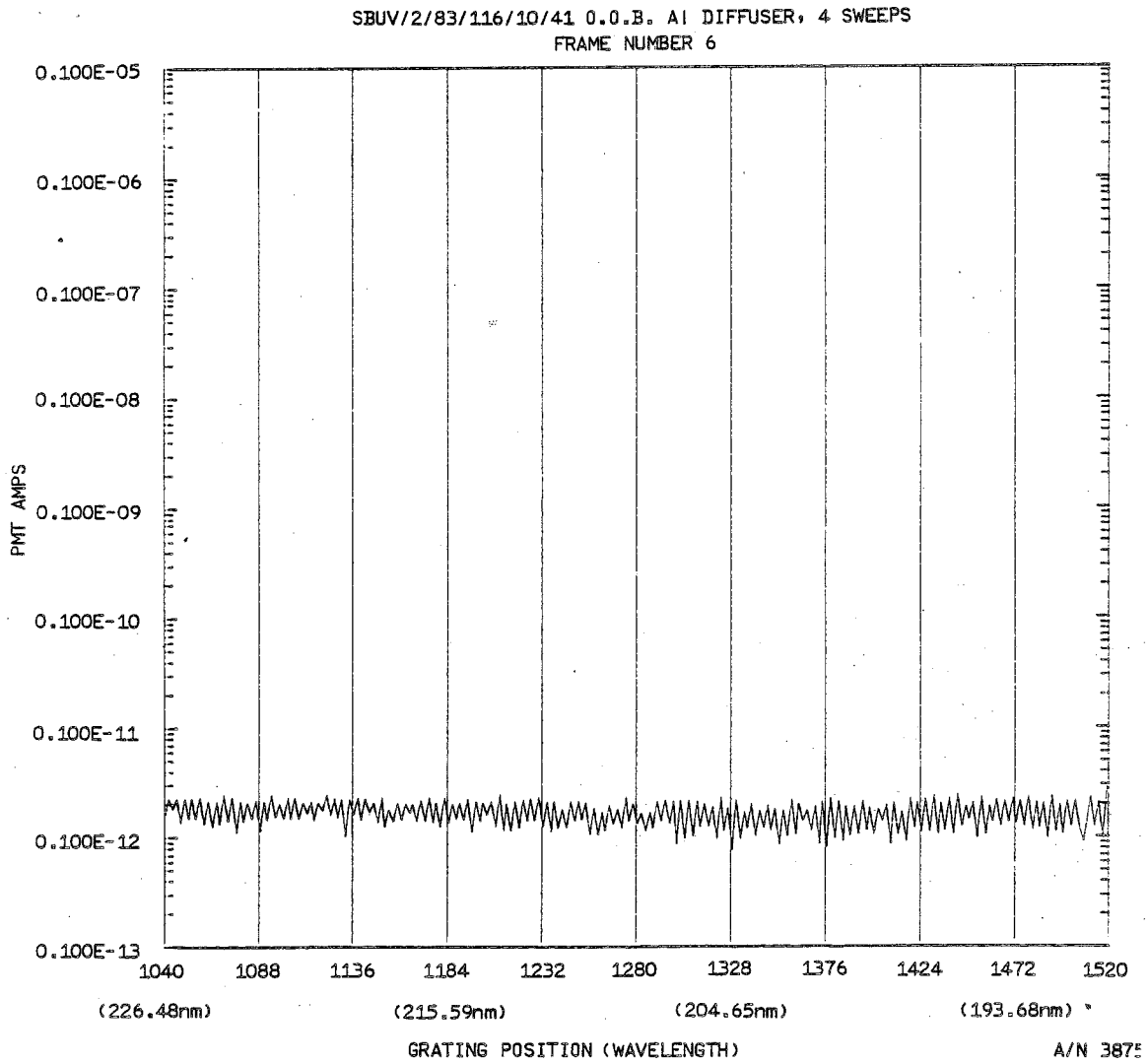


Figure 14-1f Out of Band Sweep Plot

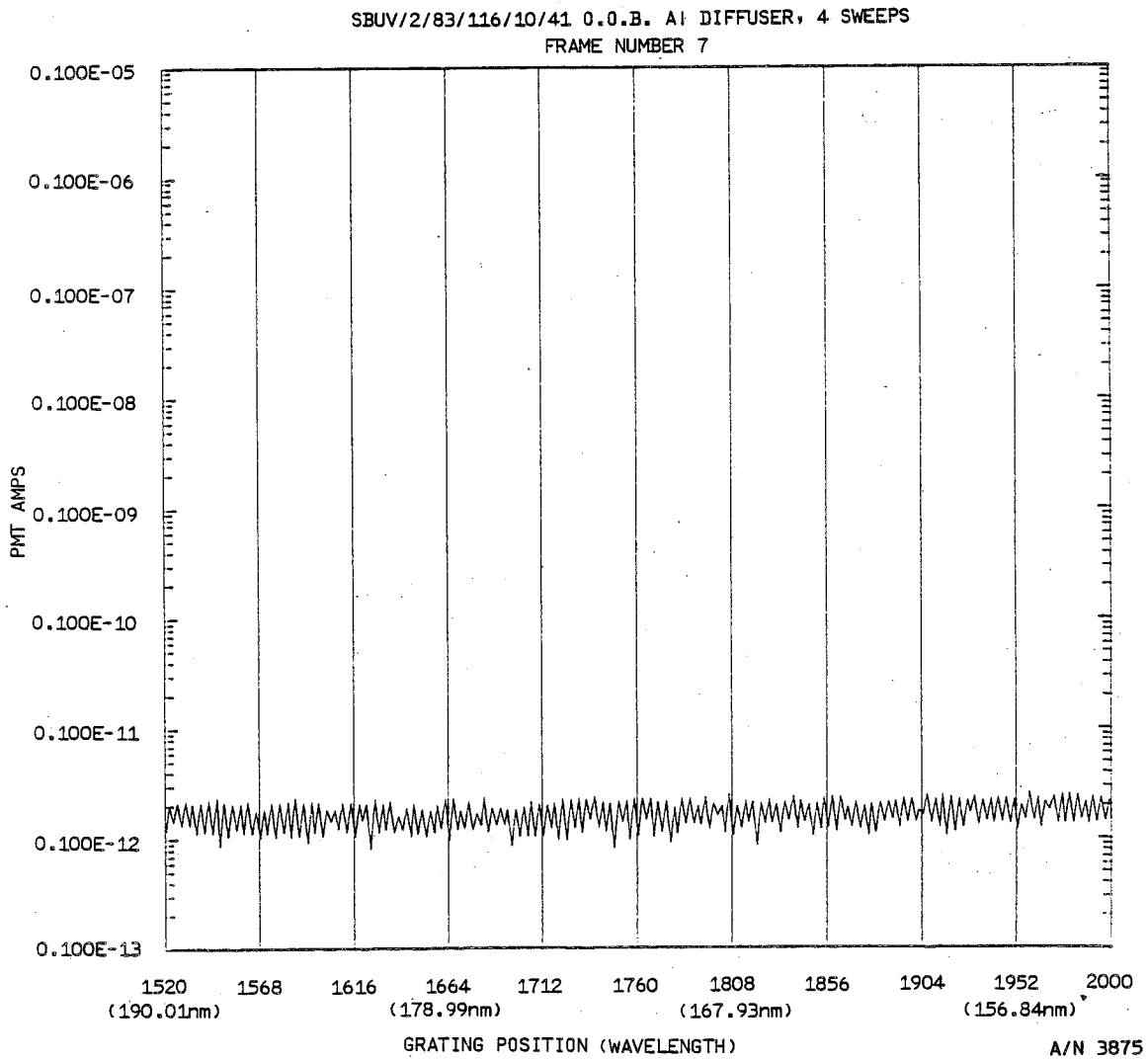


Figure 14-1g Out of Band Sweep Plot



Section 15
POLARIZATION
(Reference Test Procedure 68006)

The depolarizer efficiency was determined at the component level of test. The depolarizer was tested at the two wavelengths of 253.7 nm and 366.0 nm.

The depolarizer efficiency was tested to determine how well it scrambles the state of polarization of the incident light. A mercury pen ray lamp was used as a source. Two mercury line bandpass filters were placed in the incident beam along with a 3M Polaricoat polaroid filter. A second Polaricoat polaroid filter was used as an analyzer just in front of the photomultiplier tube detector.

With the depolarizer removed from the test fixture, the polarizer and light source were rotated 180 degrees to determine the modulation of the light beam. The depolarizer was then placed in the fixture, and again the light source and polarizer were rotated 180 degrees. The residual polarization is determined from the ratio of these measurements.

The following plot (Figure 15-1) shows the results from serial number 001 depolarizer which is installed in the EMU-FLT SBUV/2 instrument.



A/N 3875

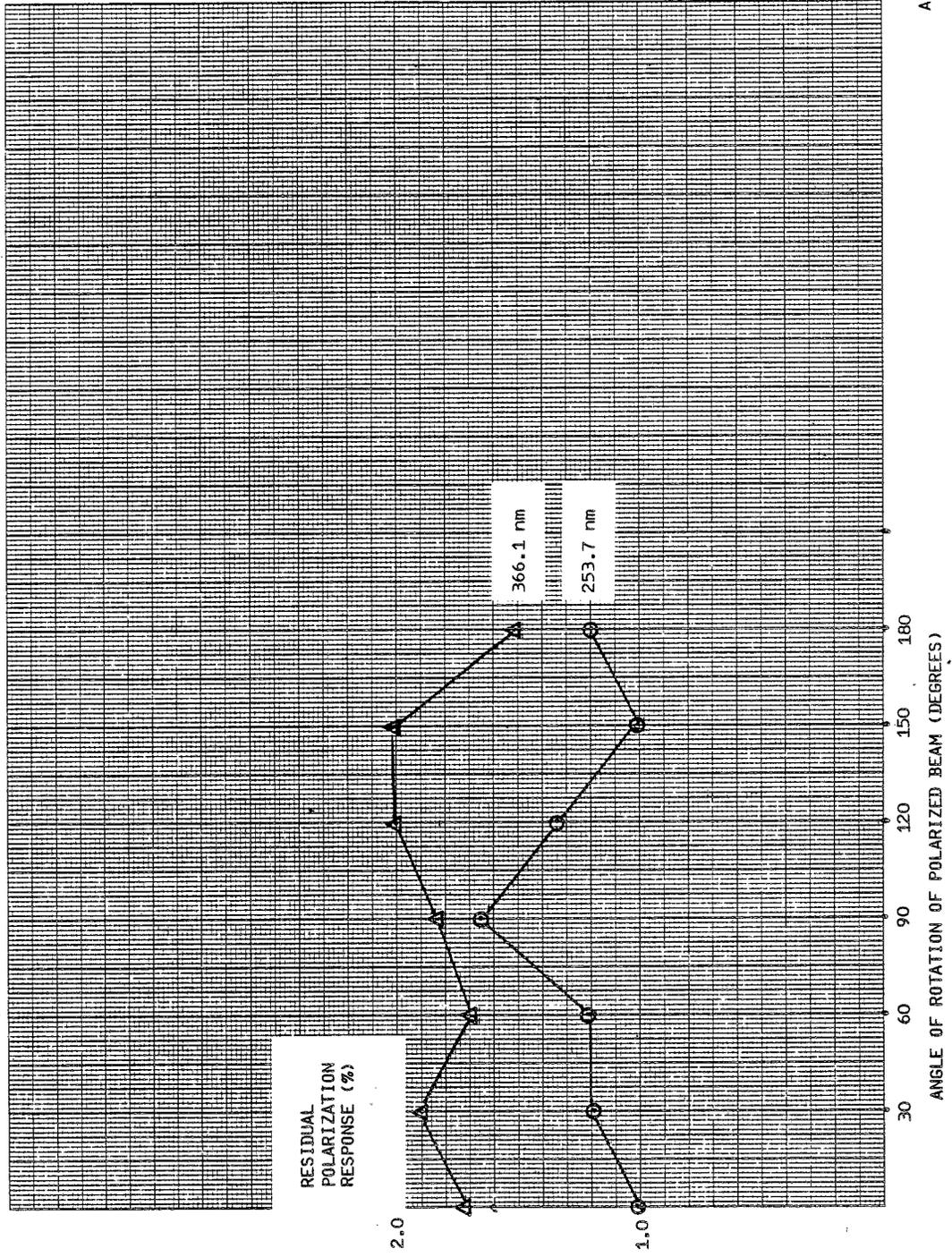


Figure 15-1 Residual Polarization Response



Section 16
LIGHT LEAK RESPONSE
(Reference Test Procedure 68031)

Two setups were used in the course of this test. First, the Sensor Module was placed in direct sunlight, without thermal blankets, and with the aperture door closed. Data was taken in Discrete Mode for five minutes. Each of the five exposed sides of the Sensor Module was tested in this manner. The data is shown in Tables 16-1a,b,c,d & e. The second test utilized a high intensity mercury vapor lamp to illuminate each side of the Sensor Module. The Sensor Module was operated in position mode at a wavelength of 253.7 nm to detect any light leak. Table 16-2 shows the data and the ratio of light leak response, resulting from the high intensity mercury vapor lamp.

No light leak was found as a result of this test. Since the test was performed without thermal blankets in place, it was concluded that a worst case test had been performed.



Table 16-1a
DATA SHEET

Light Leak Response for Side 1

Light Source Used for Test is Sunlight

DISCRETE WAVELENGTH CHANNEL (nm)	'Y' MAXIMUM LIGHT LEAK RESPONSE (COUNTS)	MEAN LIGHT LEAK RESPONSE (COUNTS)	STANDARD DEVIATION OF RESPONSE	'X' MINIMUM EXPECTED RESPONSE FOR SOLAR BACKSCATTER	RATIO OF 'X' MINIMUM TO 'Y' MAXIMUM ≤ 0.01
252.00	67	59.8	7.2	1.20×10^{-4}	.0035
273.61	75	59.1	9.6	4.98×10^{-4}	.0036
283.10	74	58.2	10.6	9.78×10^{-4}	.0018
287.70	68	55.6	7.4	1.30×10^{-3}	.0005
292.29	67	62.9	7.6	2.39×10^{-3}	.0002
297.59	76	57.1	9.8	3.48×10^{-3}	.0006
301.97	74	55.6	9.8	3.84×10^{-3}	.0004
305.87	72	57.3	13.1	6.72×10^{-3}	.0002
312.57	80	57.0	13.0	1.49×10^{-2}	.0002
317.56	69	58.9	11.1	3.09×10^{-2}	.00003
331.56	71	56.3	11.4	2.08×10^{-1}	5.0×10^{-6}
339.89	72	60.7	8.7	4.12×10^{-1}	3.0×10^{-6}

AV = .0009 A/N 3875



Table 16-1b
DATA SHEET

Light Leak Response for Side 2

Light Source Used for Test is Sunlight

DISCRETE WAVELENGTH CHANNEL (nm)	'Y' MAXIMUM LIGHT LEAK RESPONSE (COUNTS)	MEAN LIGHT LEAK RESPONSE (COUNTS)	STANDARD DEVIATION OF RESPONSE	'X', MINIMUM EXPECTED RESPONSE FOR SOLAR BACKSCATTER	RATIO OF 'X', MINIMUM 'Y', MAXIMUM ≤ 0.01 =
252.00	76	61.1	10.12	1.20×10^{-4}	.0100
273.61	72	61.4	7.0	4.98×10^{-4}	.0026
283.10	81	61.9	12.2	9.78×10^{-4}	.0030
287.70	78	65.6	8.8	1.30×10^{-3}	.0019
292.29	69	57.6	10.0	2.39×10^{-3}	.0004
297.59	71	60.4	8.6	3.48×10^{-3}	.0003
301.97	81	57.6	11.8	3.84×10^{-3}	.0007
305.87	67	59.0	7.7	6.72×10^{-3}	.0001
312.57	80	64.5	8.5	1.49×10^{-2}	.0002
317.56	73	60.1	9.6	3.09×10^{-2}	.0001
331.56	83	67.1	8.76	2.08×10^{-1}	1.4×10^{-5}
339.89	85	69.1	10.8	4.12×10^{-1}	7.0×10^{-6}

AV = .0019

A/N 3875



Table 16-1c

DATA SHEET

Light Leak Response for Side 3

Light Source Used for Test is Sunlight

DISCRETE WAVELENGTH CHANNEL (nm)	'y' MAXIMUM LIGHT LEAK RESPONSE (COUNTS)	MEAN LIGHT LEAK RESPONSE (COUNTS)	STANDARD DEVIATION OF RESPONSE	'x' MINIMUM EXPECTED RESPONSE FOR SOLAR BACKSCATTER	RATIO OF 'x' MINIMUM TO 'y' MAXIMUM ≤ 0.01
252.00	67	61.0	5.0	1.20×10^{-4}	.0035
273.61	74	60.6	7.2	4.98×10^{-4}	.0033
283.10	69	60.3	6.9	9.78×10^{-4}	.0009
287.70	69	58.7	8.0	1.30×10^{-3}	.0007
292.29	68	56.3	8.4	2.39×10^{-3}	.0003
297.59	66	56.0	8.6	3.48×10^{-3}	.0001
301.97	66	55.5	8.3	3.84×10^{-3}	.0001
305.87	66	56.8	7.6	6.72×10^{-3}	.0001
312.57	67	55.5	8.8	1.49×10^{-2}	3.5×10^{-5}
317.56	72	55.8	10.9	3.09×10^{-2}	4.7×10^{-5}
331.56	80	57.1	15.6	2.08×10^{-1}	1.2×10^{-5}
339.89	65	56.6	7.2	4.12×10^{-1}	3.3×10^{-7}

AV = .0007 A/N 3875



Table 16-1d

DATA SHEET

Light Leak Response for Side 4

Light Source Used for Test is Sunlight

DISCRETE WAVELENGTH CHANNEL (nm)	'y' MAXIMUM LIGHT LEAK RESPONSE (COUNTS)	MEAN LIGHT LEAK RESPONSE (COUNTS)	STANDARD DEVIATION OF RESPONSE	'x' MINIMUM EXPECTED RESPONSE FOR SOLAR BACKSCATTER	RATIO OF 'x' MINIMUM TO 'y' MAXIMUM ≤ 0.01
252.00	76	54.3	11.6	1.20×10^{-4}	.0100
273.61	84	60.2	14.4	4.98×10^{-4}	.0066
283.10	79	57.0	13.4	9.78×10^{-4}	.0026
287.70	82	64.7	16.3	1.30×10^{-3}	.0025
292.29	86	58.1	14.4	2.39×10^{-3}	.0016
297.59	79	62.0	14.1	3.48×10^{-3}	.0007
301.97	81	62.5	14.4	3.84×10^{-3}	.0007
305.87	93	62.9	13.9	6.72×10^{-3}	.0007
312.57	81	63.9	10.1	1.49×10^{-2}	.0002
317.56	85	64.7	11.3	3.09×10^{-2}	.0001
331.56	88	68.0	12.7	2.08×10^{-1}	1.7×10^{-5}
339.89	74	57.0	13.7	4.12×10^{-1}	3.3×10^{-6}

AV = .0025 A/N 3875



Table 16-1e

DATA SHEET

Light Leak Response for Side 5

Light Source Used for Test is Sunlight

DISCRETE WAVELENGTH CHANNEL (nm)	'Y' MAXIMUM LIGHT LEAK RESPONSE (COUNTS)	MEAN LIGHT LEAK RESPONSE (COUNTS)	STANDARD DEVIATION OF RESPONSE	'X' MINIMUM EXPECTED RESPONSE FOR SOLAR BACKSCATTER	RATIO OF 'X' MINIMUM 'Y' MAXIMUM ≤ 0.01
252.00	74	62.4	8.73	1.20×10^{-4}	.010
273.61	70	59.1	11.45	4.98×10^{-4}	.002
283.10	68	59.9	7.32	9.78×10^{-4}	.0007
287.70	73	57.1	8.91	1.30×10^{-4}	.0012
292.29	77	56.6	12.8	2.39×10^{-4}	.0010
297.59	67	54.0	11.8	3.48×10^{-4}	.0001
301.97	69	53.8	8.2	3.84×10^{-4}	.0002
305.87	69	53.2	12.2	6.72×10^{-3}	.0001
312.57	69	54.4	8.0	1.49×10^{-2}	.0001
317.56	67	55.8	8.0	3.09×10^{-2}	1.8×10^{-5}
331.56	67	60.3	5.9	2.08×10^{-1}	2.2×10^{-6}
339.89	71	58.0	10.2	4.12×10^{-1}	2.3×10^{-6}

AV = .0014 A/N 3875



Table 16-2
LIGHT LEAK RESPONSE TEST (DISCRETE WAVELENGTH 253.7 nm)

Instrument Side Being Measured	'Y' Maximum Light Leak Response (Counts)	Mean Light Leak Response (Counts)	Standard Deviation of Response	'X' Minimum Expected Response for Solar Backscatter	Ratio of	
					X' Minimum	'Y' Maximum < 0.01
1	84	58.7	8.8	1040 (counts)	.01	
2	73	53.6	6.7	For An Expected Minimum Radiance from Solar Input	.01	
3	81	55.9	8.9		.01	
4	80	62.6	8.4		.01	
5	78	69.8	8.1		.01	

A/N 3875



Section 17
SIGNAL TO NOISE RATIO
(Reference Test Procedure 68026)

The Signal-to-Noise ratio was measured at signal levels which were approximately 0.8 times, 1.2 times the required radiance, and very near the required radiance level. With three data points, a curve is established and the signal to noise ratio at the required radiance level interpolated from it.

Table 17-1 gives the resulting values measured for signal to noise ratio, and describes how the ratios were calculated.



Table 17-1
SIGNAL-TO-NOISE RATIO CALCULATION

WAVELENGTH NM	REQUIRED SOURCE INTENSITY (RADIANCE) mW/M ² -sr-Å	DISCRETE REQUIRED MINIMUM SIGNAL-TO-NOISE	MEASURED SIGNAL-TO- NOISE
252.0	1.20 x 10 ⁻⁴	35	43 NOTE 1
273.5	4.98 x 10 ⁻⁴	100	333 NOTE 2
283.0	9.78 x 10 ⁻⁴	200	632 NOTE 2
287.6	1.30 x 10 ⁻³	260	811 NOTE 2
292.2	2.39 x 10 ⁻³	400	1524 NOTE 2
297.5	3.48 x 10 ⁻³	400	2267 NOTE 2
301.9	3.84 x 10 ⁻³	400	2667 NOTE 2
305.8	6.72 x 10 ⁻³	400	4473 NOTE 2
312.5	1.49 x 10 ⁻²	400	1204 NOTE 2
317.5	3.09 x 10 ⁻²	400	2504 NOTE 2
331.2	2.08 x 10 ⁻¹	400	8992 NOTE 3
339.8	4.12 x 10 ⁻¹	400	16119 NOTE 3
CCR	0.125	100	296 NOTE 3

NOTE 1 SIGNAL TO NOISE RATIO CALCULATED AS FOLLOWS: A/N 3875

$$\frac{\text{MEAN COUNTS}}{\text{STANDARD DEVIATION}} = \text{SIGNAL TO NOISE RATIO}$$

NOTE 2 SIGNAL TO NOISE RATIO CALCULATED AS FOLLOWS:

$$\text{SIGNAL TO NOISE RATIO} = \frac{\text{MEAN COUNTS}}{\text{BACKGROUND NOISE}}$$

NOTE 3 SIGNAL TO NOISE RATIO CALCULATED AS FOLLOWS:

$$\left(\frac{\text{MEAN COUNTS}}{\text{BACKGROUND NOISE}} \right) \sqrt{\frac{\text{REQUIRED RADIANCE}}{\text{RADIANCE FOR COUNTS}}} = \text{SIGNAL TO NOISE AT REQUIRED RADIANCE}$$



Section 18
SHORT TERM STABILITY

(Reference Test Procedure 68026)

The instrument short term radiometric stability is specified as follows:

The radiometric response of the instrument shall meet the following stability requirements. The corrected mean response of the instrument shall not differ by more than 1 percent from a previous or subsequent response measurement made while viewing the same source operating at equal intensity but separated in time by at least 24 hours, for each wavelength in the Discrete Mode. The mean response is to be determined from at least 50 successive data samples taken with the wavelength drive stopped at each Discrete Mode position. This instrument data is to be corrected for changes in instrument temperature and other response-dependent parameters, if any, before comparisons are made.

The instrument was tested using the Primary Test Fixture, Target Control Console, and a FEL light source calibrated by the National Bureau of Standards. FEL source #124 was used to make these measurements.

Measurements were made for baseline, 3 days, 6 days, and 11 days later for comparison. The data is shown in Tables 18-1 and 18-2.



Table 18-1

SHORT TERM STABILITY

NOMINAL WAVELENGTH	\bar{C} BASE-LINE DATA	\bar{C} 80 HOUR DATA	Δ_1	\bar{C} 144 HOUR DATA	Δ_2	\bar{C} 264 HOUR DATA	Δ_3
252	6902	6950	48	6918	32	6830	88
273.6	20020	20010	10	19887	123	19547	340
283.1	28012	28050	38	27837	213	27345	492
287.7	33047	33126	79	32840	286	32234	606
292.3	39188	39241	53	38932	309	38230	702
297.6	47559	47644	85	47289	355	46407	882
301.9	55850	56003	153	55525	478	54511	1014
305.9	64434	64632	198	64076	556	62859	1217
312.6	816	817	1	811	6	796	15
317.6	969	972	3	964	8	944	20
331.3	1780	1787	7	1777	10	1736	41
339.9	2526	2536	10	2520	16	2457	63

$$\Delta_1 = \bar{C}_{\text{BASELINE}} - \bar{C}_{80 \text{ hour}}$$

$$\Delta_2 = \bar{C}_{144 \text{ hour}} - \bar{C}_{80 \text{ hour}}$$

$$\Delta_3 = \bar{C}_{264 \text{ hour}} - \bar{C}_{144 \text{ hour}}$$

A/N 3875



Table 18-2

CONTINUED SHORT TERM STABILITY

NOMINAL WAVELENGTH	NOTE 1 $\frac{\Sigma C}{4}$	NOTE 2 $\frac{\Sigma \Delta}{3}$	NOTE 3 $\frac{\bar{\Delta}}{C}$	REQUIREMENT
252	6900	56	0.008	< 0.01
273.6	19866	157	0.008	< 0.01
283.1	28811	248	0.009	< 0.01
287.7	32811	324	0.010	< 0.01
292.3	38898	355	0.009	< 0.01
297.6	47225	441	0.009	< 0.01
301.9	55472	548	0.010	< 0.01
305.9	64000	657	0.010	< 0.01
312.6	810	7	0.009	< 0.01
317.6	962	10	0.010	< 0.01
331.3	1770	19	0.010	< 0.01
339.9	2510	30	0.011	< 0.01

AVG. .009

$$\text{NOTE 1 } \frac{\Sigma C}{4} = \frac{C_{\text{BASELINE}} + C_{24} + C_{48} + C_{72}}{4}$$

$$\text{NOTE 2 } \frac{\Sigma \Delta}{3} = \frac{\Delta_1 + \Delta_2 + \Delta_3}{3}$$

$$\text{NOTE 3 } \frac{\bar{\Delta}}{C} = \frac{\frac{\Sigma \Delta}{3}}{\frac{\Sigma C}{4}}$$

A/N 3875



Section 19

WAVELENGTH CALIBRATION STABILITY

(Reference Test Procedure 68030)

Wavelength stability is monitored using the mercury vapor lamp onboard the instrument. A sweep mode scan is taken with the lamp door closed (lamp directly over entrance slit) and a second scan taken with the lamp door open and the diffuser in the monitor position (light being diffused off the diffuser plate).

Three spectral lines were chosen from the mercury spectrum at wavelengths 184.9, 253.7, and 404.7 nm. These lines are approximately spaced at the ends and center of the instrument's wavelength range. The grating position and corresponding wavelength of each line is determined by a linear regression curve fit to each side of the line profile. The intersection of the two curves yields the wavelength. The results are shown in Table 19-1.

The following plots (Figures 19-1 through 19-10) are line profiles from sweep mode data taken during a 25°C thermal vacuum plateau. Ten different mercury lines are plotted. The two curves on each plot are from data taken with the calibration lamp door closed and with it open and the diffuser on monitor position. These curves show that a good wavelength calibration check can be accomplished as well as constant monitoring of the condition of the diffuser over the entire wavelength of the instrument.



Table 19-1
WAVELENGTH CALIBRATION STABILITY

	184.9nm		253.7nm		404.7nm	
	GPS	λ	GPS	λ	GPS	λ
Previbration	1587.9	184.78	680.0	253.52	-1424.0	404.58
Post Z Axis Vibration	1595.8	184.18	680.5	253.48	-1424.1	404.59
Post Y Axis Vibration	1589.6	184.65	680.8	253.46	-1422.8	404.50
Post X Axis Vibration	1590.70	184.57	682.4	253.34	-1421.4	404.40
Pre Thermal Vacuum Test	1589.13	184.69	680.51	253.48	-1423.42	404.54
Post Thermal Vacuum Test	1588.43	184.74	678.75	253.61	-1423.66	404.56
EMI Retest	1587.70	184.80	679.40	253.57	-1424.38	404.60
Post Delivery Check	1585.95	184.93	681.66	253.40	-1422.3	404.46

A/N 3875



A/N 3675

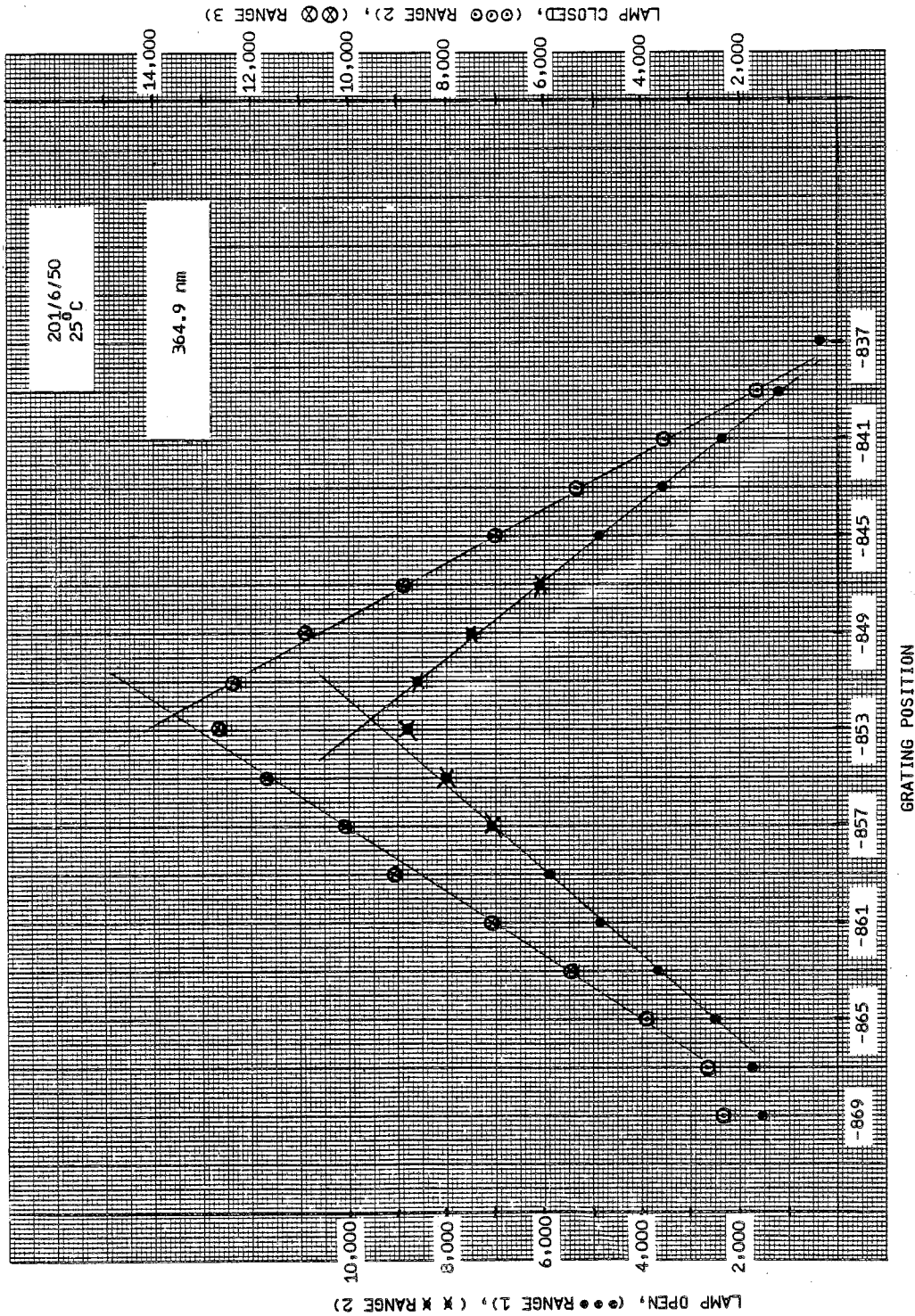
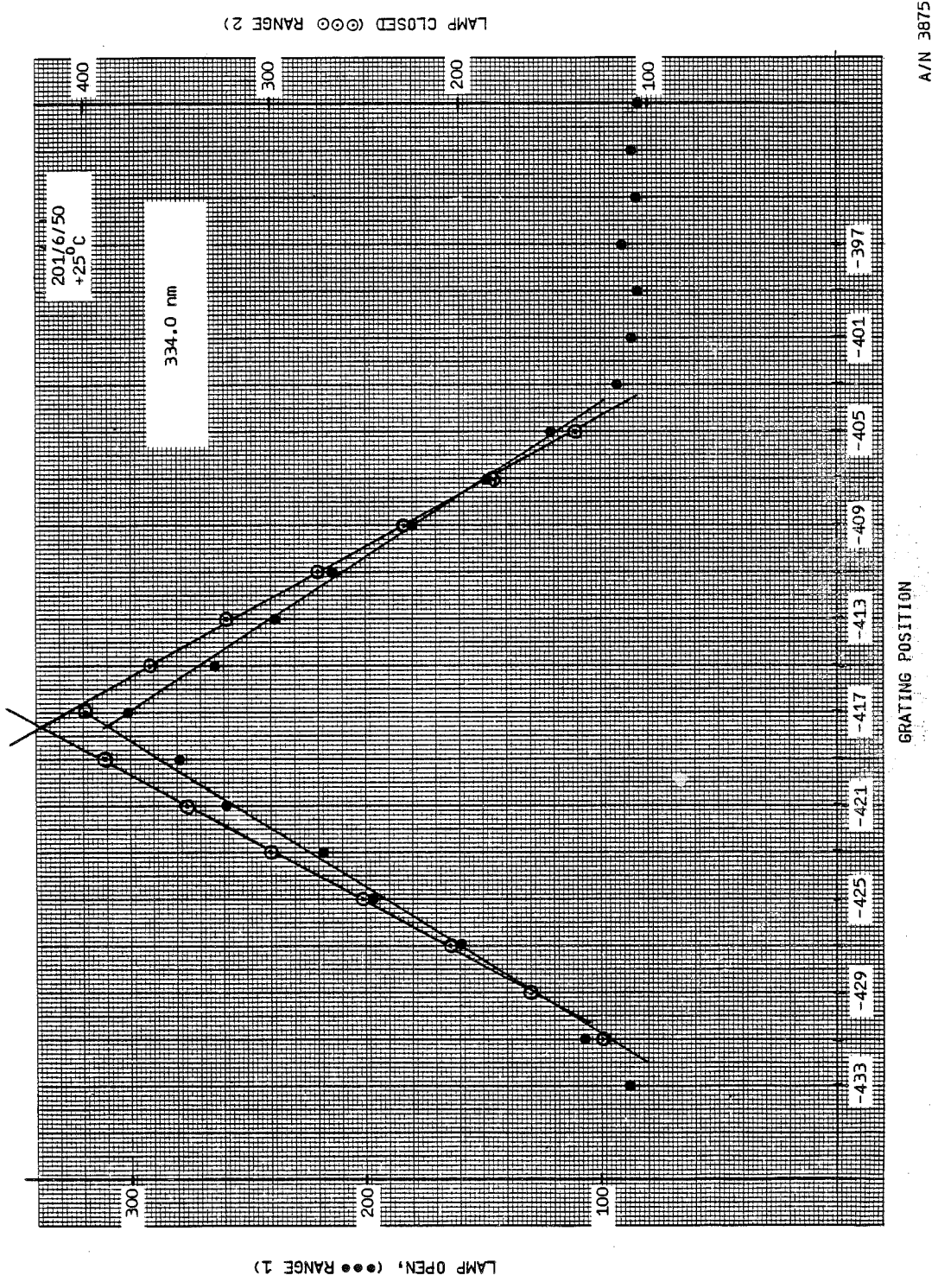
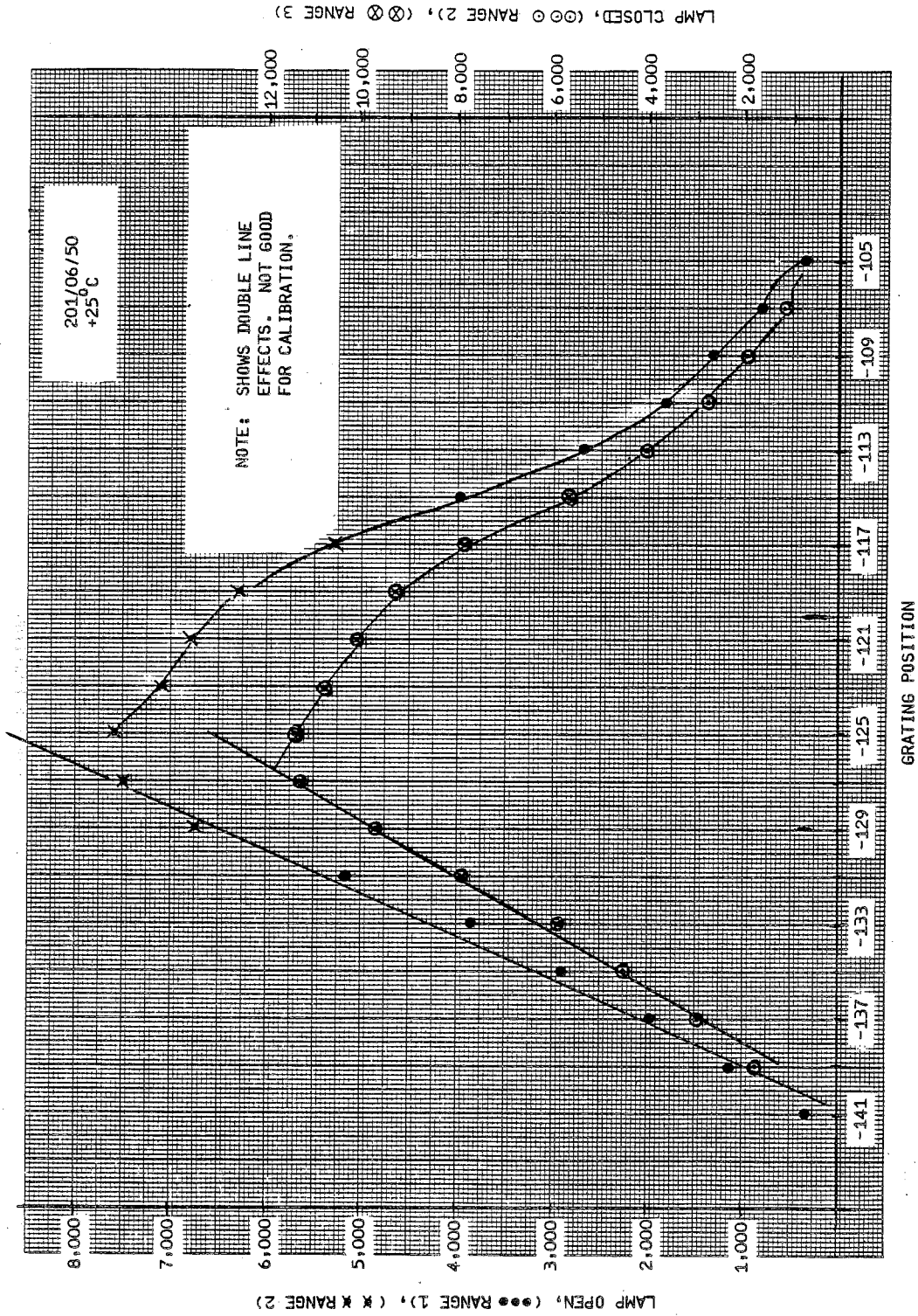


Figure 19-2 Mercury Line Profiles



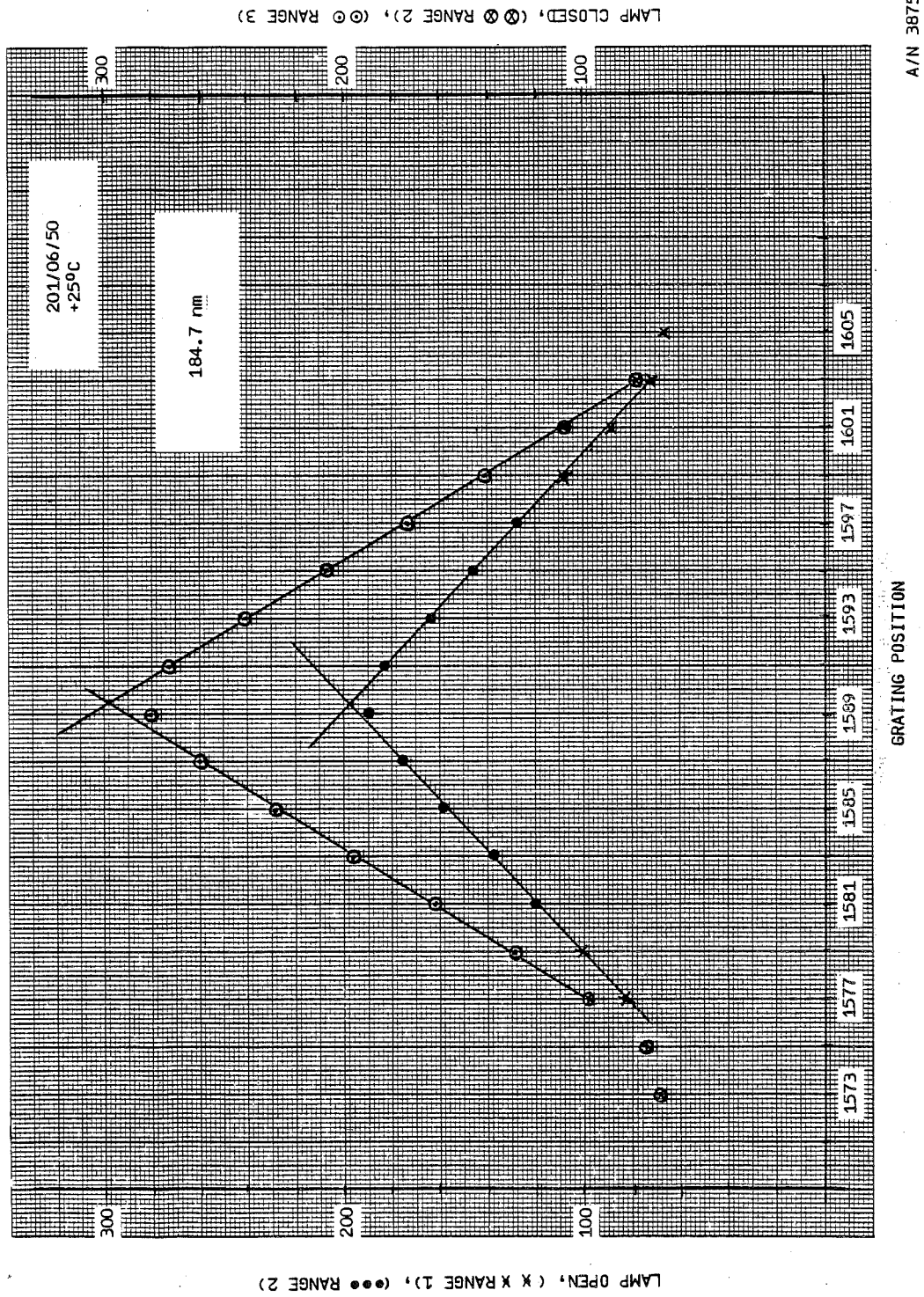
A/N 3875

Figure 19-3 Mercury Line Profiles



A/N 3875

Figure 19-4 Mercury Line Profiles



A/N 3875

GRATING POSITION

Figure 19-5 Mercury Line Profiles



A/N 3875

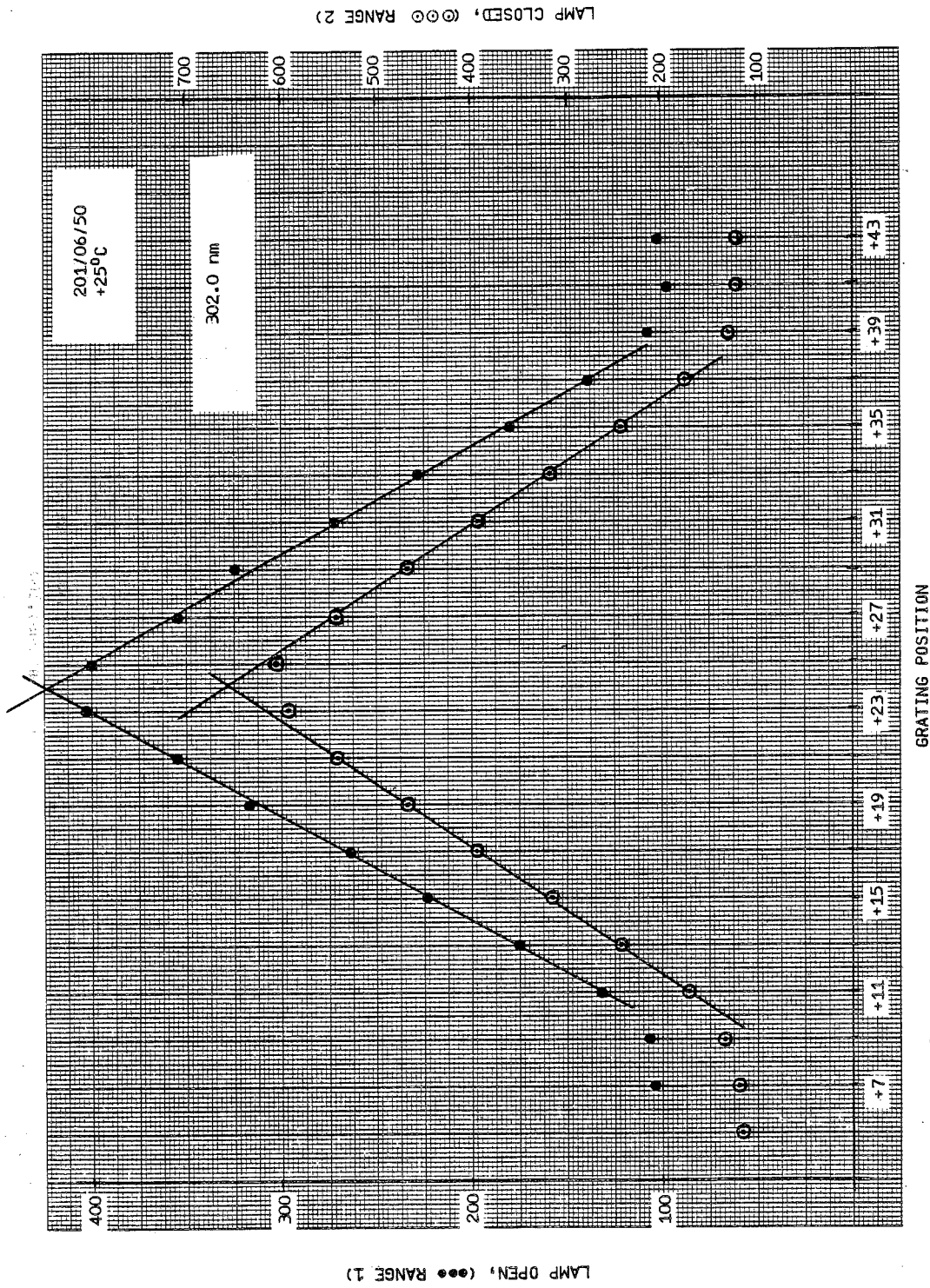
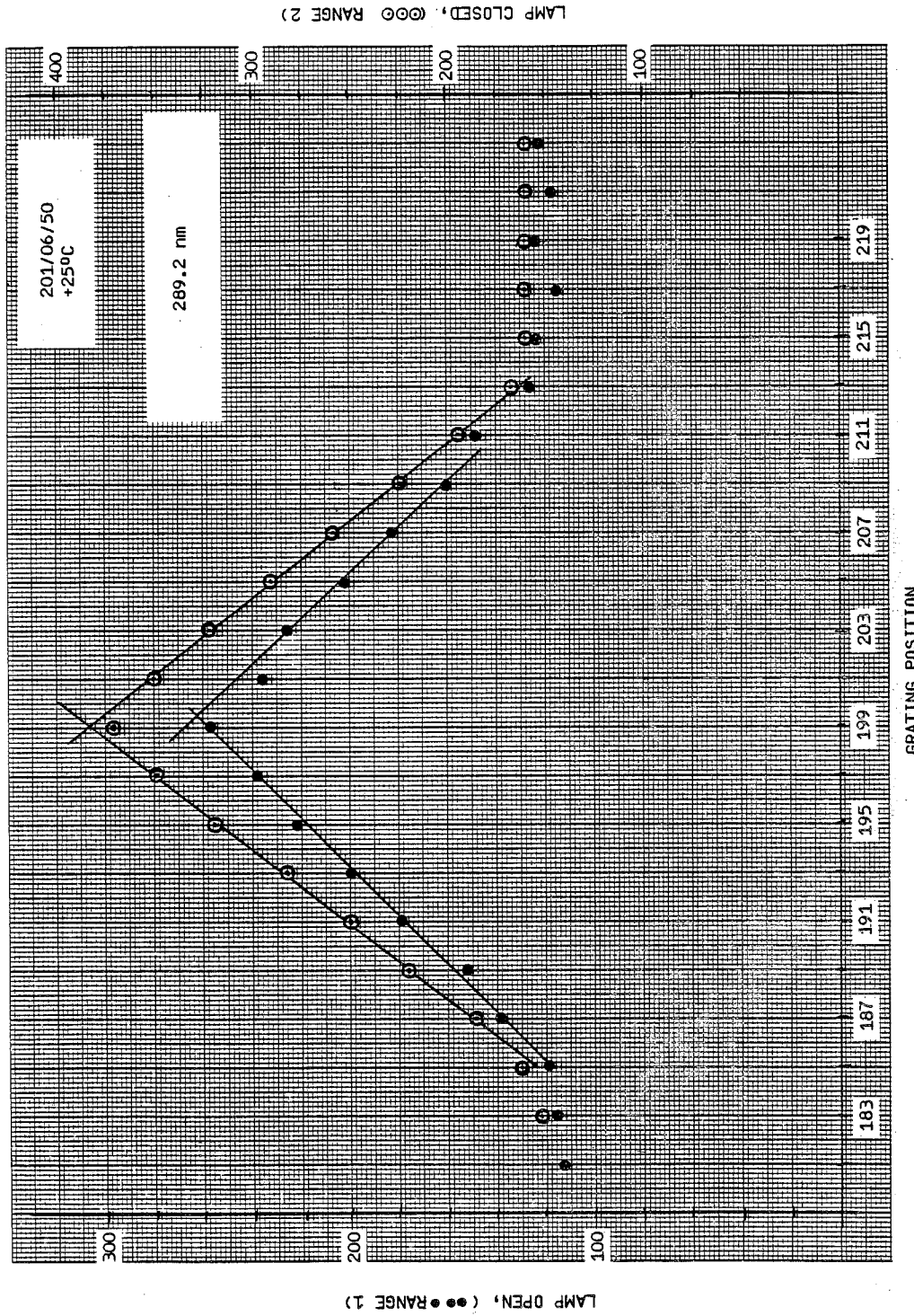


Figure 19-6 Mercury Line Profiles

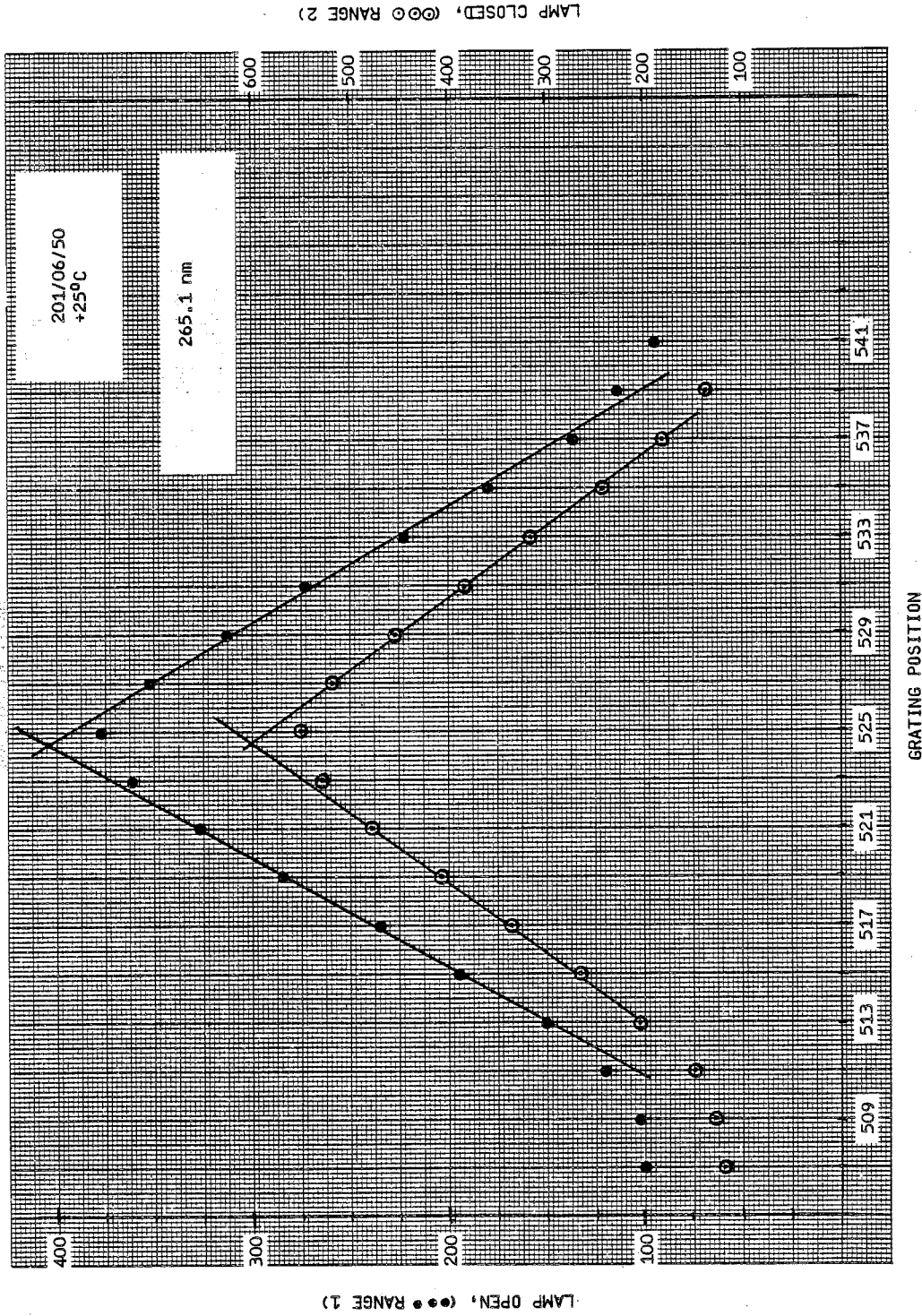


A/N 3875



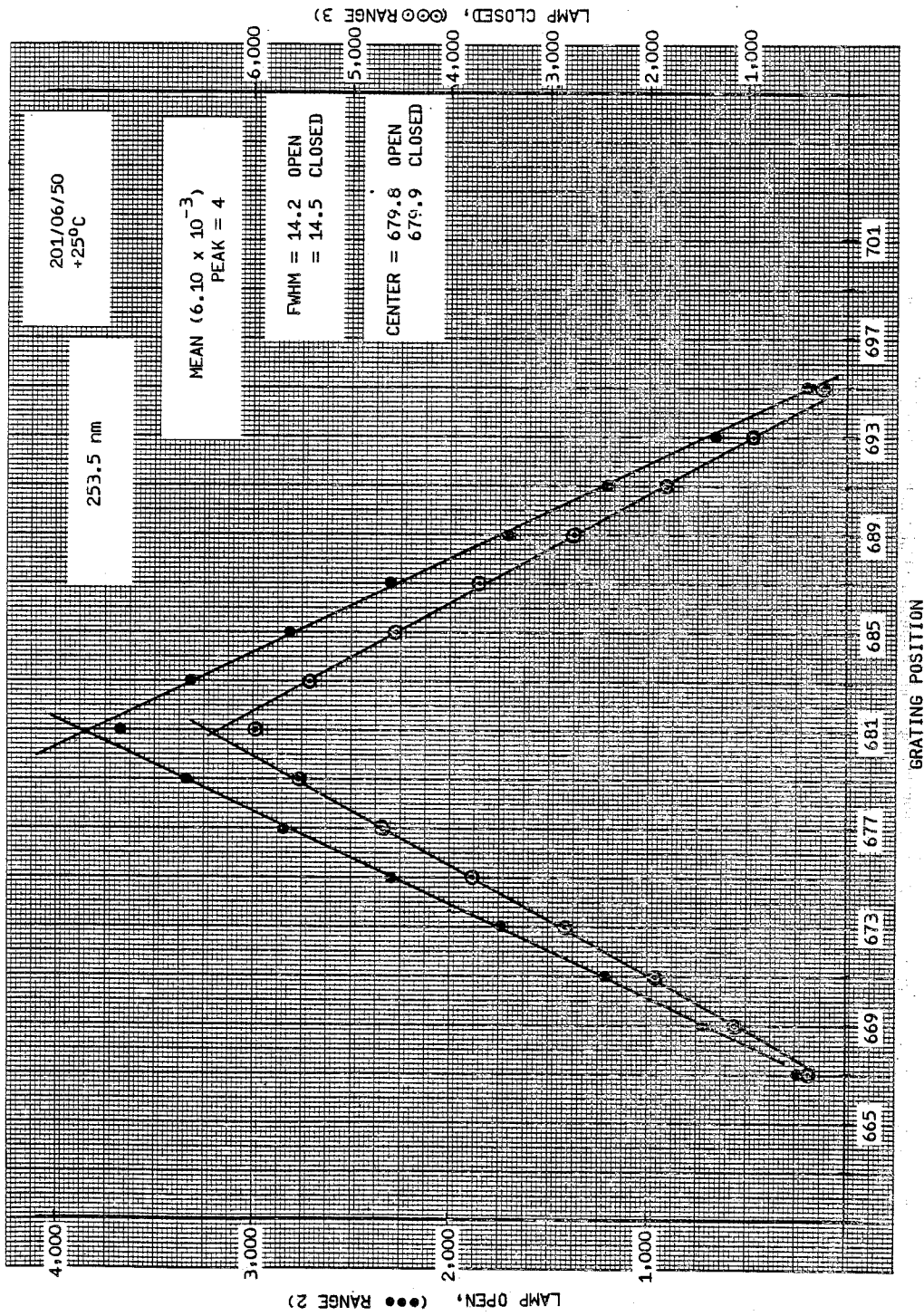
GRATING POSITION

Figure 19-7 Mercury Line Profiles



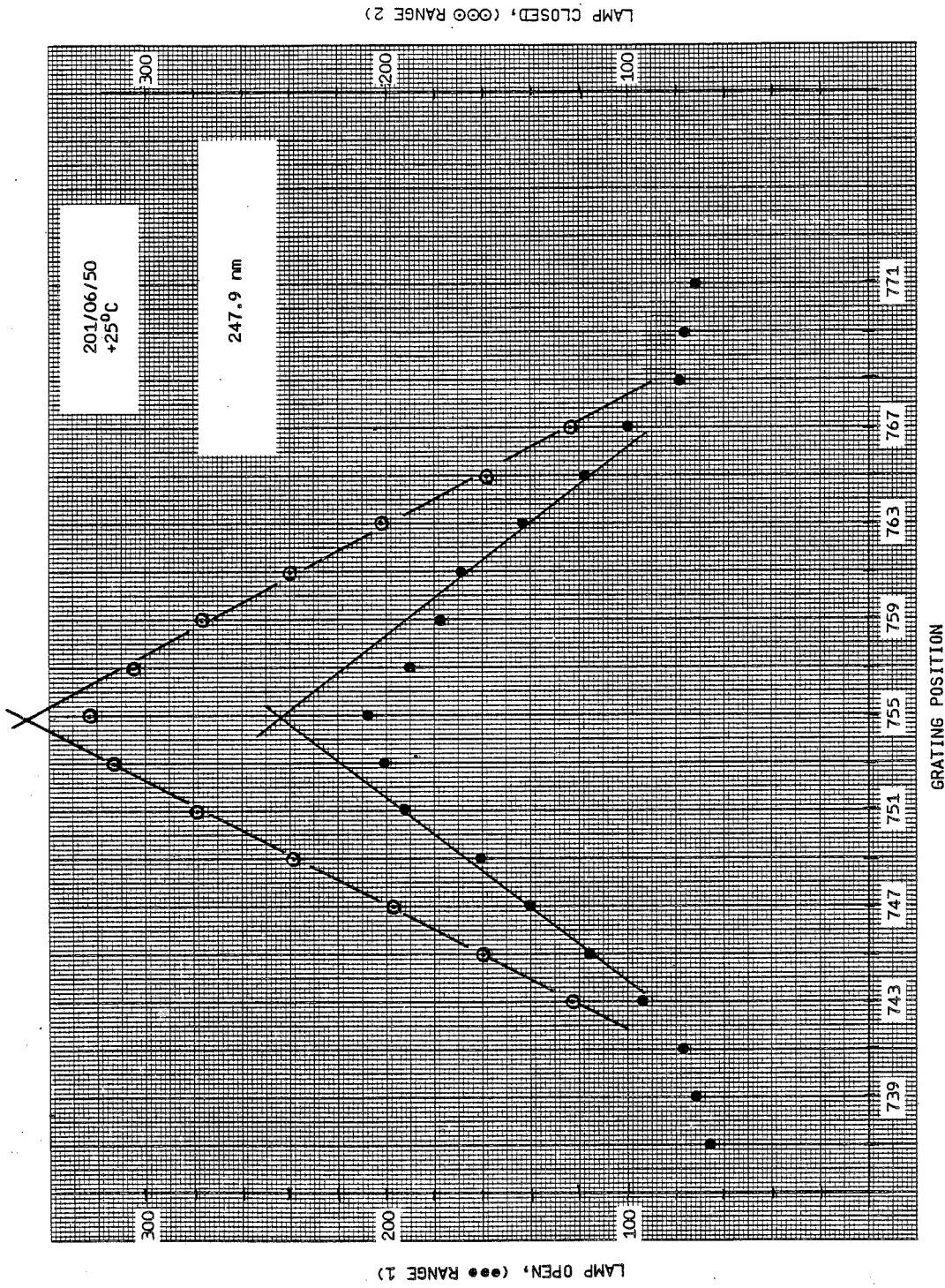
A/N 3875

Figure 19-8 Mercury Line Profiles



A/N 3875

Figure 19-9 Mercury Line Profiles



A/N 3875

GRATING POSITION

Figure 19-10 Mercury Line Profiles

Handwritten text, possibly a signature or name, located in the upper left quadrant of the page.



Section 20

ELECTRONIC CALIBRATION

(Reference Test Procedure 68026)

Tables 20-1 and 20-2 list the E-CAL counts in the Discrete and Sweep Modes for both the Cloud Cover Radiometer and Monochromator. The Tables list E-CAL values at the four temperature plateaus.



Table 20-1
DISCRETE MODE E-CAL

INSTR. TEMP °C	RANGE 1 E-CAL			
	TIME DATA TAKEN AFTER RETRACE			
	2 (SEC)	4	6	8
0	28308 *	9124	7835 *	66.79
+10	28499 *	9118	7807 *	64.39
+20	28663 *	9108	7781 *	64.79
+30	28745 *	9111	7769 *	63.59

* OVER RANGE DATA

INSTR. TEMP °C	RANGE 2 E-CAL			
	TIME DATA TAKEN AFTER RETRACE			
	2 (SEC)	4	6	8
0	10678	156.19	796	63.00
+10	10680	156.79	795	62.59
+20	10678	155.59	795	62.59
+30	10680	156.19	795	62.99

INSTR. TEMP °C	RANGE 3 E-CAL			
	TIME DATA TAKEN AFTER RETRACE			
	2 (SEC)	4	6	8
0	64.79	788	7374	38500
+10	63.99	788	7371	38461
+20	64.99	787	7374	38478
+30	64.79	787	7371	38481

INSTR. TEMP °C	CCR E-CAL			
	TIME DATA TAKEN AFTER RETRACE			
	2 (SEC)	4	6	8
0	44306	960	9164	61.79
+10	44302	959	9166	61.79
+20	44305	959	9164	61.59
+30	44294	957	9168	61.79

A/N 3875



Table 20-2
SWEEP MODE E-CAL

TIME OF RESPONSE AFTER RETRACE	INSTRUMENT TEMPERATURE				RANGE
	0°C	+10°C	+20°C	+30°C	
2 SEC	914.70	913.45	913.80	913.70	2
4	122.80	122.20	122.30	122.40	3
6	649.75	649.45	649.60	649.55	3
8	3140.95	3138.20	3139.55	3139.05	3
10	6208.50	6208.55	6209.85	6211.20	3
12	64.53	64.03	64.36	64.22	1
14	64.33	64.10	64.49	64.31	1
16	64.26	64.18	64.16	64.46	1
18	913.58	913.45	913.65	915.55	2
20	789.42	789.68	788.58	788.42	1
22	122.60	122.60	122.60	122.60	2
24	64.50	64.21	64.53	64.38	1
CLOUD COVER RADIOMETER					
2	35467.0	35465.0	35466.5	35459.5	N/A
4	772.0	771.0	771.0	770.0	
6	7345.0	7350.0	7351.0	7349.0	
8	60.5	60.5	60.0	60.0	
10	55953.0	55948.0	55968.5	55967.0	
12	64.0	64.0	64.0	64.0	
14	64.0	64.0	64.0	64.0	
16	64.0	64.0	64.0	64.0	
18	35465.0	35465.0	35466.0	35457.0	
20	771.5	772.0	771.0	770.5	
22	7347.0	7349.0	7349.0	7348.0	
24	64.0	62.0	62.5	62.0	

A/N 3875

